# Chapter 1

## *Introduction*

## 1.1 PREAMBLE

From the elucidation of the structure of DNA by Watson and Crick[1] to the sequencing and analysis of the human genome,[2] the past half-century has seen significant progress in our knowledge and understanding of nucleic acids and their role within biological systems. Nevertheless there still remain many aspects of which we have limited understanding, and so elucidation of the mechanisms behind the biological activity of DNA and RNA remains a field of considerable interest to the chemical and biological sciences.

Perhaps foremost amongst these studies have been investigations into the origins of sequence- and structure-specificity exhibited by many biological molecules when binding to DNA or RNA. A thorough understanding of the physical and chemical factors involved in such specificity will significantly influence the rational design of nucleic acid probes and sequencing agents. Furthermore, given that these principles govern some of the most elementary biological functions (replication, transcription, etc.), such knowledge may very well revolutionise the design of nucleic acid-based chemotherapeutic agents.

The ability to tailor the size and geometry of potential binding agents is an essential requirement in modulating the specificity of small molecule-polynucleotide interactions. Investigations into the nature of such specificity have been facilitated by advances in synthetic methodologies that have provided the means to design and construct DNA-binding agents encompassing a myriad of different sizes, shapes, and functionalities. These synthetic capabilities, coupled with an ever-increasing array of techniques available to investigate DNA-binding activity, present us with the ability to advance our knowledge of the structure and function of the genome.

## 1.2 NUCLEIC ACIDS

### 1.2.1 Function

The role of the naturally-occurring nucleic acids, DNA and RNA, is primarily to encode and express genetic information. In achieving this, DNA and RNA serve very different functions. DNA predominantly acts as a long-term store of hereditary information that is replicated and passed from generation to generation. It is often described as the "blueprint of life" as it contains the instructions needed to establish the cellular machinery of an organism,

and is therefore responsible for the ultimate development and function of that organism. RNA has a more transitory existence but is utilised in a variety of different tasks: as messenger, adapter and catalyst, to name a few.

Genetic information is stored in segments of DNA known as genes – the fundamental units of heredity. The "central dogma of molecular biology" states that genes are *transcribed* into messenger RNAs (mRNAs) which are subsequently *translated* into proteins that facilitate and ensure the proper structure and function of the cell (see Figure 1.1).[3] Transcription involves the synthesis of a single-stranded RNA copy of a gene by the enzyme RNA polymerase. The genetic code of the mRNA is subsequently converted into the appropriate sequence of amino acids by ribosomes, which are RNA-protein complexes that assemble proteins. Amino acids are transported to the ribosome by transfer RNAs (tRNAs), which recognise the appropriate sequences on the mRNA that represent specific amino acids. The ribosomal complex subsequently strings the amino acids together into the protein that was ultimately encoded for by the gene. While this scheme is fundamentally accurate, it may be considered an oversimplification. In reality, most of the DNA in a given genome does not directly code for proteins (as little as 1.5% in humans),[2] but rather it assumes roles in the regulation and control of various aspects of the transcription/translation machinery. Eukaryotic genes actually contain a large amount of information that is not ultimately translated. In a process called splicing these non-coding segments (*introns*) are removed from mRNA while the coding elements (*exons*) are joined together into the mature mRNA, ready for translation. One gene can give rise to different protein products via alternative splicing schemes. There is growing evidence that the discarded intron RNA is actually involved in feedback and signalling processes that modulate transcription/translation processes.[4, 5] Other non-coding RNAs include the tRNAs, ribosomal RNAs (rRNAs), ribozymes (enzymatic RNAs), microRNAs (miRNAs) that regulate gene expression, and small nuclear RNAs (snRNAs), responsible for splicing. Untranscribed DNA sequences such as promoters, enhancers and silencers facilitate the initiation, stimulation and repression of transcription (respectively) through recognition by the appropriate DNA-binding proteins.

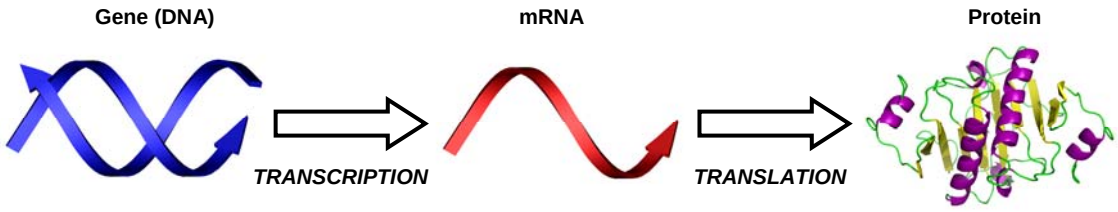


***Figure 1.1***
**The "central dogma of molecular biology".** This schematic is a simplification of the core concept of molecular biology: DNA is transcribed into RNA which is subsequently translated in to proteins. In reality, the factors and processes that drive and regulate this process are significantly more complicated.

While biological information is generally envisioned as being represented by the primary structure of nucleic acids – the linear sequences of bases from which they are composed – higher order structures are often essential to their optimal activity. Structural diversity is rife amongst biomolecules as they bend and fold to assume energy-efficient conformations, accommodate appropriate ligands and to bring isolated but functionally-related sites on the same molecule into close proximity with one another. Thus, proper appreciation of the three-dimensional structure of nucleic acids is essential to fully comprehend the mechanisms by which the information encoded within them is replicated, expressed and passed on.

### 1.2.2 Structure

Nucleic acids are essentially biopolymers comprised of repeating units known as *nucleotides*. Each nucleotide is itself a phosphate ester of the corresponding *nucleoside* – a furanose sugar (β-D-2′-deoxyribose in DNA, β-D-ribose in RNA) bound to a nitrogenous heterocyclic *base*. DNA typically contains four such bases – adenine (A), guanine (G), cytosine (C), and thymine (T) – which are planar aromatic derivatives of purine (A and G) or pyrimidine (C and T) {see Figure 1.2(a)}. RNA has adopted a somewhat larger array of construction materials {see Figure 1.2(b)}, however it is still composed primarily of these same four bases, albeit with uracil (U) in place of thymine.[†]

[†] Uracil undergoes methylation to form thymine before incorporation into DNA in order to afford greater stability and to ensure the fidelity of DNA replication. Uracil is capable of forming a variety of base pairs depending upon how it orients itself within a nucleic acid. Thymine possesses less conformational flexibility – the hydrophobic methyl group is secreted away in the major groove forcing the thymine into a conformation where it can only base pair with adenine. Restricting the number of probable base pair combinations in turn restricts the number of potential base mismatches, which ultimately results in fewer mutations. Mutation is less of a concern in RNA than in DNA because RNAs have a much shorter lifespan and are synthesised in much greater quantities.

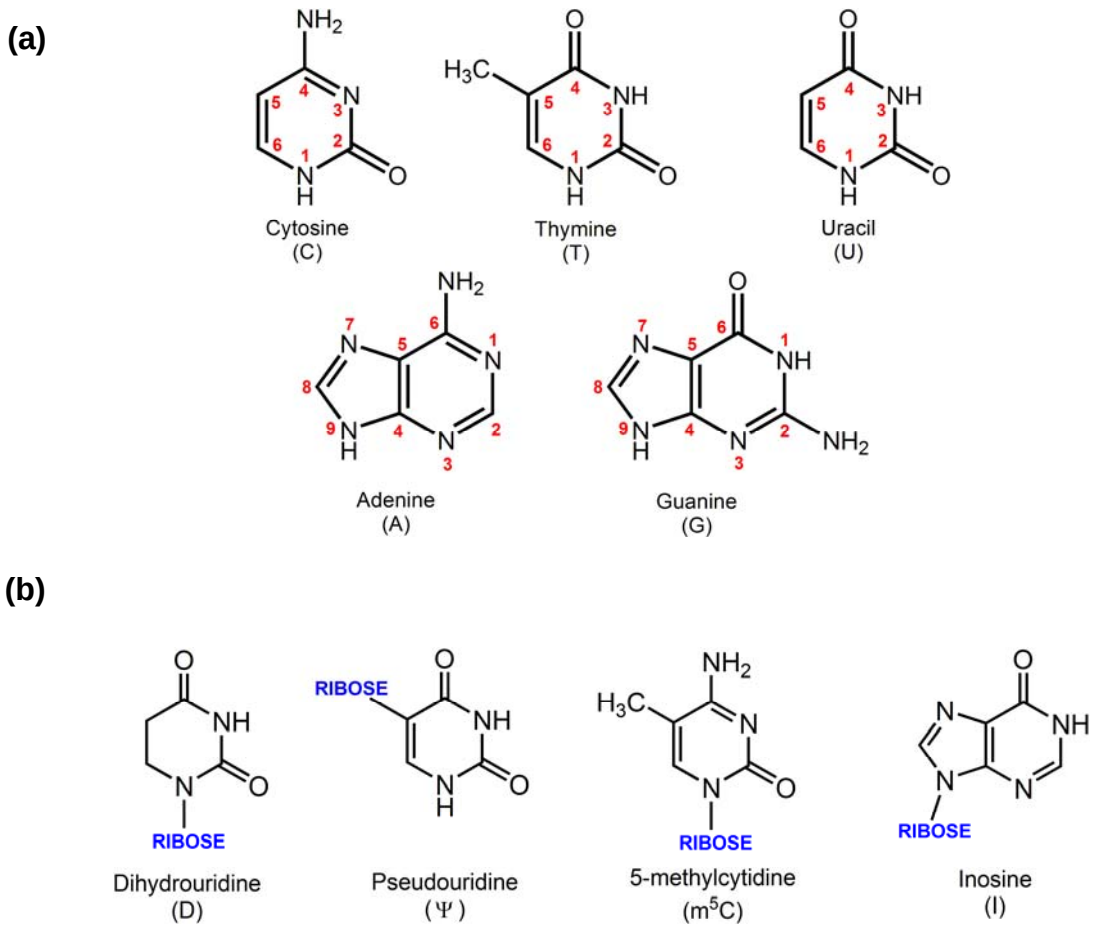


***Figure 1.2***
**The bases of DNA and RNA. (a)** The canonical bases of nucleic acids. Uracil occurs in RNA; it is replaced by thymine in DNA. **(b)** A few of the less common nucleosides, as found in RNA (particularly tRNA). Dihydrouridine is a saturated non-planar analogue of uridine. Pseudouridine differs from uridine only in the position in which the uracil base is bound to the ribose sugar. 5-Methylcytidine is one of several commonly-occurring methylated variants of standard nucleosides. Inosine is the precursor to adenosine.

Each base is attached to the sugar moiety via a glycosidic bond between the nitrogen at the 1- or 9-position of the base and the 1′-hydroxyl group of the sugar. Nucleosides are given names derived from their corresponding bases: adenine becomes adenosine, guanine becomes guanosine, cytosine become cytidine, thymine becomes thymidine, and uracil becomes uridine. DNA nucleosides are sometimes given the prefix “deoxy” to differentiate them from the RNA equivalents. Adjacent nucleosides in the polymeric chain are ligated together through a phosphodiester bond in which a phosphate group links the 5′ end of one sugar to the 3′ end of the next. The polymerisation of nucleotides in this manner gives rise to long, single-stranded polyanionic chains with a well-defined directionality (see Figure 1.3). This sequence of bases

essentially constitutes the primary structure of the nucleic acid; such sequences are traditionally described in the 5′ to 3′ direction.

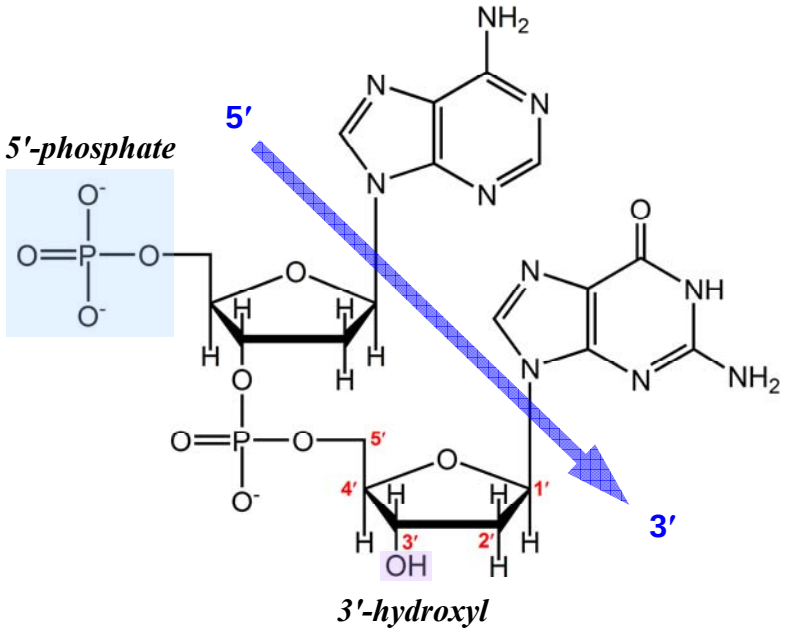


***Figure 1.3***
**The nucleotide chain.** A DNA dinucleotide illustrating the directionality inherent in polynucleotide chains. The hydroxyl and phosphate groups at the 3′ and 5′ ends of the chain, respectively, are indicated. Note the deoxyribose sugar of DNA; the equivalent RNA molecule would have an additional hydroxyl group at the 2′ position of the sugar.

Nucleic acids often adopt a double-stranded arrangement as their secondary structure – DNA is almost exclusively double-stranded in its native state and although the bulk of RNA is single-stranded, duplex regions do occur intermittently throughout the otherwise complex array of structures adopted by RNA. Such duplex arrangements arise when two polynucleotide chains (or two distally-separated regions of the same chain) coil around one another in an antiparallel manner. The resultant double-helical assembly secretes the largely hydrophobic bases away within the core of the duplex, while the hydrophilic polyanionic phosphate backbone remains exposed on the exterior of the molecule. The two strands are held together by hydrogen bonding between bases on opposite strands in a phenomenon known as base-pairing. While the free bases may potentially hydrogen-bond to each other in a multitude of different configurations, the conformational constraints imposed by the higher-order structure of the double-helix limits the range of possible interactions. The most common of the base-pairing schemes, Watson-Crick base pairing, is almost ubiquitous in canonical double-stranded DNA.

Watson-Crick base pairing {see Figure 1.4(a)} involves purine-pyrimidine (R•Y) pairs, specifically guanine bonding to cytosine and adenine bonding to thymine. G•C pairs form three hydrogen bonds whereas A•T pairs form only two, thus high G•C content in a given double-stranded polynucleotide makes for a stronger association between the two strands. A variety of other non-canonical base pairings have been found to regularly occur in non-duplex regions of nucleic acids and/or RNA; however in conventional duplex DNA they are considered mutations ("base mismatches") and typically corrected by genetic repair mechanisms. Several of the more common examples are illustrated in Figure 1.4(b). The overall stability of the double-helical arrangement is further stabilised by π-π interactions between the stacked hydrophobic aromatic rings of adjacent bases on the polynucleotide chains.[6]

While RNA is often rather vagrant (dependent upon its role), DNA is typically located within the nucleus of the cell where (in eukaryotes) it is "wrapped up" into higher-order structures. The double-stranded DNA molecule is wrapped up around assemblies of small proteins called histones to form a *nucleosome*. The nucleosomes string together and coil up into a 30 nm-thick fibre called a *solenoid*. In this condensed state the genetic material (the DNA-protein complex) is known as *chromatin*. Chromatin typically remains a disordered tangle of solenoid fibres until just prior to cell division. At this point, the chromatin further condenses around various scaffold proteins into the well-recognised four-armed structure known as a *chromosome*. Each chromosome is comprised of a single[†] DNA macromolecule (and the many genes contained therein) as well as the associated protein packaging. The human genome consists of 23 pairs of chromosomes, comprising of more than 20,000 genes over 3 billion bases.[7] By contrast, prokaryotic species generally possess a single, small circular chromosome, albeit largely free of introns. The complex packaging of eukaryotic DNA confers upon chromatin a potentially important role in the regulation of gene expression – efficient mechanisms are necessary to ensure the DNA is unpacked and made available when access is required. Indeed, epigenetics[8-10] – inheritance of genetic information not derived from the genomic DNA sequence – has been attributed to chromatin remodelling[11-14] (i.e. inherited histone modifications), as well as DNA methylation patterns[15, 16] and noncoding RNA.[17]

[†] More correctly, the classic four-armed chromosome structure is actually two copies (*chromatids*) of the same DNA molecule joined together at a region known as the *centromere*. Ideally, the two chromatids should be segregated to two different cells during cell division. Uneven segregation of chromosomes (*aneuploidy*) is usually highly detrimental, leading to disorders such as Down Syndrome as well as being associated with cancer.

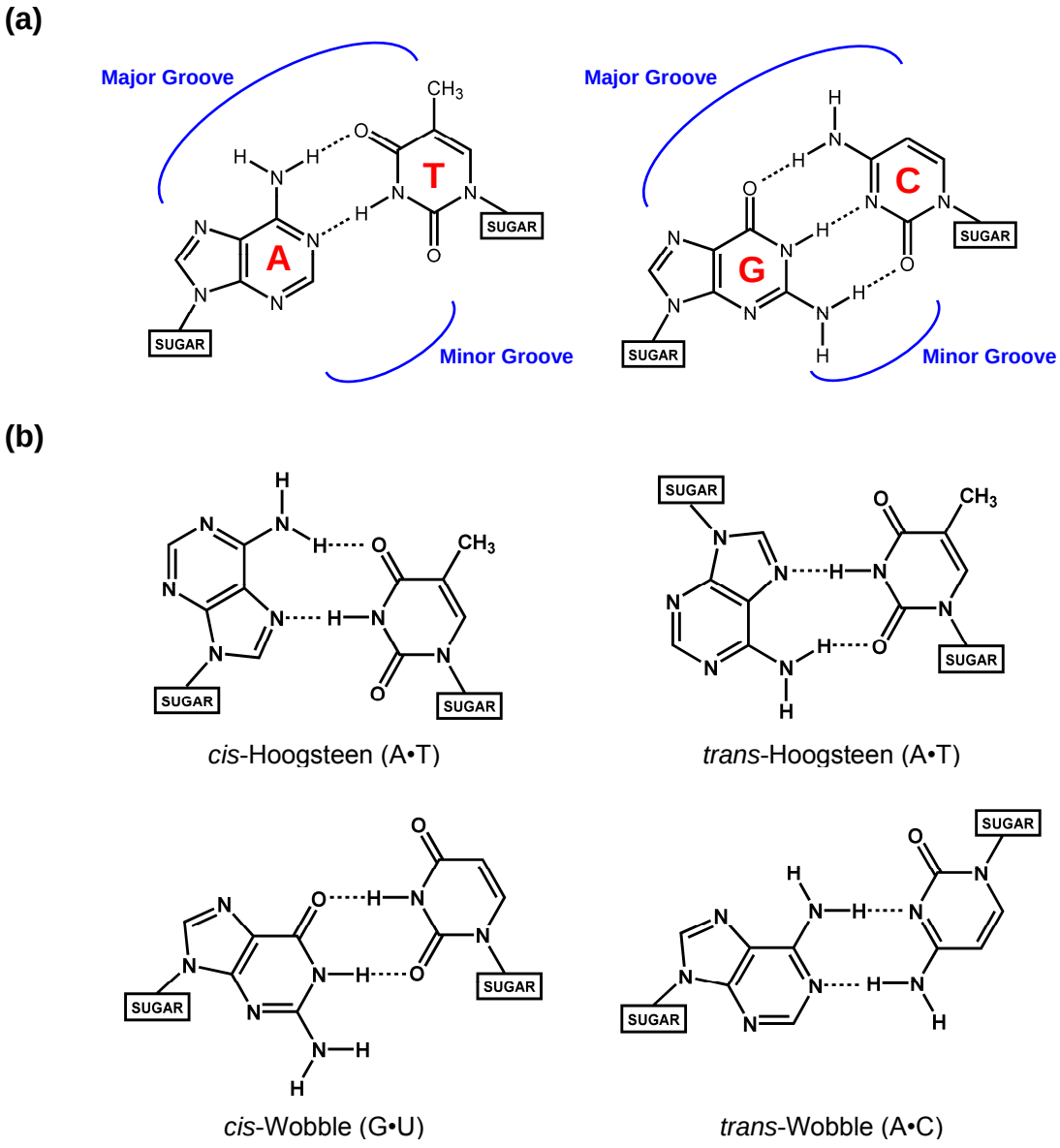


***Figure 1.4***
**Base-pairing. (a)** Watson-Crick base-pairing, the canonical hydrogen-bonding scheme of duplex DNA and RNA (uridine replacing thymidine in the latter case). **(b)** A small selection of non-canonical purine•pyrimidine base-pairs. The *cis*/*trans* nomenclature refers to the relative orientation of the glycosidic bonds of the two participating nucleosides. Standard Watson-Crick pairs, as pictured, assume the *cis* configuration, however *trans*-Watson-Crick pairs are also possible. Numerous purine•purine and pyrimidine•pyrimidine pairs, as well as base triples, are also feasible.[18]

## 1.2.3 Conformations

Duplex nucleic acids are highly polymorphic – they are able to adopt a variety of different conformations. This inherent flexibility derives from the many points of articulation found

within the nucleic acid structure.[19] Backbone torsion angles, sugar pucker geometry, and glycosidic bond rotations all work in concert to influence the ultimate conformation of a double-stranded nucleic acid. Furthermore, extensive nomenclature exists to describe the geometry and orientation of individual base-pairs (tip, inclination, opening, propeller, buckle, twist, roll, tilt, slide, shift and rise).[20, 21] Ultimately, these aspects are themselves influenced by environmental factors (hydration and ionic strength) and the primary structure (base sequence) of the polynucleotide.[22] Selected parameters of the three main DNA conformations (as depicted in Figure 1.5),[23] and the typical conformation of RNA are presented in Table 1.1.

***Table 1.1***
**Selected parameters of biologically-relevant nucleic acid conformations***

| Attribute | A-DNA | A-RNA | B-DNA | Z-DNA |
|---|---|---|---|---|
| **Helical Sense** | Right-Handed | Right-Handed | Right-Handed | Left-Handed |
| **Repeating Unit** | 1 bp | 1bp | 1bp | 2bp |
| **Residues Per Turn** | 11 | 11 | 10.5 | 11.6 |
| **Axial Rise Per Residue** | 2.55 Å | 2.8 Å | 3.4 Å | 3.7 Å |
| **Inclination of bp to Axis** | 22.6° | 15.5° | 2.8° | 0.1° |
| **Rotation Per Residue** | 32.7° | 32.7° | 36.0° | -60° (per 2 bp) |
| **Glycosyl Angle** | *anti* | *anti* | *anti* | C: *anti*<br>G: *syn* |
| **Sugar Pucker** | C3′ *endo* | C3′ *endo* | C2′ *endo* | C: C2′ *endo*<br>G: C3′ *endo* |

* Parameters adapted from Belmont *et al*.,[24] and Neidle.[19]

The conformational form of DNA most commonly encountered under physiological conditions (high hydration, low ionic strength) is known as B-DNA, first described in the seminal paper by Watson and Crick in 1953.[1] B-DNA is a right-handed helix with a diameter of approximately 20 Å, 10.5 base pairs per turn and a 3.4 Å step between base pairs that are nearly perpendicular to the helical axis. The separation of sugar-phosphate backbone chains due to base-pairing and stacking (as well as the mutual repulsion of phosphate groups) gives rise to a pair of grooves that run the length of the duplex and allow access to the bases therein {refer to Figure 1.4(a)}. Due to the non-symmetric nature of the Watson-Crick base pair – with the sugar

moieties all located on the same side of the helix – the two grooves are not equivalent.[†] In B-DNA there exists a wide *major groove* (11.6 Å wide) and a narrow *minor groove* (6.0 Å wide), with both grooves being of a similar depth. The groove dimensions of the three main DNA conformations are compared in Table 1.2. DNA-binding proteins typically associate via the major groove owing to its greater width (in B-DNA) and increased informational complexity (due to a more extensive array of potential hydrogen-bonding donors and acceptors). All four possible Watson-Crick base pairs (C•G, G•C, A•T and T•A) may be recognised via the major groove, whereas only two can be distinguished from the minor groove {C•G (≡ G•C) and A•T (≡ T•A)}.[25]

In environments of relatively low hydration (or a high concentration of cations) DNA assumes an A-form that is a wider, more compact structure (11 bp per helical turn) in which the bases are displaced off-centre resulting in an essentially hollow core.[26] The major groove of A-DNA is very deep, but restrictively narrow; conversely, the minor groove is wide and shallow. A definitive *in vivo* role of A-DNA has yet to be established, however a number of DNA-binding proteins are known to induce a B → A-DNA conformational change.[27-29] In one example, a group of proteins known as small acid-soluble proteins (SASPs) infer UV resistance upon *Bacillus subtilis* spores by binding to their DNA and causing a conformational change to the A-form which has a greater inherent UV resistance than does B-DNA.[30] Moreover, the DNA of dormant *B. subtilis* spores is believed to be permanently in the A-DNA conformation.[31] It has also been proposed that the adoption of an A-type conformation can increase the fidelity of replication due to the decreased structural variation in A-DNA compared to B-DNA.[32, 33] Duplex RNA and DNA-RNA hybrids commonly adopt an A-type conformation:[34, 35] the 2′-hydroxyl group of ribose forces the RNA sugar into a C3′ *endo* configuration {see Figure 1.6(a)}, which subsequently induces an A-type conformation in the double-helix.

[†] Grooves are typically measured as follows: groove width is defined as the perpendicular distance between phosphate groups on opposite strands, subtracting the 5.8 Å van der Waals diameter of a phosphate group; groove depth involves differences in cylindrical polar radii between phosphorous and N2 guanine (minor groove) or N6 adenine (major groove) atoms.

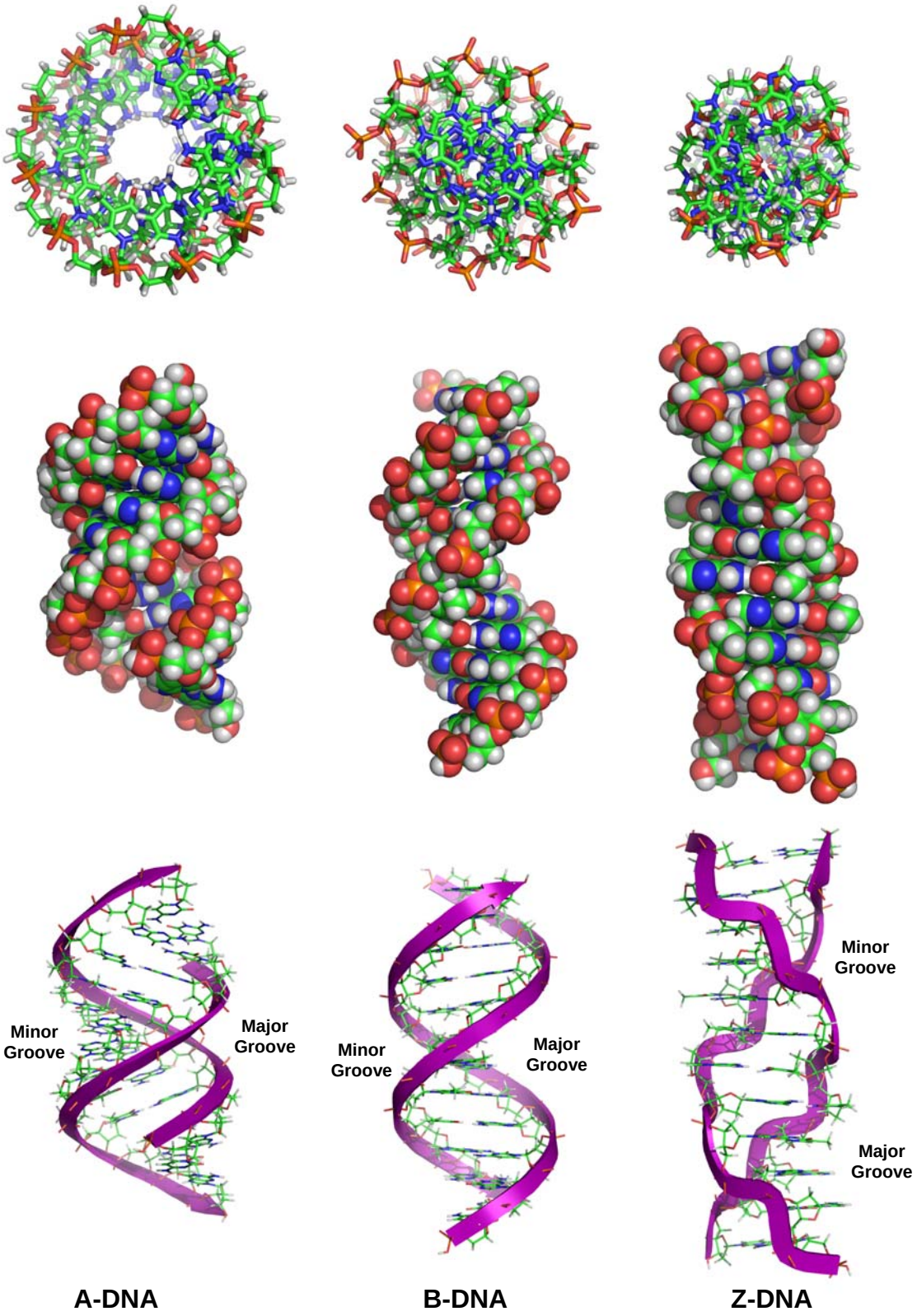


***Figure 1.5***
**The three major conformations of DNA.** Down-axis, space-filling, and backbone ribbon representations of dodecamers in the A-, B- and Z-DNA conformations. Models rendered with PyMOL.[36]

***Table 1.2***
**Groove dimensions (Å) of the three main DNA conformations***

| Conformation | Major Groove | | Minor Groove | |
|---|---|---|---|---|
| | Width | Depth | Width | Depth |
| A | 2.2 | 13.0 | 11.1 | 2.6 |
| B | 11.6 | 8.5 | 6.0 | 8.2 |
| Z | 8.8 | 3.7 | 2.0 | 13.8 |

* Information adapted from Neidle.[19]

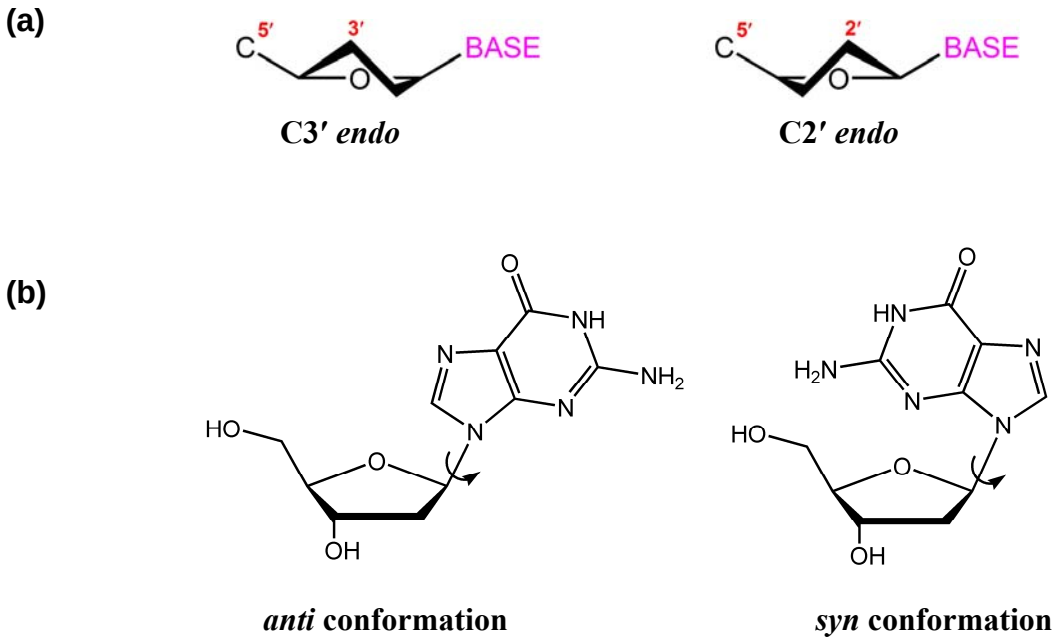


***Figure 1.6***
**Nucleoside conformations. (a)** The C3′ *endo* and C2′ *endo* pucker conformations of a furanose sugar ring. **(b)** The *anti* and *syn* orientations of a guanosine nucleoside.

A third, somewhat more drastic variation from the canonical DNA conformation is that of Z-DNA, which is a *left-handed* double helix.[37] Z-DNA, named for its zig-zagging backbone, occurs in solutions of high ionic strength (2.5 M NaCl or greater).[38] $d(GC)_n$ sequences are particularly susceptible, with runs of $d(m^5CG)_n$ – a common occurrence in eukaryotic DNA – able to assume the Z-form under salt concentrations more amenable to physiological conditions.[39, 40] Z-DNA is not a simple mirror image of B-DNA; in order to maintain Watson-Crick pairing the B → Z transition requires that bases be inverted.[41] Cytosine nucleosides invert entirely, therefore maintaining the *anti* glycosidic bond conformation of B-DNA; however, with guanosine only the base itself is rotated, forcing the nucleoside into the unusual *syn*

conformation {see Figure 1.6(b)}. The result is a zig-zagging helix with a two-base pair (bp) repeating unit. Z-DNA is elongated and thin relative to B-DNA; it has a flattened (wide and relatively shallow) major groove and a deep and narrow minor groove. The B → Z-DNA junction, a crystal structure of which was recently obtained by Ha *et al*.,[42] nicely illustrates the dichotomy between the two conformations (see Figure 1.7). Instances of Z-RNA have also been observed,[43-46] and like Z-DNA the left-handed configuration requires high ionic strengths or base/backbone modification. It is noteworthy that the 2′-hydroxyl groups of guanosine residues are located on the helical surface in Z-RNA, exposing them as potential protein binding or recognition sites. While anti-Z-RNA antibodies have been isolated,[43] very little is known about any *in vivo* role of Z-RNA which has received negligible attention since its discovery over 15 years ago.

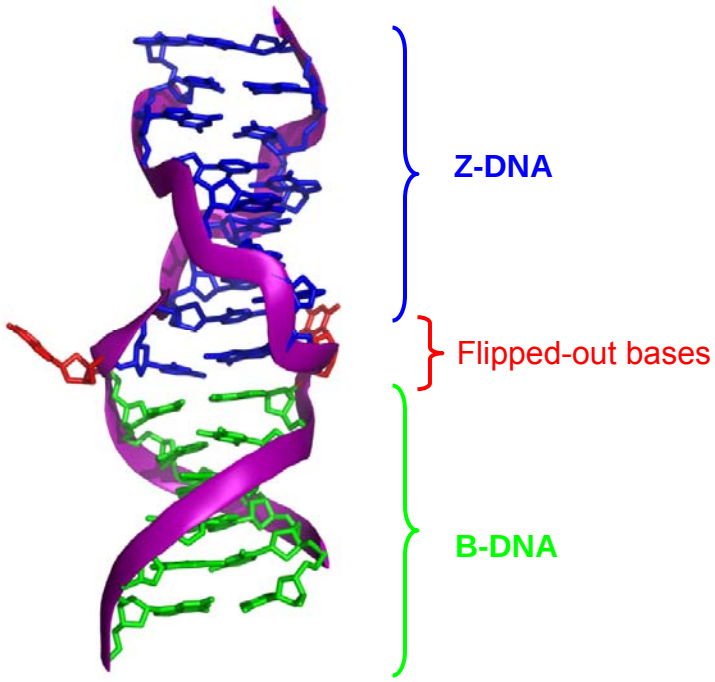


***Figure 1.7***
**The B-DNA/Z-DNA junction.** This render of PDB crystal structure **2acj** [42] illustrates how bases are flipped during a B → Z-DNA conversion. The two bases at the interface of the two conformations are made extrahelical in order to accommodate the drastic change in helical sense.

While Z-DNA has been conclusively demonstrated to occur *in vivo*[47-49] its specific function is still the matter of much speculation.[50-52] A biological role for the conformation was first hinted at by immunological studies that found Z-DNA to be highly antigenic; for example, Z-DNA specific antibodies are prolific in human autoimmune diseases such as systemic lupus

erythematosus.[53] Indeed, numerous Z-DNA-binding proteins have been characterised.[54-56] Z-DNA in known to be stabilised under negative torsional strain. The winding and unwinding of double-helical DNA executed by some enzymes can result in supercoiling of the DNA, subsequently imposing a strained topology. Unwinding of supercoiled B-DNA stabilises stretches of Z-DNA, however the significance of this observation has yet to be conclusively established. Most evidence into the biological function of Z-DNA points to a role in transcription. Anti-Z-DNA antibodies have been shown to accumulate in regions of transcriptional activity,[57] with a high degree of correlation between Z-DNA-favourable sequences and transcription start sites.[58] An RNA polymerase complex induces negative torsional strain in the DNA trailing the complex as it carries out transcription.[59] It has been proposed that this negatively-supercoiled DNA subsequently stabilises the formation of Z-DNA in a favourable sequence at or near the transcription start site. The Z-DNA, unable to be wrapped up into nucleosomes,[60] ensures the transcription site remains open, accumulating transcription factors and facilitating transcription of the appropriate gene.[52, 61]

While the A-, B- and Z-forms are perhaps the most biologically-relevant nucleic acid conformations, they are certainly not the only double-stranded configurations that have been observed. A large portion of the alphabet has been used up in the naming of various interesting nucleic acid polymorphs. However, most of these other conformations are sub-varieties of the three main polymorphs detailed above or, alternatively, remain nothing more than test tube curiosities (at least for now).

## 1.2.4 Non-Duplex Structures

### *1.2.4.1 Bulges*

Amongst the most rudimentary of deviations from the canonical duplex of nucleic acids are the stretches of unpaired nucleotides referred to as *bulges*. These features arise when one strand of the hydrogen-bonded duplex possesses one or more nucleotides which have no counterpart on the opposing strand {see Figure 1.8(a) for a schematic representation}. Bulges, typically less stable than the analogous sequence composed of standard Watson-Crick base pairs,[62] can vary in size from a single unpaired nucleotide up to a run of several residues that are capable of forming a flexible loop-like extrusion from the double helix.

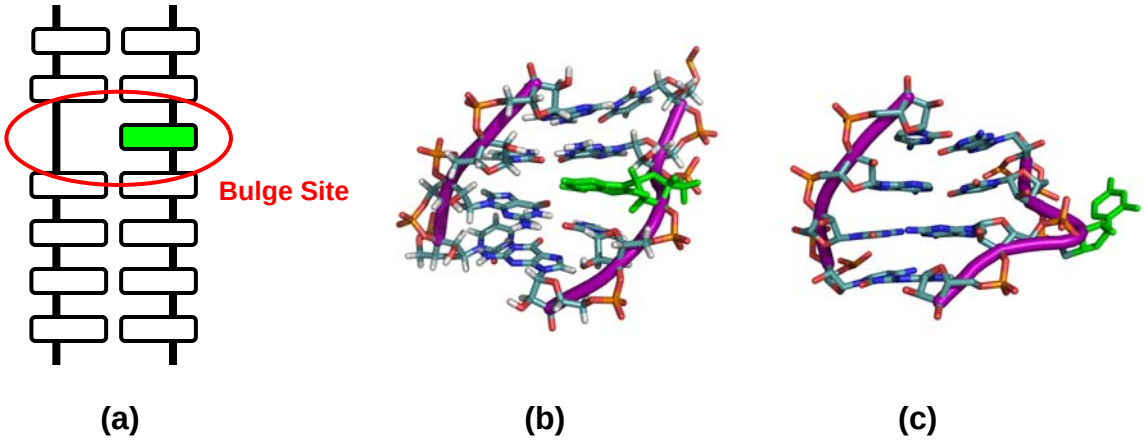


***Figure 1.8***
**Bulges.** Three representations of a single base bulge site with the unpaired base coloured green. **(a)** Schematic of a single base bulge. **(b)** Render of PDB NMR structure **1rht**,[63] a bacterial coat protein RNA binding site, featuring an *intrahelical* unpaired adenine. **(c)** Render of PDB crystal structure **1dqh**,[64] a section of 5S rRNA, featuring an *extrahelical* unpaired cytosine.

Unconstrained by the standard hydrogen-bonding schemes of base-pairing, bulged nucleotides possess considerable conformational freedom, yet generally they will assume either an intrahelical ("stacked-in") or an extrahelical ("looped-out") arrangement {see Figures 1.8(b) and 1.8(c), respectively}. Stacking arrangements secrete the hydrophobic surfaces of the unpaired bases away within the double helix of a nucleic acid, thus minimising their exposure to the polar solvent. As might be expected, solution (NMR) structures of nucleic acids with bulge sites typically adopt such a stacked arrangement.[63, 65, 66] Conversely, crystal structures of bulge sequences often advocate a looped-out arrangement with the unpaired base projecting out of the helix, most likely due to stabilising intermolecular interactions between bulged nucleotides and/or other regions of the nucleic acid in the crystal packing.[67, 68] While the looping-out of unpaired bases results in relatively little distortion of a typical double-helical conformation, the incorporation of bulged bases between the π-stacked base pairs of the duplex can induce kinking in the nucleic acid, the extent of which is dependent upon the identity of the bulged bases and the size of the bulge.[69-74] In some instances, a bulged nucleotide has been found to fold back onto adjacent hydrophobic surfaces of the double-helix, forming a "pocket-like" structure.[75] Ultimately, the stability of any given bulge structure is governed by multiple factors including the identity of the bulged base and those bases flanking it,[62, 65, 76]

intramolecular contacts between bulges and/or other regions of the nucleic acid,[77, 78] and interactions with cationic metal ions.[79-82]

Biological occurrences of bulges are found in both DNA and RNA, but characterisation and understanding of such structures are much more extensive in the latter. Bulges in RNA tend to be of particular and well-defined architectural and functional significance, whereas in DNA they tend to be more transient in nature and are typically associated with mutagenic events. The disadvantageous formation of DNA bulges can give rise to frameshift mutations in which one or more nucleotides are inserted into or deleted from a DNA strand. Since gene expression is based on nucleotide triplets (codons) encoding for a specific amino acid, additions or subtractions from the base sequence leads to an alteration of the reading frame.[83-85] Because every codon following the mutation site is changed as a consequence of the mutation, the translation product of the gene will be significantly different from that of the original unmutated gene. The extent of alteration to the resultant protein is dependent upon the proximity of the mutation site to the end of the gene. While frameshift mutations can be beneficial to an organism – conferring resistance to HIV,[86] for instance – the protein is often incomplete and/or non-functional as the stop codon cannot be read (or a premature stop codon could arise due to the frameshift); accordingly, such mutations are often implicated in a variety of common diseases, including hypercholesterolemia[87] and cancer.[88, 89] Indeed, the tumour suppressor protein p53 is known to have a high affinity for bulges,[90] as does the MutS DNA mismatch repair protein.[91]

The initial formation of bulges is attributed to events such as replication errors, the recombination of imperfectly homologous sequences, or the repair of carcinogen- or radiation-induced DNA damage. The most accepted mechanism by which bulges lead to frameshift mutations was proposed by Streisinger *et al*.[92] It involves the slippage of one DNA strand relative to the other during replication (most commonly encountered in regions of repeated base sequences). This slippage results in one or more unpaired bases which, upon subsequent replication, invoke either an addition or deletion to the DNA sequence depending on which strand contained the bulge. Larger slippages (and the resultant metastable bulge loops) have been implicated in the expansion of trinucleotide repeat regions of the genome and the associated diseases.[93, 94] However, the structure usually associated with such an event is the hairpin loop, and in this context the topic is covered in more depth in a later Section.

While DNA bulges are most often considered an unwanted aberration of the duplex DNA structure, there is some evidence of their involvement in some regulatory processes by serving as recognition points for DNA-binding proteins. For instance, the High Mobility Group (HMG) DNA-binding domains, found in a number of chromosome architectural proteins, have been found to preferentially bind B-DNA distortions such as bulges.[95, 96] These proteins play a role in bending DNA into the appropriate topology for transcriptional events, a process that may potentially be facilitated by the increased flexibility (and preliminary kinking) afforded by bulge sites.[97] Specificity for DNA kinks is not unusual – the catabolite activator protein (CAP) of *Escherichia coli* is known to exhibit selectivity for a T•A base pair, not through direct contact but rather via selectivity for the kink induced by the increased flexibility of a T•A/G•C step.[98, 99] It is therefore quite conceivable that the transient occurrence of unpaired nucleotides in DNA may serve as another source of such flexibility and subsequent protein-binding specificity.

In contrast to DNA, bulges are ubiquitous in RNA secondary structures as potential protein recognition sites.[100, 101] Unpaired nucleotides may fulfil this role by either acting as direct contact points with RNA-binding proteins, or in an indirect manner by facilitating distortion of the RNA backbone. As the standard A-form of duplex RNA possesses a deep but narrow major groove, the information contained therein is largely unavailable to RNA-binding proteins.[102] Thus, distortions to the RNA backbone induced by bulge sites may potentially widen the information-rich major groove, allowing direct read-out of base sequence by a protein. Generally speaking, RNA-binding proteins have a tendency to target imperfections in the double helix,[103] whereas in DNA the major groove is readily accessible and DNA-binding proteins are often *sequence* (primary structure)-specific.

Perhaps the best-characterised of all the biologically-relevant RNA bulges is that belonging to the *trans*-activation response (TAR) element of human immunodeficiency virus-1 (HIV-1) mRNAs. The TAR element is a 59-nucleotide stretch of RNA in a stem-loop structure near the 5′ end of HIV-1 transcripts.[104-107] TAR serves as the binding site of the Tat protein, with the TAR-Tat complex greatly enhancing viral transcription.[108-110] Tat specifically targets the site of a three-base bulge (either UCU or UUU) on the stem of the TAR element, most likely due to the increased flexibility and more open major groove in this region.[74, 102, 107, 111-116] Indeed, the TAR structure is believed to undergo a significant conformational change upon the binding of Tat as the intrahelical bulge bases are extruded, resulting in straightening of the RNA.[117, 118]

The TAR-Tat interaction is mediated by a short region of basic amino acids on the protein, with a single arginine residue making the only sequence-specific contact with select phosphates near the bulge site (specifically, those between G21-A22 and A22-U23).[105, 115] Thus, while the widened major groove facilitates initial binding of the protein to the RNA, the affinity and selectivity of the binding are provided by folding of the TAR around the basic Tat domain and indirect readout of base sequence via the phosphate backbone.[111, 119, 120] Numerous studies of TAR derivatives and mutants featuring systematic changes to the TAR sequence have demonstrated that the three-base bulge is necessary for optimal function of the TAR-Tat complex.[104, 113, 121, 122] The first of the unpaired nucleotides in the three-base bulge, U23, is essential for the association of the Tat protein – possibly due to the formation of a TAR-stabilising, major groove-widening base triple with one of the two base pairs immediately above the bulge site (which are also essential to Tat binding).[105, 123, 124] The other two bases of the three-base bulge are thought to serve as a spacer.[106, 107] While the general stem-loop structure of the HIV-1 TAR element – including several important base pairs – is necessary for the full transcriptional activity, it is the three nucleotide bulge that serves as the heart of the TAR-Tat complex.[125, 126] The TAR element of HIV-2, the less virulent species of HIV, is identical to that of HIV-1 TAR except for the deletion of the unpaired nucleotide (U or C) at position 24 of the RNA, resulting in a two-base bulge that is also essential for the binding of Tat.[124, 127] The structures of HIV-1 and HIV-2 TAR RNA are illustrated in Figure 1.9.

Like many RNA bulges, the three unpaired nucleotides are believed to be stabilised by the binding of metal cations.[82] Backbone distortions induced by bulges have a tendency to force negatively-charged phosphate groups together; cation binding to such sites serves to alleviate some of that negative charge density, thereby stabilising bulge loops and kinks. The crystal structure of free HIV-1 TAR RNA shows the three-base bulge to be stabilised by $Ca^{2+}$ ions.[80] Cate *et al*. make the analogy that while proteins tend to fold around a hydrophobic core, RNA folds around a *metal* core.[128]

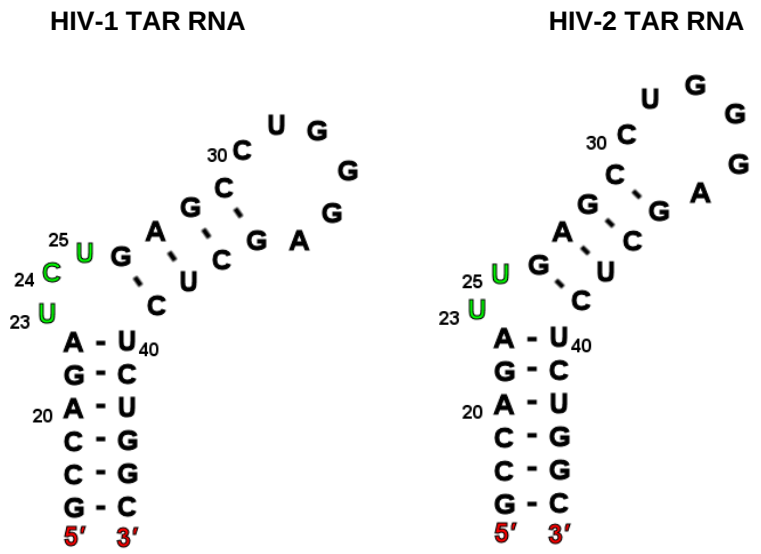


***Figure 1.9***
**TAR RNA.** The sequences of the Tat binding sites of HIV-1 and HIV-2 TAR RNAs illustrating the stem-loop/bulge secondary structures of each. HIV-2 TAR RNA is identical to that of HIV-1 with the exception of the deletion of a single nucleotide (at position 24) within the bulge site (depicted in green). Note the bulge-induced kinking of each structure.

While the TAR bulge has received the most attention, it is certainly not the only documented RNA bulge of biological significance. A number of bacteriophage coat proteins, such as those that bind the replicase genes of R17 and MS2, have been found to target hairpin loop structures featuring a single bulge in the stem.[129-132] A general model of these RNA structures is depicted in Figure 1.10, showing the essential features needed for coat protein binding. While there is some leniency in the identity of the bulged nucleotide – it need only be a pyrimidine – the bulge itself plays an essential role in the regulation of the viral replicase. In the free RNAs the unpaired nucleotides are believed to stack within the helix[63] (thus influencing helical structure and facilitating protein binding), whereas the protein-bound bulge of MS2 is found to loop out of the helix and bind in a hydrophobic pocket on the surface of the coat protein.[132]

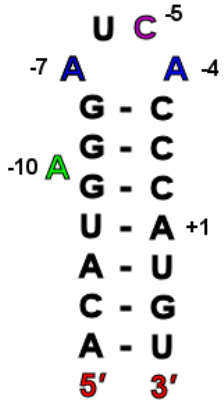


***Figure 1.10***
**Conservation of a bulge at a bacteriophage coat protein binding site.** The general sequence of the stem-loop/bulge R17/MS2 bacteriophage coat protein binding site. Bases are numbered relative to the AUG start codon of the replicase gene at position +1. The exact identity of the loop adenines (positions -4 and -7, in blue) must be retained for coat protein binding, whereas the bases at positions -5 (purple) and -10 (green; the bulge site) must be a pyrimidine and a purine, respectively, to ensure tight binding.

Bulges are also a common feature of ribosomal RNA. The ribosomal protein L18 binds specifically to a region of *E. coli* 5S rRNA that possesses an adenine bulge. Interestingly, the bulged nucleotide of 5S rRNA appears to be conserved through evolution, with the identity of the nucleotide varying between major phylogenetic divisions (A for aerobic bacteria, dinoflagellates and yeast; C for animals; U for plants, cyanobacteria, halophilic bacteria and anaerobic bacteria – see Table 1.3 for examples).[133]

Similarly, a two-base bulge has been demonstrated to mediate the interaction between the L5 ribosomal protein and the appropriate region of *Xenopus* 5S rRNA.[134] On the other hand, deletion studies with *Xenopus laevis* (the African clawed frog) have shown that bulges are *not* necessary to the binding of transcription factor IIIA to an alternate section of 5S rRNA.[135] The binding of the L11 ribosomal protein to 23S rRNA is believed to be facilitated by the tertiary structure of the RNA, which itself is stabilised by long range interactions between bulge sites. These interactions include a *trans*-Hoogsteen base pair between two bulged nucleotides (A•U) and a long-range stacking interaction between two extruded, unpaired adenines (a “high-five” motif).[78, 136] The sequence and tertiary structure of the L11 binding site are depicted in Figure 1.11.

***Table 1.3***
**Evolutionary conservation of a 5S rRNA bulge site**[*]

| Central Helix Base Sequence[†] | Organism |
|---|---|
| GC GUUAUG<br>CGAUAAUGC | *Phosphobacterium phosphoreum* |
| GC GCGGUG<br>CGAUGCCGC | *Yersinia pestis, Serratia marcescens, Erwinia aeriodae, Proteus mirabilis, Aerobacter aerogenes, Salmonella typhimurium, Escherichia coli* |
| GC GGCGUG<br>CGACCGCGC | *Thermus aquaticus* |
| GC GAAGAG<br>CGAUUUCUC | *Bacillus megaterium, Bacillus pasteurii, Bacillus licheniformis, Bacillus subtilus* |
| GC GGAGRG<br>CGACCUCYC | *Bacillus stearothermophilus, Bacillus brevis* |
| GC GARRAG<br>CGACUYYUC | *Bacillus Q, Bacillus firmus* |
| GC AUUGAG<br>CGAUAACUC | *Lactobacillus viridescens* |
| GC GUGRGG<br>CGAYAYYCC | *Streptomyces griseus, Micrococcus lysodeikticus* |
| GC GAGAAG<br>CGAUUCUUC | *Streptococcus faecalis* |
| CC GUGUCG<br>GGACACGGC | *Crypthecodinium cohnii* |
| GC GGUAUG<br>CGUCCAUAC | *Anacystis nidulans* |
| GC GGUGGG<br>CGUCCGCCC | *Halobacterium cutirubrum* |
| AC UUAGAG<br>UGUAAUCUC | *Clostridium pasteurianum* |
| CC ACCACG<br>GGUUGGUGC | *Chlorella pyrenoidosa* |
| YC AGCAC<br>GGUUCGUG | Rye, tomato, sunflower, dwarf bean, broad bean, wheat embryo |
| UC UACCAG<br>AGAAUGGUC | *Saccharomyces cerevisiae, Saccharomyces carlsbergensis, Kluyvermeyces lactis* |
| UC UAGCAG<br>AGAAUCGUC | *Torulopsis utilis, Pichia membranafaciens* |
| CU AGGUUG<br>GACUCCAGC | *Dictyostelium discoideum* |
| CC ACCCUG<br>GGCUGGUAC | Human KB and HeLa cells, *Iguana iguana*, turtle, chicken, mouse, kangaroo rat, *Xenopus laevis*, *Xenopus mulleri* |

[*] Adapted from Peattie *et al.*[133]
[†] Unpaired base in red; R = purine, Y = pyrimidine.

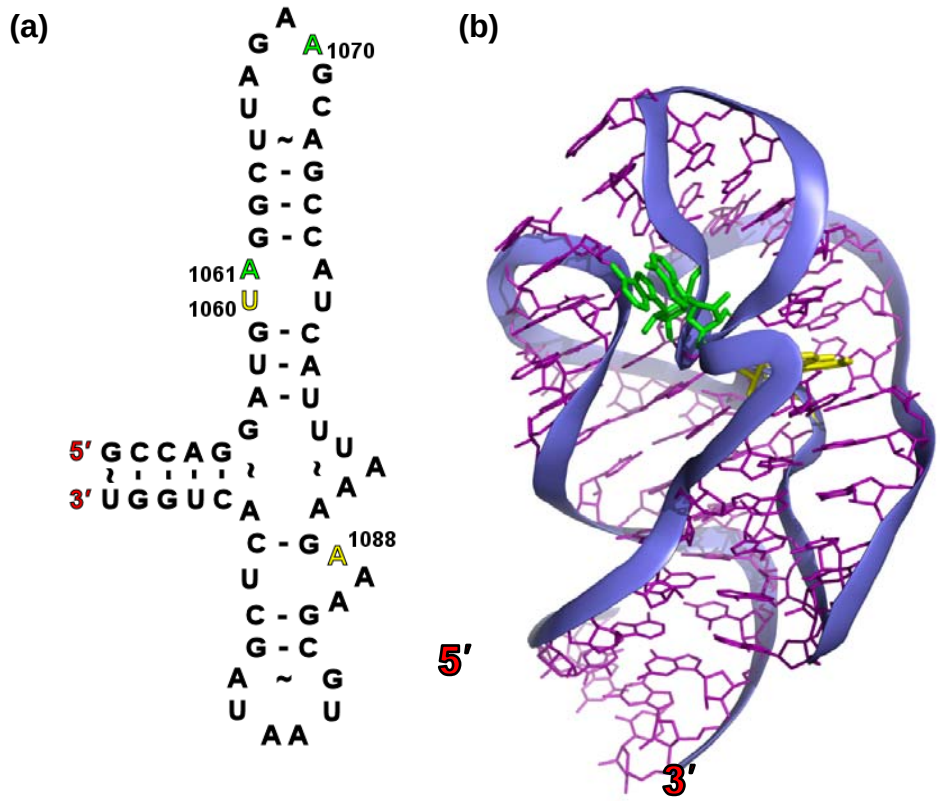


***Figure 1.11***
**The bulge-stabilised structure of 23S rRNA. (a)** Schematic representation of the nucleotide sequence of interest (Watson-Crick base pairs indicated by a '—', non-Watson-Crick base pairs indicated by a '~'), and **(b)** the three-dimensional crystal structure of L11-bound 23S rRNA (PDB structure **1qa6**).[136] The unpaired nucleotides A1061 and A1070 (green) participate in a long-range stacking interaction; U1060 and A1088 (yellow), also unpaired, form a long-range *trans*-Hoogsteen A•U base pair. Solvent molecules, counterions, and the L11 protein itself have been removed from the crystal structure for clarity.

Tertiary stabilisation of RNA structures is another important role of bulged bases as the function of several classes of RNA are very much dependent on their three-dimensional topology. One good example of this is the structure of the splice site of archaeal pre-tRNA endonuclease: a bulge-helix-bulge configuration with the pre-tRNA being cleaved at two 3-nucleotide bulges. These bulges induce abrupt conformational changes to the RNA backbone either side of the central helix, resulting in a Z-like shape with approximately two-fold symmetry.[77] This stretch of pre-tRNA is therefore the ideal shape for attack from symmetrical dimers like the archaeal spicing endonucleases. Substantial conservation of this motif has been observed amongst the archaea.[137]

### *1.2.4.2 Internal Loops*

Internal loops differ from bulges in that the Watson-Crick base-pairing of a duplex polynucleotide is interrupted on *both* strands (see Figure 1.12).[100, 138] Such loops can be described as being symmetric (in which the same number of non-complementary bases occur on each strand), or asymmetric (differing numbers of non-complementary bases on each strand).[†] Although uncommon in DNA, RNA internal loops are stabilised by a myriad of different non-canonical base pairings between the two strands[139] and, as with bulges, they introduce a site of local flexibility.[140]

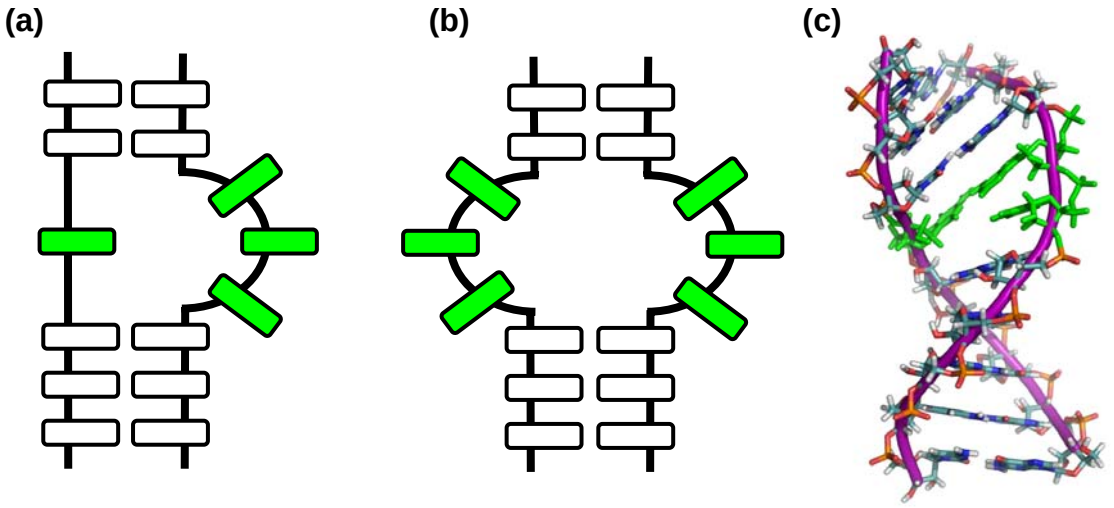


***Figure 1.12***
**Internal Loops.** Three representations of an internal loop single with unpaired bases coloured green. **(a)** Schematic of an asymmetric loop. **(b)** Schematic of a symmetric loop. **(c)** NMR structure (PDB identifier **1lc6**,[64] of an internal loop in U6 RNA.[141] Note the kink induced in the duplex structure by the unpaired loop bases (in green).

There are numerous cases of internal loops serving as recognition sites for RNA-binding proteins, the best example of which is perhaps HIV Rev-responsive element (RRE) RNA. The HIV-regulatory protein Rev binds with high affinity to the RRE viral transcript, with specific recognition of an internal loop.[142, 143] This asymmetric internal loop contains a purine•purine base pair which has been found to be essential to protein binding.[144-146] While the Rev protein selectively targets the unusual conformation of the phosphate backbone rather than the bases themselves, the non-canonical base pair is thought to widen the major groove of the RNA,

[†] The "symmetric"/"asymmetric" nomenclature used here is the biochemical parlance rather than the strictest mathematical sense of the words.

turning the internal loop into a relatively deep binding pocket.[115, 147, 148] Another well-characterised internal loop system occurs in the pre-mRNA of U1A, one of the constituent proteins of the U1 small nuclear ribonucleoprotein (snRNP) complex that is involved in mRNA splicing. The 3′-untranslated region (UTR) of U1A pre-mRNA features a pair of asymmetric internal loops within close proximity to one another. Each loop is comprised of a 7-nucleotide bulge on one strand opposite a single-nucleotide bulge on the other, with the respective strands reversed between loops. This pair of loops actually serves as a binding site for the U1A protein itself in an autoregulatory process controlling polyadenylation (an important step along the road to developing mature mRNA fit for translation).[149-151] The flexibility of the loops, their close proximity, and findings that two U1A proteins bind the U1A pre-mRNA in a cooperative fashion, have led some to speculate that the RNA may bend in such a matter as to allow direct protein-protein interactions at adjacent binding sites.[152, 153]

#### *1.2.4.3 Hairpin Loops*

Hairpin loops are deviations from the canonical duplex DNA or RNA structure that arise when a polynucleotide chain possessing self-complementarity loops back on itself to form a duplex stem terminating in a loop of unpaired bases (see Figure 1.13). This "stem-loop" structure, as it is often called, is stabilised by base pairing (both canonical and non-canonical) within the stem. In DNA the stem typically assumes a B-type conformation, whereas in RNA it is typically of the A-form.

The stability of hairpin structures is governed primarily by the length and sequence of the loop rather than the sequence of the stem.[154, 155] While *in vivo* hairpin loops are usually closed by a G•C base pair (offering a greater stability than an A•T base pair), it is base interactions (both stacking and hydrogen-bonding) within the loop that account for the stability of a given hairpin loop.[156-158] In fact, loop length has been attributed a greater significance than loop sequence, with *in vitro* experiments suggesting an optimal loop length of 4-5 nucleotides in DNA and 6-7 nucleotides in RNA.[154, 155, 159, 160] In reality, tetraloops appear to be the most common, particularly in (ribosomal) RNA.[161] The sequences UNCG, GNRA and CUUG (where N is any nucleotide and R is a purine) have been found to occur quite frequently in RNA (especially rRNA), owing to their exceptional stability.[162-165] For example, the r[C(UUCG)G] loop present throughout 16S rRNA has been found to adopt a compact and

stable structure,[166, 167] whereas the DNA equivalent d[C(TTCG)G] is relatively flexible and lacks well-defined base interactions in the loop, resulting in a structure of ordinary stability.[168] The difference in stability between the two has been credited to a greater network of interactions in the RNA as mediated by the 2′-OH groups, which are absent from DNA.[163, 169] Additional hydrogen bonding afforded by the 2′-OH groups of RNA is believed to contribute to the differences in cooperativity between RNA and DNA loops: DNA loops have been found to fold in a concerted manner whereas RNA loops are less cooperative and fold in a stepwise, modular fashion.[169] The lesser cooperativity of RNA loops may potentially enhance their robustness, allowing them to better withstand mutations without loss of stability, and hence enhance the evolutionary ability of RNA. On the other hand, GNRA-type loops are very stable in both RNA and DNA.[154] Unusually stable DNA loops have been found to include the sequences GNA, GNNA and GNAB (where B = C, G or T), each of which have been associated with regions possessing some regulatory role in biological systems.[170-173]

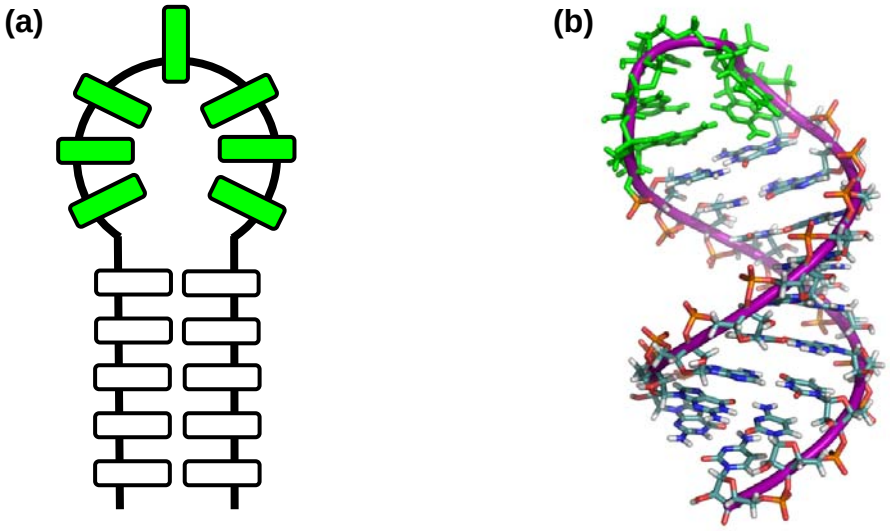


***Figure 1.13***
**Hairpin Loop. (a)** Schematic of a hairpin loop, with the unpaired bases of the loop depicted in green. **(b)** NMR structure (PDB identifier **15ki**) of a conserved ribosomal RNA 5-base loop (CUCAA), loop bases rendered in green.[174]

As with bulges, loops are most often considered “imperfections” to duplex DNA but are essential to the higher structure and functionality of RNA. In DNA they are commonly associated with the biophysical mechanism believed to be causative in a number of neurodegenerative diseases. Disorders such as Huntington disease,[175, 176] myotonic

dystrophy,[177, 178] and fragile X syndrome[179, 180] are all attributed to instabilities in trinucleotide repeat regions of particular genes.[181, 182] Repetitive DNA sequences such as these are both abundant in the genome and highly polymorphic – expansions of such regions via many-fold duplication of the trinucleotide repeat are common during replication, repair and recombination events.[183-185] The instability of such repeat sequences is dependent upon both their composition and their length, with particular triplets having a threshold repeat length at which the associated disease will emerge in the form of abnormal transcription products. Huntington Disease, for example, involves an expansion of the CAG triplet repeat in the *IT15* gene[186] from a normal length of approximately 5-30 CAG triplets to a mutant with a repeat length of 40-100 triplets.[94, 187] Because the CAG codon encodes for glutamine, the result of this expansion is a transcription product (the huntingtin protein) with a polyglutamine mutation that forms harmful aggregates.[188, 189] Expansions are a dynamic mutation: as the length of a repeat grows, so does the size and likelihood of any successive expansion events. Consequently, subsequent generations inheriting a pathogenic allele face a decrease in the age of onset and an increase in the severity of the disorder.[190] Several expansion-related diseases and their associated trinucleotide repeats are listed in Table 1.4.

***Table 1.4***
**Several trinucleotide repeat expansion-related disorders**

| Disorder | Locus | Repeat Allele | |
|---|---|---|---|
| | | ***Normal*** | ***Pathogenic*** |
| Fragile X syndrome | *FMR1* | $(CGG)_{6-52}$ | $(CGG)_{60-200}$ {premutation}<br>$(CGG)_{230-1000}$ [191] |
| Fragile XE mental retardation | *FMR2* (*AFF2*) | $(GCC)_{7-35}$ | $(CGG)_{130-150}$ {premutation}<br>$(CGG)_{230-750}$ [191] |
| Huntington disease | *IT15* | $(CAG)_{10-35}$ | $(CAG)_{36-39}$ {increased risk}<br>$(CAG)_{40-121}$ [191] |
| Friedreich's ataxia | *FXN* | $(GAA)_{7-34}$ | $(GAA)_{100+}$ |
| Myotonic Dystrophy | *DMPK* | $(CTG)_{5-37}$ | $(CTG)_{50-3000}$ |
| Machado-Joseph disease | *MJD1* | $(CAG)_{12-37}$ | $(CAG)_{61-84}$ |
| Spincerebellar ataxia Type 1 | *SCA1* | $(CAG)_{6-39}$ | $(CAG)_{41-81}$ |
| Spincerebellar ataxia Type 8 | *SCA8* (*IOSCA*) | $(CTG)_{16-37}$ | $(CTG)_{110-250}$ |
| Spinobulbar muscular atrophy (Kennedy disease) | *AR* | $(CAG)_{11-33}$ | $(CAG)_{38-66}$ |

One of the more accepted mechanisms explaining expansion phenomena is that of *polymerase slippage* (illustrated in Figure 1.14). It is proposed that during replication events

DNA polymerase may potentially pause and dissociate from the template DNA strand, causing local strand separation.[192-197] If this occurs in a trinucleotide[†] repeat region, the polymerase is confronted with multiple identical codons at which to reattach. Improper re-annealing of the two DNA strands will result in the formation of a bulged-out loop and the daughter strand being displaced (slipped) relative to the template strand by an integral number of triplets.[198, 199] Subsequent replication and repair mechanisms give rise to an expansion of the repeat region by an appropriate number of codons.[‡ 94, 202-205]

While the initial dissociation of the polymerase in DNA expansion events has been attributed to the formation of impassable non-canonical DNA secondary structures (often triple helices) within the repeat region,[194, 197, 206-209] long-range slippage events are energetically unfavourable. Slippage requires that numerous hydrogen bonds be broken as base-pairs are separated, thus necessitating a mediator to minimise the energy difference between duplex and slipped DNA structures. Hairpin loops are most often implicated in this role (particularly amongst repeats of the general form CNG, where N = A, C, T, or G).[183, 187, 190, 210-212] Many experiments have demonstrated the propensity of trinucleotide repeat structures to form stem-loop structures *in vitro* and have found the stability of these structures to be dependent upon both their length and their sequence.[187, 213-218] Futhermore, the sequences most likely to form hairpin loops (CNG repeats) have been shown to be more elusive to repair mechanisms than sequences less proficient at forming hairpin loops (AAG, CAA, and AGT).[219] This increases the likelihood that the slipped structure will be overlooked, subsequently giving rise to expansion.

While efficient base-stacking and the presence of strong G•C base-pairing in the stem are important factors in determining the stability of a particular hairpin loop sequence, so too are the identity of the *mismatched* base-pairs that are a common feature of these stem-loop structures.[220] Indeed, expansion events often exhibit a dependence on orientation (i.e. which direction the polymerase is travelling)[221] that was originally attributed to the greater stability of the hairpin intermediate of one strand over the other. Myotonic dystrophy type 1, for instance,

---

[†] While the majority of disorders related to the expansion of tandem repeats have been attributed to *tri*nucleotide repeats, di-, tetra- and pentanucleotide expansions have also been associated with disease.

[‡] Deletions/contractions of repeat regions can also occur, depending upon which strand (daughter or template) the loop arises in. Contractions are significantly less common than expansions. [200, 201]

is associated with the expansion of a $(CTG)_n$•$(CAG)_n$ repeat sequence. The hairpin loop responsible for this expansion was believed to arise in the CTG strand because the T•T mismatches contained within the stem of that hairpin loop would be more stable than the A•A mismatches that would arise in the complementary CAG strand.[94, 210, 220] However, experiments proving the *in vivo* formation of hairpin loops in trinucleotide repeat sequences have also shown that the loops form equally well in either strand of a $(CTG)_n$•$(CAG)_n$ repeat in yeast,[219] confirming the near-equivalent stabilities observed *in vitro*.[215, 217] Thus, the reason behind the orientation-dependence of expansion events remains elusive.

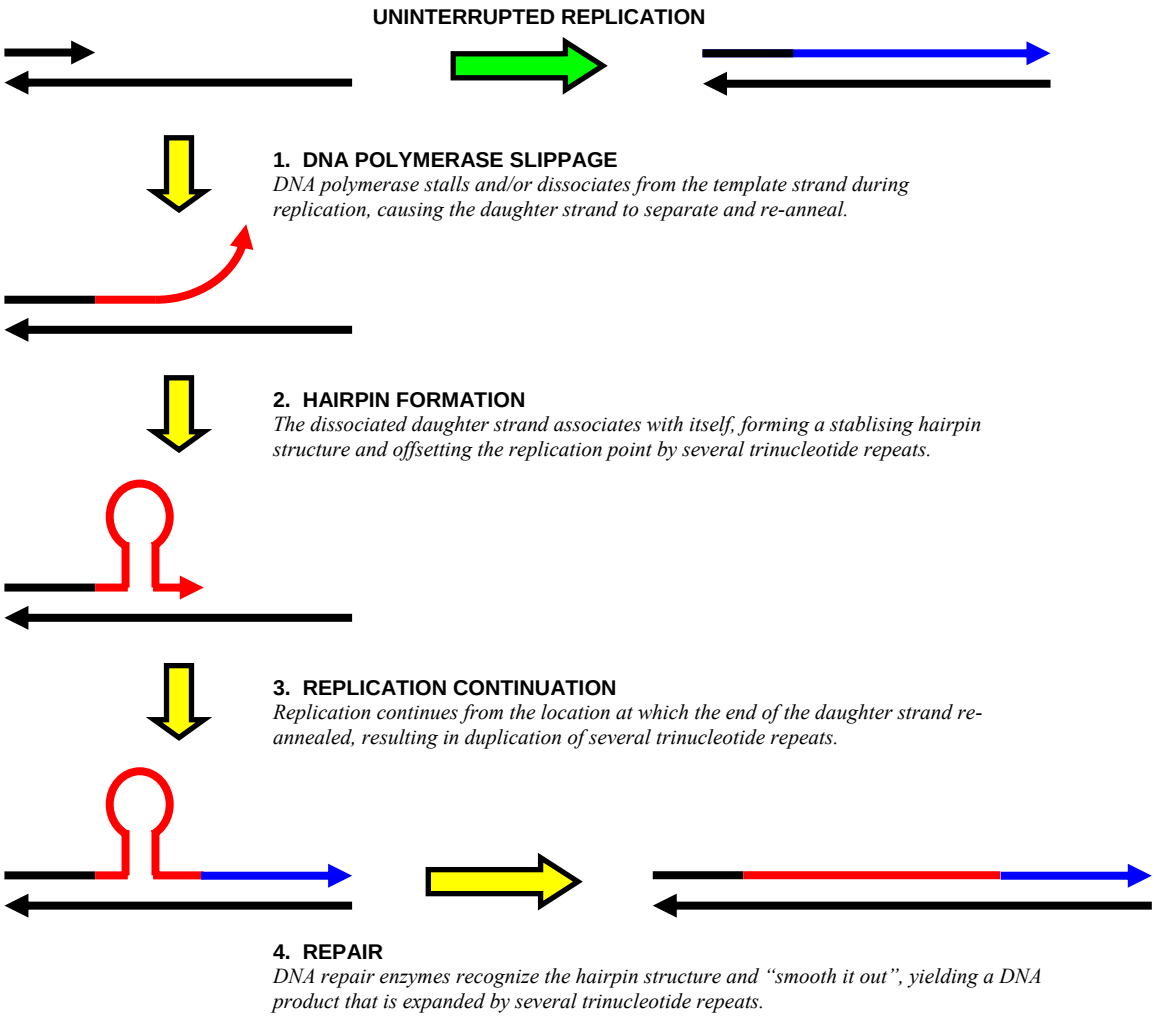


***Figure 1.14***
**Hairpin-mediated polymerase slippage model of repeat expansion.** A trinucleotide repeat sequence of DNA (in black) undergoes replication. A typical replication event (green arrow) would yield a DNA product (blue) with the same number of repeats as the original template strand; however, during the polymerase slippage mechanism (yellow arrows) the DNA polymerase dissociates, a stablising hairpin is formed, and replication continues resulting in the duplication of several repeats. DNA repair enzymes subsequently eliminate the hairpin, yielding a product that has been expanded in length by several trinucleotide repeats (red).

Although the expansion of CNG-type repeat sequences is most often attributed to the formation of hairpin loops, a variety of other secondary structures have been implicated in the expansion of alternate repeat sequences.[210] Expansion of AT-rich repeats, such as the pentanucleotide repeat ATTCT•AGAAT associated with spinocerebellar ataxia type 10, has been attributed to the formation of DNA-unwinding elements.[203, 222] Differing studies have found the fragile X repeat, CGG•CCG, to adopt either hairpin[217, 223] or tetraplex structures,[224, 225] both of which would potentially facilitate enhanced methyltransferase activity,[226] thus explaining the hypermethylation of cytosine observed in the CGG repeats of those afflicted with fragile X syndrome.[179] The GAA•TTC repeat associated with Friedrich's ataxia has been attributed both a triple helix conformation[227, 228] and a "sticky DNA" structure.[229, 230] Ultimately, the mechanisms behind the expansion of tandem repeat regions of DNA may be complicated and many-fold, but the *in vitro* and *in vivo* tendency of many of these sequences to form hairpin loops suggests that such a structure does indeed play a prominent role.

As with DNA bulges, the formation of DNA hairpin loops is usually considered disadvantageous. Nevertheless, there are a number of instances in which DNA hairpin loops have been attributed regulatory roles in genome expression through either hairpin-induced conformational changes to DNA or direct protein contact.[154, 231] As previously mentioned, a number of DNA-binding proteins preferentially target non-B-DNA structures, including hairpin loops. IRIP, a ribosome-inactivating plant protein isolated from *Iris hollandica*, bound preferentially to DNA fragments that shared no common sequences, but rather, contained one or more possible free energy-stable hairpin structures.[232] Likewise, the DAX-1 protein, implicated in sex determination,[233] has been found to bind to hairpin structures *in vitro* and *in vivo*.[234] Conversely, a number of specific genomic sequences have been found to adopt hairpin-like structures. For instance, the origin or replication region of M13 bacteriophage DNA may adopt a structure featuring two hairpins, one of which features a specific protein cleavage site within its large loop.[235] Yafe *et al*. have reported that the promoter and enhancer regions of several muscle-specific genes adopt diverse secondary structures. Of these, the guanine-rich human *sMtCK* (sarcomeric mitochondrial creatine kinase) sequence folded into a hairpin structure.[236] In one particularly interesting example of hairpin-mediated gene regulation, the proenkephalin gene – involved in pain regulation – possesses a sequence that has been found to switch between two different conformations, thus providing two distinct factor binding sites.[237] The palindromic nature of the sequence facilitates switching between a linear duplex and a

cruciform structure, each of which provides a unique binding site essential for correct transcription of the gene.

Cruciforms are intramolecular structures consisting of two hairpins opposite each other on antiparallel DNA strands, thus giving rise to a four-way junction. They occur in DNA inverted repeats or palindromes where the sequences read the same (5′ to 3′) on each strand.[24, 231] Cruciforms are believed to form from supercoiled DNA: the extrusion of the cruciform structure lowers the superhelical free energy of the system.[238-240] While supercoiling is itself linked to gene regulation,[241-243] hairpin and cruciform structures extruded from supercoiled DNA are believed to often serve as protein recognition sites.[244-246] For instance, there are a number of examples of endonucleases selectively cleaving plasmid DNA at cruciform-forming palindromic sites.[247, 248] Indeed, topoisomerase II, one of the class of enzymes dedicated to acting upon the topology of DNA,[249] has been demonstrated to cleave a specific site only when a hairpin loop was present.[250] The same site, when present in conventional dsDNA or ssDNA, was not utilised by the topoisomerase suggesting that the DNA hairpin serves as a potential substrate for topoisomerase II-mediated illegitimate recombination. Another well-characterised regulatory DNA hairpin structure is that which arises in bacteriophage N4 virion RNA polymerase (N4 vRNAP) promoter regions. This stable structure (a 5- to 7-base pair stem and a 3-base loop) extrudes under physiological superhelical densities in a $Mg^{2+}$-dependent manner and appears to regulate transcription *in vivo*.[251, 252]

RNA hairpin loops are ubiquitous. 16S rRNA, for example, has some 70% of its length folded into 31 stem-loop structures.[154] Like bulges, hairpin loops are integral to the structure and function of the various types of RNA, providing stabilising tertiary contacts and nucleation sites for RNA folding, as well as distinct protein recognition sites.

Perhaps the most prominent occurrence of RNA hairpin loops takes place in the characteristic cloverleaf structure of tRNAs. The archetypical tRNA structure comprises three stem-loop structures, as well as an acceptor stem and a variable bulge/loop (see Figure 1.15a). The acceptor stem binds the amino acid which is specific to that particular tRNA, while at the other end of the molecule the anticodon loop possesses a three-base sequence representative of the attached amino acid. During translation, this anticodon matches up with the complimentary codon of an mRNA and the appropriate amino acid is appended to the protein being synthesised. The roles of the D- and T-loops in the function of tRNAs are less well established. Both are known to contribute towards the overall folding of the molecules into the more

realistic L-shape (see Figure 1.15b) via tertiary interactions between the two loops.[253] It is postulated that the D-loop (named for the abundance of the base dihydrouracil found therein) acts as a recognition site for aminoacyl-tRNA synthetase, the enzyme responsible for "charging" the acceptor stem with the appropriate amino acid.[254, 255] Conversely, the T-loop (named for the near-invariant TΨC sequence found across tRNAs) is believed to serve as a recognition site for the ribosome during the formation of tRNA-ribosome complexes.[256]

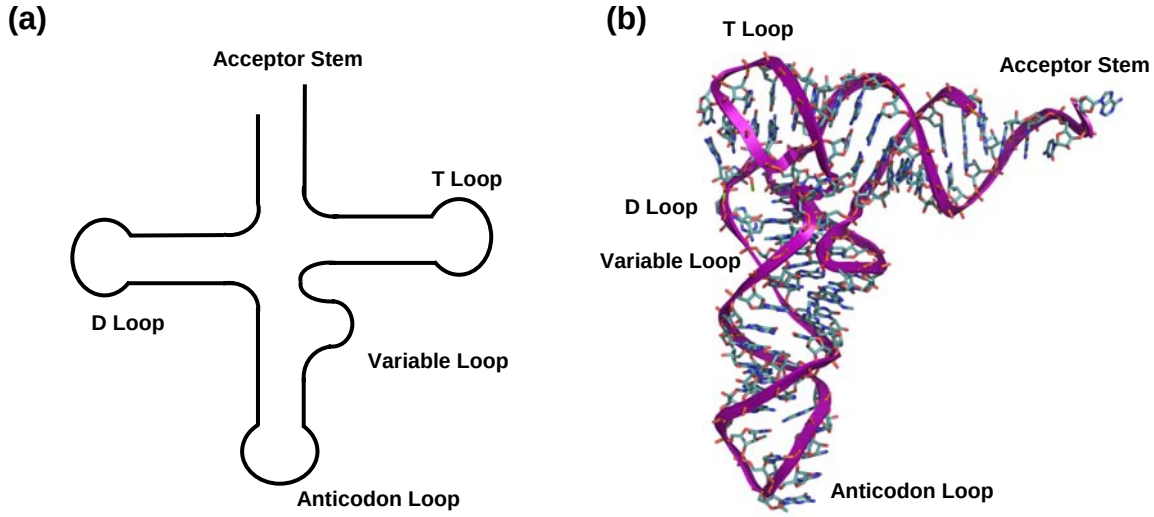


***Figure 1.15***
**tRNA. (a)** Schematic represenatation of tRNA illustrating the functional arms of the molecule. **(b)** Crystal structure (PDB identifier **6tna**)[257] of yeast phenylalanine tRNA demonstrating the three-dimensional conformation of the molecule. Crystal structure rendered with PyMOL.[36]

The TAR and RRE HIV mRNAs mentioned earlier feature stable hairpin loops structures that are involved in binding-site recognition by the Tat and Rev proteins, respectively. Mutational studies conducted with HIV-1 TAR have demonstrated that the sequence of bases in the loop is relatively unimportant in comparison to certain stem and bulge sequences, however the overall hairpin structure is still necessary for efficient protein binding.[104, 125, 258] Similarly, the structure of the bulge-containing stem-loop arrangement of RNA selectively bound by the R17 bacteriophage coat protein has also been well characterised.[63, 129, 130]

Stem-loop structures are quite common at the 5′- and 3′-UTRs (that is, the ends) of prokaryotic[259-264] and eukaryotic[265] mRNAs, respectively. In this context they are believed to be crucial in modulating the longevity of transcripts by either facilitating the correct folding of the mRNA or by serving as binding sites for protective and regulatory proteins. One particularly interesting example of the latter case involves the post-transcriptional iron-mediated regulation

of ferritin and transferrin receptor (TfR) proteins. Ferritin is the ubiquitous iron-storage protein of mammals and TfR is involved in the mediation of iron uptake into the cell. The mRNAs of each protein possess a number of similar hairpin structures in their untranslated regions (5′ end for ferritin, 3′ end for TfR) known as iron-responsive elements (IREs). These highly-conserved structures are bound by IRE binding proteins that (i) modulate the translational repression of ferritin in response to iron, and (ii) regulate the stability of the TfR mRNA.[266, 267] Accordingly, these hairpin loop structures may be considered integral to the maintenance of cellular iron homeostasis.

#### *1.2.4.4 Multiplexes*

Certain nucleic acid sequences are able, if not prone, to form complexes of more than two strands, blurring the line between secondary and tertiary structure. Triple helices are typically comprised of a purine•pyrimidine Watson-Crick base-paired duplex with a third strand binding via a Hoogsteen bonding scheme in the major groove (see Figure 1.16).[268] Pyrimidine-rich strands bind parallel to the purine strand, whereas a purine-rich third strand binds in an antiparallel manner. While early crystal and NMR structures have depicted a somewhat A-like helical form,[269, 270] more recent investigations are suggestive of a B-type conformation.[271, 272] While T•AT triplexes are most common, $C^+$•GC structures are also feasible at low pH or given appropriate substitution upon the cytosine bases.[273] These two structures represent the most stable base-triple configurations, however some 16 possible combinations have been described, including various base mismatches.[19] Intramolecular triplexes, wherein a single strand folds back on itself, are particularly stable. A likely *in vivo* occurrence of triple helical structures is in the DNA structures known as H-DNA[†]. These arrangements feature a stretch of double-helical DNA with the extremities of one strand looping back around to associate in the major groove of the duplex to form a triple helix. The formation of such structures has been associated with negative supercoiling or low pH of the appropriate repeat sequences.[274-276] An H-DNA conformation is believed to be a possible stabilising structure in trinucleotide expansion events relating to the GAA repeat of Friedrich's ataxia.[227] While little is known about the biological

[†] So-called because original observations of such structures seemed to indicate that base protonation (i.e. an abundance of "H") was a requirement in their formation.

implications of naturally-occurring triple helices, synthetic triplex-forming strands show promising application as diagnostic and therapeutic agents possessing sequence selectivity for relatively large polynucleotide strands.[277-283] Upon binding, the third strand may be utilised as a means of modulating gene expression or, properly functionalised, a sequence-specific cleavage agent.

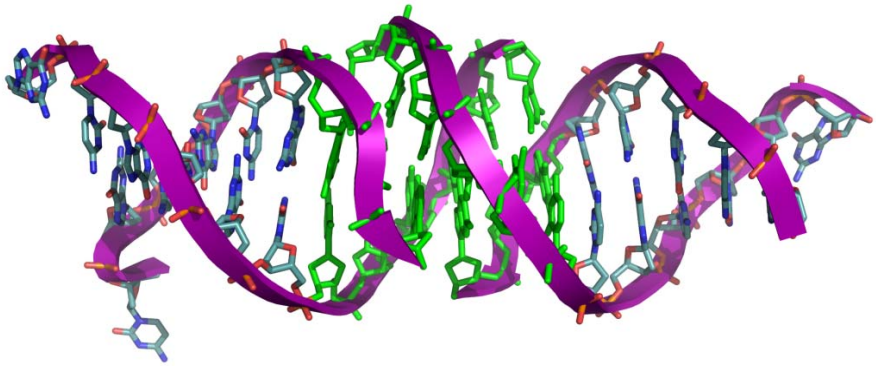

***Figure 1.16***
**Triple Helix.** Crystal structure (PDB identifier **1d3r**)[273] of triple helical DNA with a triplex-duplex junction. Base triples are depicted in green. Crystal structure rendered with PyMOL.[36]

The other common multi-stranded nucleic acid configuration is the quadruplex. Such structures are usually associated with guanine-rich sequences which have been found to aggregate together when properly stabilised by cations. In doing so a structure forms in which groups of four guanines are able to hydrogen bond to one another in an arrangement known as a G-tetrad {Figure 1.17(a)}. The end result is a four-stranded structure that can be configured in a number of different ways: an intermolecular arrangement with four separate polynucleotide chains bonding together, a single strand folded back on itself several times, or the intermediate case in which two individual strands are folded into adjacent hairpin structures which subsequently bond with each other {illustrated in Figures 1.19(b)-(d), respectively}.[284, 285] Several different quadruplex structures have been characterised via crystallographic and NMR techniques, with factors such as strand length and sequence, as well as the size of the stabilising counterions, dictating the ultimate configuration.[286-290] While typically composed primarily of guanine residues, other bases can be incorporated into the structure.

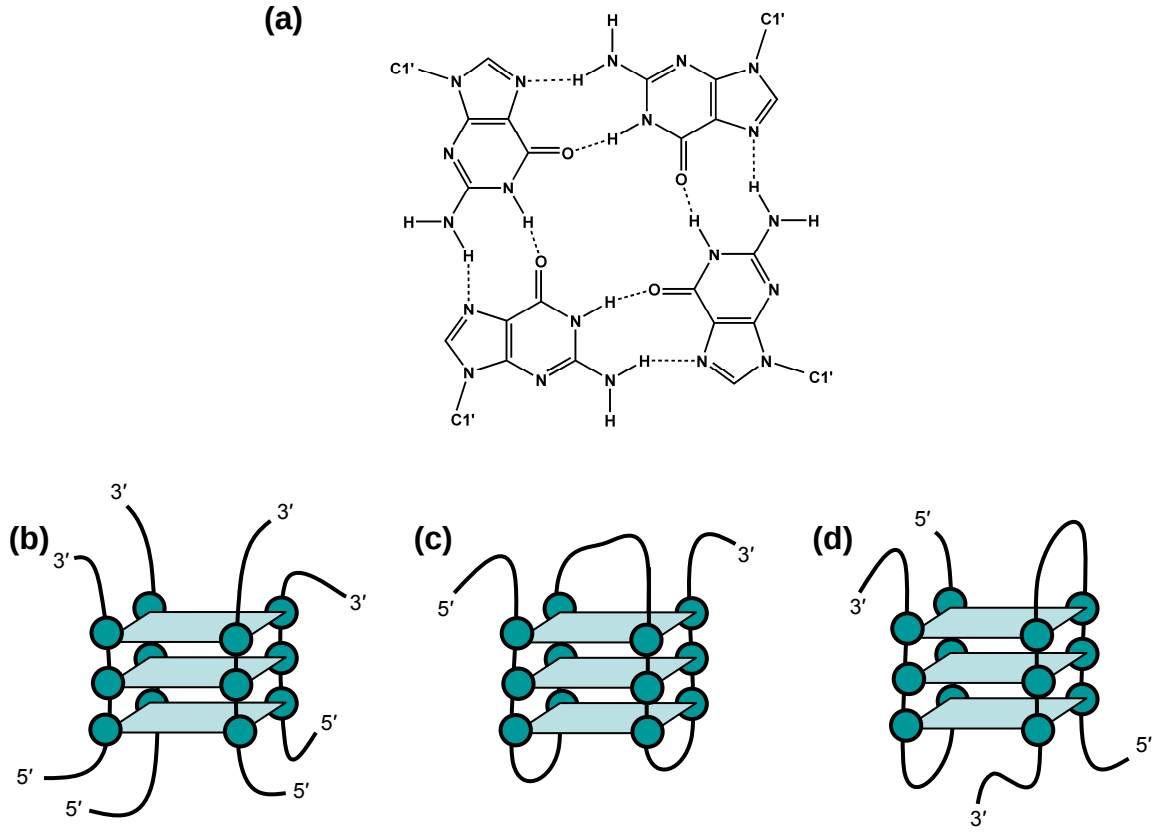


***Figure 1.17***
**Quadruplexes. (a)** The hydrogen-bonding scheme of a guanine-quartet, and schematic representations of several quadruplex configurations: **(b)** a four-stranded, all-parallel intermolecular quadruplex arrangement, **(c)** a single-stranded intramolecular quadruplex, and **(d)** a two-stranded hairpin-dimer type quadruplex. Teal circles represent guanine bases while the light blue rectangles illustrate the G-quartet formations between them.

The most likely *in vivo* role of quadruplex structures is as a structural feature of *telomeres*. Telomeres are guanine-rich repeat sequences (TTAGGG in humans) several thousand bases long that occur on the 3′-end of eukaryotic chromosomes where they essentially serve as a disposable buffer.[291-293] One strand of the telomere has a single-stranded overhang several hundred bases long which has the potential to fold back into quadruplex configurations. During replication, DNA polymerase is unable to read to the very end of the chromosome; without a buffer, each successive cell division would result in the loss of information from the end of the chromosome. Instead, the telomeric DNA in somatic cells shrinks with every replication, ultimately leading to apoptosis when the telomere becomes too short. As such, telomeres have been likened to a "biological clock", limiting the number of times cells can proliferate, and they have subsequently been linked to aging. This process is counteracted by a reverse-transcriptase

enzyme known as telomerase that elongates the 3′-end of telomeric DNA.[294] Ordinarily, somatic cells are free of telomerase activity, however the majority of tumour cells do exhibit such activity which bolsters the replicative longevity of these cell lines and contributes to tumourigenesis. However, quadruplex DNA proves to be an impediment to telomerase activity.[295] As a result, the design of quadruplex inducing/stabilising ligands is a growing field of investigation in the fight against cancer.[296-298] Potential quadruplex-forming sequences are prevalent throughout the human genome,[299, 300] many of which have been associated with the promoter regions of a number of genes,[301-306] suggesting a regulatory role for quadruplex formation.

#### *1.2.4.5 Junctions*

Branched nucleic acid species, or junctions, are a common feature in the more convoluted landscape of higher-order RNA structures.[100, 307] They arise as an inevitable consequence of the multiple arms ever-present in tRNAs and rRNAs, and play an important role in the global folding of RNA structures as well as protein recognition and enzymatic processes. However, like so many of the more complex structural elements of nucleic acids, junctions typically occur as transient features in DNA.[308] The formation of cruciforms, as described earlier, gives rise to four-way junctions where the stem-loop structures extrude from the main duplex.[309] The process of homologous recombination, the exchanging of genetic material between chromosomes, also requires an intermediate four-way construct known as a Holliday Junction. When the DNA from two duplexes crosses over, the four strands arrange themselves into four anti-parallel base-paired arms, adopting a stacked X-like structure (see Figure 1.18).[310-312] Migration of the branches and subsequent enzymatic resolution (cleavage) of the strands ultimately yields two recombinant helices.[313, 314] Somewhat more complex junctions have been found in crystal structures of "DNA enzymes,"[315] which as the name suggests are DNA sequences that exhibit enzymatic capabilities.

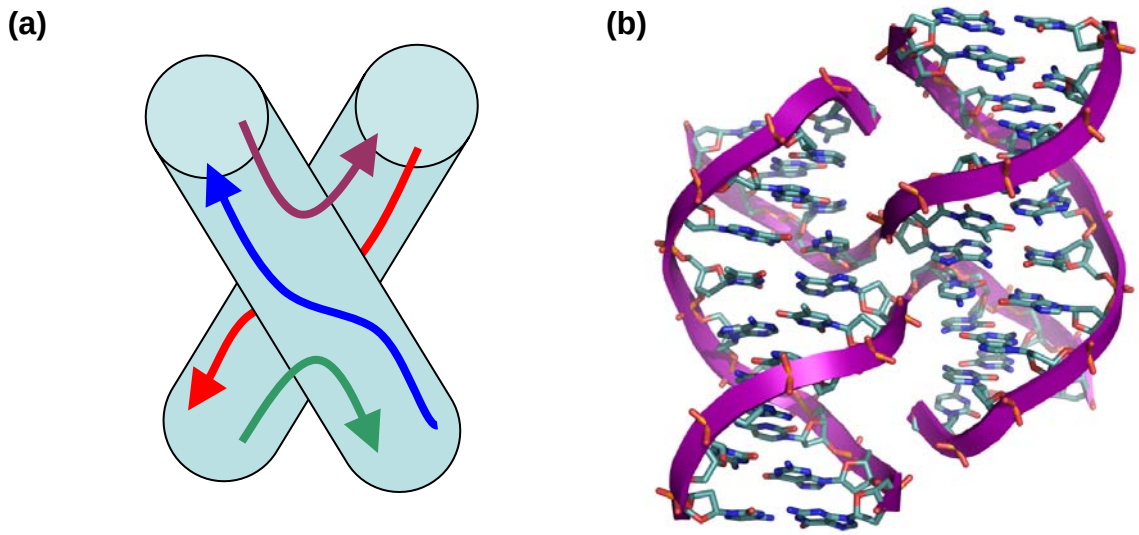


***Figure 1.18***
**Holliday Junction. (a)** Schematic representation of a four-way Holliday junction. The duplex arms of the structure are represented as cylinders while the directionality of each strand is shown by an arrow. (**b**) Crystal structure (PDB identifier **1dcw**)[310] of triple helical DNA with a triplex-duplex junction. Base triples are depicted in green. Crystal structure rendered with PyMOL.[36]

### *1.2.4.6 Tertiary Structures*

With respect to nucleic acids, "tertiary structure" is typically reserved for reference to the overall three-dimensional configurations of RNAs. DNA does not typically assume structures of sufficient complexity to warrant references to its tertiary organisation. Structure at this level is generally described in terms of interactions between secondary structural elements. Such motifs include kissing hairpins, wherein the unpaired bases of one hairpin loop pair up with those of another; pseudoknots, consisting of two stem-loop structures in which the loop of the first forms part of the stem of the second; and myriad loop-loop, bulge-loop, and bulge-bulge interactions.[138, 253, 307, 316] These intramolecular interactions ultimately define the global folding and structure of an RNA, and by extension, contribute to the functionality of the molecule. While the tertiary architecture of some RNAs (tRNA[253] and the hammerhead ribozyme,[317, 318] for instance) are fairly well established, a firm understanding of structure and its recognition at this level remains elusive.

## 1.3 SMALL MOLECULE-NUCLEIC ACID INTERACTIONS

### 1.4.1 General Comments

The vast array of different nucleic acid structural features present themselves as a daunting selection of targets in the design of small diagnostic and therapeutic molecules. To achieve maximum effectiveness and efficiency, sequence- and structure-selectivity must be considered alongside the intended function of the drug. A long-term goal of this line of work is the regulation of gene expression accomplished by means of enhancing or inhibiting the action of nucleic acid-binding proteins. Such regulation might be realised via either direct mediation of the polynucleotide-protein interaction or by stabilisation/de-stabilisation of modulating structures. While significant progress is being made in our understanding of both the nature of nucleic acids and the factors that govern their interactions with other species, there is still much to be learnt through probing the structure of nucleic acids with small molecules. Success in this endeavour requires fine-tuning of the chirality, topology, electrostatics, hydrophobicity and hydrogen-bonding characteristics of the guest molecule to best match its host.

### 1.4.2 Modes of Interaction

Nucleic acid-ligand interactions can be broadly categorised as being either covalent or non-covalent in nature. While most biological nucleic acid-binding molecules interact non-covalently with their target, many of the more successful synthetic DNA-based pharmaceuticals developed thus far been covalently-binding species. Typically, such interactions involve electrophilic attacks by the binding agent on the DNA bases, with the favourable electronic charge distribution of the purines making them particularly susceptible (guanine more so than adenine).[19, 319] Common sites of attack are the O6 (guanine), N6 (adenine) and N7 atoms in the major groove and the N1, N2 (guanine) and N3 atoms in the minor groove.

The earliest DNA-binding antitumour agents were nitrogen mustards, derived from chemical warfare agents of the First World War, which demonstrated a propensity for alkylating the N7 position of guanine bases within guanine-rich sequences.[320] While contemporary derivatives of such species are still in use today, a significant number of modern chemotherapeutic drugs are platinum complexes. This apparent predilection may be attributed to the success of the archetypical platinum anti-cancer drug, *cis*-diamminedichloroplatinum(II)

(cisplatin).[321-324] The ability of this complex to inhibit cell division was discovered serendipitously by Rosenberg in the 1960s,[325-327] with subsequent investigations attributing the cytotoxicity of the complex to its tendency to covalently bind to (predominantly) the N7 atoms of adjacent guanosine residues.[328] While the mechanisms by which it subsequently invokes cell death are still not completely understood,[329] the intrastrand cross-linking caused by cisplatin binding is believed to induce distortions in the DNA which subsequently impede replication and ultimately induce apoptosis.[330-333] Despite showing impressive success against particular types of tumour (a >90% cure rate in the case of testicular cancer) and subsequently becoming one of the world's most widely utilised anticancer drugs, the effectiveness of cisplatin is hampered by resistance amongst many cancer lines. Furthermore, cisplatin causes a number of unpleasant side-effects owing to its lack of selectivity for cancerous cells. As a result there has been extensive research into the development of alternative platinum-based drugs with lower toxicities and wider applicability.[321, 330, 331] While early candidates such as carboplatin[334] and oxaliplatin[335] are relatively simple derivatives of the cisplatin archetype, the rational design of antitumour platinum complexes has advanced to more elaborate schemes in hopes of avoiding the mechanisms involved in the resistance and toxicity of first-generation platinum drugs. Promising recent advances include multinuclear species such as the trinuclear platinum complex BBR 3464, which has performed well in preclinical evaluations.[321, 336] While popular, platinum complexes are not unique in their ability to participate in inner-sphere coordination with nucleic acids. Dirhodium "lantern" complexes[337-342] and organometallic ruthenium-arene complexes[343-347] are two more classes of promising metallopharmaceuticals that covalently bind to DNA, while another labile ruthenium-based anticancer drug, imidazolium *trans*-imidazoledimethylsulfoxidetetrachlororuthenate(III) (NAMI-A), has demonstrated relatively low toxicity levels relative to its platinum counterparts.[348-350]

The non-covalent interaction of molecules with nucleic acids may be further sub-categorised as being electrostatic, groove-binding, or intercalative in nature.[351] While many non-covalent binders utilise at least two of the three different modes, appropriate electrostatic attractions between the ligand and the polyanionic nucleic acid are, understandably, essential. Consequently, most polynucleotide binders tend to be cationic in nature. These cations vary in complexity from simple counter-ions such as $Na^+$ and $Mg^{2+}$ that influence and stabilise higher-order structures of DNA and RNA,[101, 352] through natural polyamines such as spermine and spermidine,[353] up to proteins with positively-charged arginine or lysine residues.[354] However,

ligands binding solely (or predominantly) via electrostatic interactions tend to be relatively mobile within the nucleic acid structure and as a result exhibit little structure- or sequence-selectivity. Accordingly, electrostatics are best utilised in cooperation with the other modes of interaction.

Groove-binding, the second of the three classes of non-covalent nucleic acid-binding, involves the association of a guest molecule (or part thereof) within the major and/or minor grooves of the polynucleotide. Such associations are driven by a combination of electrostatics, van der Waals contacts, hydrophobic interactions, and hydrogen-bonding (where applicable). The suitability of a particular substrate for a given groove may be dependent upon the conformation of the polynucleotide, as changes in sequence and structure can influence the dimensions and functionality of both the major and minor grooves. The DNA stains DAPI (4′,6-diamidino-2-phenylindole)[355-357] and Hoechst 33258,[358-360] and the antiviral antibiotic netropsin[361, 362] (see Figure 1.19), are typical of minor groove-binding molecules in that they are (i) positively charged, (ii) roughly crescent-shaped to neatly match the groove floor, and (iii) consist largely of a series of linked, but not fused, aromatic/heteroaromatic rings.[363] Such species exhibit a preference for A•T-rich sequences over those containing G•C base pairs for the following reasons:[360, 364-367]

- It has been established that the minor groove possesses a greater electronegativity at A•T steps, making it more attractive than G•C-rich sites to positively-charged ligands.
- The minor groove is considerably narrower at A•T runs, albeit more flexible, thus enabling the backbones of the polynucleotide to make closer van der Waals contacts with the ligand.
- In stretches of G•C base pairs, the exocyclic amino group of the guanine base protrudes into the minor groove, obstructing with the complementarity of the concave ligand with the convex groove floor.

Conversely, most proteins bind nucleic acids largely via the major groove owing to its larger width (enabling accommodation of protein α-helices or zinc fingers,[368-370] for example), and richer information content (by which greater sequence selectivity can be obtained). In situations where the groove dimensions have been significantly altered, such as in A-form helices, binding affinity is affected. Indeed, DAPI has been found to bind via an alternate, intercalative mode (see below) when the minor groove is unfavourable (as in A-form

conformations or GC-rich sequences).[371-373] This is also the reason that many double-helical RNA binding sites utilise bulges or loops to confer increased flexibility upon the duplex; proteins are able to manipulate the more flexible major groove and gain access to the hydrogen-bonding donors and acceptors within.[374] Triple-helical nucleic acid structures also arise through the association of a hydrogen-bonding third polynucleotide strand in the major groove.[268, 269, 375]

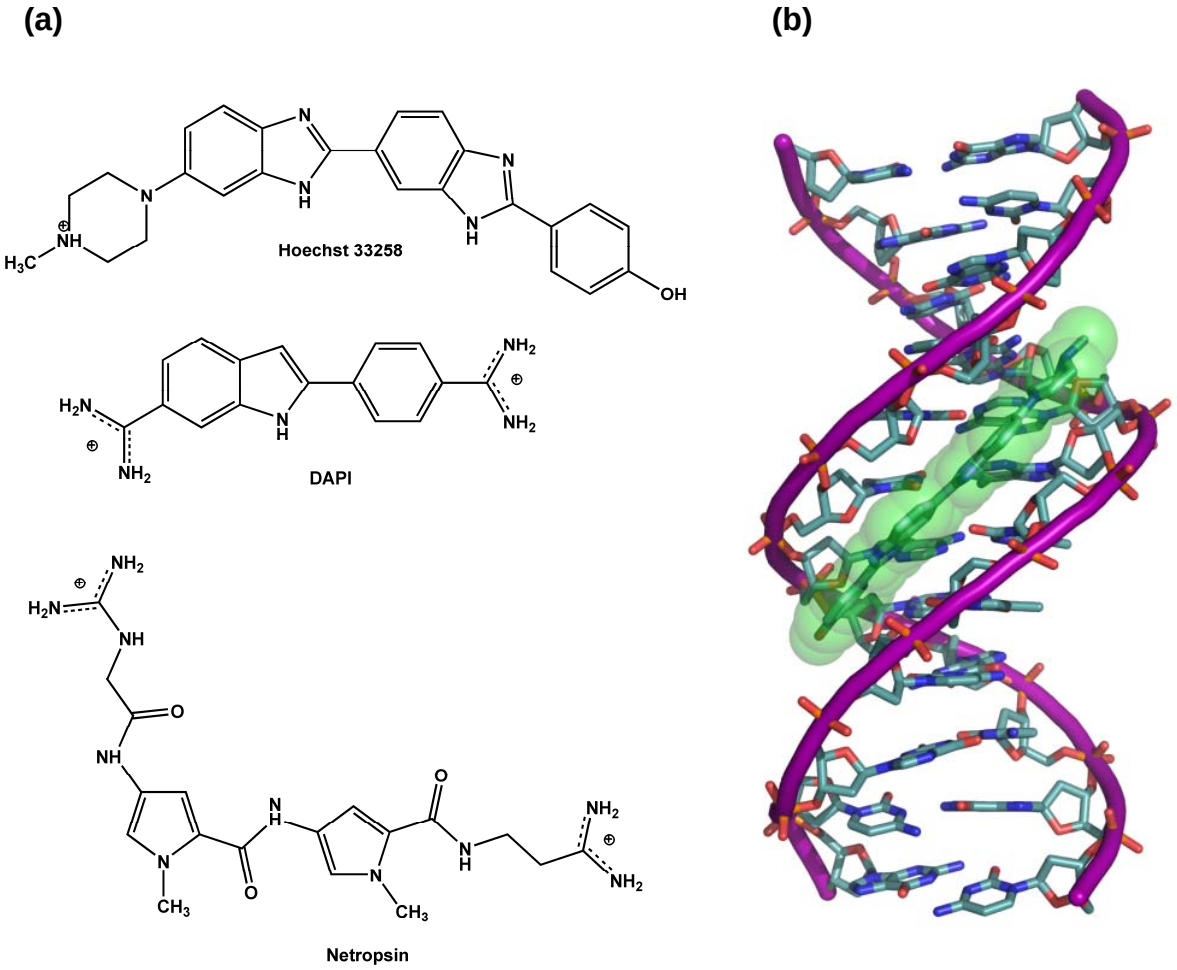


***Figure 1.19***
**Minor Groove Binders.** (a) Three examples of minor groove-binding drugs. (b) A crystal structure (PDB identifier **1d43**)[376] depicting Hoechst 33258 bound in the AT-rich region of the minor groove of the oligonucleotide d(CGCGAATTCGCG)$_2$. Crystal structure rendered with PyMOL.[36]

With regards to metal complexes, square planar species such as $[Pt(en)_2]^{2+}$ {en = ehtylenediamine; see Appendix A for ligand structures} or amino acid complexes of Ni(II) have demonstrated an affinity for the AT-rich minor groove, for similar reasons to those detailed above.[377, 378] Alternatively, bulkier octahedral complexes have typically found the major groove a more inviting target. The complexes $[Co(NH_3)_6]^{3+}$ and $[Co(en)_3]^{3+}$ exploit the greater size and

hydrogen-bonding potential of the major groove, with a particular affinity for the N7 and O6 atoms of adjacent guanine residues while exhibiting some degree of enantioselectivity in the case of the ethylenediamine complex.[379-383] Major groove-binding has also been seen in a number of metallo-supramolecular cylinders that emulate the cylindrical binding units of proteins.[384-386]

The final major class of non-covalent interactions, intercalation, has been the binding mode of the majority of DNA-binding transition metal complexes studied to date.[387] Intercalative associations involve favourable stacking interactions between the electron-deficient π-system of a planar, polyaromatic substrate and the nucleobases above and below it.[6, 19, 351] Nucleic acids themselves make use of such interactions to stabilise their secondary and tertiary structures by means of base-on-base stacking. Intercalation of guest molecules can take place via the major or minor grooves; bulkier compounds can insert an extended planar moiety between the bases of a nucleic acid while the rest of the molecule interacts via a groove-binding mode. In accommodating intercalating ligands the DNA base-pairs need to separate to some extent, resulting in DNA helix unwinding/lengthening which is dependent upon the nature of the intercalating species.[388] Intercalative binding adheres to a neighbour-exclusion principle whereby backbone geometry structural constraints restrict maximal binding to one intercalator per three base pairs. Although intercalation is generally not sequence-specific, stacking requirements do result in a small preference for pyrimidine-purine steps.[19]

Simple intercalators include the fluorescent nucleic acid stain ethidium[389-391] and the antiviral agent proflavine[392-394] (see Figure 1.20) interact primarily via electrostatic and polarisation forces. More complex intercalators feature additional groove binding moieties in the form of hydrophobic groups, peptide chains and/or carbohydrate rings that can enhance van der Waals contacts and provide potential sequence-selectivity via direct readout of hydrogen bonding schemes.[395] Examples here include chemotherapeutic drugs such as daunorubicin[396, 397] and actinomycin D[398-401] which intercalate via the minor groove, various mononuclear rhodium and ruthenium complexes that intercalate via the major groove (discussed in greater detail below), and even species such as porphyrins[402-404] or the antitumour antibiotic nogalamycin,[405] which possess substituents that occupy both grooves simultaneously.

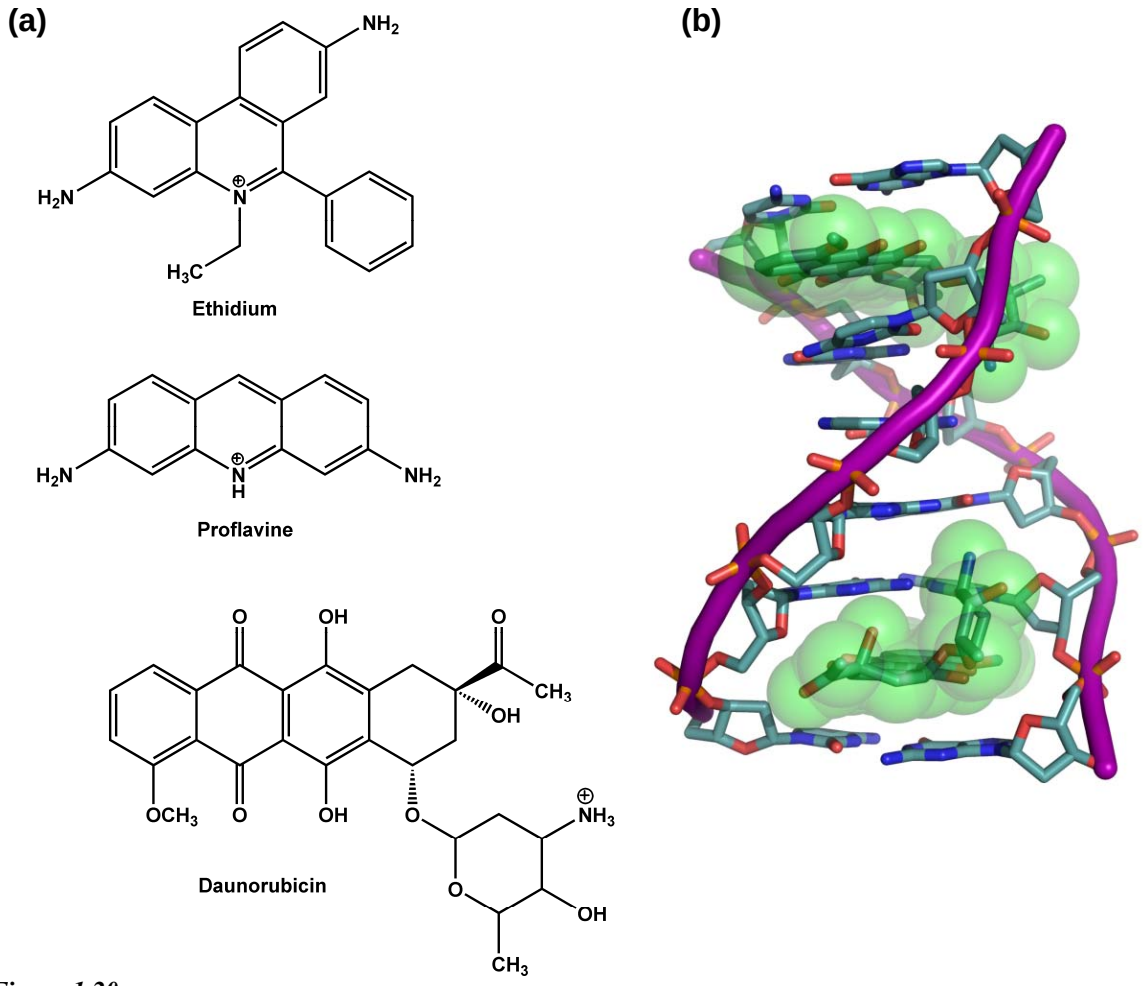


***Figure 1.20***
**Intercalators.** (a) Three examples of intercalating drugs. (b) A crystal structure (PDB identifier **110d**)[406] depicting two daunorubicin (aka daunomycin) molecules (green space-filling models) intercalated into the terminal CG steps of the hexanucleotide $d(CGGCCG)_2$. Crystal structure rendered with PyMOL.[36]

## 1.4.3 Selectivity of Interaction

Selectivity is fundamental to the rational design of efficient and effective nucleic acid-binding pharmaceuticals and probes. The myriad of different sequences and structures present within a given genome provide potential ligands with a wide array of prospective targets. This is well illustrated by current chemotherapeutic drugs: often they lack specificity for *cancerous* cells (and the distinctive biomolecular targets therein), instead attacking cancerous and healthy cells alike, thus inducing severe side-effects in the patient. Identifying, and subsequently targeting, molecular features specific to cancer cells would subsequently result in increased efficiency and fewer side-effects.

The most conspicuous means by which selectivity might be obtained is to target a specific base sequence. Such a sequence might belong to a specific gene or its promoter or enhancer regions, with the subsequent binding resulting in some degree of modulation of the gene itself. Selectively binding a *unique* DNA sequence in the human genome would require an incredibly complex drug able to recognise a sequence of some 15-16 bases[†].[407-409] Molecules possessed of such a binding footprint present a significant synthetic challenge and potential candidates have, to date, have had limited success.[407, 409] Even so, a smaller target sequence of 6-10 bases (for example) would still occur relatively infrequently within the genome and therefore still represent a viable objective. The lower end of this range corresponds to the footprint size of some of the more specific nucleic acid binders in use today. These ligands are typically polyamide minor groove binders such as netropsin and derivatives thereof. Selectivity is achieved via specific hydrogen-bonding patterns between amide functionalities on the drug molecules and polar minor groove atoms on the target bases. Species featuring pyrrole subunits favourably bind A•T and T•A base pairs, whereas those with imidazole subunits preferably bind to G•C and C•G base pairs.[410-412] Unfortunately, a mismatch in the geometries between the DNA minor groove and polyamide geometries means that the hydrogen-bonding functionalities on each eventually become out of phase (within approximately 10 base pairs). Multiple functionalities (i.e. a pair of groove-binding moieties joined by a central intercalating segment) and flexible linkers have been utilised in attempts to combat this problem.[407, 412] Furthermore, polyamides have demonstrated an affinity for mismatched bases,[413] a role at which polypyridyl rhodium complexes have also proven especially adept.[414-416] As mentioned above, simple intercalators possess little sequence selectivity, however more complex species usually incorporate minor groove-binding moieties with a preferences for GC-rich regions (specifically, the guanine amino group and N3 atom).[400, 417, 418]

Although selectivity in nucleic acid-binding is generally considered in terms of specific binding to a linear sequence of bases, the higher-order structures of polynucleotides are receiving more and more attention as potential targets. For example, the bending of DNA duplexes inherent in runs of adenine bases ("A-tracts")[419] presents itself as a more favourable target to a terbenzimidazole derivative than does the analogous sequence with an alternating AT

[†] The human genome is reportedly some $3 \times 10^9$ base pairs in length.[7] Being comprised of four different bases, a unique 15 base sequence should occur every $4^{15} = 1.1 \times 10^9$ bases, or $4^{16} = 4.3 \times 10^9$ bases for a 16 base sequence.

sequence.[420] Aminoglycoside antibiotics, although relatively unselective sequence-wise, have demonstrated a preference for RNA over DNA.[421, 422] The A-form double helix is also reportedly the target of choice for the tris(tetramethylphenanthroline)ruthenium(II) complex.[423] Z-DNA has received considerable attention:[41] a number of peptide chains,[424, 425] major groove-binding polamides[426] and cationic metal complexes[39, 427, 428] induce a B → Z transition, while a plethora of intercalators, including ethidium monoazide,[429] proflavine,[430] actinomycin D,[430] and adriamycin[431, 432] have been found to inhibit the B → Z transition by stabilising the B-DNA structure. Furthermore, compounds such as elsamicin A,[433] daunomycin,[434] ethidium bromide,[43] NC-182 (a benzo[*a*]phenazine derivative),[435] and netropsin[436] have been demonstrated to induce the reverse Z → B-DNA transition.

The flexibility inherent in and around bulge sites makes them promising targets for small nucleic acid-binding drugs. Simple intercalators like ethidium and 9-aminoacridine have been found to possess an increased affinity for DNA and RNA sequences that contain a bulge site,[24, 437, 438] and it is believed that such intercalators bind strongly to intercalation sites either side of the bulge.[439] Introducing hydrogen-bonding functionality to the intercalator can confer selectivity for a particular bulge upon the drug. For example, melting temperature experiments have shown that 2-acylamino-1,8-napthyridine can increase the stability of a duplex containing a single G bulge, but not the equivalent structures with A or T bulges.[440] The neocarzinostatin chromophore and its spirocyclic derivatives have demonstrated a high affinity and selectivity for bulge sites when cleaving nucleic acids,[441-447] specifically those of DNA due to steric clashes with the 2′-OH group in RNA.[448] While many metal complexes show promising artificial nuclease activity,[449] they usually do so without a great deal of selectivity. However, the complex $[Co^{II}(HAPP)(TFA)_2]$ {where HAPP is hexaazaphenantholine-cyclophane and TFA is trifluoroacetate} has been found to preferentially bind and cleave bulges.[450]

In contrast to bulges, loops have received little attention as potential small molecule binding sites. A few instances of selective cleavage of hairpin loops by neocarzinostatin chromophore antibiotics[451] and anthraquinone[452] have been reported, however most loop-related binding studies relate to selective binding of the bulge/loop structure of TAR and RRE RNA. Hoechst 33258,[453] diphenylfuran derivatives,[454-456] quinoxaline and quinozaline derivatives[457] and the aminoglycosides[101, 374, 457-459] have all been found to bind preferentially to the TAR and/or RRE RNA structures and impede the binding of the Tat or Rev proteins. Nonetheless, these reports

suggest that the bulge site is the major influencing factor in such binding, not the loop. Cationic porphyrin complexes have demonstrated some propensity for binding small DNA hairpin loop structures, with the affinity and binding mode (intercalation or external binding) of the complex dependent upon both stem and loop sequences.[402, 460-464] Porphyrins, alongside anthraquinones and acridines, have also been found to bind to and stabilise quadruplex DNA structures, albeit with little selectivity over duplex DNA.[296, 298, 465] It is believed such ligands bind via external stacking onto the quadruplex, rather than direct intercalation within the G-quartets.[466] Careful design of dibenzophenanthroline derivatives and tri-substituted acridines that better exploit the difference in groove dimensions between duplex and quadruplex DNA, has resulted in an increased affinity for the latter.[467, 468] Additionally, macrocyclic oxazoles and bistriazoles have exhibited a particular selectivity for quadruplexes over duplexes.[469-472] The stabilisation of the quadruplex upon the binding of such ligands has proven to exert an inhibitory effect of telomerase. Additionally, triplex-binding species, typically intercalative in nature, have commonly been utilised to stabilise triple helical nucleic acids for further study. These have usually taken the form of polyaromatic indole and quinoxaline derivatives.[473-477] Higher-order, branched DNA structures have been largely neglected with regards to their role as potential ligands, however recent investigations have demonstrated selective binding by an iron-based supramolecular helicate to a three-way junction[478] and a bis-acridine derivative to a four-way (Holliday) junction.[479] One particularly interesting study has found that the furocoumarin drug psoralen is capable of inducing and stabilising a Holliday junction-like structure in DNA, thus potentially promoting recombination events and the subsequent repair of strand lesions.[480]

It is clear that the abundance of potential nucleic acid structures presents a plethora of different targets for small ligands. Furthermore, the brief review above makes it evident that there is still much room for improvement with regards to the selectivities of nucleic acid-binding drugs and probes. The design of more potent ligands will ultimately necessitate the exploitation of not only subtleties in the electrostatics and hydrogen-bonding functionality of different sequences, but also the recognition of characteristic secondary structures within specific polynucleotide targets. A concept of particular importance to the latter form of specificity, yet largely absent in the above review, is that of *stereochemistry*. Nucleic acids are inherently chiral molecules, able to adopt a variety of different stereochemical conformations dependent upon their role and environment, yet the design of organic ligands has largely neglected this aspect of nucleic acid-substrate interactions. Studies into enantioselective

interactions between small molecules and nucleic acids have largely been confined to octahedral metal complexes, particularly ruthenium-based species possessing polypyridyl ligands.

## 1.4 POLYPYRIDYLRUTHENIUM COMPLEX-NUCLEIC ACID INTERACTIONS

### 1.4.1 Mononuclear Complexes

The application of polypyridyl transition metal complexes to the structural elucidation of biological molecules has its origins in the observations of Dwyer *et al*. in the 1950s. This group noted that the Δ (right-handed) and Λ (left-handed) enantiomers of tris(phenanthroline) complexes of Fe(II), Ni(II), Ru(II), Os(II), Co(II), and Zn(II) exhibited different biological activity in laboratory rats.[481] Upon being administered a racemic mixture of the two enantiomers, the Λ isomer essentially passed through the rats without effect – it was expelled in their urine. Intriguingly (or, from the perspective of the rats, unfortunately) the Δ enantiomer lingered in the rodents' systems and proved to be quite toxic, ultimately proving fatal. As such complexes are chemically inert, Dwyer *et al*. reasoned that any effect they had must be based primarily on their *physical* interactions with biological systems.

Ruthenium is often the metal of choice when studying the interactions of polypyridyl transition metal complexes with nucleic acids owing to its well-established chemistry and rich photophysical properties.[482] Polypyridylruthenium complexes are typically chemically inert, meaning their interactions with nucleic acids are usually non-covalent and hence reversible. Additionally, such octahedral tris(bidentate) species possess an inherent chirality which can be exploited in their interactions with chiral polynucleotides. Futhermore, these complexes exhibit strong metal-to-ligand charge transfer (MLCT)-induced absorbances in the visible portion of the spectrum and notable luminescent emissions – perturbations of these spectral characteristics upon nucleic acid-binding provide a convenient means to appraise the extent or nature of the interaction.

$[Ru(phen)_3]^{2+}$ {phen = 1,10-phenanthroline} has been adopted as the archetypical inert metalloprobe of DNA. The DNA-binding ability of this complex has been most extensively investigated by Barton and co-workers, who in the early 1980s elaborated upon the work of Dwyer *et al*. by investigating the *in vitro* enantioselectivity of the complex. Building upon

earlier studies involving $[Cu(phen)_2]^{+}$ [483] and $[Zn(phen)_3]^{2+}$,[484] the spectroscopic, electrophoretic, and dialytic experiments of Barton *et al*. demonstrated a preferential association between right-handed B-DNA and the right handed chirality of the Δ enantiomer of the tris(phenanthroline) complex.[485] On the basis of hypochromicity measurements it was proposed that the complex bound via intercalation of a single phenanthroline ligand. Such a binding mode leads to a complementary association between the right-handed propeller-like arrangement of the non-intercalated phenanthroline moieties of the Δ enantiomer and the walls of the DNA groove. Conversely, the non-intercalated ligands of the Λ enantiomer would encounter steric clashes with the right-handed phosphate backbone, inhibiting its binding ability. This scenario is illustrated in Figure 1.21. No such enantioselectivity was observed in experiments conducted with left-handed Z-DNA, presumably due to the altered groove dimensions. Were Z-DNA the exact mirror image of B-DNA, one might imagine Λ-$[Ru(phen)_3]^{2+}$ to have the greater affinity of the two enantiomers. Ultimately, the ability of the complex (and analogues) to discriminate between right- and left-handed DNA came into doubt as it appeared to induce local Z → B-DNA transitions as it bound to certain polynucleotides.

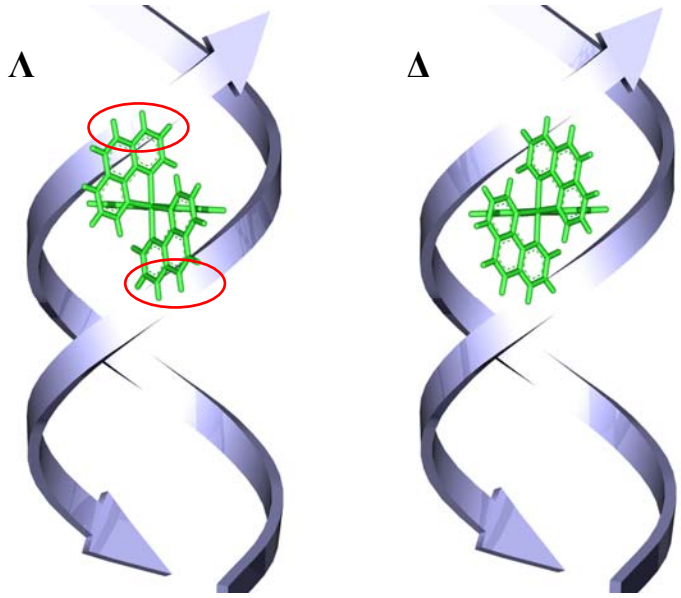


***Figure 1.21***
**The enantioselectivity of metal complex-DNA interactions.** The Λ enantiomer of $[Ru(phen)_3]^{2+}$ (left) experiences more significant steric interactions (designated by red ovals) with the backbone of a right-handed DNA helix than does the Δ enantiomer (right).

The intercalative model proposed by Barton *et al*. was supported by experiments utilising the analogous complex with diphenyl-substituted phenanthroline ligands. As expected, the phenyl groups heightened the observed enantioselectivity, purportedly by exaggerating the steric interactions between the Λ enantiomer and the phosphate backbone as well as enhancing the extent of intercalation.[486] Again, both enantiomers were found to bind to Z-DNA with equal affinity. Experiments conducted with the analogous cobalt complex, $[Co(DIP)_3]^{3+}$ {DIP = 4,7-diphenyl-1,10-phenanthroline}, revealed similar results with the cobalt analogue able to affect stereoselective photocleavage (the Λ enantiomer was capable of cleaving Z-DNA but not B-DNA).[487, 488] $[Ru(DIP)_3]^{2+}$ exhibited a greater binding affinity for B-DNA than did $[Ru(phen)_3]^{2+}$.[486] By contrast, $[Ru(bpy)_3]^{2+}$ {bpy = 2,2′-bipyridine}, lacking sufficiently elongated polyaromatic ligands to participate in intercalation, associates with DNA only weakly in what is believed to be primarily an electrostatic interaction.[489] It was proposed that the observed increase in binding affinity (bpy < phen < DIP) could be attributed to the increasing hydrophobicity and aromatic surface area of the ligands, and hence a greater intercalative ability.[490] Further photophysical studies gave the impression that while the Δ isomers of $[Ru(phen)_3]^{2+}$ and $[Ru(DIP)_3]^{2+}$ were indeed intercalating, the Λ isomers instead associated via a rather shallow groove-binding interaction (being based primarily on electrostatic attraction to the DNA).[489, 491] Ultimately, however, an intercalative binding mode for *either* enantiomer was brought into question.

Satyanarayana and co-workers used equilibrium dialysis and fluorescence titration experiments to confirm the enantioselectivity of $[Ru(phen)_3]^{2+}$; however, based on the outcome of viscosity experiments they concluded that neither enantiomer undergoes intercalation in the classical sense.[492] As previously discussed, classical intercalation results in a lengthening of the double helix which may be ascertained by an increased relative viscosity in electrophoretic mobility measurements. No increase was observed for either enantiomer of $[Ru(phen)_3]^{2+}$. By contrast, Kalsbeck and Thorp used thermodynamic calculations to confirm the presence of a significant non-electrostatic contribution towards the DNA-binding of $[Ru(phen)_3]^{2+}$ (although electrostatics were indeed deemed to be the dominating factor).[493] Scanning force microscopy investigations by Coury and co-workers also suggested a non-intercalative mode of binding.[494]

The NMR experiments of Collins *et al*. gave some indication that $[Ru(phen)_3]^{2+}$ may indeed be partially intercalating,[495] a result confirmed by more recent linear dichroism studies by Nordén and Lincoln.[496] They found that both enantiomers of the complex may bind with one

phenanthroline ligand partially (or "semi"- or "quasi"-) intercalated (via the minor groove), and their proposed binding geometry is in reasonable agreement with the available NMR data. This partial intercalation model is commonly seen amongst complexes which have polyaromatic ligands that are either of insufficient length to insert fully between stacked base pairs, or in cases where the intercalating ligand deviates from planarity, inhibiting complete insertion.[497] Indeed, a circular and linear dichroism study by Nordén and co-workers eventually dismissed not only the enantioselectivity of $[Ru(DIP)_3]^{2+}$, but also eliminated an intercalative binding mode for this complex.[498] It should be noted that in square-planar metal complexes such as $[Pt(en)(phen)]^{2+}$ the phen ligand *is* capable of participating in classical intercalation.[499]

The controversy surrounding the exact mode of binding adopted by $[Ru(phen)_3]^{2+}$, heightened by the relatively low binding affinity of the complex ($\sim 6 \times 10^3$ $M^{-1}$, dependent upon DNA sequence),[485, 491] was exacerbated by debate over *where* the complex was ultimately binding. Specifically, the identity of the groove via which the complex did or did not intercalate was the topic of considerable contention. The initial assumptions of Barton *et al*. were that, given the dimensions of the complex, it would be more readily accommodated if it were to intercalate from and/or bind in the *major* groove.[485, 489] These assumptions were reinforced experimentally with binding studies conducted with T4-DNA and double-stranded RNA.[491] T4-DNA is extensively glycosylated in the major groove, while the A-type conformation of double-stranded RNA possesses a very narrow major groove. Consequently, a major groove-binding complex would be expected to bind poorly to each of these nucleic acids – exactly what was observed in these studies. However, NMR studies conducted by Barton and co-workers suggested that the Λ isomer may actually bind in the *minor* groove of B-DNA.[500, 501] Further confusion arose when circular and linear dichroism studies by Nordén *et al*. indicated that both enantiomers were binding in the major groove – the Λ and Δ isomers with one and two phenanthroline "wings" projecting into the groove, respectively.[502] Importantly, such an orientation would rule out any intercalation of the Δ isomer. Despite molecular modeling/energy minimisation calculations supporting the major groove binding of both enantiomers,[503] Nordén and co-workers ultimately rejected their original major groove-binding model due to errors in the interpretation of the LD spectra. Two-dimensional NMR experiments revealed that both enantiomers of $[Ru(phen)_3]^{2+}$ bound in the minor groove of DNA.[504]

The numerous conflicting results regarding the site and orientation of binding have been attributed to variations in technique, DNA sequence and even metal complex/DNA/salt

concentrations.[505, 506] A minor groove-binding mode was consistent with the trend observed amongst the bulk of other polypyridylruthenium(II) complexes studied.[507-513] Competitive binding experiments conducted against distamycin A (a known minor groove-binder) supported the minor groove-binding model,[514] as did additional NMR experiments by Collins *et al*.[495] NMR experiments of Nordén and co-workers indicated that Δ-$[Ru(phen)_3]^{2+}$ binds preferentially to the central, electrostatically-favourable minor groove of the AT region of the decanucleotide $d(CGCGATCGCG)_2$,[504, 513] whereas experiments by Collins and co-workers established a preference for the adjacent CC/GG bases on a similar oligonucleotide, $d(TCGGGATCCCGA)_2$, where the minor groove is probably wider.[495] It therefore appears that sequence-dependent structural features influence the minor groove binding of $[Ru(phen)_3]^{2+}$. Even so, a minor groove-binding site remains far from universally accepted. For instance, Kuwabara and co-workers report on a technique for establishing the DNA-binding mode of antitumour and antiviral agents based on the electrochemiluminescence of *major* groove-bound $[Ru(phen)_3]^{2+}$.[515]

Amidst the $[Ru(phen)_3]^{2+}$ controversy, the binding nature of the related complex $[Ru(phen)_2(dppz)]^{2+}$ {dppz = dipyrido[3,2-*a*:2′,3′-*c*]phenazine} has also invoked vigorous debate.[516] Complexes based on the dppz ligand have received considerable attention due to their function as "molecular light switches". In aqueous solution $[Ru(bpy)_2(dppz)]^{2+}$ and $[Ru(phen)_2(dppz)]^{2+}$ are effectively quenched by the proton-donating solvent and show no luminescence, but when intercalated in DNA the hydrophobic environment allows them to luminesce strongly.[517-521] This luminescence enhancement is particularly large upon binding to triple-helical nucleic acids, making dppz-based complexes ideal probes for triplex structures.[522] Additionally, the facile electron transfer capabilities of intercalated ruthenium dppz complexes has seen their frequent use in studies of long-range DNA-mediated electron transfer.[517, 523-529] Unlike $[Ru(phen)_3]^{2+}$, the intercalative ability of the dppz ligand is unambiguous and undisputed, having been proven using a variety of techniques and methodologies.[507, 518, 530-534] $[Ru(phen)_2(dppz)]^{2+}$ has been found to bind to DNA with an association constant in excess of $10^6$ $M^{-1}$ [530, 532]. The extended planar aromatic ring system of the dppz ligand lends itself to intercalative stacking between base pairs much more readily than its smaller phen counterpart. Several complexes possessing intercalating ligands of similar structure to dppz have also been reported to exhibit the light-switch effect.[523, 535, 536] Nevertheless, there still exists a significant electrostatic contribution to the binding of dppz complexes:[530] the monocationic, achiral

analogue, $[RuCl(tpm)(dppz)]^+$ {where tpm is tris(1-pyrazolyl)methane}, has been found to bind to DNA with an affinity which is at least an order of magnitude below that of its dicationic dppz/tpm counterpart.[537]

Despite universal support for the intercalative binding mode of dppz-based complexes, the groove via which the complexes intercalated became a point of contention. Based on NMR studies, Barton and co-workers proposed intercalation of $[Ru(phen)_2dppz]^{2+}$ via the major groove.[538, 539] The addition of the minor groove-binder distamycin to a $[Ru(phen)_2(dppz)]^{2+}$-poly[$d(AT)_2$] system resulted in an increase in the luminescence intensity of the ruthenium complex, whereas the addition of the major-groove binder Δ-*α*-[Rh(*R*,*R*-$Me_2$trien)(phi)]$^{3+}$ {$Me_2$trien = 2,9-diamino-4,7-diazadecane; phi = 9,10-phenanthrernequinonediimine} to a $[Ru(phen)_2(dppz)]^{2+}$-[$d(GAGTGCACTC)_2$] complex produced a *decrease* in ruthenium emission:[540] these observations are consistent with intercalation of $[Ru(phen)_2(dppz)]^{2+}$ via the major groove.

Conversely, Nordén and co-workers have proposed intercalation via the minor groove. Their conclusions were based primarily upon linear dichroism experiments in which $[Ru(phen)_2(dppz)]^{2+}$ was found to have a binding geometry similar to that of actinomycin D, a known minor groove binder.[507] Photophysical studies involving T4-DNA[510] and a synthetic triplex in which the major groove is obstructed by a Hoogsteen-paired third strand also support intercalation from the minor groove.[508] Furthermore, linear dichroism studies of $[Ru(phen)_3]^{2+}$ (generally accepted as a minor groove-binder by this point) conducted by the Nordén group revealed a similar binding geometry to that of $[Ru(phen)_2(dppz)]^{2+}$.[496] Molecular modeling studies conducted on $[Co(phen)_2(dppz)]^{3+}$ are in agreement with the minor groove-binding model of Nordén et al.[541]

NMR studies have suggested that both Δ-$[Ru(phen)_2(dpq)]^{2+}$ {dpq = dipyrido[3,2-*d*:2′,3′-*f*]quinoxaline} and Δ-$[Ru(phen)_2(dpqC)]^{2+}$ {dpqC = dipyrido[3,2-*a*:2′,3′-*c*](6,7,8,9-tetrahydro)phenazine} bind via the minor groove.[495, 509] Given the similar shape of the dpq and dpqC ligands to dppz it is not unreasonable to infer that the complexes possessing these ligands might assume similar binding geometries (that is, they may all bind via the minor groove). However, the dpq and dpqC complexes do not bind to DNA as strongly as do their dppz or dppx {dppx = 7,8-dimethyldipyridophenazine} analogues.[542] It is believed that dpq and dpqC do not intercalate as effectively as dppz or dppx, both of which possess larger aromatic areas that may potentially stack between DNA bases. This increased π-stacking ability not only

enhances binding affinity, but also increases the efficiency of DNA-mediated charge transfer, as demonstrated in oxidative damage investigations. In experiments by Delaney *et al*., $[Ru(bpy)_2(dppz)]^{2+}$ and $[Ru(bpy)_2(dppx)]^{2+}$ exhibited the highest extent of charge transport damage, the (partially) intercalating $[Ru(bpy)_2(dpq)]^{2+}$ and $[Ru(bpy)_2(dpqC)]^{2+}$ complexes showed intermediate levels of damage, and $[Ru(bpy)_3]^{2+}$ – a non-intercalator – demonstrated negligible effects.[542]

Additional NMR experiments conducted by the Collins *et al.* on $[Ru(Me_2phen)_2(dpq)]^{2+}$ and $[Ru(Me_2phen)_2(dppz)]^{2+}$ {$Me_2$phen = 2,9-dimethyl-1,10-phenanthroline} also suggested intercalation via the minor groove (methylated phenanthroline ligands were used to simplify the NMR spectra and to provide strong NOE signals in NOESY spectra).[511, 512] Recently, Nordén and co-workers conceded the possibility of intercalation from either groove when the other is blocked; this concession was based in-part on spectroscopic investigations into the properties of DNA-bound $[Ru(phen)_2(dppz)]^{2+}$ in the presence and absence of the minor-groove binder DAPI.[543, 544]

Negligible enantioselectivity was observed in the DNA-binding of the complex $[Ru(phen)_2(dppz)]^{2+}$ [511, 532] and its 2,2′-bipyridine analogue $[Ru(bpy)_2(dppz)]^{2+}$,[544] although in each case differential luminescence and binding rates were observed between the Δ and Λ isomers, suggesting different binding geometries for each enantiomer. While $[Ru(phen)_2(dppz)]^{2+}$,[540] $[Ru(TAP)_2(dppz)]^{2+}$ {TAP = 1,4,5,8-tetraazaphenanthrene},[545] and $[Os(phen)_2(dppz)]^{2+}$ [546] each exhibited decidedly different photophysical and photochemical properties, they possess nearly identical DNA-binding profiles (including a small preference for AT-rich sequences). These similar binding modes would seemingly reflect the efficient intercalative ability of the dppz ligand.

The bulk of studies conducted into polypyridyl complex-nucleic acid interactions have concerned themselves with intercalating mononuclear complexes, typically of the form $[Ru(ancillary)_2(intercalator)]^{2+}$, where there is a single dedicated intercalating ligand and a pair of ancillary ligands that occupy the groove (to a variable extent). Due to the three-dimensional nature of the association between these octahedral complexes and their chiral polynucleotide targets, the nature of all the ligands, ancillary or intercalating, influences the binding affinity of the complex. As evidenced above with the comparisons between dpq/dpqC and dppz/dppx, a larger intercalative surface area generally correlates with a greater binding affinity.[547] Molecular modeling experiments suggest that increasing the *length* of the intercalating ligand

favours binding via the minor groove, whereas increases to the *width* of this ligand promotes binding from the major groove.[548] These findings are corroborated by experimental results obtained with Ru(II) and Rh(III) complexes featuring the relatively wide intercalating ligand phi. NMR experiments suggest that Δ-cis-*α*-[Ru(RR-picchxnMe$_2$)(dpq)]$^{2+}$ {picchxnMe$_2$ = *N*,*N*′-dimethyl-*N*,*N*′-di(2-picolyl)-1,2-diaminocyclohexane} intercalates via the minor groove of DNA, whereas the analogous complex with a phi intercalator, Δ-cis-*α*-[Ru(RR-picchxnMe$_2$)(phi)]$^{2+}$, binds via the major groove.[549] Intriguingly, complexes with a pair of diimine quinone ligands have been found to stabilise double-stranded DNA and impair transcription, while their single diimine quinone counterparts were less effective in this regard.[550] Enhanced binding by a complex with a single ancillary and two intercalating ligands has been reported for other intercalators as well.[551] Studies of octahedral rhodium complexes featuring the phi ligand have been particularly prolific, and such species almost invariably intercalate via the major groove.[552] Rhodium complexes containing phi, or derivatives thereof, have demonstrated an impressive degree of selectivity for features such as base sequences,[552, 553] sequence-dependent twisting,[554, 555] base mismatches,[415, 556] and base triples.[557] They have also proven useful in selectively targeting specific RNA structures, such as folded tRNA[558] or the HIV-1 TAR bulge site.[559] The usual enantioselectivity favouring the Δ enantiomer is typically observed in nucleic acid-binding experiments with these complexes.[560]

As previously alluded to, the planarity of the intercalating ligand is also of particular significance in governing the binding affinity of these complexes.[561] A major factor in the dismissal of a probable intercalating binding mode for [Ru(DIP)$_3$]$^{2+}$ is the non-planarity of the diphenylphenanthroline ligand. The torsion angle between the phenanthroline moiety and its phenyl substituent prohibits a deep insertion of the ligand into the groove, making intercalation unlikely.[498, 562] The issue of planarity is further highlighted by comparisons between the DNA-binding of the complexes [Ru(bpy)$_2$(CIP)]$^{2+}$ and [Ru(bpy)$_2$(NIP)]$^{2+}$, which possess non-planar intercalating ligands, and their parent complex [Ru(bpy)$_2$(PIP)]$^{2+}$ which has a planar intercalating ligand {CIP = 2-(2-chlorophenyl)imidazo[4,5-*f*]1,10-phenanthroline; NIP = 2-(2-nitrophenyl)imidazo[4,5-*f*]1,10-phenanthroline; PIP = 2-phenylimidazo[4,5-*f*]1,10-phenanthroline}. DNA viscosity experiments suggest a classical intercalation mode for the PIP complex, whereas the derivatives can only achieve partial intercalation due to the non-planarity of the ligands.[563, 564] Similarly, comparisons between the binding affinities of [Ru(bpy)$_2$(taptp)]$^{2+}$ {taptp = 4,5,9,18-tetraazaphenanthreno[9,10-*b*]triphenylene} and

$[Ru(bpy)_2(dptatp)]^{2+}$ {dptatp = 2,3-diphenyl-1,4,8,9-tetraazatriphenylene} reveal that the former complex, with its planar intercalating ligand, binds with greater affinity than does the latter, which possesses an analogous non-planar intercalator.[565] Luedtke and Tor have demonstrated the biological ramifications of such selectivity in experiments involving HIV-1 RNA and complexes of the form $[Ru(bpy)_2(L)]^{2+}$, where L is either the planar, aromatic ligand eilatin or a non-planar precursor "pre-eilatin": the complexes possessing the "pre-eilatin" ligand had a significantly lower binding affinity and anti-HIV activity than did those with eilatin.[142, 566, 567] Substituents on the intercalating ligand can be influential even if they do not significantly affect the planarity of the ligand:[568, 569] the addition of an electron-withdrawing –CN substituent on the dpq ligand greatly enhances its DNA affinity,[570] while an $–NO_2$ substituted dppz ligand proves to be a more effective DNA binder than does the analogous –OH substituted ligand.[571]

The role of ancillary ligands should also not be overlooked, as the steric bulk of the nonintercalating ligand directly influences how deeply the complex may intercalate. Alternatively, hydrophobic interactions, van der Waals contacts, and hydrogen bonding brought about by the ancillary ligands are believed to be the major driving forces behind many DNA/complex associations.[512, 530] A good illustration of this is the complex $[Ru(IP)_2(dppz)]^{2+}$ {IP = imidazole[4,5-*f*][1,10]phenanthroline}, which with its bulkier aromatic ancillary ligands, binds to DNA with an affinity several times that of its parent complex $[Ru(bpy)_2(dppz)]^{2+}$.[572] Likewise, $[Ru(phen)_2(DMHBT)]^{2+}$ {DMHBT = 11,13-dimethyl-13H-4,5,9,11,14-hexaaza-benzo[*b*]triphenylene-10,12-dione} binds to calf thymus DNA with a greater affinity than $[Ru(bpy)_2(DMHBT)]^{2+}$.[573] Increased hydrophobicity in the form of carefully-placed methyl groups can also strengthen the DNA-complex interaction: $[Ru(5,6\text{-}Me_2phen)_2(dppz)]^{2+}$ {5,6-$Me_2$phen = 5,6-dimethyl-1,10-phenanthroline} binds stronger than does $[Ru(phen)_2(dppz)]^{2+}$ [574] and, similarly, $[Ru(NH_3)_4(5,6\text{-}Me_2phen)]^{2+}$ binds stronger than does $[Ru(NH_3)_4(phen)]^{2+}$ even though the former cannot intercalate due to the bulky substituents on the intercalative ligand.[575] However, methylation at the 2- and 9-positions of phenanthroline ligands introduces steric hinderance, preventing deep groove binding of octahedral metal complexes.[574, 575] As originally postulated for $[Ru(DIP)_3]^{2+}$, increasing the relative bulk of the ancillary ligands, which exaggerates any unfavourable chiral interactions with the groove walls, is the predominant factor in governing enantiopreferential interactions with the nucleic acids. Although the enantioselectivity of $[Ru(DIP)_3]^{2+}$ was brought into doubt, bulky ancillary ligand substituents, when correctly placed, can certainly lead to the preferential binding of one complex enantiomer

(typically Δ) over the other.[511, 547, 576, 577] The ability of particular enantiomers to recognise specific nucleic acid conformations has been demonstrated in several different complexes. For instance, Δ-$[Ru(5,6\text{-}Me_2phen)_3]^{2+}$ preferentially binds B-DNA whereas the Λ enantiomer prefers Z-DNA,[578] while Λ-$[Ru(Me_4phen)_3]^{2+}$ {$Me_4$phen = 3,4,7,8-tetramethyl-1,10-phenanthroline} has been touted as a probe of A-form DNA and RNA.[423, 579, 580] Ultimately, how well the ancillary ligands complement the shape of the groove in which they are binding (which itself depends on the nature of the target nucleic acid) may be the most significant factor governing binding.[562]

### 1.4.2 Dinuclear Complexes

The utility of *mononuclear* metal complexes as probes into the structural recognition mechanisms of polynucleotides is limited by their relatively small size. A typical mononuclear complex may, at best, span only 4-6 base-pairs; typically they only have a footprint of two bases.[581] Clearly, larger species will be required to mimic the selectivity of nucleic acid-binding proteins. Additionally, mononuclear complexes generally possess low binding affinities (typically ~$10^3$-$10^5$ $M^{-1}$, with the exception of strong intercalators like the dppz complexes) and consequently they are displaced from nucleic acids at relatively low ionic strengths, limiting their application in environments encountered *in vivo*.[582] In contrast, di-, tri- and oligonuclear metal complexes are not only larger (and therefore able to span a greater number of base-pairs), but they also possess a greater stereochemical diversity, allowing them to more effectively probe the shape- and structure-recognition mechanisms of nucleic acids than their mononuclear counterparts. Furthermore, dinuclear species possess a larger cationic charge; they may potentially have greater nucleic acid-binding affinities than mononuclear complexes; the presence of *two* metal centres amplifies any possible chiral discrimination effects; and the larger size of the complex results in considerably slower DNA-dissociation rates (a property that is advantageous to both the biological activity and NMR studies of such complexes). However, the nucleic acid-binding of multinuclear polypyridyl ruthenium complexes has received relatively little attention.

The potential appeal of a dinuclear binding species was first explored in the form of bis-intercalating organic molecules. These essentially consisted of two intercalating chromophores (ethidium or similar) joined via a flexible polyamine/alkane linker.[583] Such dyes bound double-

stranded DNA with an affinity several orders of magnitude higher than their monomeric analogues, a result that would encourage the design of flexibly-bridged dinuclear nucleic acid-binding metal complexes. For example, Kelly and co-workers have compared the binding behaviour of the dinuclear complex $[(bpy)_2Ru\{Mebpy(CH_2)_nbpyMe\}Ru(bpy)_2]$ {Mebpy = 4-methyl-2,2′-bipyridine; $n$ = 3 or 5} with its mononuclear analogues $[Ru(bpy)_3]^{2+}$ and $[Ru(bpy)_2(Me_2bpy)]^{2+}$ {$Me_2$bpy = 4,4′-dimethyl-2,2′-bipyridine} and found that the bimetallic species has a much higher binding affinity, is more efficient at photosensitising DNA strand breaks, and its binding affinity is less sensitive to ionic strength.[584, 585] The complex appeared to assume several different binding modes (possibly attributable to the different stereoisomers), each of which were mainly electrostatic in nature. Additional investigations were undertaken with $[(phen)_2Ru\{Mebpy(CH_2)_nbpyMe\}Ru(phen)_2]$ {where $n$ = 5, 7, or 10}.[582] Again, the dinuclear complex was found to have a stronger binding affinity than its mononuclear counterpart, $[Ru(phen)_2(Me_2bpy)]^{2+}$, and that the binding affinity was dependent upon the linker chain length. The most effective binding was observed at $n$ = 7, somewhat shorter than the optimal chain length ($n$ > 8) of the classical intercalators with polymethylene chains.[583] This shorter chain length is consistent with partial intercalation of a phenanthroline ligand on each metal centre.[582] Aldrich-Wright *et al*. have investigated a similar flexible-linker dimer, $[\{Ru(dpq)_2\}_2(\mu\text{-phen-}x\text{–SOS–}x\text{-phen})]^{4+}$ {SOS = 2-mercaptoethyl ether; the attachment position of the linker, $x$, is 4 or 5}, featuring intercalating terminal ligands on each of the metal centres.[581] The complex was found to have a binding affinity of approximately $6 \times 10^7$ $M^{-1}$, far in excess of its mononuclear counterpart $[Ru(dpq)_2(phen)]^{2+}$ ($K = 5.4 \times 10^4$ $M^{-1}$).[542] Furthermore, the complex demonstrated some degree of specificity for purine-purine steps and has the potential for hydrogen-bonding interactions with the S—O—S bridge. Nakabayashi and co-workers also describe a series of flexible diamine-bridged dinuclear ruthenium(II) complexes that vary in their affinity based on length. Unlike the examples discussed above, these complexes formed covalent bonds with a specificity for guanine residues.[586]

While the species described above interact with DNA largely via their metal centres (and terminal ligands), a number of complexes that bind via an intercalating *bridging* ligand have also been reported. Perhaps the earliest example of this was the 2,3-bis(2-pyridyl)bezo[*g*]quinoxaline {dpb} bridged species described by Carlson *et al*.[587] It was found that $[\{Ru(NH_3)_4\}_2(\mu\text{-dpb})]^{4+}$ bound with an affinity similar to that of a mononuclear dppz-based intercalator, whereas $[\{Ru(bpy)_2\}_2(\mu\text{-dpb})]^{4+}$ bound rather weakly. This discrimination between

the two complexes was attributed to the increased steric bulk of the bpy ancillary ligands interfering with complete insertion of the intercalating dpb moiety in the latter case and potential affinity-enhancing hydrogen-bonding from the $NH_3$ ligands in the former.

Further studies on complexes in which the bridging ligand was extended into a bis-intercalating moiety revealed very interesting binding dynamics. Complexes of the form [$\mu$-(11,11′-bidppz)$(L)_4Ru_2]^{4+}$ {11,11′-bidppz = 11,11′-bis(dipyrido[3,2-*a*:2′,3′-*c*]phenazine; L = bpy or phen}, bridged by a bis-dppz moiety, have been found to assume different binding geometries dependent upon the stereochemistry and ancillary ligands of the metal centres. Linear dichroism experiments originally suggested that both metal centres were associating in the major groove, albeit with slightly different orientations between the enantiomers (ΔΔ and ΛΛ).[588] Phen terminal ligands invoked some degree of enantioselectivity, whereas bpy ligands had no such effect. A serendipitous re-examination of the binding some two weeks later revealed a dramatically different binding profile: one end of the complex had effectively threaded through the DNA helix.[589] This threading was accompanied by a luminescence increase akin to that observed for the strongly-intercalating dppz complexes. Further investigation showed that, for both enantiomers of the species with bpy terminal ligands and for the ΛΛ enantiomer of the phen complex, one $Ru(L)_2$ moiety was located in each groove. ΔΔ-[$\mu$-(11,11′-bidppz)$(phen)_4Ru_2]^{4+}$ remained orientated such that both metal centres still occupied the major groove.[589, 590] The *meso* diastereoisomer of the complex was subsequently used to establish the preferential binding of the Λ moiety in the minor groove and the Δ moiety in the major groove, with the bidppz linker intercalated between the nucleobases.[590] It appears that the complex initially assumed a metastable major groove-bound state before threading through the double helix. Interestingly, the threading kinetics appeared to operate remarkably slowly for GC-rich oligonucleotides and calf thymus DNA, but was near instantaneous for AT-rich oligonucleotides.[590] The threaded complex demonstrated a very high affinity for DNA ($\sim 10^{12}$ $M^{-1}$).

The introduction of some greater degree of flexibility between the two bridging dppz moieties was found to result in more expedient threading. The complex [$\mu$-$C4(cpdppz)_2(phen)_4Ru_2]^{4+}$ {$C4(cpdppz)_2$ = *N*,*N*′-bis(12-cyano-12,13-dihydro-11H-8-cyclopenta[*b*]dipyrido[3,2-*h*:2′,3′-*j*]phenazine-12-carbonyl)-1,4-diaminobutane} threaded through the DNA helix such that the ancillary phen ligands sat in the minor groove while the flexible linker occupied the major groove.[591, 592] In contrast to the semi-rigid bis-dppz bridge

described above, this complex was fully intercalated within approximately 30 minutes. The threading process is believed to require extensive conformational changes to the DNA helix, including the breaking and re-forming of base pairs. This is supported by the observation that, as with the bidppz-bridged species, AT-threading was faster than that for GC-rich sequences due to the stronger base-pairing of the latter. Dissociation of the ΛΛ-enantiomer from calf thymus DNA was considerably faster and more dependent upon ionic strength than was the ΔΔ-enantiomer. Nevertheless, the two enantiomers were found to possess very similar binding affinities.[592]

Other intercalative bridging moieties used in the study of DNA-binding dinuclear ruthenium complexes include phenanthroline/imidazole derivatives[593, 594] and porphyrins,[595] each of which yielded only moderate binding affinities. In one notable example of the former category, the complex $[(bpy)_2Ru(ebipcH2)Ru(bpy)_2]^{4+}$ {ebipcH2 = N-ethyl-4,7-bis(imidazolo[4,5-*f*]-(1,10-phenanthrolin)-2-yl)carbazole} was found to intercalate in yeast tRNA with a much greater affinity than calf thymus DNA.[596] Another particularly interesting species utilised the intercalative bridge bipp {bipp = 2,9-bis(2-imidazo[4,5-f][1,10]phenanthroline)-1,10-phenanthroline} which features vacant chelating sites well-suited to the binding of a third metal ion, specifically $Cu^{2+}$. The emissive properties of the complex were quenched upon binding of the copper ion, whereas the DNA-bound complex exhibited a large increase in emission. Subsequent addition of copper ions to the complex-DNA system had no effect because the chelating site was blocked upon intercalation.[597, 598] This is in contrast with the so-called "molecular nut and bolt" system of $[Ru(bpy)_2(tpphz)]^{2+}$ {tpphz = tetrapyrido[3,2-*a*:2′,3′-*c*:3″,2″-*h*: 2″,3″-*j*]phenazine}, which possesses a similar chelating site on the tpphz ligand. Upon intercalation with DNA, the chelating site projects out of the opposite side of the helix where it can coordinate a copper ion, quenching the emission of the complex and locking it in place.[599] Many multi-nuclear species incorporating mixed-metal polypyridyl systems have shown considerable promise as photoactivated drugs: for instance, trinuclear Ru-Rh species (essentially two $Ru(L)_2$ moieties linked to a $RhCl_2$ core via 2,3-dpp bridges {2,3-dpp = 2,3-bis(2-pyridyl)pyrazine}) have demonstrated visible light-induced photocleavage of DNA.[600] This has been attributed to a Ru → Rh metal-to-metal charge-transfer excited state and is dependent upon the nature of the bridging ligand (the analogous complex with 2,2′-bipyrimidine {bpm} bridges was inactive).[601] Ru/Pt mixed species, bridged by 2,3-dpp, dpq and

dpb ligands, have been found to bind DNA covalently via the square-planar platinum moiety.[602, 603]

Several non-intercalative, semi-rigid dinuclear complexes have also been investigated. Complexes bridged by the asymmetric phenanthroline derivative pztp {(3-pyrazin-2-yl)-*as*-triazino[5,6-*f*]-1,10-phenanthroline} have been found to bind via electrostatic/groove binding interactions whereas the mononuclear equivalent intercalates.[604] Furthermore, the groove complementarity necessary for intercalation means that the mononuclear complex exhibits enantioselectivity whereas the (relatively) loosely-associating dinuclear species does not. Jiang and co-workers have surveyed a number of dinuclear complexes featuring bridges derived from bpy.[605-608] They all bind via a non-intercalative mode with modest binding affinities, however in a number of cases they exhibit intriguing enantiopreferences in which the ΛΛ enantiomer appears to be the stronger binding.[605, 608]

Collaborations between the laboratories of Keene and Collins have adopted a somewhat different approach to investigations of dinuclear DNA-binding complexes by utilising rigid, groove-binding complexes instead of the intercalating or semi-rigid species described above. These studies have extended from initial investigations, conducted by the laboratories of Kirsch-De Mesmaeker and Keene into the complex $[\{Ru(phen)_2\}_2(\mu\text{-HAT})]^{4+}$ {HAT = 1,4,5,8,9,12-hexaazatriphenylene}, a relatively weak minor groove-binder. Photophysical investigations revealed that very little luminescence increase was observed upon interaction with double-stranded DNA, however in the presence of *denatured* (partially single-stranded) DNA, a large increase was observed.[609-611] Indeed, the complex was found to form photoadducts with guanosine monophosphate and single-stranded DNA, but not double-stranded DNA.[612] Subsequent NMR investigations into the binding of bpm-bridged species to double-stranded oligonucleotides reaffirmed the apparent selectivity of this class of complex for more open and/or flexible sites within polynucleotides.[613, 614] Initial studies by Keene, Collins, *et al.* found that the complex $[\{Ru(Me_2bpy)_2\}_2(\mu\text{-bpm})]^{4+}$ bound to the minor groove of the duplex DNA sequence $d(CAATCCGGATTG)_2$ with a modest affinity (~2-3 × $10^3$ $M^{-1}$) and a small enantioselectivity in favour of the ΔΔ enantiomer. Two-dimensional NMR experiments demonstrated that the complex preferably bound to the central CCGG sequence of the oligonucleotide. Conversely, the analogous complex with unmethylated bipyridine terminal ligands, $[\{Ru(bpy)_2\}_2(\mu\text{-bpm})]^{4+}$, bound with a greater degree of enantioselectivity (again for the ΔΔ enantiomer) and a larger binding affinity (*ca.* 1 × $10^4$ $M^{-1}$ for the ΔΔ enantiomer, 4 ×

$10^3$ $M^{-1}$ for the ΛΛ enantiomer).[615] Furthermore, the unmethylated complexes favoured the peripheral AAT/ATT region of the duplex. It was believed that the bulkier methylated bipyridine ligands are not readily accommodated by the narrow minor groove of the duplex, thus decreasing both binding affinity and enantioselectivity. This conclusion was further supported by experiments utilising $[\{Ru(Me_2bpy)_2\}_2(\mu\text{-bpm})]^{4+}$ and an oligonucleotide in which the central GC-rich sequence was subtly altered: *viz*. $d(CAATCGCGATTG)_2$. In this instance the methylated complex also bound at the peripheral AT-rich regions with an affinity of similar magnitude to that of the unmethylated species. Overall the results suggested a compromise between more a favourable electrostatic environment (the more electronegative minor groove of AT-rich sequences) and a binding site more accommodating of a bulky complex (the wider minor groove of the central CCGG sequence). The increased steric bulk of $[\{Ru(Me_2bpy)_2\}_2(\mu\text{-bpm})]^{4+}$, not easily accommodated within the narrow minor groove of the AT-rich region, bound instead at the more open CCGG sequence. Changing this sequence to CGCG is believed to have invoked steric clashes between the complex and the now-alternating guanine amino groups within the minor groove. Consequently, $[\{Ru(Me_2bpy)_2\}_2(\mu\text{-bpm})]^{4+}$ preferentially binds the AT-rich regions of $d(CAATCGCGATTG)_2$.

The utility of these complexes as probes of distinct secondary structure features within nucleic acids, specifically more open binding sites, was confirmed by further experiments demonstrating total enantioselectivity in the binding of $[\{Ru(Me_2bpy)_2\}_2(\mu\text{-bpm})]^{4+}$ to an oligonucleotide possessing a single-base bulge $\{d(CCGAGAATTCCGG)_2\}$.[616, 617] Two-dimensional NMR spectra showed that the ΔΔ enantiomer bound reasonably strongly (in excess of $10^5$ $M^{-1}$) to the oligonucleotide at the site of the unpaired adenine base, whereas the ΛΛ enantiomer bound weakly to the central AT-rich region and frayed ends of the oligonucleotide. As might be expected, the *meso* (ΔΛ) stereoisomer bound with intermediate selectivity and affinity. The ability of the non-symmetric dinuclear species, ΔΔ-$[\{Ru(Me_2bpy)_2\}(\mu\text{-bpm})\{Ru(bpy)_2\}]^{4+}$, to bind to the bulge sequence was also investigated.[616] In contrast to the experiments conducted with canonical duplex sequences described above, methylation in this instance seems to be a boon rather than a hindrance. NMR spectra showed definitively that the complex bound selectively at the bulge site with the $Ru(Me_2bpy)_2$ moiety projecting more deeply into the bulge site than the non-methylated end of the complex. Such a result would seem to be indicative of the more open and flexible bulge site being able to better facilitate a

hydrophobic interaction between the complex, secreting its $Me_2$bpy ligands away from the bulk solution, and the minor groove of the oligonucleotide.

This thesis builds upon these latter revelations by investigating a series of dinuclear polypyridylruthenium(II) complexes and their stereoselective interactions with nucleic acids of diverse secondary structures. The function – and dysfunction – of nucleic acids is largely influenced by their structure, thus a firm understanding of those structures and their intermolecular interactions is invaluable to the rational design of more effective and efficient diagnostic and therapeutic agents. Inert metal complexes have proven themselves to be well suited to probing those factors that govern these structure-specific interactions owing to the reversibility of their association with nucleic acids, their useful spectro- and electrochemical properties, and the synthetic versatility of such species. The experiments described above demonstrated the considerable potential of rigid dinuclear complexes as stereoselective probes of a single-base bulge site within a DNA duplex; the present study expands upon these findings by exploring the effects of changes to the geometry and size of these complexes through variations in bridging and terminal ligands on their affinity to a variety of different nucleic acid structures and sequences. These experiments imply that one may potentially fine-tune the structure and functionality of this genre of metal complex in order to target specific nucleic acid sites.

- Chapter 2 details the synthetic methodologies used to prepare an array of complexes of the form $[\{Ru(pp)_2\}_2(\mu\text{-BL})]^{4+}$ {where pp represents one of the non-intercalating polypyridyl terminal ligands bpy, $Me_2$bpy, phen, or $Me_2$phen, and BL represents one of the symmetrical, non-intercalating bridging ligands bpm, HAT, ppz, 2,3-dpp, or 2,5-dpp; see Figure 1.22}, as well as describing the cation-exchange chromatographic techniques used to purify and isolate the various stereochemical (diastereoisomeric and enantiomeric) forms of each.

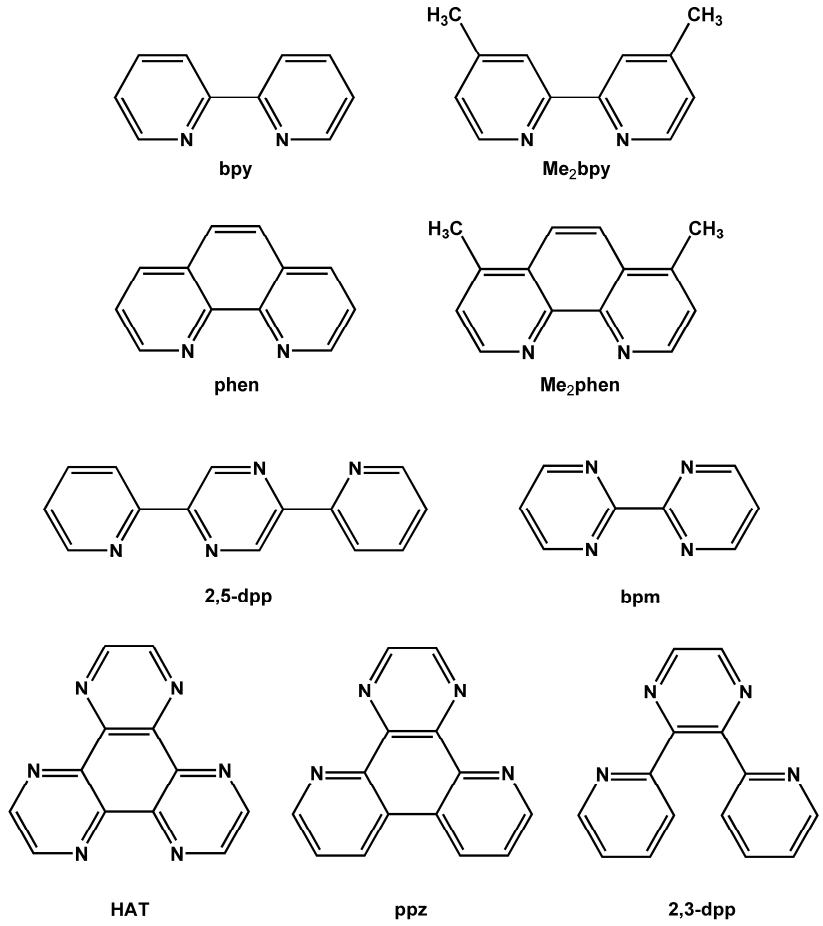


***Figure 1.22***
**Ligands used in these studies.** The polypyridyl bridging and terminal ligands used in the synthesis of complexes of the form $[\{Ru(pp)_2\}_2(\mu\text{-BL})]^{4+}$ for DNA-binding studies. The structure of other ligands mentioned in the text may be found in Appendix A.

- Chapter 3 discusses spectrophotometric surveys of the interactions between these complexes and a variety of different nucleic acids. Fluorescent intercalator displacement (FID) assays (and modifications of the assay using DAPI, a non-intercalative fluorescent agent) were used to qualitatively assess the relative binding affinities of this range of complexes against a large selection of oligonucleotides possessing distinctive sequences and secondary structures. These surveys reveal that those complexes based upon angular bridging ligands like HAT, ppz and 2,3-dpp typically exhibit the greatest binding affinities, with a particular propensity for more open secondary structures. Complementary UV/Vis spectroscopy titrations are employed to further quantify the interactions between these metal complexes and generic nucleic acids.

- Chapter 4 reports upon the results of a number of more comprehensive, NMR-based investigations into the specific oligonucleotide interactions of HAT- and ppz-bridged complexes. These species demonstrated particularly strong affinities for hairpin and AT-rich oligonucleotides, respectively, in the spectroscopic surveys, and were subjected to one- and two-dimensional NMR experiments which (in association with molecular modelling studies) provide a more detailed picture of the selectivity inherent in this genre of nucleic acid-binding metal complexes.

2 Finally, Chapter 5 describes a high-resolution affinity chromatography technique arising from the reverse application of the principles of DNA-binding specificity elaborated upon in the rest of the thesis. The stereo- and structure-selective affinities of the dinuclear polypyridylruthenium(II) complexes employed in these studies result in highly efficient separations of diastereoisomers and resolutions of enantiomers on a non-duplex DNA medium. The technique is employed as a simple means to establish the relative binding affinities of different complexes or stereoisomers.

## 1.5 REFERENCES


1. J. D. Watson and F. H. C. Crick, *Nature*, **1953**, *171*, 737-738.
2. International Human Genome Sequencing Consortium, *Nature*, **2001**, *409*, 860-921.
3. F. Crick, *Nature*, **1970**, *227*, 561-563.
4. J. S. Mattick, *Science*, **2005**, *309*, 1527-1528.
5. J. S. Mattick and I. V. Makunin, *Hum. Mol. Genet.*, **2006**, *15*, R17-R29.
6. C. A. Hunter, K. R. Lawson, J. Perkins and C. J. Urch, *J. Chem. Soc., Perkin Trans.*, **2001**, *2*, 651-669.
7. E. Pennisi, *Science*, **2007**, *316*, 1113.
8. Z. Herceg, *Mutagenesis*, **2007**, *22*, 91-103.
9. A. D. Goldberg, C. D. Allis and E. Bernstein, *Cell*, **2007**, *128*, 635-368.
10. M. F. Fraga, E. Ballestar, M. F. Paz, S. Ropero, F. Setien, M. L. Ballestar, D. Heine-Suñer, J. C. Cigudosa, M. Urioste, J. Benitez, M. Boix-Chornet, A. Sanchez-Aguilera, C. Ling, E. Carlsson, P. Poulsen, A. Vaag, Z. Stephan, T. D. Spector, Y.-Z. Wu, C. Plass and M. Esteller, *Proc. Natl. Acad. Sci. USA*, **2005**, *102*, 10604-10609.
11. J. Wysocka, T. Swigut, H. Xiao, T. A. Milne, S. Y. Kwon, J. Landry, M. Kauer, A. J. Tackett, B. T. Chait, P. Badenhorst, C. Wu and C. D. Allis, *Nature*, **2006**, *440*, 86-90.
12. T. Kouzarides, *Cell*, **2007**, *128*, 693-705.
13. T. Jenuwein and C. D. Allis, *Science*, **2001**, *293*, 1074-1080.
14. G. Egger, G. Liang, A. Aparicio and P. A. Jones, *Nature*, **2004**, *429*, 457-463.
15. A. C. D'Alessio and M. Szyf, *Biochem. Cell Biol.*, **2006**, *84*, 463-476.
16. B. F. Vanyushin, *Russian J. Genet.*, **2006**, *42*, 985-997.
17. M. Rassoulzadegan, V. Grandjean, P. Gounon, S. Vincent, I. Gillot and F. Cuzin, *Nature*, **2006**, *441*, 469-474.
18. N. B. Leontis, J. Stombaugh and E. Westhof, *Nucleic Acids Res.*, **2002**, *30*, 3497-3531.
19. S. Neidle, *Nucleic Acid Structure and Recognition*, Oxford University Press, New York, NY, USA, **2002**.
20. S. Diekmann, *J. Mol. Biol.*, **1989**, *205*, 787-791.
21. R. E. Dickerson, M. Bansal, C. R. Calladine, S. Diekmann, W. N. Hunter, O. Kennard, E. von Kitzing, R. Lavery, H. C. M. Nelson, W. K. Olson, W. Saenger, Z. Shakked, H. Sklenar, D. M. Soumpasis, C.-S. Tung, A. H.-J. Wang and V. B. Zhurkin, *Nucleic Acids Res.*, **1989**, *17*, 1797-1803.
22. Z. Shakked, G. Guerstein-Guzikevich, M. Eisenstein, F. Frolow and D. Rabinovich, *Nature*, **1989**, *342*, 456-460.
23. R. E. Dickerson, H. R. Drew, B. N. Conner, R. M. Wing, A. V. Fratini and M. L. Kopka, *Science*, **1982**, *216*, 475-485.
24. P. Belmont, J.-F. Constant and M. Demeunynck, *Chem. Soc. Rev.*, **2001**, *30*, 70-81.
25. N. C. Seeman, J. M. Rosenberg and A. Rich, *Proc. Nat. Acad. Sci. USA*, **1976**, *73*, 804-808.
26. R. E. Franklin and R. G. Gosling, *Nature*, **1953**, *172*, 156-157.
27. X.-J. Lu, Z. Shakked and W. K. Olson, *J. Med. Biol.*, **2000**, *300*, 819-840.
28. V. I. Ivanov, L. E. Minchenkova, B. K. Chernov, P. McPhie, S. Rya, S. Garges, A. M. Barber, V. B. Zhurkin and S. Adhya, *J. Mol. Biol.*, **1995**, *245*, 228-240.
29. Y. Mo, B. Vaessen, K. Johnston and R. Marmorstein, *Mol. Cell*, **1998**, *2*, 201-212.

30. S. C. Mohr, N. V. H. A. Sokolov, C. He and P. Setlow, *Proc. Natl. Acad. Sci. USA*, **1991**, *88*, 77-81.
31. P. Setlow, *Molec. Microbiol.*, **1992**, *6*, 563-567.
32. J. R. Kiefer, C. Mao, J. C. Braman and L. S. Beese, *Nature*, **1998**, *391*, 304-307.
33. Y. Timsit, *J. Mol. Biol.*, **1999**, *293*, 835-853.
34. J. I. Gyi, A. N. Lane, G. L. Conn and T. Brown, *Nucleic Acids Res.*, **1998**, *26*, 3104-3110.
35. J. Fohrer, M. Hennig and T. Carlomagno, *J. Mol. Biol.*, **2006**, *356*, 280-287.
36. W. L. De Lano, *The PyMOL Molecular Graphics System*, De Lano Scientific, Palo Alto, CA, USA, **2002**, http://www.pymol.org.
37. A. H.-J. Wang, G. J. Quigley, F. J. Kolpak, J. L. Crawford, J. H. van Boom, G. van der Marel and A. Rich, *Nature*, **1979**, *282*, 680-686.
38. F. M. Pohl and T. M. Jovin, *J. Mol. Biol.*, **1972**, *67*, 375-396.
39. M. Behe and G. Felsenfeld, *Proc. Natl. Acad. Sci. USA*, **1981**, *78*, 1619-1623.
40. W. Zacharias, A. Jaworski and R. D. Wells, *J. Bacteriol.*, **1990**, *172*, 3278-3283.
41. M. A. Fuertes, V. Cepeda, C. Alonso and J. M. Perez, *Chem. Rev.*, **2006**, *106*, 2045-2064.
42. S. C. Ha, K. Lowenhaupt, A. Rich, Y.-G. Kim and K. K. Kim, *Nature*, **2005**, *437*, 1183-1186.
43. C. C. Hardin, G. T. Walker and J. Tinoco, I., *Biochem.*, **1988**, *27*, 4178-4184.
44. K. Hall, P. Cruz, I. Tinoco Jr., T. M. Jovin and J. H. van de Sande, *Nature*, **1984**, *311*, 584-586.
45. M.-K. Teng, Y.-C. Liaw, G. A. van der Marel, J. H. van Boom and A. H.-J. Wang, *Biochemistry*, **1989**, *28*, 4923-4928.
46. P. W. Davis, K. Hall, P. Cruz, J. Ignacio Tinoco and T. Neilson, *Nucleic Acids Res.*, **1986**, *14*, 1279-1291.
47. A. Jaworski, W.-T. Hsieh, J. A. Blaho, J. E. Larson and R. D. Wells, *Science*, **1987**, *238*, 773-777.
48. A. R. Rahmouni and R. D. Wells, *Science*, **1989**, *246*, 358-363.
49. W. Zacharias, A. Jaworski, J. E. Larson and R. D. Wells, *Proc. Natl. Acad. Sci. USA*, **1988**, *85*, 7069-7073.
50. A. Herbert and A. Rich, *J. Biol. Chem.*, **1996**, *271*, 11595-11598.
51. A. Herbert and A. Rich, *Genetica*, **1999**, *106*, 37-47.
52. A. Rich and S. Zhang, *Nature*, **2003**, *4*, 566-573.
53. E. M. Lafer, R. P. Valle, A. Möller, A. Nordheim, P. H. Schur, A. Rich and B. D. Stollar, *J. Clin. Invest.*, **1983**, *71*, 314-321.
54. A. Herbert, K. Lowenhaupt, J. Spitzner and A. Rich, *Proc. Natl. Acad. Sci. USA*, **1995**, *92*, 7550-7554.
55. T. Schwartz, J. Behlke, K. Lowenhaupt, U. Heinermann and A. Rich, *Nature Struct. Biol.*, **2001**, *8*, 761-765.
56. S. Zhang, C. Lockshin, A. Herbert, E. Winter and A. Rich, *EMBO J.*, **1992**, *11*, 3787-3796.
57. F. Lancillotti, M. C. Lopez, P. Arias and C. Alonso, *Proc. Natl. Acad. Sci. USA*, **1987**, *81*, 1560-1564.
58. G. P. Schroth, P.-J. Chou and P. S. Ho, *J. Biol. Chem.*, **1992**, *267*, 11846-11855.
59. L. F. Liu and J. C. Wang, *Proc. Natl. Acad. Sci. USA*, **1987**, *84*, 7024-7027.
60. M. M. Garner and G. Felsenfeld, *J. Mol. Biol.*, **1987**, *196*, 581-590.

61. R. Liu, H. Liu, X. Chen, M. Kirby, P. O. Brown and K. Zhao, *Cell*, **2001**, *106*, 309-318.
62. S.-H. Ke and R. M. Wartell, *Biochemistry*, **1995**, *34*, 4593-4600.
63. P. N. Borer, Y. Lin, S. Wang, M. W. Roggenbuck, J. M. Gott, O. C. Uhlenbeck and I. Pelczer, *Biochemistry*, **1995**, *34*, 6488-6503.
64. Y. Xiong and M. Sundaralingam, *RNA*, **2000**, *6*, 1316-1324.
65. M. W. Kalnik, D. G. Norman, P. F. Swann and D. J. Patel, *J. Biol. Chem.*, **1989**, *264*, 3702-3712.
66. L. Varani, M. Hasegawa, M. G. Spillantini, M. J. Smith, J. R. Murrell, B. Ghetti, A. Klug, M. Goedert and G. Varani, *Proc. Natl. Acad. Sci. USA*, **1999**, *96*, 8229-8234.
67. L. Joshua-Tor, F. Frolow, E. Appella, H. Hope, D. Rabinovich and J. L. Sussman, *J. Mol. Biol.*, **1992**, *225*, 397-431.
68. S. Portmann, S. Grimm, C. Workman, N. Usman and M. Egli, *Chem. Biol.*, **1996**, *3*, 173-184.
69. A. Bhattacharyya, A. I. H. Murchie and D. M. Lilley, *Nature*, **1990**, *343*, 484-487.
70. D. M. J. Lilley, *Proc. Natl. Acad. Sci. USA*, **1995**, *92*, 7140-7142.
71. C. Gohlke, A. I. Murchie, D. M. Lilley and R. M. Clegg, *Proc. Natl. Acad. Sci. USA*, **1994**, *91*, 11660-11664.
72. F. A. Gollmick, M. Lorenz, U. Dornberger, J. von Langen, S. Diekmann and H. Fritzsche, *Nucleic Acids Res.*, **2002**, *30*, 2669-2677.
73. R. S. Tang and D. E. Draper, *Biochemistry*, **1990**, *29*, 5232-5237.
74. F. A. Riordan, A. Bhattacharyya, S. McAteer and D. M. Lilley, *J. Mol. Biol.*, **1992**, *226*, 305-310.
75. N. L. Greenbaum, I. Radhakrishnan, D. J. Patel and D. Hirsh, *Structure*, **1996**, *4*, 725-733.
76. J. Zhu and R. M. Wartell, *Biochemistry*, **1999**, *38*, 15986-15993.
77. J. L. Diener and P. B. Moore, *Mol. Cell*, **1998**, *1*, 883-894.
78. B. T. Wimberly, R. Guymon, J. P. McCutcheon, S. W. White and V. Ramakrishnan, *Cell*, **1999**, *97*, 491-502.
79. J. H. Cate, A. R. Gooding, E. Podell, K. Zhou, B. L. Golden, C. E. Kundrot, T. Cech and J. A. Doudina, *Science*, **1996**, *273*, 1678-1696.
80. J. A. Ippolito and T. A. Steitz, *Proc. Natl. Acad. Sci. USA*, **1998**, *95*, 9819-9824.
81. T. E. Edwards and S. T. Sigurdsson, *Biochem. Biophys. Res. Commun.*, **2003**, *303*, 721-725.
82. T. Hermann and E. Westhof, *Structure*, **1998**, *6*, 1303-1314.
83. T. A. Kunkel, *Biochemistry*, **1990**, *29*, 8003-8011.
84. G. R. Hoffmann and R. P. P. Fuchs, *Chem. Res. Toxicol.*, **1997**, *10*, 347-359.
85. B. S. Strauss, *Mutat. Res.*, **1999**, *437*, 195-203.
86. M. Samson, F. Libert, B. J. Doranz, J. Rucker, C. Liesnard, C.-M. Farber, S. Saragosti, C. Lapouméroulie, J. Cognaux, C. Forceille, G. Muyldermans, C. Verhofstede, G. Burtonboy, M. Georges, T. Imai, S. Rana, Y. Yi, R. J. Smyth, R. G. Collman, R. W. Doms, G. Vassart and M. Parmentier, *Nature*, **1996**, *382*, 722-725.
87. M. A. Austin, C. M. Hutter, R. L. Zimmern and S. E. Humphries, *Am. J. Epidemiol.*, **2004**, *160*, 407-420.
88. N. Papadopolus, N. C. Nicoladies, Y.-F. Wei, S. M. Ruben, K. C. Carter, C. A. Rosen, W. A. Haseltine, R. D. Fleischmann, C. M. Fraser, M. D. Adams, A. J. C. Venter, S. R. Hamilton, G. M. Petersen, P. Watson, H. T. Lynch, P. Peltomaki, J.-P. Mechlin, A. de la Chapelle, K. W. Kinzler and B. Vogelstein, *Science*, **1994**, *263*, 1625-1629.

89. J. Li, C. Yen, D. Liaw, K. Podsypanina, S. Bose, S. I. Wang, J. Puc, C. Miliaresis, L. Rogers, R. McCombie, S. H. Bigner, B. C. Giovanella, M. Ittmann, B. Tycko, H. Hibshoosh, M. H. Wigler and R. Parsons, *Science*, **1997**, *275*, 1943-1947.
90. N. Degtyareva, D. Subramanian and J. D. Griffith, *J. Biol. Chem.*, **2001**, *276*, 8778-8784.
91. V. A. Malkov, I. Biswas, R. D. Camerini-Otero and P. Hsieh, *J. Biol. Chem.* , **1997**, *272*, 23811-23817.
92. G. Streisinger and J. E. Owen, *Genetics*, **1985**, *109*, 633-659.
93. J. Völker, H. H. Klump and K. J. Breslauer, *J. Am. Chem. Soc.*, **2007**, *129*, 5272-5280.
94. R. D. Wells, *J. Biol. Chem.*, **1996**, *271*, 2875-2878.
95. D. Payet, A. Hillisch, N. Lowe, S. Diekmann and A. Travers, *J. Mol. Biol.*, **1999**, *294*, 79-91.
96. R. Cerdan, D. Payet, J.-C. Yang, A. A. Travers and D. Neuhaus, *Prot. Sci.*, **2001**, *10*, 504-518.
97. D. Payet and A. Tavers, *J. Mol. Biol.*, **1997**, *266*, 66-75.
98. S. Chen, A. Gunasekera, X. Zhang, T. A. Kunkel, R. H. Ebright and H. M. Berman, *J. Mol. Biol.*, **2001**, *314*, 75-82.
99. S. Chen, J. Vojtechovsky, G. N. Parkinson, R. H. Ebright and H. M. Berman, *J. Mol. Biol.*, **2001**, *314*, 63-74.
100. D. M. J. Lilley, *Biopolymers*, **1998**, *48*, 101-112.
101. T. Hermann and D. J. Patel, *Structure*, **2000**, *8*, R47-R54.
102. K. M. Weeks and D. M. Crothers, *Science*, **1993**, *261*, 1574-1577.
103. B. Tian, P. C. Bevilacqua, A. Diegelman-Parente and M. B. Matthews, *Nature Rev. Molec. Cell. Biol.*, **2004**, *5*, 1013-1023.
104. B. Berkhout and K.-T. Jeang, *J. Virol.*, **1989**, *63*, 5501-5504.
105. U. Delling, L. S. Reid, R. W. Barnett, M. Y.-X. Ma, S. Climie, M. Sumner-Smith and N. Sonenberg, *J. Virol.*, **1992**, *66*, 3018-3025.
106. M. J. Churcher, C. Lamont, F. Hamy, C. Dingwall, S. M. Green, A. D. Lowe, J. G. Butler, M. J. Gait and J. Karn, *J. Mol. Biol.*, **1993**, *230*, 90-110.
107. F. Aboul-ela, J. Karn and G. Varani, *J. Mol. Biol.*, **1995**, *253*, 313-332.
108. J. Karn, *J. Mol. Biol.*, **1999**, *293*, 235-254.
109. T. M. Rana and K.-T. Jeang, *Arch. Biochem. Biophys.*, **1999**, *365*, 175-185.
110. Y. N. Vaishnav and F. Wong-Staal, *Annu. Rev. Biochem.*, **1991**, *60*, 577-630.
111. F. Aboul-ela, J. Karn and G. Varani, *Nucleic Acids Res.*, **1996**, *24*, 3974-3981.
112. C. Dingwall, I. Ernberg, M. J. Gait, S. M. Green, S. Heaphy, J. Karn, A. D. Lowe, M. Singh and M. A. Skinner, *EMBO J.*, **1990**, *9*, 4145-4153.
113. D. Harrich, G. Mavankal, A. Mette-Snider and R. B. Gaynor, *J. Virol.*, **1995**, *69*, 4906-4913.
114. F. Hamy, U. Asseline, J. Grasby, S. Iwai, C. Pritchard, G. Slim, J. G. Butler, J. Karn and M. J. Gair, *J. Mol. Biol.*, **1993**, *230*, 111-123.
115. C. E. Pritchard, J. A. Grasby, F. Ham, A. M. Zacharek, M. Singh, J. Karn and M. J. Gait, *Nucleic Acids Res.*, **1994**, *22*, 2592-2600.
116. K. M. Weeks and D. M. Crothers, *Cell*, **1991**, *66*, 577-588.
117. H. Huthoff, F. Girard, S. S. Wijmenga and B. Berkhout, *RNA*, **2004**, *10*, 412-423.
118. M. Zacharias and P. J. Hagerman, *Proc. Natl. Acad. Sci. USA*, **1995**, *92*, 6052-6056.
119. B. J. Calnan, B. Tidor, S. Biancalana, D. Hudson and A. D. Frankel, *Science*, **1991**, *252*, 1167-1171.

120. J. Tao and A. D. Frankel, *Proc. Natl. Acad. Sci. USA*, **1992**, *89*, 2723-2726.
121. K. A. Sannes-Lowery, P. Hu, D. P. Mack, H.-Y. Mei and J. A. Loo, *Anal. Chem.*, **1997**, *69*, 5130-5135.
122. K. M. Weeks and D. M. Crothers, *Biochemistry*, **1992**, *31*, 10281-10287.
123. J. D. Puglisi, R. Tan, B. J. Calnan, A. D. Frankel and J. R. Williamson, *Science*, **1992**, *257*, 76-80.
124. A. S. Brodsky and J. R. Williamson, *J. Mol. Biol.*, **1997**, *267*, 624-639.
125. M. G. Cordingley, R. L. LaFemina, P. L. Callahan, J. H. Condra, V. V. Sardana, D. J. Graham, T. M. Nguyen, K. LeGrow, L. Gotlib, A. J. Schlabach and R. J. Colonno, *Proc. Natl. Acad. Sci. USA*, **1990**, *87*, 8985-8989.
126. S. Roy, N. T. Parkin, C. Rosen, J. Itovitch and N. Sonenberg, *J. Virol.*, **1990**, *64*, 1402-1406.
127. K. T. Dayie, A. S. Brodsky and J. R. Williamson, *J. Mol. Biol.*, **2002**, *317*, 263-278.
128. J. H. Cate, R. L. Hanna and J. A. Doudna, *Nature Struct. Biol.*, **1997**, *4*, 553-558.
129. P. J. Romaniuk, P. Lowary, H.-N. Wu, G. Stormo and O. C. Uhlenbeck, *Biochemistry*, **1987**, *26*, 1563-1568.
130. J. Gralla, J. A. Steitz and D. M. Crothers, *Nature*, **1974**, *248*, 204-208.
131. H.-N. Wu and O. C. Uhlenbeck, *Biochemistry*, **1987**, *26*, 8221-8227.
132. K. Valegård, J. B. Murray, P. G. Stockley, N. J. Stonehouse and L. Liljas, *Nature*, **1994**, *371*, 623-626.
133. D. A. Peattie, S. Douthwaite, R. A. Garrett and H. F. Noller, *Proc. Natl. Acad. Sci. USA*, **1981**, *78*, 7331-7335.
134. P. W. Huber, J. P. Rife and P. B. Moore, *J. Mol. Biol.*, **2001**, *312*, 823-832.
135. F. Baudin and P. J. Romaniuk, *Nucleic Acids Res.*, **1989**, *17*, 2043-2056.
136. G. L. Conn, D. E. Draper, E. E. Lattman and A. G. Gittis, *Science*, **1999**, *284*, 1171-1174.
137. J. Lykke-Andersen and R. A. Garrett, *J. Mol. Biol.*, **1994**, *243*, 846-855.
138. J. Nowakowski and I. Tinocco Jr., *Sem. Virol.*, **1997**, *8*, 153-165.
139. U. Nagaswamy, N. Voss, Z. Zhang and G. E. Fox, *Nucleic Acids Res.*, **2000**, *28*, 375-376.
140. R. S. Tang and D. E. Draper, *Biochemistry*, **1994**, *33*, 10089-10093.
141. A. Huppler, L. J. Nikstad, A. M. Allmann, D. A. Brow and S. E. Butcher, *Nature Struct. Biol.*, **2002**, *9*, 431-435.
142. N. W. Luedtke and Y. Tor, *Biopolymers*, **2003**, *70*, 103-119.
143. R. Tan and A. D. Frankel, *Biochemistry*, **1994**, *33*, 14579-14585.
144. J. L. Battiste, R. Tan, A. D. Frankel and J. R. Williamson, *Biochemistry*, **1994**, *33*, 2741-2747.
145. R. D. Peterson, D. P. Bartel, J. W. Szostak, S. J. Horvath and J. Feigon, *Biochemistry*, **1994**, *33*, 5357-5366.
146. G. Werstuck, M. L. Zapp and M. R. Green, *Chem. Biol.*, **1996**, *3*, 129-137.
147. J. L. Battiste, H. Mao, N. S. Rao, R. T. Tan, D. R. Muhandiram, L. E. Kay, A. D. Frankel and J. R. Williamson, *Science*, **1996**, *273*, 1547-1551.
148. D. Grate and C. Wilson, *Structure*, **1997**, *5*, 7-11.
149. F. H.-T. Allain, C. C. Gubser, P. W. A. Howe, K. Nagai, D. Neuhaus and G. Varani, *Nature*, **1996**, *380*, 646-650.
150. C. C. Gubser and G. Varani, *Biochemistry*, **1996**, *35*, 2253-2267.
151. R. J. Grainger, D. G. Norman and D. M. J. Lilley, *J. Mol. Biol.*, **1999**, *288*, 585-594.

152. R. J. Grainger, A. I. H. Murchie, D. G. Norman and D. M. J. Lilley, *J. Mol. Biol.*, **1997**, *273*, 84-92.
153. C. W. van Gelder, S. I. Gunderson, E. J. R. Jansen, W. C. Boelens, M. Polycarpou-Schwartz, I. W. Mattaj and W. J. van Venrooij, *EMBO J.*, **1993**, *12*, 5191-5200.
154. G. Varani, *Annu. Rev. Biophys. Biomol. Struct.*, **1995**, *24*, 379-404.
155. M. M. Senior, R. A. Jones and K. J. Breslauer, *Proc. Natl. Acad. Sci. USA*, **1988**, *85*, 6242-6246.
156. M. J. J. Blommers, J. A. L. I. Walters, C. A. G. Haasnoot, J. M. A. Aelen, G. A. van der Marel, J. H. van Boom and C. W. Hilbers, *Biochemistry*, **1989**, *28*, 7491-7498.
157. V. P. Antao and I. Tinoco Jr., *Nucleic Acids Res.*, **1992**, *20*, 819-824.
158. P. M. Vallone, T. M. Paner, J. Hilario, M. J. Lane, B. D. Faldasz and A. S. Benight, *Biopoly.*, **1999**, *50*, 425-442.
159. J. Gralla and D. M. Crothers, *J. Mol. Biol.*, **1973**, *73*, 497-511.
160. O. C. Uhlenbeck, P. N. Borer, B. Dengler and I. Tinoco Jr., *J. Mol. Biol.*, **1973**, *73*, 483-496.
161. J. Wolters, *Nucleic Acids Res.*, **1992**, *20*, 1843-1850.
162. H. A. Heus and A. Pardi, *Science*, **1991**, *253*, 191-194.
163. V. P. Antao, S. Y. Lai and I. Tinoco Jr., *Nucleic Acids Res.*, **1991**, *19*, 5901-5905.
164. C. Tuerk, P. Gauss, C. Thermes, D. R. Groebe, M. Gayle, N. Guild, G. Stormo, Y. d'Aubenton-Carafa, O. C. Uhlenbeck, I. Tinoco, E. N. Brody and L. Gold, *Proc. Natl. Acad. Sci. USA*, **1988**, *85*, 1364-1368.
165. C. R. Woese, S. Winker and R. R. Gutell, *Proc. Natl. Acad. Sci. USA*, **1990**, *87*, 8467-8471.
166. C. Cheong, G. Varani and I. Tinoco Jr., *Nature*, **1990**, *346*, 680-682.
167. G. Varani, C. Cheong and I. Tinoco Jr., *Biochemistry*, **1991**, *30*, 3280-3289.
168. J. K. James and J. Tinoco, I., *Nucleic Acids Res.*, **1993**, *21*, 3287-3293.
169. E. M. Moody, J. C. Ferrar and P. C. Bevilacqua, *Biochemistry*, **2004**, *43*, 7992-7998.
170. I. Hirao, G. Kawai, S. Yoshizawa, Y. Nishimura and Y. Inshido, *Nucleic Acids Res.*, **1994**, *22*, 576-582.
171. E. M. Moody and P. C. Bevilacqua, *J. Am. Chem. Soc.*, **2004**, *126*, 9570-9577.
172. S. Yoshizawa, G. Kawai, K. Wantabe, K.-I. Miura and I. Hirao, *Biochemistry*, **1997**, *36*, 4761-4767.
173. M. Nakano, E. M. Moody, J. Liang and P. C. Bevilacqua, *Biochemistry*, **2002**, *41*, 14281-14292.
174. U. Nagaswamy, X. Gao, S. A. Martinis and G. E. Fox, *Nucleic Acids Res.*, **2001**, *29*, 5129-5139.
175. S. Li and X.-J. Li, *Molec. Neurodeg.*, **2006**, *1*, 19-28.
176. G. P. Bates, *Nature Rev. Genet.*, **2005**, *6*, 766-773.
177. D. H. Cho and S. J. Tapscott, *Biochem. Biophys. Acta*, **2007**, *1772*, 195-204.
178. L. Machuca-Tzili, D. Brook and D. Hilton-Jones, *Mucle Nerve*, **2005**, *32*, 1-18.
179. S. Jacquemont, R. J. Hagerman, P. Hagerman and M. A. Leehey, *Lancet Neurol.*, **2007**, *6*, 45-55.
180. S. T. Warren and C. T. Ashley Jr., *Annu. Rev. Neurosci.*, **1995**, *18*, 77-99.
181. J. R. Gatchel and H. Y. Zoghbi, *Nature Rev. Genet.*, **2005**, *6*, 743-755.
182. H. L. Paulson and K. H. Fischbeck, *Annu. Rev. Neurosci.*, **1996**, *19*, 79-107.
183. C. E. Pearson, K. N. Edamura and J. D. Cleary, *Nature Rev. Genet.*, **2005**, *6*, 729-742.
184. G. R. Sutherland and R. I. Richards, *Proc. Natl. Acad. Sci. USA*, **1995**, *92*, 3636-3641.

185. C. T. Ashley Jr. and S. T. Warren, *Annu. Rev. Genet.*, **1995**, *29*, 703-728.
186. G. Gàrdiàn and L. Vécsei, *J. Neural. Transm.*, **2004**, *111*, 1485-1494.
187. M. J. Hartenstine, M. F. Goodman and J. Petruska, *J. Biol. Chem.*, **2000**, *275*, 18382-18390.
188. G. Bates, *Lancet*, **2003**, *361*, 1642-1644.
189. E. Cattaneo, *News Physiol. Sci.*, **2003**, *18*, 34-37.
190. C. T. McMurray, *Proc. Natl. Acad. Sci. USA*, **1999**, *96*, 1823-1825.
191. K. W. Jones, W. J. Berry, D. J. Borsay, H. T. Cline, W. C. J. Conner and C. S. Fullmer, *X-ray Spect.* , **1997**, *26*, 350-358.
192. E. Viguera, D. Canceill and S. D. Ehrlich, *J. Mol. Biol.*, **2001**, *312*, 323-333.
193. E. Viguera, D. Canceill and S. D. Ehrlich, *EMBO J.*, **2001**, *20*, 2587-2595.
194. S. Kang, K. Ohshima, M. Shimizu, S. Amirhaeri and R. D. Wells, *J. Biol. Chem.*, **1995**, *270*, 27014-27021.
195. K. Ohshima and R. D. Wells, *J. Biol. Chem.*, **1997**, *272*, 16798-16806.
196. R. Pelletier, M. M. Krasilnikova, G. M. Samadashwily, R. Lahue and S. M. Mirkin, *Mol. Cell. Biol.*, **2003**, *23*, 1349-1357.
197. G. M. Samadashwily, G. Raca and S. M. Mirkin, *Nature Genet.*, **1997**, *17*, 298-304.
198. G. Levinson and G. A. Gutman, *Mol. Biol. Evol.*, **1987**, *4*, 203-221.
199. C. Schlötterer and D. Tautz, *Nucleic Acids Res.*, **1992**, *20*, 211-215.
200. H. G. Brunner, G. jansen, W. Nillesen, M. Nelen, C. de Die, C. J. Howeler, B. A. van Oost, B. Wieringa, H.-H. Ropers and H. Smeets, *New. Eng. J. Med.*, **1993**, *328*, 476-480.
201. K. L. O'Hoy, C. Tsilfidis, M. S. Mahadevan, C. E. Neville, J. Barcelo, A. G. W. Hunter and R. G. Korneluk, *Science*, **1993**, *259*, 809-812.
202. J. Petruska, M. J. Hartenstine and M. F. Goodman, *J. Biol. Chem.*, **1998**, *273*, 5204-5210.
203. V. N. Potaman, J. J. Bissler, V. I. Hashem, E. A. Oussatcheva, L. Lu, L. S. Shlyakhtenko, Y. L. Lyubchenko, T. Matsuura, T. Ashizawa, M. Leffak, C. J. Benham and R. R. Sinden, *J. Mol. Biol.*, **2003**, *326*, 1095-1111.
204. R. D. Wells, P. Parniewski, A. Pluciennik, A. Bacolla, R. Gellibolian and A. Jaworski, *J. Biol. Chem.*, **1998**, *273*, 19532-19541.
205. R. R. Sinden, V. N. Potaman, E. A. Oussatcheva, C. E. Pearson, Y. L. Lyubchenko and L. S. Shlyakhtenko, *J. Biosci.*, **2002**, *27*, 53-65.
206. M. M. Krasilnikova and S. M. Mirkin, *Mol. Cell. Biol.*, **2004**, *24*, 2286-2295.
207. A. S. Krasilnikov, I. G. Panyutin, G. M. Samadashwily, R. Cox, Y. S. Lazurkin and S. M. Mirkin, *Nucleic Acids Res.*, **1997**, *25*, 1339-1346.
208. K. Usdin and K. J. Woodford, *Nucleic Acids Res.*, **1995**, *23*, 4202-4209.
209. A. Pluciennik, R. R. Iyer, P. Parniewski and R. D. Wells, *J. Biol. Chem.*, **2000**, *275*, 28386-28397.
210. R. D. Wells, R. Dere, M. L. Hebert, M. Napierala and L. S. Son, *Nucleic Acids Res.*, **2005**, *33*, 3785-3798.
211. I. V. Kovtun, G. Goeliner and C. T. McMurray, *Biochem. Cell. Biol.*, **2001**, *79*, 325-336.
212. B. A. Lenzmeier and C. H. Freudenreich, *Cytogenet. Genome Res.*, **2003**, *100*, 7-24.
213. M. Vorlickova, M. Zimulova, J. Kovanda, P. Fojtik and J. Kypr, *Nucleic Acids Res.*, **1998**, *26*, 2679-2685.

214. S. Amrane, B. Sacca, M. Mills, M. Chauhan, H. H. Klump and J.-L. Mergny, *Nucleic Acids Res.*, **2005**, *33*, 4065-4077.
215. A. M. Gacy and C. T. McMurray, *Biochemistry*, **1998**, *37*, 9426-9434.
216. J. Petruska, N. Arnheim and M. F. Goodman, *Nucleic Acids Res.*, **1996**, *24*, 1992-1998.
217. A. M. Gacy, G. Goellner, N. Juranić, S. Macura and C. T. McMurray, *Cell*, **1995**, *81*, 533-540.
218. A. M. Paiva and R. D. Sheardy, *Biochemistry*, **2004**, *43*, 14218-14227.
219. H. Moore, P. W. Greenwell, C. Liu, N. Arnheim and T. D. Petes, *Proc. Natl. Acad. Sci. USA*, **1999**, *96*, 1504-1509.
220. M. Mitas, *Nucleic Acids Res.*, **1997**, *25*, 2245-2253.
221. S. Kang, A. Jaworski, K. Ohshima and R. D. Wells, *Nature Genet.*, **1995**, *10*, 213-218.
222. T. Matsuura, P. Fang, X. Lin, M. Khajavi, K. Tsuji, A. Rasmussen, R. P. Grewal, M. Achari, M. E. Alonso, S. M. Pulst, H. Y. Zoghbi, D. L. Nelson, B. B. Roa and T. Ashizawa, *Am. J. Hum. Genet.*, **2004**, *74*, 1216-1224.
223. Y. Nadel, P. Weisman-Shomer and M. Fry, *J. Biol. Chem.*, **1995**, *270*, 28970-28977.
224. M. Fry and L. A. Loeb, *Proc. Natl. Acad. Sci. USA*, **1994**, *91*, 4950-4954.
225. P. Fojtík and M. Vorlícková, *Nucleic Acids Res.*, **2001**, *29*, 4684-4690.
226. S. S. Smith, A. Laayoun, R. G. Lingerman, D. J. Baker and J. Riley, *J. Mol. Biol.*, **1994**, *243*, 143-151.
227. A. M. Gacy, G. M. Goeliner, C. Spiro, X. Chen, G. Gupta, E. M. Bradbury, R. B. Dyer, M. J. Mikesell, J. Z. Yao, A. J. Johnson, A. Richter, S. B. Melançon and C. T. McMurray, *Molecular Cell*, **1998**, *1*, 583-593.
228. S. V. S. Mariappan, P. Catasti, L. A. Silks III, E. M. Bradbury and G. Gupta, *J. Mol. Biol.*, **1999**, *285*, 2035-2052.
229. N. Sakamoto, P. D. Chastain, P. Parniewski, K. Ohshima, M. Pandolfo, J. D. Griffith and R. D. Wells, *Mol. Cell*, **1999**, *3*, 465-475.
230. A. A. Vetcher, M. Napierala, R. R. Iyer, P. D. Chastain, J. D. Griffith and R. D. Wells, *J. Biol. Chem.*, **2002**, *277*, 39217-39227.
231. C. E. Pearson, H. Zorbas, G. B. Price and M. Zannis-Hadjopoulos, *J. Cell. Biochem.*, **1996**, *63*, 1-22.
232. Q. Hao, W. J. Peumans and E. J. M. Van Damme, *Biochem. J.*, **2001**, *357*, 875-880.
233. J. J. Meeks, J. Weiss and J. L. Jameson, *Nature Gen.*, **2003**, *34*, 32-33.
234. E. Zazopoulos, E. Lalli, D. M. Stocco and P. Sassone-Corsi, *Nature*, **1997**, *390*, 311-315.
235. A. van Belkum, M. J. J. Blommers, H. van den Elst, J. H. van Boom and C. W. Hilbers, *Nucleic Acids Res.*, **1990**, *18*, 4703-4710.
236. A. Yafe, S. Etzioni, P. Weisman-Shomer and M. Fry, *Nucleic Acids Res.*, **2005**, *33*, 2887-2900.
237. C. Spiro and M. C. T., *J. Biol. Chem.*, **1997**, *272*, 33145-33152.
238. K. Mizuuchi, M. Mizuuchi and M. Gellert, *J. Mol. Biol.*, **1982**, *156*, 229-243.
239. D. M. J. Lilley, *Nucleic Acids Res.*, **1981**, *9*, 1271-1289.
240. N. Panayotatos and R. D. Wells, *Nature*, **1981**, *289*, 466-470.
241. J. G. Brahms, O. Dargouge, S. Brahms, Y. Ohara and V. Vagner, *J. Mol. Biol.*, **1985**, *181*, 455-465.
242. F. Rojo, B. Nuez, M. Mencía and M. Salas, *Nucleic Acids Res.*, **1993**, *21*, 935-940.
243. E. Richet and O. Raibaud, *J. Mol. Biol.*, **1991**, *218*, 529-542.
244. M. S. Z. Horwitz and L. A. Loeb, *Science*, **1988**, *241*, 703-705.

245. K. Robbe and E. Bonnefoy, *Biochimie*, **1998**, *88*, 665-6671.
246. S. Waga, S. Mizuno and M. Yoshida, *J. Biol. Chem.*, **1990**, *265*, 19424-19428.
247. D. M. J. Lilley, *Proc. Natl. Acad. Sci. USA*, **1980**, *77*, 6468-6472.
248. N. Panayotatos and A. Fontaine, *J. Biol. Chem.*, **1987**, *262*, 11364-11368.
249. J. J. Champoux, *Annu. Rev. Biochem.*, **2001**, *70*, 369-413.
250. S. J. Froelich-Ammon, K. C. Gale and N. Osheroff, *J. Biol. Chem.*, **1994**, *269*, 7719-7725.
251. M. A. Glucksmann, P. Markiewicz, C. Malone and L. B. Rothman-Denes, *Cell*, **1992**, *70*, 491-500.
252. E. K. Davydova, T. J. Santangelo and L. B. Rothman-Denes, *Proc. Natl. Acad. Sci. USA*, **2007**, *104*, 7033-7038.
253. S. H. Kim, F. L. Suddath, G. J. Quigley, A. McPherson, J. L. Sussman, A. H. J. Wang, N. C. Seeman and A. Rich, *Science*, **1974**, *185*, 435-440.
254. T. L. Hendrickson, *Proc. Natl. Acad. Sci. USA*, **2001**, *98*, 13473-13475.
255. A. Shimada, O. Nureki, M. Goto, S. Takahashi and S. Yokoyama, *Proc. Natl. Acad. Sci. USA*, **2001**, *98*, 13537-13542.
256. M. M. Yusupov, Y. G.Z., A. Baucorn, K. Lieberman, T. N. Earnest, J. H. D. Cate and H. F. Noller, *Science*, **2007**, *292*, 883-896.
257. J. L. Sussman, S. R. Holbrook, R. W. Warrant, G. M. Church and S.-H. Kim, *J. Mol. Biol.*, **1978**, *123*, 607-360.
258. B. Klaver and B. Berkhout, *EMBO J.*, **1994**, *13*, 2650-2659.
259. S. A. Emory, P. Bouvet and J. G. Belasco, *Genes Dev.*, **1992**, *6*, 135-148.
260. A. Diwa, A. L. Bricker, C. Jain and J. G. Belasco, *Genes Dev.*, **2000**, *14*, 1249-1260.
261. G. Hambraeus, K. Karhumaa and B. Rutberg, *Microbology*, **2002**, *148*, 1795-1803.
262. D. C. Higgs, R. S. Shapiro, K. L. Kindle and D. B. Stern, *Mol. Cell. Biol.*, **1999**, *19*, 8479-8491.
263. Z. Zou, C. Eibl and H.-U. Koop, *Mol. Gen. Genomics*, **2003**, *269*, 340-349.
264. L. Suay, M. L. Salvador, E. Abesha and U. Klein, *Nucleic Acids Res.*, **2005**, *33*, 4754-4761.
265. N. B. Pandey, A. S. Williams, J.-H. Sun, V. D. Brown, U. Bond and W. F. Marzluff, *Mol. Cell. Biol.*, **1994**, *14*, 1709-1720.
266. H. A. Barton, R. S. Eisenstein, A. Bomford and H. N. Munro, *J. Biol. Chem.*, **1990**, *265*, 7000-7008.
267. E. A. Leibold, A. Laudano and Y. Yu, *Nucleic Acids Res.*, **1990**, *18*, 1819-1824.
268. G. Felsenfeld, D. R. Davies and A. Rich, *J. Am. Chem. Soc.*, **1957**, *79*, 2023-2024.
269. S. Arnott and E. Selsing, *J. Mol. Biol*, **1974**, *88*, 509-521.
270. C. de los Santos, M. Rosen and D. Patel, *Biochemistry*, **1989**, *28*, 7282-7289.
271. R. Macaya, E. Wang, P. Schultze, V. Sklenář and J. Feigon, *J. Mol. Biol.*, **1992**, *225*, 755-773.
272. I. Radhakrishnan and D. J. Patel, *J. Am. Chem. Soc*, **1992**, *114*, 6913-6915.
273. S. Rhee, Z.-J. Ham, K. Liu, H. T. Miles and D. R. Davies, *Biochemistry*, **1999**, *38*, 16810-16815.
274. H. Htun and J. E. Dahlberg, *Science*, **1989**, *243*, 1571-1576.
275. M. Frank-Kamenetskii and S. M. Mirkin, *Annu. Rev. Biochem.*, **1995**, *64*, 65-95.
276. R. W. Roberts and D. M. Crothers, *J. Mol. Biol.*, **1996**, *260*, 135-146.
277. K. A. Shahid, A. Majumdar, R. Alam, S. Liu, J. Y. Kuan, X. Sui, B. Cuenoud, P. M. Glazer, P. S. Miller and M. M. Seidman, *Biochemistry*, **2006**, *45*, 1970-1978.

278. H. E. Moser and P. B. Dervan, *Science*, **1987**, *238*, 645-650.
279. M. Cooney, G. Czernuszewicz, E. H. Postel, S. J. Flint and M. E. Hogan, *Science*, **1988**, *241*, 456-459.
280. T. Le Doan, L. Perrouault and C. Helene, *Biochemistry*, **1986**, *25*, 6736-6739.
281. P. A. Beal and P. B. Dervan, *Science*, **1991**, *251*, 1360-1363.
282. K. M. Vasquez, L. Narayanan and P. M. Glazer, *Science*, **2000**, *290*, 530-533.
283. J. M. Kalish, M. M. Seidman, D. L. Weeks and P. M. Glazer, *Nucleic Acids Res.*, **2005**, *33*, 3492-3502.
284. S. Burge, G. N. Parkinson, P. Hazel, A. K. Todd and S. Neidle, *Nucleic Acids Res.*, **2006**, *34*, 5402-5415.
285. D. Sen and W. Gilbert, *Nature*, **1988**, *334*, 364-366.
286. V. Dapic, V. Abdomerovic, R. Marrington, J. Peberdy, A. Rodger, J. O. Trent and P. J. Bates, *Nucleic Acids Res.*, **2003**, *31*, 2097-9107.
287. G. N. Parkinson, M. P. H. Lee and S. Neidle, *Nature*, **2002**, *417*, 876-880.
288. T. Phan, K. N. Luu and D. J. Patel, *Nucleic Acids Res.*, **2006**, *34*, 5715-5719.
289. C. Kang, X. Zhang, R. Ratliff, R. Moyzis and A. Rich, *Nature*, **1992**, *356*, 126-131.
290. D. Sen and W. Gilbert, *Nature*, **1990**, *344*, 410-414.
291. C. Antonacci, J. B. Chaires and R. D. Sheardy, *Biochemistry*, **2007**, *46*, 4654-4660.
292. E. H. Blackburn, *Cell*, **2001**, *106*, 661-673.
293. M. Chakhparonian and R. J. Wellinger, *Trends Genet.*, **2003**, *19*, 439-446.
294. L. Oganesian, I. K. Moon, T. M. Bryan and M. B. Jarstfer, *EMBO J.*, **2006**, *25*, 1148-1159.
295. A. M. Zahler, J. R. Williamson, T. R. Cech and D. M. Prescott, *Nature*, **1991**, *350*, 718-720.
296. M. A. Read, A. A. Wood, J. R. Harrison, S. M. Gowan, L. R. Kelland, H. S. Dosanjh and S. Neidle, *J. Med. Chem.*, **1999**, *42*, 4538-4546.
297. T. Tauchi, K. Shin-ya, G. Sashida, M. Sumi, A. Nakajima, T. Shimamoto, J. H. Ohyashiki and K. Ohyashiki, *Oncogene*, **2003**, *22*, 5338-5347.
298. R. T. Wheelhouse, D. Sun, H. Han, F. X. Han and L. H. Hurley, *J. Am. Chem. Soc.*, **1998**, *120*, 3261-3262.
299. J. L. Huppert and S. Balasubramanian, *Nucleic Acids Res.*, **2005**, *33*, 2908-2916.
300. A. K. Todd, M. Johnston and S. Neidle, *Nucleic Acids Res.*, **2005**, *33*, 2901-2907.
301. J. L. Huppert and S. Balasubramanian, *Nucleic Acids Res.*, **2007**, *35*, 406-413.
302. J. Dai, T. S. Dexheimer, D. Chen, M. Carver, A. Ambrus, R. A. Jones and D. Tang, *J. Am. Chem. Soc.*, **2005**, *128*, 1096-1098.
303. S. Cogoi, F. Quadrifoglio and L. E. Xodo, *Biochemistry*, **2004**, *2004*.
304. A. T. Phan, Y. S. Modi and D. J. Patel, *J. Am. Chem. Soc*, **2004**, *126*, 8710-8716.
305. A. Siddiqui-jain, C. L. Grand, D. J. Bearss and L. H. Hurley, *Proc. Natl. Acad. Sci. USA*, **2002**, *99*, 11593-11598.
306. T. Saha and K. Usdin, *FEBS Lett.*, **2001**, *491*, 184-187.
307. R. T. Batey, R. P. Rambo and J. A. Doudna, *Angew. Chem. Int. Ed.*, **1999**, *38*, 2326-2343.
308. P. S. Ho and B. F. Eichman, *Curr. Opin. Struct. Biol.*, **2001**, *11*, 302-308.
309. A. L. Mikheikin, A. Y. Lushnikov and Y. L. Lyubchenko, *Biochemistry*, **2006**, *45*, 12998-13006.
310. B. F. Eichman, J. M. Vargason, B. H. Mooers and P. S. Ho, *Proc. Natl. Acad. Sci. USA*, **2000**, *97*, 3971-3976.

311. F. A. Hays, V. Schirif, P. Ho and B. Demeler, *J. Am. Chem. Soc.* , **2006**, *45*, 2467-2471.
312. E. von Kitzing, D. M. Lilley and S. Diekmann, *Nucleic Acids Rev.*, **1990**, *18*, 2671-2683.
313. G. LeRoy, R. Carroll, S. Kyin, M. Seki and M. D. Cole, *Nucleic Acids Res.*, **2005**, *33*, 6251-6257.
314. M. F. White, M.-J. E. Giraud-Panis, J. R. G. Pöhler and D. M. J. Lilley, *J. Mol. Biol.*, **1997**, *269*, 647-664.
315. J. Nowakowski, P. J. Shim, G. S. Prasad, C. D. Stout and G. F. Joyce, *Nature Struct. Biol.*, **1999**, *6*, 151-156.
316. J.-L. Chen and C. W. Greider, *Proc. Natl. Acad. Sci. USA*, **2005**, *102*, 8080-8085.
317. M. Martick and W. G. Scott, *Cell*, **2006**, *126*, 309-320.
318. W. G. Scott, J. T. Finch and A. Klug, *Cell*, **1995**, *81*, 991-1002.
319. H. Sigel, *Chem. Soc. Rev.*, **1993**, 255-267.
320. J. A. Hartley, J. P. Bingham and R. L. Souhami, *Nucleic Acids Res.*, **1992**, *20*, 3175-3178.
321. E. Wong and C. M. Giandomenico, *Chem. Rev.*, **1999**, *99*, 2451-2466.
322. J. Reedijk, *Proc. Nat. Acad. Sci. USA*, **2003**, *100*, 3611-3616.
323. E. R. Jamieson and S. J. Lippard, *Chem. Rev*, **1999**, *99*, 2467-2498.
324. S. E. Shermann and S. J. Lippard, *Chem. Rev.*, **1987**, *87*, 1153-1181.
325. B. Rosenberg, *Plat. Met. Rev.*, **1971**, *15*.
326. B. Rosenberg, L. Van Camp and T. Krigas, *Nature*, **1965**, *205*, 698-699.
327. B. Rosenberg, L. VanCamp, J. E. Trosko and V. H. Mansour, *Nature*, **1969**, *222*, 385-386.
328. J. P. Caradonna and S. J. Lippard, *J. Am. Chem. Soc.*, **1982**, *104*, 5793-5795.
329. H. Zorbas and B. K. Keppler, *ChemBioChem*, **2005**, *6*, 1157-1166.
330. T. W. Hambley, *J. Chem. Soc., Dalton Trans.*, **2001**, 2711-2718.
331. Z. Guo and P. J. Sadler, *Angew. Chem. Int. Ed.*, **1999**, *38*, 1512-1531.
332. L. Marrot and M. Leng, *Biochemistry*, **1989**, *28*, 1454-1461.
333. M. A. Fuertes, V. Cepeda, C. Alonso and J. M. Pérez, *Chem. Rev.*, **2006**, *106*, 2045-2064.
334. R. J. Knox, F. Friedlos, D. A. Lydall and J. J. Roberts, *Cancer Res.*, **1986**, *46*, 1972-1979.
335. A. M. Di Francesco, A. Ruggiero and R. Riccardi, *Cell. Mol. Life Sci.*, **2002**, *59*, 1914-1927.
336. N. J. Wheate and J. G. Collins, *Coord. Chem. Rev.*, **2003**, *241*, 133-145.
337. H. T. Chifotides and K. R. Dunbar, *Acc. Chem. Res.* , **2005**, *38*, 146-156.
338. K. Sorasaenee, P. K.-L. Fu, A. M. Angeles-Boza, K. R. Dunbar and C. Turro, *Inorg. Chem.*, **2003**, *42*, 1267-1271.
339. R. A. Howard, E. Sherwood, A. Erck, A. P. Kimball and J. L. Bear, *J. Med. Chem.*, **1977**, *20*, 943-946.
340. K. R. Dunbar, J. H. Matonic, V. P. Saharan, C. A. Crawford and G. Christou, *J. Am. Chem. Soc.*, **1994**, *116*, 2201-2202.
341. A. M. Angeles-Boza, H. T. Chifotides, J. D. Aguirre, A. Chouai, P. K.-L. Fu, K. R. Dunbar and C. Turro, *J. Med. Chem.*, **2006**, *49*, 6841-6847.
342. H. T. Chifotides and K. R. Dunbar, *Chem. Eur. J.*, **2006**, *12*, 6458-6468.
343. C. S. Allardyce, P. J. Dyson, D. J. Ellis and S. L. Heath, *Chem. Commun.*, **2001**, 1396-1397.

344. O. Novakova, H. Chen, O. Vrana, A. Rodger, P. J. Sadler and V. Brabec, *Biochemistry*, **2003**, *42*, 11544-11554.
345. C. Scolaro, T. J. Geldbach, S. Rochat, A. Dorcier, C. Gossens, A. Bergamo, M. Cocchietto, I. Tavernelli, G. Sava, U. Rothlisberger and P. J. Dyson, *Organometallics*, **2006**, *25*, 756-765.
346. C. A. Vock, W. H. Ang, C. Scolaro, A. D. Phillips, L. Lagopoulos, L. Juillerat-Jeanneret, G. Sava, R. Scopelliti and P. J. Dyson, *J. Med. Chem.*, **2007**, *50*, 2166-2175.
347. Y. K. Yan, M. Melchart, A. Habtemariam and P. J. Sadler, *Chem. Commun.*, **2005**, 4764-4776.
348. A. Bergamo and G. Sava, *Dalton Trans.*, **2007**, 1267-1272.
349. D. Pluim, R. C. A. M. van Waardenburg, J. H. Beijnen and J. H. M. Schellens, *Cancer Chemother. Pharmacol.*, **2004**, *54*, 71-78.
350. J. M. Rademaker-Lakhai, D. van den Bongard, D. Pluim, J. H. Beijnen and J. H. M. Schellens, *Clin. Cancer Res.*, **2004**, *10*, 3717-3727.
351. J. R. Aldrich-Wright, I. D. Greguric, C. H. Y. Lau, P. Pellegrini and J. G. Collins, *Recent Res. Devel. in Inorganic Chem.*, **1998**, *1*, 13-35.
352. P. Várnai and K. Zakrzewska, *Nucleic Acids Res.*, **2004**, *32*, 4269-4280.
353. H. Deng, V. A. Bloomfield, J. M. Benevides and G. J. Thomas Jr., *Nucleic Acids Res.*, **2000**, *28*, 3379-3385.
354. N. M. Luscombe, R. A. Laskowski and J. M. Thornton, *Nucleic Acids Res.*, **2001**, *29*, 2860-2874.
355. K. Jansen, B. Norden and M. Kubista, *J. Am. Chem. Soc.*, **1993**, *115*, 10527-10530.
356. J. Kapuscinski and W. Szer, *Nucleic Acids Res.*, **1979**, *6*, 3519-3534.
357. E. Trotta, E. D'Ambrosio, G. Ravagnan and M. Paci, *J. Biol. Chem.*, **1996**, *271*, 27608-27614.
358. C. E. Bostock-Smith and M. S. Searle, *Nucleic Acids Res.*, **1999**, *27*, 1619-1624.
359. S. Y. Breusegem, R. M. Clegg and F. G. Loontiens, *J. Mol. Biol.*, **2002**, *315*, 1049-1061.
360. P. E. Pjura, K. Grzeskowiak and R. E. Dickerson, *J. Mol. Biol.*, **1987**, *197*, 257-271.
361. C. Alemán, M. C. Vega, L. Tabernero and J. Bella, *J. Phys. Chem.*, **1996**, *100*, 11480-11487.
362. C. Bailly and J. B. Chaires, *Bioconjugate Chem.*, **1998**, *9*, 513-538.
363. P. R. Turner and W. A. Denny, *Curr. Drug Targets*, **2000**, *1*, 1-14.
364. S. Neidle, *Nat. Prod. Rep.*, **2001**, *18*, 291-309.
365. R. Lavery and B. Pullman, *Nucleic Acids Res.*, **1982**, *10*, 4383-4395.
366. A. V. Fratini, M. L. Kopka, H. R. Drew and R. E. Dickerson, *J. Biol. Chem.*, **1982**, *257*, 14686-14707.
367. M. L. Kopka, C. Yoon, D. Goodsell, P. Pjura and R. E. Dickerson, *Proc. Natl. Acad. Sci. USA*, **1985**, *82*, 1376-1380.
368. D. E. Draper, *J. Mol. Biol.*, **1999**, *293*, 255-270.
369. Y. Choo and A. Klug, *Curr. Opin. Struct. Biol.*, **1997**, *7*, 117-125.
370. H. C. M. Nelson, *Curr. Opin. Cell. Biol.*, **1995**, *5*, 180-189.
371. W. D. Wilson, L. Ratmeyer, M. Zhao, L. Strekowski and D. Boykin, *Biochemistry*, **1993**, *32*, 4098-4104.
372. F. A. Tanious, J. M. Veal, H. Buczak, L. S. Ratmeyer and W. D. Wilson, *Biochemistry*, **1992**, *31*, 3103-3112.

373. C. Bailly, P. Colson, C. Houssier and F. Hamy, *Nucleic Acids Res.*, **1996**, *24*, 1460-1464.
374. T. Hermann and E. Westhof, *J. Med. Chem.*, **1999**, *42*, 1250-1261.
375. P. M. Brown and K. R. Fox, *Biochem. J.*, **1998**, *333*, 259-267.
376. J. R. Quintana, A. A. Lipanov and R. E. Dickerson, *Biochemistry*, **1991**, *30*, 10294-10306.
377. C. A. Franklin, J. V. Fry and J. G. Collins, *Inorg. Chem.*, **1996**, *35*, 7541-7545.
378. Q. Liang, P. Denney Eason and E. C. Long, *J. Am. Chem. Soc.*, **1995**, *117*, 9625-9631.
379. A. Rodger, K. J. Sanders, M. J. Hannon, I. Meistermann, A. Parkinson, D. S. Vidler and I. S. Haworth, *Chirality*, **2000**, *12*, 221-236.
380. T. A. Watt, *Inorg. Chem.*, **1994**, *33*, 609-610.
381. Q. Xu, R. K. Shoemaker and W. H. Braunlin, *Biophys. J.*, **1993**, *65*, 1039-1049.
382. H. Robinson and A. H.-J. Wang, *Nucleic Acids Res.*, **1996**, *24*, 676-682.
383. Q. Xu, S. R. B. Jampani and W. H. Braunlin, *Biochemistry*, **1993**, *32*, 11754-11760.
384. I. Meistermann, V. Moreno, M. J. Prieto, E. Moldrheim, E. Sletten, S. Khalid, P. M. Rodger, J. C. Peberdy, C. J. Isaac, A. Rodger and M. J. Hannon, *Proc. Nat. Acad. Sci. USA*, **2002**, *99*, 5069-5074.
385. E. Moldrheim, M. J. Hannon, I. Meistermann, A. Rodger and E. Sletten, *J. Biol. Inorg. Chem.*, **2002**, *7*, 770-780.
386. C. Uerpmann, J. Malina, M. Pascu, G. J. Clarkson, M. V., A. Rodger, A. Grandas and M. J. Hannon, *Chem. Eur. J.* , **2005**, *11*, 1750-1756.
387. K. E. Erkkila, D. T. Odom and J. K. Barton, *Chem. Rev.*, **1999**, *99*, 2777-2795.
388. M. Waring, *J. Mol. Biol.*, **1970**, *54*, 247-279.
389. N. W. Luedtke, Q. Liu and Y. Tor, *Chem. Eur. J.* , **2005**, *11*, 495-508.
390. D. J. Patel and L. L. Canuel, *Proc. Natl. Acad. Sci. USA*, **1976**, *73*, 3343-3347.
391. P. O. Vardevanyan, A. P. Antonyan, M. A. Parsadanyan, H. G. Davtyan and A. T. Karapetyan, *Exp. Mol. Med.*, **2003**, *35*, 527-533.
392. H. D. Kumar, H. N. Singh and G. Prakash, *Plant Cell Physiol.*, **1967**, *8*, 171-179.
393. S. Neidle, A. Achari, G. L. Taylor, H. M. Berman, H. L. Carrell, J. P. Glusker and W. C. Stallings, *Nature*, **1977**, *269*, 304-307.
394. P. Tang, C.-L. Juang and G. S. Harbison, *Science*, **1990**, *249*, 70-72.
395. J. B. Chaires, *Biopolymers*, **1997**, *44*, 201-215.
396. D. J. Cashman and G. E. Kellogg, *J. Med. Chem.*, **2004**, *47*, 1360-1374.
397. F. Leng, R. Savkur, I. Fokt, T. Przewloka, W. Priebe and J. B. Chaires, *J. Am. Chem. Soc.* , **1996**, *118*, 4731-4738.
398. R. L. Jones, E. V. Scott, G. Zon, L. G. Marzilli and W. D. Wilson, *Biochemistry*, **1988**, *27*, 6021-6026.
399. D. J. Patel, *Biochemistry*, **1974**, *13*, 2396-2402.
400. D. R. Brown, M. Kurz, D. R. Kearns and V. L. Hsu, *Biochemistry*, **1994**, *33*, 651-664.
401. C. Lian, H. Robinson and A. H.-J. Wang, *J. Am. Chem. Soc.*, **1996**, *118*, 8791-8801.
402. S. A. Bejune, A. H. Shelton and D. R. McMillin, *Inorg. Chem.*, **2003**, *42*, 8465-8475.
403. L. G. Marzilli, D. L. Banville, G. Zon and W. D. Wilson, *J. Am. Chem. Soc.*, **1986**, *108*, 4188-4192.
404. K. Zupán, L. Herényi, K. Tóth, Z. Majer and G. Csík, *Biochemistry*, **2004**, *43*, 9151-9159.
405. Y.-C. Liaw, Y.-G. Gao, H. Robinson, G. A. v. d. Marel, J. H. v. Boom and A. H.-J. Wang, *Biochemistry*, **1989**, *28*, 9913-9918.

406. G. A. Leonard, T. W. Hambley, K. McAuley-Hecht, T. Brown and W. N. Hunter, *Acta Crystallogr. D: Biol. Crystallogr.*, **1993**, *49*, 458-467.
407. P. B. Dervan, *Science*, **1986**, *232*, 464-471.
408. R. L. Souhami, *Q. J. Med.*, **1994**, *87*, 195-197.
409. H. L. Takusagawa and F. Takusagawa, *Acta Cryst.*, **2000**, *D56*, 344-347.
410. J. W. Trauger, E. E. Baird and P. B. Dervan, *Nature*, **1996**, *382*, 559-561.
411. C. L. Kielkopf, S. White, J. W. Szewczyk, J. M. Turner, E. E. Baird, P. B. Dervan and D. C. Rees, *Science*, **1998**, *282*, 111-115.
412. W. L. Walker, M. L. Kopka and D. S. Goodsell, *Biopolymers*, **1997**, *44*, 323-334.
413. E. R. Lacy, B. Nguyen, M. Le, K. K. Cox, C. O'Hare, J. A. Hartley, M. Lee and W. D. Wilson, *Nucleic Acids Res.*, **2004**, *32*, 2000-2007.
414. C. S. Chow and J. K. Barton, *Biochemistry*, **1992**, *31*, 5423-5429.
415. B. A. Jackson and J. K. Barton, *J. Am. Chem. Soc.*, **1997**, *119*, 12986-12987.
416. H. Junicke, J. R. Hart, J. Kisko, O. Glebov, I. R. Kirsch and J. K. Barton, *Proc. Nat. Acad. Sci. USA*, **2003**, *100*, 3737-3742.
417. F. Barceló, C. Scotta, M. Ortiz-Lombardía, C. Méndez, J. A. Salas and J. Portugal, *Nucleic Acids Res.*, **2007**, *35*, 2215-2226.
418. S.-Y. Chiang, J. C. Azizkhan and T. A. Beerman, *Biochemistry*, **1998**, *37*, 3109-3115.
419. L. E. Ulanovsky and E. N. Trifonov, *Nature*, **1987**, *326*, 720-722.
420. D. S. Pilch, Z. Xu, Q. Sun, E. J. LaVoie, L. F. Liu and K. J. Breslauer, *Proc. Natl. Acad. Sci. USA*, **1997**, *94*, 13565-13570.
421. Y. Tor, *ChemBioChem*, **2003**, *4*, 998-1007.
422. R. Schroeder, C. Waldsich and H. Wank, *EMBO J.*, **2000**, *19*, 1-9.
423. H.-Y. Mei and J. K. Barton, *J. Am. Chem. Soc.*, **1986**, *108*, 7414-7416.
424. H. Takeuchi, N. Hanamura and I. Harada, *J. Mol. Biol.*, **1994**, *236*, 610-617.
425. H. Takeuchi, N. Hanamura, H. Hayasaku and I. Harada, *FEBS Lett.*, **1991**, *279*, 253-255.
426. T. J. Thomas, U. b. Gunnia and T. Thomas, *J. Biol. Chem.*, **1991**, *266*, 6137-6141.
427. S. Mahadevan and M. Palaniandavar, *Inorg. Chem.*, **1998**, *37*, 3927-3934.
428. Y. Qu, A. Harris, A. Hegmans, A. Petz, P. Kabolizadeh, H. Penazova and N. Farrell, *J. Inorg. Biochem.*, **2004**, *98*, 1591-1598.
429. P. L. Gilbert, D. E. Graves, M. Britt and J. B. Chaires, *Biochemistry*, **1991**, *30*, 10931-10937.
430. O. A. Mirau and D. R. Kearns, *Nucleic Acids Res.*, **1983**, *11*, 1931-1941.
431. M. Britt, F. Zunino and J. B. Chaires, *Molec. Pharmacol.*, **1985**, *29*, 74-80.
432. P. D. van Helden, *Nucleic Acids Res.*, **1983**, *11*, 8415-8420.
433. E. Jiménez-García and J. Portugal, *Biochemistry*, **1992**, *31*, 11641-11646.
434. J. B. Chaires, *J. Biol. Chem.*, **1986**, *261*, 8899-8907.
435. M. Tarui, M. Doi, T. Ishida, M. Inoue, S. Nakaike and K. Kitamura, *Biochem. J.*, **1994**, *304*, 271-279.
436. C. Zimmer, C. Marck and W. Guschlbauer, *FEBS Lett.*, **1983**, *154*, 156-160.
437. S. A. White and D. E. Draper, *Nucleic Acids Res.*, **1987**, *15*, 4049-4064.
438. S. A. White and D. E. Draper, *Biochemistry*, **1989**, *28*, 1892-1897.
439. J. W. Nelson and J. Tinoco, I., *Biochemistry*, **1985**, *24*, 6416-6421.
440. K. Nakatani, S. Sando and I. Saito, *J. Am. Chem. Soc.*, **2000**, *122*, 2172-2177.
441. L. S. Kappen, Y. Lin, G. B. Jones and I. H. Goldberg, *Biochemistry*, **2007**, *46*, 561-567.
442. Z. Xi, D. Ouyang and H. Mu, *Bioorg. Med. Chem. Lett.*, **2006**, *16*, 1185-1190.

443. C. F. Yang, P. J. Jackson, Z. Xi and I. H. Goldberg, *Bioorg. Med. Chem.* , **2002**, *10*, 1329-1335.
444. Z. Xiao, N. Zhang, y. Lin, G. B. Jones and I. H. Goldberg, *Chem. Commun.*, **2006**, 4431-4433.
445. G. B. Jones, Y. Lin, Z. Xiao, L. Kappen and I. H. Goldberg, *Bioorg. Med. Chem.*, **2007**, *15*, 784-790.
446. A. Stassinopoulos, J. Ji, X. Gao and I. H. Goldberg, *Science*, **1996**, *272*, 1943-1946.
447. Z. Xi, Q. K. Mao and I. H. Goldberg, *Biochemistry*, **1999**, *38*, 4342-4354.
448. L. S. Kappen, Z. Xi and I. H. Goldberg, *Bioorg. Med. Chem.*, **1997**, *5*, 1221-1227.
449. L. J. Boerner and J. M. Zaleski, *Curr. Opin. Chem. Biol*, **2005**, *9*, 135-144.
450. C.-C. Cheng, W.-C. Huang-Fu, K.-C. Hung, P.-J. Chen, W. J. Wang and Y.-J. Chen, *Nucleic Acids Res.*, **2003**, *31*, 2227-2233.
451. J.-M. A. Battigello, M. Cui, S. Roshong and B. J. Carter, *Bioorg. Med. Chem.*, **1995**, *3*, 839-849.
452. P. T. Henderson, B. Armitage and G. B. Schuster, *Biochemistry*, **1998**, *37*, 2991-3000.
453. L. Dassonneville, F. Hamy, P. Colson, C. Houssier and C. Bailly, *Nucleic Acids Res.*, **1997**, *25*, 4487-4492.
454. N. Gelus, C. Bailly, F. Hamy, T. Klimkait, W. D. Wilson and D. W. Boykin, *Bioorg. Med. Chem.*, **1999**, *7*, 1089-1096.
455. L. Ratmeyer, M. L. Zapp, M. R. Green, R. Vinayak, A. Kumar, D. W. Boykin and W. D. Wilson, *Biochemistry*, **1996**, *35*, 13689-13696.
456. W. D. Wilson, L. Ratmeyer, M. Zhao, D. Ding, A. W. McConnaughie, A. Kumar and D. W. Boykin, *J. Mol. Recog.*, **1996**, *9*, 187-196.
457. H.-Y. Mei, M. Cui, A. Heldsinger, S. M. Lemrow, J. A. Loo, K. A. Sannes-Lowery, L. Sharmeen and A. W. Czarnik, *Biochemistry*, **1998**, *37*, 14204-14212.
458. H.-Y. Mei, A. A. Galan, N. S. Halim, D. P. Mack, D. W. Moreland, K. B. Sanders, H. N. Truong and A. W. Czarnik, *Bioorg. Med. Chem. Lett.*, **1995**, *5*, 2755-2760.
459. F. Leclerc and R. Cedergren, *J. Med. Chem.*, **1998**, *41*, 175-182.
460. S. A. Bejune and D. R. McMillin, *Chem. Commun.*, **2004**, 1320-1321.
461. M. K. Eggleston, D. K. Crites and D. R. McMillin, *J. Phys. Chem.*, **1998**, *102*, 5506-5511.
462. D. K. Crites Tears and D. R. McMillin, *Chem. Commun.*, **1998**, 2517-2518.
463. D. K. C. Tears and D. R. McMillin, *Chem. Commun.*, **1998**, 2517-2518.
464. P. Lugo-Ponce and D. R. McMillin, *Coord. Chem. Rev.*, **2000**, *208*, 169-191.
465. D. Sun, B. Thompson, B. E. Cathers, M. Salazar, S. M. Kerwin, J. O. Trent, T. C. Jenkins, S. Neidle and L. H. Hurley, *J. Med. Chem.*, **1997**, *40*, 2113-2116.
466. M. A. Read and S. Neidle, *Biochemistry*, **2000**, *39*, 13422-13432.
467. J.-L. Mergny, L. Lacroix, M.-P. Teulade-Fichou, C. Hounsou, L. Guittat, M. Hoarau, P. B. Arimondo, J.-P. Vigneron, J.-M. Lehn, J.-F. Riou, T. Garestier and C. Hélène, *Proc. Natl. Acad. Sci. USA*, **2001**, *98*, 3062-3067.
468. M. A. Read, J. Harrison, B. Romagnoli, F. A. Tanious, S. H. Gowan, A. P. Reszka, W. D. Wilson, L. R. Kelland and S. Neidle, *PNAS*, **2001**, *98*, 4844-4849.
469. C. M. Barbieri, A. R. Srinivasan, S. G. Rzuczek, J. E. Rice, E. J. LaVoie and D. S. Pilch, *Nucleic Acids Res.*, **2007**, *35*, 3272-3286.
470. M.-Y. Kim, H. Mankayalapati, K. Shin-ya, K. Wierzba and L. H. Hurley, *J. Am. Chem. Soc.*, **2002**, *124*, 2098-2099.

471. A. D. Moorhouse, A. M. Santos, M. Gunaratnam, M. Moore, S. Neidle and J. E. Moses, *J. Am. Chem. Soc.*, **2006**, *128*, 15972-15973.
472. G. S. Minhas, D. S. Pilch, J. E. Kerrigan, E. J. LaVoie and J. E. Rice, *Bioorg. Med. Chem. Lett.*, **2006**, *16*, 3891-3895.
473. C. Escudé, C. H. Nguyen, S. Kukreti, Y. Janin, J.-S. Sun, E. Bisagni, T. Garestier and C. Hélene, *Proc. Natl. Acad. Sci. USA*, **1998**, *95*, 3591-3596.
474. J. L. Mergny, G. Duval-Valentin, C. H. Nguyen, L. Perrouault, B. Faucon, M. Rougee, T. Montenay-Garestier, E. Bisagni and C. Hélene, *Science*, **1992**, *256*, 1681-1684.
475. R. Zain, D. Polverari, C.-H. Nguyen, Y. Blouquit, E. Bisagni, T. Garestier, D. S. Grierson and J.-S. Sun, *ChemBioChem*, **2003**, *4*, 856-862.
476. G. C. Silver, J.-S. Sun, C. H. Nguyen, A. S. Boutorine, E. Bisagni and C. Hélène, *J. Am. Chem. Soc.*, **1997**, *119*, 263-268.
477. A. Zaid, J.-S. Sun, C.-H. Nguyen, E. Bisagni, T. Garestier, D. G. Grierson and R. Zain, *ChemBioChem*, **2004**, *5*, 1550-1557.
478. A. Oleksi, A. G. Blanco, R. Boer, I. Usón, J. Aymamí, A. Rodger, M. J. Hannon and M. Coll, *Angew. Chem. Int. Ed.*, **2006**, *45*, 1227-1231.
479. A. L. Brogden, N. H. Hopcroft, M. Searcey and C. J. Cardin, *Angew. Chem. Int. Ed.*, **2007**, *46*, 3850-3854.
480. B. F. Eichman, B. H. Mooers, M. Alberti, J. E. Hearst and P. S. Ho, *J. Mol. Biol.*, **2001**, *308*, 15-26.
481. A. Shulman and F. P. Dwyer, *Metal Chelates in Biological Systems*, in *Chelating Agents and Metal Chelates*, eds. F. P. Dwyer and D. P. Mellor, Academic Press, New York, NY, USA, **1964**, pp. 383-439.
482. A. Juris, S. Barigelletti, S. Campagna, V. Balzani, P. Belser and A. von Zelewsky, *Coord. Chem. Rev.*, **1988**, *84*, 85-277.
483. L. E. Marshall, D. R. Graham, K. A. Reich and D. S. Sigman, *Biochemistry*, **1981**, *20*, 244-250.
484. J. K. Barton, J. J. Dannenberg and A. L. Raphael, *J. Am. Chem. Soc.*, **1982**, *104*, 4967-4969.
485. J. K. Barton, A. T. Danishefsky and J. M. Goldberg, *J. Am. Chem. Soc.*, **1984**, *106*, 2172-2176.
486. J. K. Barton, L. A. Basile, A. Danishefsky and A. Alexandrescu, *Proc. Natl. Acad. Sci. USA*, **1984**, *81*, 1961-1965.
487. J. K. Barton and A. L. Raphael, *Proc. Natl. Acad. Sci. USA*, **1985**, *82*, 6460-6464.
488. J. K. Barton and A. L. Raphael, *J. Am. Chem. Soc.*, **1984**, *106*, 2466-2468.
489. C. V. Kumar, J. K. Barton and N. J. Turro, *J. Am. Chem. Soc.*, **1985**, *107*, 5518-5523.
490. N. J. Turro, J. K. Barton and D. A. Tomalia, *Acc. Chem. Res.*, **1991**, *24*, 332-340.
491. J. K. Barton, J. M. Goldberg, C. V. Kumar and N. J. Turro, *J. Am. Chem. Soc.*, **1986**, *108*, 2081-2088.
492. S. Satyanarayana, J. C. Dabrowiak and J. B. Chaires, *Biochemistry*, **1992**, *31*, 9320-9323.
493. W. A. Kalsbeck and H. H. Thorp, *Inorg. Chem.*, **1994**, *33*, 3427-3429.
494. J. E. Coury, J. R. Anderson, L. McFailIsom, L. D. Williams and L. A. Bottomley, *J. Am. Chem. Soc.*, **1997**, *119*, 3792-3796.
495. J. G. Collins, A. D. Sleeman, J. R. Aldrich-Wright, I. Greguric and T. W. Hambley, *Inorg. Chem.*, **1998**, *37*, 3133-3141.
496. P. Lincoln and B. Norden, *J. Phys. Chem.*, **1998**, *102*, 9583-9594.

497. L.-N. Ji, X.-H. Zou and J.-G. Liu, *Coord. Chem. Rev.*, **2001**, *216-217*, 513-536.
498. H. K. Kim, P. Lincoln, B. Nordén and E. Tuite, *Chem. Commun.*, **1997**, 2375-2376.
499. J. G. Collins, R. M. Rixon and J. R. Aldrich-Wright, *Inorg. Chem.* , **2000**, *39*, 4377-4379.
500. J. P. Rehmann and J. K. Barton, *Biochemistry*, **1990**, *29*, 1701-1709.
501. J. P. Rehmann and J. K. Barton, *Biochemistry*, **1990**, *29*, 1710-1717.
502. C. Hiort, B. Nordén and A. Rodger, *J. Am. Chem. Soc.*, **1990**, *112*, 1971-1982.
503. I. S. Haworth, A. H. Elcock, J. Freeman, A. Rodger and W. G. Richards, *J. Biomol. Struct. Dyn.*, **1991**, *9*, 23-44.
504. M. Eriksson, M. Leijon, C. Hiort, B. Nordén and A. Gräslund, *J. Am. Chem. Soc.*, **1992**, *114*, 4933-4934.
505. M. F. Ottaviani, N. D. Ghatlia, S. H. Bossmann, J. K. Barton, H. Dürr and N. J. Turro, *J. Am. Chem. Soc.*, **1992**, *114*, 8946-8952.
506. D. Z. M. Coggan, I. S. Haworth, P. J. Bates, A. Robinson and A. Rodger, *Inorg. Chem.*, **1999**, *38*, 4486-4497.
507. P. Lincoln, A. Broo and B. Nordén, *J. Am. Chem. Soc.*, **1996**, *118*, 2644-2653.
508. S.-D. Choi, M.-S. Kim, S. K. Kim, P. Lincoln, E. Tuite and B. Nordén, *Biochemistry*, **1997**, *36*, 214-223.
509. I. Greguric, J. R. Aldrich-Wright and J. G. Collins, *J. Am. Chem. Soc.*, **1997**, *119*, 3621-3622.
510. E. Tuite, P. Lincoln and B. Nordén, *J. Am. Chem. Soc.*, **1997**, *119*, 239-240.
511. J. G. Collins, J. R. Aldrich-Wright, I. D. Greguric and P. A. Pellegrini, *Inorg. Chem.*, **1999**, *38*, 5502-5509.
512. A. Greguric, I. D. Greguric, T. W. Hambley, J. R. Aldrich-Wright and J. G. Collins, *J. Chem. Soc., Dalton Trans.*, **2002**, 849-855.
513. M. Eriksson, M. Leijon, C. Hiort, B. Norden and A. Graslund, *Biochemistry*, **1994**, *33*, 5031-5040.
514. N. A. P. Kane-Maguire and J. F. Wheeler, *Coord. Chem. Rev.*, **2001**, *211*, 145-162.
515. T. Kuwabara, T. Noda, H. Ohtake, T. Ohtake, S. Toyama and Y. Ikariyamab, *Anal. Biochem.*, **2003**, *314*, 30-37.
516. C. Metcalfe and J. A. Thomas, *Chem. Soc. Rev.*, **2003**, *32*, 215-224.
517. Y. Jenkins and J. K. Barton, *J. Am. Chem. Soc.*, **1992**, *114*, 8736-8738.
518. A. E. Friedman, J.-C. Chambron, J.-P. Sauvage, N. J. Turro and J. K. Barton, *J. Am. Chem. Soc.*, **1990**, *112*, 4960-4962.
519. E. J. C. Olson, D. Hu, A. Hormann, A. M. Jonkman, M. R. Arkin, E. D. A. Stemp, J. K. Barton and P. F. Barbara, *J. Am. Chem. Soc.*, **1997**, *119*, 11458-11467.
520. A. E. Friedman, C. V. Kumar, N. J. Turro and J. K. Barton, *Nucleic Acids Res.*, **1991**, *19*, 2595-2601.
521. B. Önfelt, P. Lincoln, B. Norden, J. S. Baskin and A. H. Zewail, *Proc. Natl. Acad. Sci. USA*, **2000**, *97*, 5708-5713.
522. Y. Jenkins, A. E. Friedman, N. J. Turro and J. K. Barton, *Biochemistry*, **1992**, *31*, 10809-10816.
523. C. Moucheron, A. Kirsch-De Mesmaeker and S. Choua, *Inorg. Chem.*, **1997**, *36*, 584-592.
524. C. J. Murphy, M. R. Arkin, Y. Jenkins, N. D. Ghatlia, S. H. Bossmann, N. J. Turro and J. K. Barton, *Science*, **1993**, *262*, 1025-1029.

525. E. D. A. Stemp, M. R. Arkin and J. K. Barton, *J. Am. Chem. Soc.*, **1995**, *117*, 2375-2376.
526. M. R. Arkin, E. D. A. Stemp, R. E. Holmlin, J. K. Barton, A. Hormann, E. J. C. Olson and P. F. Barbara, *Science*, **1996**, *273*, 475-480.
527. P. Lincoln, E. Tuite and B. Nordén, *J. Am. Chem. Soc.*, **1997**, *119*, 1454-1455.
528. S. Priyadarshy, S. M. Risser and D. N. Beratan, *J. Phys. Chem.*, **1996**, *100*, 17678-17682.
529. L. S. Schulman, S. H. Bossmann and N. J. Turro, *J. Phys. Chem.*, **1995**, *99*, 9283-9292.
530. I. Haq, P. Lincoln, D. C. Suh, B. Nordén, B. Z. Chowdhry and J. B. Chaires, *J. Am. Chem. Soc.*, **1995**, *117*, 4788-4796.
531. R. M. Hartshorn and J. K. Barton, *J. Am. Chem. Soc.*, **1992**, *114*, 5919-5925.
532. C. Hiort, P. Lincoln and B. Nordén, *J. Am. Chem. Soc.*, **1993**, *115*, 3448-3454.
533. C. G. Coates, L. Jacquet, J. J. McGarvey, S. E. J. Bell, A. H. R. Al-Obaidi and J. M. Kelly, *Chem. Commun.,*, **1996**, 35-36.
534. A. Mihailovic, I. Vladescu, M. McCauley, E. Ly, M. C. Williams, E. M. Spain and M. E. Nunez, *Langmuir*, **2006**, *22*, 4699-4709.
535. J. Bolger, A. Gourdon, E. Ishow and J.-P. Launnay, *Inorg. Chem.*, **1996**, *35*, 2937-2944.
536. Q.-X. Zhen, B.-H. Ye, J.-G. Liu, Q.-L. Zhang, L.-N. Ji and L. Wang, *Inorg. Chim. Acta*, **2000**, *303*, 141-147.
537. S. P. Foxon, C. Metcalfe, H. Adams, M. Webb and J. A. Thomas, *Inorg. Chem.*, **2007**, *46*, 409-416.
538. C. M. Dupureur and J. K. Barton, *J. Am. Chem. Soc.*, **1994**, *116*, 10286-10287.
539. C. M. Dupureur and J. K. Barton, *Inorg. Chem.*, **1997**, *36*, 33-43.
540. R. E. Holmlin, E. D. A. Stemp and J. K. Barton, *Inorg. Chem.*, **1998**, *37*, 29-34.
541. Y. Pin and H. Daxiong, *Sci. China, Ser. B*, **2000**, *43*, 516-523.
542. S. Delaney, M. Pascaly, P. K. Bhattacharya, K. Han and J. K. Barton, *Inorg. Chem.*, **2002**, *41*, 1966-1974.
543. B. H. Yun, J.-O. Kim, B. W. Lee, P. Lincoln, B. Nordén, J.-M. Kim and S. K. Kim, *J. Phys. Chem. B*, **2003**, *107*, 9858-9864.
544. B. W. Lee, S. J. Moon, M. R. Youn, J. H. Kim, H. G. Jang and S. K. Kim, *Biophys. J.*, **2003**, *85*, 3865-3871.
545. I. Ortmans, B. Elias, J. M. Kelly, C. Moucheron and A. Kirsch-De Mesmaeker, *Dalton Trans.*, **2004**, 668-676.
546. R. E. Holmlin, J. A. Yao and J. K. Baton, *Inorg. Chem.*, **1999**, *38*, 174- 189.
547. L. Ji, X. Zou and J. Liu, *Coord. Chem. Rev.* , **2001**, 513-536.
548. D. Han, H. Wang and N. Ren, *J. Mol. Model.*, **2004**, *10*, 216-222.
549. E. M. Proudfoot, J. P. Mackay and P. Karuso, *Biochemistry*, **2001**, *40*, 4867-4878.
550. P. K.-L. Fu, P. M. Bradley and C. Turro, *Inorg. Chem.*, **2003**, *42*, 878-884.
551. B. Wu, L. Gao, Z. Duan and K. Wang, *Inorg. Biochem.*, **2005**, *99*, 1685-1691.
552. R. H. Terbrueggen, T. W. Johann and J. K. Barton, *Inorg. Chem.*, **1998**, *37*, 6874-6883.
553. S. S. David and J. K. Barton, *J. Am. Chem. Soc.*, **1993**, *115*, 2984-2985.
554. D. Campisi, T. Morii and J. K. Barton, *Biochemistry*, **1994**, *33*, 4130-4139.
555. R. H. Terbrueggen and J. K. Barton, *Biochemistry*, **1995**, *34*, 8227-8234.
556. E. Rüba, J. R. Hart and J. K. Barton, *Inorg. Chem.*, **2004**, *43*, 4570-4578.
557. C. S. Chow and J. K. Barton, *J. Am. Chem. Soc.*, **1990**, *112*, 2839-2841.
558. C. S. Chow, L. S. Behlen, O. C. Uhlenbeck and J. K. Barton, *Biochemistry*, **1992**, *31*, 972-982.

559. H. R. Neenhold and T. M. Rana, *Biochemistry*, **1995**, *34*, 6303-6309.
560. B. P. Hudson and J. K. Barton, *J. Am. Chem. Soc.*, **1998**, *120*, 6877-6888.
561. R. J. Morgan, S. Chatterjee, A. D. Baker and T. C. Strekas, *Inorg. Chem.*, **1991**, *30*, 2687-2692.
562. A. M. Pyle, J. P. Rehmann, R. Meshoyrer, C. V. Kumar, N. J. Turro and J. K. Barton, *J. Am. Chem. Soc.*, **1989**, *111*, 3051-3058.
563. J.-Z. Wu, B.-H. Ye, L. Wang, L.-N. Ji, J.-Y. Zhou, R.-H. Li and Z.-Y. Zhou, *J. Chem. Soc., Dalton Trans.*, **1997**, 1395-1401.
564. Y. Xiong, X. F. He, X. H. Zou, J. Z. Wu, X. M. Chen, L. N. Ji, R. H. Li, J. Y. Zhou and K. B. Yu, *J. Chem. Soc., Dalton Trans.*, **1999**, 19- 23.
565. Q.-X. Zhen, B.-H. Ye, Q.-L. Zhang, J.-G. Liu, H. Li, L.-N. Ji and L. Wang, *J. Inorg. Biochem.*, **1999**, *76*, 47-53.
566. N. W. Luedtke, J. S. Hwang, E. C. Glazer, D. Gut, M. Kol and Y. Tor, *ChemBioChem*, **2002**, *3*, 766-771.
567. N. W. Luedtke, J. S. Hwang, E. Nava, D. Gut, M. Kol and Y. Tor, *Nucleic Acids Res.*, **2003**, *31*, 5732-5740.
568. S. Shi, J. Liu, K. C. Zheng, C. P. Tan, L. M. Chen and L. N. Ji, *Dalton Trans.*, **2005**, 2038-2046.
569. P. U. Maheswari and M. Palaniandavar, *J. Inorg. Biochem.*, **2004**, *98*, 219-230.
570. X. W. Liu, J. Li, H. Deng, K. C. Zheng, Z. W. Mao and L. N. Ji, *Inorg. Chim. Acta*, **2005**, *358*, 3311-3319.
571. X. W. Liu, J. Li, H. Li, K. Zheng, H. Chao and L. Ji, *Inorg. Chem.*, **2005**, *99*, 2372-2380.
572. J.-G. Liu, B.-H. Ye, H. Li, L.-N. Ji, R.-H. Li and J.-Y. Zhou, *J. Inorg. Biochem.*, **1999**, *73*, 117-122.
573. D. Lawrence, V. G. Vaidyanathab and B. U. Nair, *J. Inorg. Biochem.* , **2006**, *100*, 1244-1251.
574. P. U. Maheswari, V. Rajendiran, M. Palaniandavar, R. Parthasarathi and V. Subramanian, *J. Inorg. Biochem.*, **2006**, *100*, 3-17.
575. P. U. Maheswari and M. Palaniandavar, *Inorg. Chim. Acta*, **2004**, *357*, 901-912.
576. P. P. Pellegrini and J. R. Aldrich-Wright, *Dalton Trans.*, **2003**, 176-183.
577. R. Caspar, L. Musatkina, A. Tatosyan, H. Amouri, M. Gruselle, C. Guyard-Duhayon, R. Duval and C. Cordier, *Inorg. Chem.*, **2004**, *43*, 7986-7993.
578. P. U. Maheswari, V. Rajendiran, H. Stoeckli-Evans and M. Palaniandavar, *Inorg. Chem.*, **2006**, *45*, 37-50.
579. H.-Y. Mei and J. K. Barton, *Proc. Natl. Acad. Sci. USA*, **1988**, *85*, 1339-1343.
580. P. W. Huber, T. Morii, H. Mei and J. K. Barton, *Proc. Natl. Acad. Sci. USA*, **1991**, *88*, 10801-10805.
581. J. Aldrich-Wright, C. Brodie, E. C. Glazer, N. W. Luedtke, L. Elson-Schwaband and Y. Tor, *Chem. Commun.*, **2004**, 1018-1019.
582. F. M. O'Reilly and J. M. Kelly, *New J. Chem.*, **1998**, *22*, 215-217.
583. A. N. Glazer and H. S. Rye, *Nature*, **1992**, *359*, 859-861.
584. F. O'Reilly, J. Kelly and A. Kirsch-De Mesmaeker, *Chem. Commun.*, **1996**, 1013-1014.
585. F. M. O'Reilly and J. M. Kelly, *J. Phys. Chem. B*, **2000**, *104*, 7206-7213.
586. Y. Nakabayashi, N. Iwamoto, H. Inada and O. Yamauchi, *Inorg. Chem. Commun.*, **2006**, *9*, 1033-1036.

587. D. L. Carlson, D. H. Huchital, E. J. Mantilla, R. D. Sheardy and W. R. Murphy, *J. Am. Chem. Soc.*, **1993**, *115*, 6424-6425.
588. P. Lincoln and B. Nordén, *J. Chem. Soc., Chem. Commun.*, **1996**, *18*, 2145-2146.
589. L. M. Wilhelmsson, F. Westerlund, P. Lincoln and B. Nordén, *J. Am. Chem. Soc.*, **2002**, *124*, 12092-12093.
590. L. M. Wilhelmsson, E. K. Esbjörner, F. Westerlund, B. Nordén and P. Lincoln, *J. Phys. Chem. B*, **2003**, *107*, 11784-11793.
591. B. Önfelt, P. Lincoln and B. Nordén, *J. Am. Chem. Soc.*, **1999**, *121*, 10846-10847.
592. B. Önfelt, P. Lincoln and B. Nordén, *J. Am. Chem. Soc.*, **2001**, *123*, 3630-3637.
593. H. Chao, Y. Yuan, F. Zhou and L. Ji, *Transit. Metal Chem.*, **2006**, *31*, 465-469.
594. F. Liu, K. Wang, G. Bai, Y. Zhang and L. Gao, *Inorg. Chem.*, **2004**, *43*, 1799-1806.
595. M. Narra, P. Elliot and S. Swavey, *Inorg. Chim. Acta*, **2006**, *359*, 2256-2262.
596. S.-D. Jiang, K.-Z. Wang, F.-R. Liu, Y.-A. Zhang and L.-H. Gao, *Huaxue Xuebao*, **2005**, *63*, 783-786.
597. J.-Z. Wu, L. Yuan and Y. Yu, *Inorg. Chim. Acta*, **2006**, *359*, 718-720.
598. J.-Z. Wu and L. Yuan, *J. Inorg. Biochem.*, **2004**, *98*, 41-45.
599. S. A. Tysoe, R. Kopelman and D. Schelzig, *Inorg. Chem.*, **1999**, *38*, 5196-5197.
600. A. A. Holder, *Inorg. Chem.*, **2004**, *43*, 303-308.
601. S. Swavey and K. J. Brewer, *Inorg. Chem.*, **2002**, *41*, 6196-6198.
602. M. Milkevitch, H. Storrie, E. Brauns, K. J. Brewer and B. W. Shirley, *Inorg. Chem.*, **1997**, *36*, 4534-4538.
603. R. L. Williams, H. N. Toft, B. Winkel and K. J. Brewer, *Inorg. Chem.*, **2003**, *42*, 4394-4400.
604. X.-H. Zou, *J. Chem. Soc., Dalton Trans.*, **1999**, 1423-1428.
605. C.-W. Jiang, H. Chao, X.-L. Hong, H. Li, W.-J. Mei and L.-N. Ji, *Inorg. Chem. Commun.*, **2003**, *6*, 773-775.
606. C.-W. Jiang, *Inorg. Chim. Acta*, **2005**, *358*, 1231-1236.
607. C.-W. Jiang, *Inorg. Chim. Acta*, **2004**, *357*, 3403-3406.
608. C.-W. Jiang, *Eur. J. Inorg. Chem.*, **2004**, 2277-2282.
609. A. Kirsch-De Mesmaeker, C. Moucheron and N. Boutonnet, *J. Phys. Org. Chem.*, **1998**, *11*, 566-576.
610. O. van Gijte and A. Kirsch-De Mesmaeker, *J. Chem. Soc., Dalton Trans.*, **1999**, 951-956.
611. A. Brodkorb, A. Kirsch-De Mesmaeker, T. J. Rutherford and F. R. Keene, *Eur. J. Inorg. Chem.*, **2001**, 2151-2160.
612. T. J. Rutherford, O. Van Gijte, A. Kirsch-De Mesmaeker and F. R. Keene, *Inorg. Chem.*, **1997**, *36*, 4465-4474.
613. F. M. Foley, F. R. Keene and J. G. Collins, *J. Chem. Soc., Dalton Trans.*, **2001**, 2968-2974.
614. F. M. Foley, *DNA Interactions of Mono- and Dinuclear Polypyridylruthenium(II) Complexes*, Honours Thesis, James Cook University, Townsville, **2000**.
615. B. T. Patterson, *Stereochemistry and Applications of Mono- and Oligo-nuclear Complexes of Iron, Ruthenium and Osmium*, PhD Thesis, James Cook University, Townsville, **2002**.
616. B. T. Patterson, J. G. Collins, F. M. Foley and F. R. Keene, *J. Chem. Soc., Dalton Trans.*, **2002**, 4343-4350.
617. J. A. Smith, J. G. Collins, B. T. Patterson and F. R. Keene, *Dalton Trans.*, **2004**, 1277-1283.

# Chapter 2

## *Synthesis and Stereochemical Purification of Dinuclear Ruthenium Complexes*

## 2.1 INTRODUCTION

### 2.1.1 Background

Over the past two decades the field of supramolecular chemistry has become one of the most active within the discipline of chemistry. The importance of the field was acknowledged by the awarding of the 1987 Nobel Prize for Chemistry to Cram, Lehn and Pedersen in recognition of their contributions to supramolecular chemistry, particularly their studies of structure-specific recognition and complex formation.[1] Essentially, supramolecular chemistry involves the study of non-covalent interactions – hydrogen bonding, van der Waals forces, electrostatics, π-stacking, hydrophobic contacts, and metal-ligand coordination – between otherwise chemically-independent molecules.[2] Such studies arose from the desire to emulate the specificity of interactions between biological molecules – an enzyme and its substrate or two strands of DNA, for instance – and today encompasses a variety of different areas of innovation including host-guest chemistry, molecular recognition, molecular self-assembly, and mechanically-interlocked architectures. Ultimately, these systems will see potential applications as photochemical molecular devices, catalysts, magnetic storage systems, molecular machines, and probes of biological systems.

Polypyridyl complexes of $d^6$ transition metals – such as osmium(II), rhenium(I), rhodium(III), and particularly ruthenium(II) – have received considerable attention as potential building blocks of metallosupramolecular assemblies. This interest stems from the favourable photophysical and redox properties of such species and their well-defined synthetic chemistry. Complexes of this type often exhibit strong spectroscopic absorbances and luminescent emissions, and they frequently demonstrate facile electron transfer properties. Furthermore, they are relatively inert (a vital attribute when one is studying non-covalent interactions) and the synthetic methodologies exist to exert a high degree of control over the size and shape of their structure, including the production of ligand-bridged oligo-metallic species. Given the importance attributed to the fundamental concept of "shape" in intermolecular interactions amongst natural systems, it is apparent that careful control over the stereochemistry of these large synthetic supramolecular systems may well be fundamental to their successful application.

### 2.1.2 Polypyridylruthenium Complexes

The first reported use of polypyridyl ligands as coordinating agents was by Blau in 1888, where he described the binding of the now-archetypical bidentate chelates 1,10-phenanthroline (phen) and 2,2′-bipyridine (bpy) to iron(II).[3] Such heterocyclic aromatic ligands are not only excellent σ-donors due to the presence of lone pairs of electrons in the $sp^2$ orbitals of the aromatic nitrogen atoms, but the delocalised π*-orbitals associated with their aromatic ring systems bestow on them a significant acceptor ability as well. Coupling these ligands to a $d^6$ ruthenium(II) centre gives rise to inert complexes possessing impressive metal-to-ligand charge transfer (MLCT) characteristics, relatively long excited-state lifetimes, and redox properties that make them ideally suited to a variety of applications. Additionally, the rigid coordination geometry of such species and well-established methodologies for manipulating the shape and functionalities of polypyridyl ligands allows for fine control over the overall size and stereochemistry of polypyridylruthenium(II) complexes.[4, 5]

To date, the majority of studies into the properties and applications of polypyridylruthenium(II) complexes have focused upon mononuclear species. The configuration of the ligands in tris(bidentate) complexes of octahedral metal centres {e.g. $[Ru(bpy)_3]^{2+}$} is such that the complex possesses either a left-handed (Λ) or right-handed (Δ) configuration (see Figure 2.1). In most regards these enantiomers are indistinguishable from one another unless introduced to an environment which is itself chiral. For instance, Δ-$[Ru(bpy)_3]^{2+}$ cannot be differentiated from Λ-$[Ru(bpy)_3]^{2+}$ using NMR spectroscopy,[†] but the two optical isomers give opposite Cotton Effects in circular dichroism spectra.

Through a bridging ligand two or more of these mononuclear units may be linked together. The most basic example of such a system is a dinuclear complex of the form $[\{Ru(pp)_2\}_2(\mu\text{-BL})]^{4+}$ {where pp is a symmetrical bidentate terminal ligand ($C_{2v}$ point group symmetry) such as bpy, and BL is a symmetrical ($D_{2h}$) bridging ligand such as 2,2′-bipyrimidine (bpm)}. Since $[\{Ru(pp)_2\}_2(\mu\text{-BL})]^{4+}$ is composed of two metal centres, each possessing its own chirality, this complex exists in two diastereoisomeric forms: *meso* (ΔΛ/ΛΔ; $C_{2h}$ point group symmetry) and *rac* (ΔΔ/ΛΛ; $D_2$ point group symmetry) {see Figure 2.2}.[4, 5] The racemic mixture of the *rac*

[†] In the strictest sense, the "enantiomers" discussed here are actually *diastereoisomers* that can conceivably be distinguished through ultra-high-resolution NMR.[6] True enantiomers are not only space-inverted (i.e. mirror images), but also *charge* inverted. Consequently, the true enantiomeric counterpart of Δ-$[Ru(bpy)_3]^{2+}$ would be Λ-$[Ru(bpy)_3]^{2+}$ composed of *antimatter*.

diastereoisomer can be resolved into its enantiomeric constituents (ΔΔ and ΛΛ) under the appropriate chiral conditions, however symmetry dictates that the two forms of the *meso* diastereoisomer are indistinguishable (ΔΛ ≡ ΛΔ) under conditions in which both metal centres are equivalent. Introduction of non-equivalence to the two halves of the complex, $[\{M(pp)_2\}(\mu\text{-}BL)\{M'(pp')_2\}]^{4+}$, by means of coordinating different terminal ligands to each metal centre {pp ≠ pp′} and/or by introducing heterometallic centres {M ≠ M′}, results in a lowering of the symmetry of both the "*meso*" and *rac* diastereoisomers to $C_2$. Consequently, the two stereoisomers of the "*meso*" set would no longer be configurationally internally compensated and hence would constitute an enantiomeric pair (see Figure 2.3).[4, 7, 8]

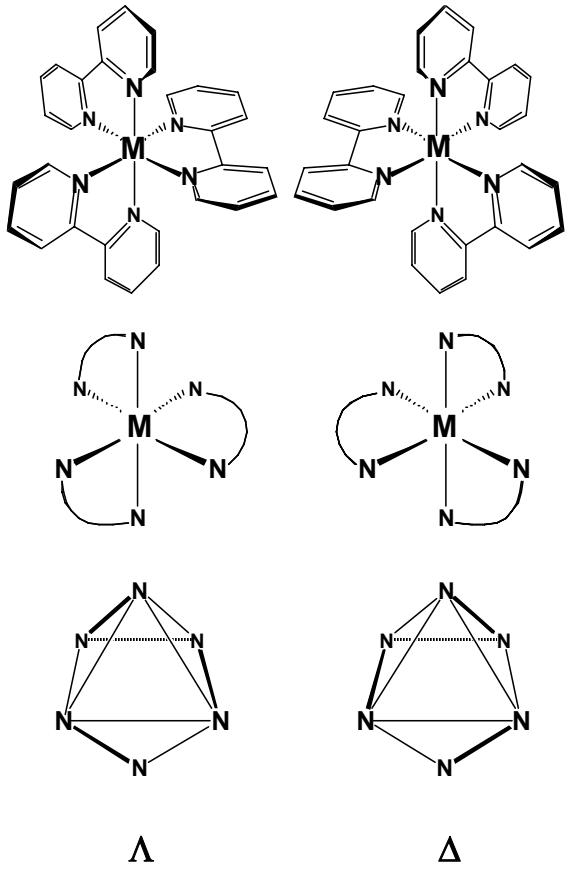


***Figure 2.1***
**Enantiomers.** Three different representations of the enantiomeric forms of $[M(bpy)_3]^{2+}$ {and by extension any tris(bidentate) system} where M is an octahedral metal centre.

Dinuclear systems are further complicated in instances where the metal centres have mixed terminal ligands {i.e. $[\{M(pp)(pp')\}_2(\mu\text{-}BL)]^{4+}$, again where pp ≠ pp′} as this leads to geometric

isomerism.[9] In such cases the *meso* and *rac* diastereoisomers exist as *cis* and *trans* geometric forms depending upon whether the equivalent ligands are located on the same or opposite sides of the plane of the bridging ligand. The *cis* and *trans* forms of the *meso* diastereoisomer have $C_s$ and $C_i$ point group symmetries, respectively, while both geometric isomers of the *rac* diastereoisomer have $C_2$ point group symmetry, albeit each with a $C_2$ axis of different orientation (see Figure 2.4). It is evident that an increase in the nuclearity of the complex from the mono- to the dinuclear species yields an increase in the potential stereochemical complexity of the system, a trend that continues with further expansion into trinuclear assemblies and beyond.[10, 11]

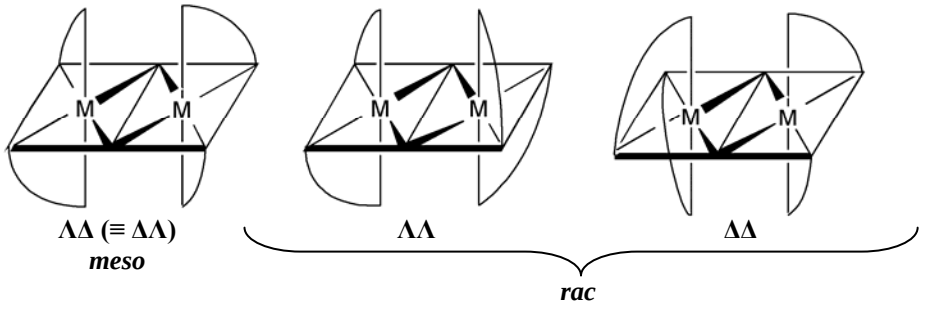


***Figure 2.2***
**Stereoisomers of a dinuclear complex.** Complexes of the form $[\{M(pp)_2\}_2(\mu\text{-BL})]^{4+}$ exist in two diastereoisomeric forms, *meso* and *rac*, the latter being a mixture of two enantiomers (ΔΔ and ΛΛ).

The bulk of studies conducted into polymetallic systems have generally concerned themselves with isomeric mixtures,[12-18] either due to the inherent difficulties in isolating individual stereoisomers from multinuclear systems or the misapprehension that the influence of isomerism on molecular properties is negligible. However, it has been demonstrated that the geometric isomers of mononuclear species[5, 19-21] and the diastereoisomers of di- and trinuclear systems[5, 10, 22-25] do indeed exhibit significant differences in their physical properties. The influence of the spatial configuration of polymetallic assemblies makes it clear that careful control over the stereochemistry will be necessary to ensure maximum efficiency of such systems in whichever role they are to be employed. This level of structural control remains a daunting prospect when faced with multiple stereocentres and as a result the issue has received limited attention to date.

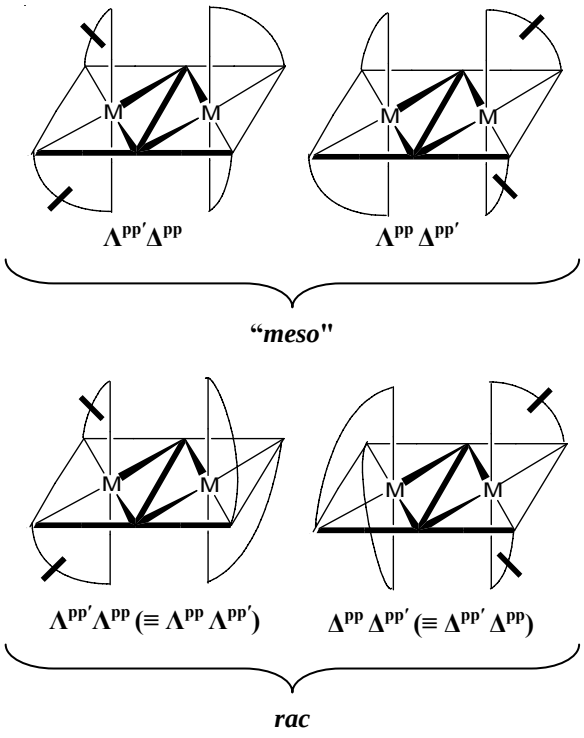


***Figure 2.3***
**Non-equivalent ends results in lower symmetry.** Complexes of the form $[\{M(pp)_2\}(\mu\text{-BL})\{M(pp')_2\}]^{4+}$ exist in four stereoisomeric forms, two sets of enantiomers arising from each of the *meso* and *rac* diastereoisomers. pp ≠ pp′, with the latter marked with a bar in the above diagram.

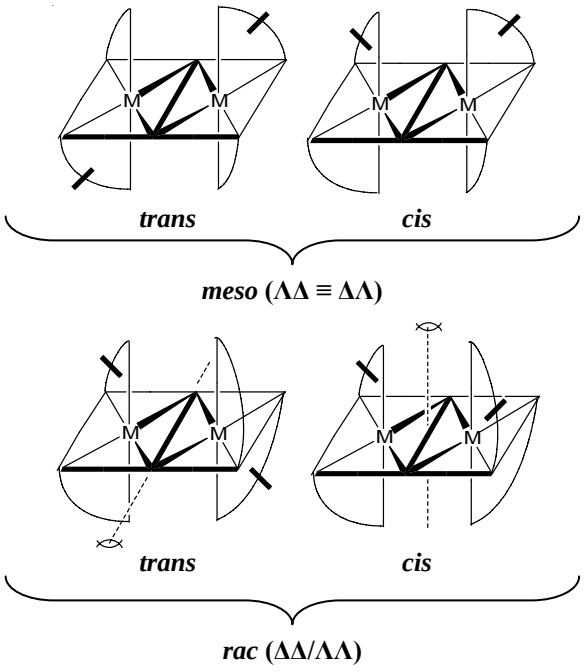


***Figure 2.4***
**Geometric isomerism in a dinuclear species.** The diastereoisomers of complexes of the form $[\{M(pp)(pp')\}_2(\mu\text{-BL})]^{4+}$ exist in *cis* and *trans* geometric isomers. pp ≠ pp′, with the latter marked with a bar in the above diagram. $C_2$ symmetry axes are shown for the *rac* isomers.

### 2.1.3 Chromatography

Traditionally, chiral resolutions of mononuclear polypyridyl complexes have been accomplished by means of diastereoisomeric salt formation.[7, 26-30] This technique typically involves mixing a racemic mixture of the ionic complex of interest with a single enantiomer of a chiral auxiliary counterion, resulting in the formation of two possible diastereoisomeric salts. Differences in the solubilities of the diastereoisomers allows for their separation (and, hence, the separation of the enantiomers of the complex) via fractional crystallisation. A variety of different chiral anions have been employed, including (+/-)-*O*,*O*′-dibenzoyl-D/L-tartrate,[29] arsenyl-(+/-)-tartrate,[28] (+)-tartrate,[26, 31] antimonyl-(+)-tartrate,[27, 30, 32] (+)-camphorsulfonic acid and derivatives,[33-36] and Δ-[tris(tetrachlorobenzenediolato)phosphate(V)]$^-$ {TRISPHAT}.[37, 38]

An alternative method of achieving chiral control is stereoselective synthesis. This technique entails the use of precursors of definitive stereochemistry (often obtained via diastereoisomeric salt formation) and substituting ligands without loss of configuration. The resultant product will be of high enantiomeric purity and may itself be used as a basis for the stereoselective synthesis of larger assemblies.[4, 5, 7, 29, 39-41] Unfortunately, such procedures require great care to maintain the chirality of the metal centre during each step of the synthetic process. Furthermore, the conditions required for such reactions often lead to some degree of loss of stereochemical integrity.

Chromatographic techniques have long been utilised as a means of separating and purifying mixtures of metal complex isomers.[31] This has classically been accomplished by exploiting the differing affinities of isomers for a chiral adsorbent such as quartz,[42] starch,[43-45] cellulose,[46-48] or alumina treated with chiral agents.[49] However, such techniques often demonstrated limited resolving powers due to the relatively poor adsorbency of the stationary phase. Greater success has been achieved through the use of ion-exchange gels, notably Sephadex which is a three dimensional network of functionalised dextran (a polysaccharide composed of D-glucose subunits linked via α-1,6-glycosidic bonds {and to a lesser extent α-1,3 and/or α-1,4 bonds}) bridged by epichlorohydrin.[50] Use of this medium was pioneered by in the laboratories of Yoshikawa[50-52] and Searle[52, 53] who utilised it to affect the separation of geometric and optical isomers of numerous cobalt(III)-amine complexes. More recently, Keene and co-workers have coupled column chromatography using the chiral Sephadex stationary phase (typically SP Sephadex C-25, featuring strongly acidic propylsulfonate functional groups) with optically-

active eluents, enabling highly efficient resolutions of many transition metal complexes, including multinuclear systems.[5, 7, 32, 54]

The technique developed by Keene *et al.* has proven to be an effective means of separating the stereoisomers of mono-, di- and trinuclear polypyridyl metal complexes.[4, 5, 9, 10, 54, 55] While the coulombic interactions governing the process of cation-exchange chromatography separate on the basis of the charge, some differentiation between substrates possessing the *same* overall charge may also be achieved based on variations in the charge density or polarity of the cations.[53, 54] Discrimination between the *meso* and *rac* diastereoisomers of such complexes is believed to be based upon "host-guest"-type interactions between the eluent anion and complex cation.[55] These interactions are thought to be largely hydrophobic and/or π-stacking in nature, with the extent of association governed by the stereochemistry of the complex. In the case of the dinuclear complex $[\{Ru(Me_2bpy)_2\}_2(\mu\text{-bpm})]^{4+}$, the orthogonal arrangement of the terminal ligands in the *meso* diastereoisomer gives rise to clefts above and below the plane of the bridging ligand in which an eluent anion can be accomodated, whereas the *rac* form lacks such well-defined features. NMR studies suggest that these clefts are sufficiently large to accommodate the bulk of an eluent anion such as toluene-4-sulfonate, thus reducing the effective charge of the complex. With regards to $[\{Ru(Me_2bpy)_2\}_2(\mu\text{-bpm})]^{4+}$ the *meso* diastereoisomer would be expected to have a lowered relative charge and therefore be eluted faster than did the racemic mixture. This technique has also been successfully applied to the separation of *geometric* isomers.[9]

The resolution of enantiomers of mono- and dinuclear species via this technique operates on a similar principle, albeit with the use of a chiral eluent anion to discriminate between the enantomers.[32] Again, the eluent anion forms a stronger association with one isomer than it does the other resulting in a diminished effective charge on the favoured enantiomer, which subsequently elutes faster. For example, in the resolution of the complex $[Ru(bpy)_3]^{2+}$ using a solution of disodium (-)-*O*,*O*′-dibenzoyl-L-tartrate the Δ enantiomer eluted before the Λ enantiomer. Conversely, the use of an eluent anion of the opposite handedness, disodium (+)-*O*,*O*′-dibenzoyl-D-tartrate, resulted in a reversal of the elution order, albeit with a noticeable decrease in efficiency as the chirality of the eluent opposes that of the support.[32, 55]

It is noteworthy that in some instances chiral resolution can be achieved through the use of an achiral eluent.[32, 54] In the absence of a chiral eluent the two enantiomers of a mononuclear complex should be of equivalent effective charge and polarity – the resolution must therefore

be attributed to the chiral nature of the Sephadex support material alone. Consequently, a typical resolution utilising a chiral eluent *and* support might be considered to be the result of a synergistic effort between the two.[32] Hence, optimal resolution of a racemic mixture necessitates the choice of an eluent that not only exhibits the greatest discrimination between enantiomers but also complements the chirality of the stationary phase. Indeed, while factors such as temperature and eluent concentration are known to be influential,[54] it is often a judicious choice of eluent that governs the overall efficiency of separations/resolutions using these techniques.

### 2.1.4 Applications

As mentioned above, the synthetic versatility and inertness of polypyridylruthenium(II) complexes, coupled with their advantageous photophysical and electrochemical properties, makes such species ideally suited to a variety of potential applications including photocatalysis,[56-58] small-molecule/ion recognition and optical sensing,[59-67] the development of non-linear optical materials,[68-73] and as templates for molecular machines.[74-78] Larger supramolecular and/or polymetallic assemblies based upon the polypyridylruthenium moiety have demonstrated promising activity as the basis of photochemical molecular devices (PMDs) – molecular constructs that perform light-induced functions such as photoswitching, solar energy conversion and information storage.[79-86] Inspired by natural energy/electron-transfer systems (such as those involved in photosynthesis) PMDs are essentially comprised of donor and acceptor moieties separated by a spacer; these may be relatively simple linear arrangement resembling a molecular wire,[85, 87, 88] or be part of more elaborate dendrimeric ”antenna” systems in which multiple polypyridyl transition metal centres are linked via bridging ligands such as 2,3-dpp.[12, 89-91] Energy absorption and transfer is facilitated by the strong MLCT properties of polypyridylruthenium species, while electron transfer is aided by intervalence charge transfer (IVCT) mechanisms arising from the notable stability of ruthenium (and related transition metals) in multiple oxidation states.[80, 92-94]

The specific application at the crux of this thesis is the use of polypyridylruthenium(II) complexes as probes of biological molecules, particularly the secondary structure of nucleic acids. Again, the photophysical and redox properties that make such complexes so applicable to the design of new materials have been extensively employed in the exploration of the energy-

and electron-transfer properties of DNA.[95-98] Furthermore, this genre of complexes have been utilised as a means to investigate oxidative damage/cleavage of nucleic acids,[99-101] and by extension as artificial nucleases,[102-104] as well as probes of specific nucleic acid structures and conformations.[105-110] The ability to systematically vary the geometry of these complexes allows for the "fine-tuning" of the overall shape, size and stereochemistry.[4, 5, 84] This, in turn, facilitates the design of probes intended to target specific nucleic acid structural features such as bulges or hairpin loops. Thus, polypyridylruthenium(II) complexes provide a means by which to elucidate the structure and structure-recognition principles of nucleic acids, with the potential long-term outcomes including the development of metallopharmaceuticals possessing exceptional specificity and efficacy.

### 2.1.5 Present Studies

The syntheses described within this Chapter were intended to provide a series of dinuclear polypyridylruthenium(II) complexes of the form $[\{Ru(pp)_2\}_2(\mu\text{-BL})]^{4+}$ for use in DNA-binding studies {where pp represents the terminal ligands 2,2′-bipridine (bpy), 4,4′-dimethyl-2,2′-bipridine ($Me_2$bpy), 5,5′- dimethyl-2,2′-bipridine (5,5′-$Me_2$bpy), 1,10-phenanthroline (phen), or 4,7-dimethyl-1,10-phenanthroline ($Me_2$phen), and BL represents the bridging ligands 2,2′-bipyrimidine (bpm), 1,4,5,8,9,12-hexaazatriphenylene (HAT), 1,4,5,12-tetraazatriphenylene (4,7-phenanthrolino-5,6:5′,6′-pyrazine; ppz), 2,3-bis(2-pyridyl)pyrazine (2,3-dpp), or 2,5-bis(2-pyridyl)pyrazine (2,5-dpp)}. Established synthetic and chromatographic techniques allowed for the synthesis and isolation of stereochemically-pure complexes encompassing a variety of geometries. Specifically, complexes possessing linear, stepped-parallel and angular bridging ligands (see below) were prepared in order to investigate the effects of differing metal centre arrangements and proximities and the resultant influence on the overall geometry of the complex. Additionally, the consequences of subtle variations to the bulk, aromaticity and hydrophobicity of terminal ligands were able to be explored through the use of both bpy and phen terminal ligands and their methylated analogues. This systematic variation to the ligand environment of the complexes was intended to identify and give insight into the nature of structure-specific interactions with nucleic acids through the experiments detailed in subsequent Chapters.

## 2.2 EXPERIMENTAL

### 2.2.1 Materials

Ruthenium trichloride hydrate ($RuCl_3.xH_2O$; Strem, 99.9%), 2,2′-bipyridine (bpy; Aldrich, 99+%), 4,4′-dimethyl-2,2′-bipyridine ($Me_2$bpy; Aldrich, 99%), 5,5′-dimethyl-2,2′-bipyridine (5,5′-$Me_2$bpy, Aldrich, 98%), 1,10-phenanthroline (phen; Aldrich, 99+%), 4,7-dimethyl-1,10-phenathroline ($Me_2$phen; Lancaster), 2,2′-bipyrimidine (bpm; Aldrich, 97%), 2,3-bis(2-pyridyl)pyrazine (2,3-dpp; Aldrich, 98%), ethylene glycol (Sigma-Aldrich), dimethyl sulfoxide (DMSO; Fluka), 1-methyl-2-pyrrolidinone (Aldrich), lithium chloride (LiCl; Aldrich, 99%), stannous chloride ($SnCl_2$; Aldrich, 99.99%), ammonium hexfluorophosphate ($NH_4PF_6$; Aldrich, 95+%), potassium hexafluorophosphate ($KPF_6$; Aldrich, 98%), and anhydrous sodium sulfate ($Na_2SO_4$; Ajax) were used as supplied. 1,4,5,8,9,12-Hexaazatriphenylene (HAT), 1,4,5,12-tetraazatriphenylene (ppz), and 2,5-bis(2-pyridyl)pyrazine were supplied by other members of the Keene laboratory – Dr. Nick Fletcher, Dr. Rob Gauci, and Dr. Lawrence Keslo, respectively. Laboratory-grade organic solvents (APS Ajax) were used except for purification procedures or unless otherwise noted. HPLC-grade acetonitrile (Ajax) was used for electronic spectroscopy experiments while $d_3$-acetonitrile (Cambridge Isotopes, 99.9%) was used for NMR spectroscopy experiments. SP Sephadex C-25 (GE Healthcare), silica gel (Sigma-Aldrich, 200-400 mesh, 60 Å), Amberlite IRA-400 (chloride form; Aldrich) anion exchange resin, sodium toluene-4-sulfonate (Aldrich, 95%), sodium benzoate (Aldrich, 99%), and sodium chloride (Ajax) were used as supplied. Aqueous solutions of (-)-*O*,*O*′-dibenzoyl-L-tartrate were prepared by neutralisation of the corresponding acid (Fluka, ≥99%) using sodium hydroxide pellets (APS).

### 2.2.2 Physical Measurements

One- and two-dimensional $^1$H NMR spectra were recorded on either a Varian Mercury (JCU) or a Bruker AV300 (Australian Institute of Marine Science) 300 MHz spectrometer and are reported relative to 99.9% $d_3$-acetonitrile ($CD_3CN$, $\delta$ = 1.95 ppm). IR spectra were recorded using a Nicolet Nexus 670 FT-IR spectrometer. Electronic absorption spectra were recorded on a Cary 5E spectrophotometer in HPLC-grade acetonitrile (complex concentrations of 10-20 μM) using quartz cells at room temperature. Circular dichroism spectra were recorded on a

Jasco J-715 spectropolarimeter and are reported as $\Delta\varepsilon$ versus $\lambda$ (nm) using the same acetonitrile solutions.

## 2.2.3 Synthetic Procedures

### *2.2.3.1 Microwave Syntheses*

All microwave-assisted syntheses[111] were performed in a modified Sharp microwave oven (Model R-2V55; 600 W, 2450 MHz) using the "medium-high" power setting. Reactions were carried out in ethylene glycol in a round-bottomed flask fitted with a reflux condenser that had been mounted within the modified oven.

### *2.2.3.2 Cation-Exchange Column Chromatography*

The synthesised complexes were each subjected to a preliminary purification step intended to separate the dinuclear species from any unreacted or mononuclear material. Following microwave reflux, the reaction mixture was allowed to cool before being diluted with distilled water to 4-5 times its original volume. The dilute solution was subsequently loaded onto a column (*ca*. 300 mm in length by 40 mm in diameter) of SP Sephadex C-25 cation-exchange support. Once the intensely-coloured reaction mixture had settled onto the surface of the Sephadex an additional layer of support was applied in order to prevent back-elution of the complex into the head solution. The complex was ultimately eluted from the column using a concentration gradient of aqueous NaCl solution. Mononuclear by-products (typically orange-red in colour) were eluted with a 0.2 M NaCl solution, dinuclear species with 0.5 M NaCl solution, and any trinuclear species (when applicable, i.e. HAT complexes) with 1.0 M NaCl solution. The aqueous complex eluate solution was treated with saturated $KPF_6$ solution to precipitate out the hexafluorophosphate salt of the complex which was then collected via filtration, washed with water and dried *in vacuo*. Alternatively, if precipitation did not occur or was particularly fine, the $PF_6^-$ salt of the complex would be isolated by extraction into dichloromethane which was subsequently dried using $Na_2SO_4$, filtered, and the dichloromethane removed on a rotary evaporator. A yield of 80-90% of the dinuclear species was usually recovered following this step.

Separations of the stereoisomeric forms of the complexes were conducted using chromatographic techniques developed by Keene and co-workers.[5, 10, 32] In a typical procedure, the complex as the hexfluorophosphate salt (approximately 40-80 mg) was converted to the water-soluble chloride salt by dissolution in a minimum volume of acetone and stirring with an aqueous slurry of IRA-400 Amberlite anion-exchange resin (chloride form). Upon filtration and removal of the acetone *in vacuo* the complex solution was loaded on another SP Sephadex C-25 column, albeit significantly longer than that used in the preliminary purification (1000 mm by 30 mm). Despite their increased length, the columns were generally too short to effect a sufficient separation of the stereoisomers within a single. Consequently, it was necessary to extend the effective column length (ECL, the distance travelled before visible separation of stereoisomer bands was observed) of the system. This was accomplished by sealing the column after the complex was loaded and the support matrix had equilibrated with the eluent, and attaching the system to a peristaltic pump. Upon reaching the end of the column (a distance of approximately one metre) the stereoisomer mixture was made to recycle back to the top for another passage down the column. Several cycles through the column were needed for most separations/resolutions, with the ECL dependent upon the nature of the complex being separated. Diffusion of the substrate over successive passages down the column occasionally necessitated "clipping" of the front of the leading band and/or the back of the trailing band in order to prevent the extremities from overlapping each other. Separations of diastereoisomers (*meso* and *rac*) were performed using aqueous 0.25 M sodium toluene-4-sulfonate (sodium tosylate) solution as the eluent; after isolation, the racemic mixture was re-loaded on a Sephadex column and the ΔΔ and ΛΛ forms resolved using 0.15 M disodium (-)-*O*,*O*′-dibenzoyl-L-tartrate solution. Individual diastereoisomers and enantiomers were typically isolated in yields of 35-45% of the starting stereoisomer mixture. As with the preliminary chromatography, the stereoisomers were recovered from solution by precipitating out the hexafluorophosphate salt, filtering, washing and drying *in vacuo,* or by extraction into dichloromethane as required.

Collected stereoisomers were further purified on a short (*ca.* 5 cm) column of 300-400 mesh silica gel equilibrated with AR acetone. The impure complex (typically containing extraneous eluent salts remaining from chromatographic separations) was dissolved in a minimum volume of acetone and loaded onto the column. The complex was washed with water and then AR acetone, before being eluted from the column with a solution of 5% $NH_4PF_6$ in

AR acetone. Upon dilution with a small volume of water, the eluate was subjected to rotary evaporation and as the acetone was removed the ruthenium complex precipitated out of solution. The solution was subsequently cooled and the purified complex collected by means of vacuum filtration and washed with water and diethyl ether before being dried in a vacuum desiccator.

#### *2.2.3.3 Synthesis of Mononuclear Precursors*

**$[Ru(DMSO)_4Cl_2]$** was prepared using the method of Evans *et al*.:[112] $RuCl_3.xH_2O$ (1 g) was refluxed in DMSO (5 mL) for 5 min before the volume of the purple-black reaction mixture was reduced by half *in vacuo*. The addition of acetone (20 mL) yielded a pale yellow precipitate which, upon cooling, was filtered off, washed with small volumes of acetone and diethyl ether, and then dried in a vacuum desiccator. Yield: 1.12 g (61%). IR spectroscopy was used to confirm the identity of the product by comparison with the literature.[112]

**$[Ru(pp)_2Cl_2]$, where pp is bpy, $Me_2$bpy, phen, or $Me_2$phen,** was prepared by either of two synthetic routes:

(a) ***The 1-methyl-2-pyrrolidinone method*** – a modification of the method used by Anderson *et al*. to prepare $[Ru(Me_4bpy)_2Cl_2]$,[113] scaled up to ten times that of the original procedure. $[Ru(DMSO)_4Cl_2]$ (300 mg, 0.6 mmol), the ligand of interest (*ca.* 200-270 mg, 1.3 mmol), and LiCl (1 g, 23 mmol) were refluxed in 1-methyl-2-pyrrolidinone (10 mL) for 15 min. The dark purple-brown mixture was left to cool before being added to dichloromethane (120 mL). Water (100 mL) was added, the mixture was shaken vigorously in a separating funnel, and the dark dichloromethane layer was separated and dried over anhydrous $Na_2SO_4$. Following filtration, the dichloromethane was removed by means of rotary evaporation and diethyl ether (400 mL) was added to the residue, which was then refrigerated. The resultant purple-brown precipitate was collected by filtration and washed with diethyl ether. While reasonable yields (*ca.* 65%) could be obtained for the $Me_2$bpy and $Me_2$phen complexes using this technique, it was less effective for the bpy and phen complexes due to their lower solubility in dichloromethane. Consequently, an alternative method was adopted for the synthesis of both the substituted *and* unsubstituted complexes, namely the "Ruthenium Blue" method of Togano *et al*.,[114] typically performed at five times the scale of the literature.

(b) ***The "Ruthenium Blue" method*** – $RuCl_3.xH_2O$ (2.5 g, *ca.* 10 mmol) was refluxed in a solution of ethanol (75 mL) and water (50 mL) for approximately 4 h. During this time the colour of the solution had changed from dark brown to deep blue via dark green, and a shiny black material – believed to be ruthenium oxide or a cluster compound of some form[114] – was deposited on the walls of the flask.

A solution of the desired ligand (bpy, $Me_2$bpy, 5,5′-$Me_2$bpy, phen or $Me_2$phen; *ca.* 3.5-4.0 g, 20 mmol) in ethanol (50 mL) was added to the hot "ruthenium blue" solution along with hydrochloric acid (32%, 10 mL). The mixture was refluxed for 30 min, during which time the colour of the solution changed from deep blue to dark brown. The solution was allowed to cool before being evaporated to dryness on a rotary evaporator, leaving a brown crystalline residue. This residue, *cis*-$[Ru^{III}(pp)_2Cl_2]Cl.2H_2O$, was collected and washed with small volumes of acetone and diethyl ether. Typical yield: 85-90%.

The Ru(III) complex, $[Ru(pp)_2Cl_2]Cl$, was subsequently reduced to $[Ru(pp)_2Cl_2]$ (the analogous Ru(II) complex) by adding $SnCl_2$ (100 mg, 0.5 mmol) to a hydrochloric acid solution (2 M, 150 mL) containing *cis*-$[Ru(pp)_2Cl_2]Cl.2H_2O$ (500 mg, *ca.* 1 mmol). The solution darkened upon the addition of the stannous chloride and it was reduced in volume on a hot plate until $[Ru(L)_2Cl_2]$ precipitated out as a black solid which was collected by filtration, washed with a small volume of water, and dried in a vacuum desiccator. Typical yield: 60-70%.

#### *2.2.3.4 Synthesis of Dinuclear Complexes*

All dinuclear complexes of the form $[\{Ru(pp)_2\}_2(\mu\text{-BL})](PF_6)_4$ were synthesised and purified using the general microwave-synthesis technique described by Fletcher *et al*.,[54] usually at one-fifth the reported scale, using the appropriate precursors and bridging ligands (BL). The general procedure involved dissolving the mononuclear precursor $[Ru(pp)_2Cl_2]$ (*ca*. 200 mg, 0.34 mmol) and the desired bridging ligand (bpm, 2,3-dpp, 2,5-dpp, ppz or HAT; *ca.* 40 mg, 0.17 mmol) in ethylene glycol (2 mL) and refluxing the mixture in a microwave oven for approximately 9 min (a colour change marked reaction completion). The complex was then subjected to a preliminary purification procedure, as described above. In instances where the complex has been previously described in the literature, spectra were identical to those reported for the complex unless otherwise noted.

**[{Ru(bpy)$_2$}$_2$(μ-bpm)](PF$_6$)$_4$** [115] was isolated as a dark green solid from the initial post-synthesis purification step. Chromatographic separation of the *meso* (first band) and *rac* (second band) diastereoisomers was achieved with an ECL of *ca.* 1.5 m. Resolution of the ΔΔ (first band) and ΛΛ (second band) enantiomers required an ECL of *ca.* 3 m. **UV/Vis** {λ/nm (ε/M$^{-1}$ cm$^{-1}$), $CH_3CN$)}: 597 (7,700), 549 (sh, 5,700), 413 (26,800), 281 (89,300), 246 (41,000). **CD** {λ/nm (Δε/M$^{-1}$ cm$^{-1}$), $CH_3CN$}: ΔΔ: 205 (-81), 236 (65), 258 (70), 280 (-209), 319 (-68), 390 (44); ΛΛ: 205 (79), 236 (-62), 258 (-67), 280 (200), 319 (66), 390 (-41).

**[{Ru(Me$_2$bpy)$_2$}$_2$(μ-bpm)](PF$_6$)$_4$** [116] was isolated as a dark green solid. Chromatographic separation of the *meso* (first band) and *rac* (second band) diastereoisomers was achieved with an ECL of *ca.* 60 cm. Resolution of the ΔΔ (first band) and ΛΛ (second band) enantiomers required an ECL of *ca.* 2 m. **UV/Vis** {λ/nm (ε/M$^{-1}$ cm$^{-1}$), $CH_3CN$)}: 204 (114,600), 259 (sh, 48,200), 280 (93,500), 415 (30,000), 566 (sh, 6,000), 612 (7,700). **CD** {λ/nm (Δε/M$^{-1}$ cm$^{-1}$), $CH_3CN$}: ΔΔ: 216 (-54), 248 (62), 279 (-103), 320 (-30), 391 (23); ΛΛ: 215 (54), 248 (-56), 279 (97), 320 (30), 391 (-20).

**[{Ru(5,5′-Me$_2$bpy)$_2$}$_2$(μ-bpm)](PF$_6$)$_4$** [24, 117] was isolated as a dark green solid. Chromatographic separation of the *meso* (first band) and *rac* (second band) diastereoisomers was achieved with an ECL of *ca.* 20 cm. Resolution of the ΔΔ (first band) and ΛΛ (second band) enantiomers required an ECL of *ca.* 4 m. **UV/Vis** {λ/nm (ε/M$^{-1}$ cm$^{-1}$), $CH_3CN$)}: 260 (66,000), 285 (102,800), 410 (30,100), 560 (sh, 6,200), 605 (8,300). **CD** {λ/nm (Δε/M$^{-1}$ cm$^{-1}$), $CH_3CN$}: ΔΔ: 240 (54), 257 (49), 282 (-160), 303 (47), 327 (-67), 386 (25); ΛΛ: 240 (-55), 257 (-51), 282 (159), 303 (-49), 327 (67), 386 (-27).

**[{Ru(phen)$_2$}$_2$(μ-bpm)](PF$_6$)$_4$** [118] was isolated as a dark green solid. Chromatographic separation of the *meso* (first band) and *rac* (second band) diastereoisomers was achieved with an ECL of *ca.* 50 cm. Resolution of the ΔΔ (first band) and ΛΛ (second band) enantiomers required an ECL of *ca.* 1.5 m. **UV/Vis** {λ/nm (ε/M$^{-1}$ cm$^{-1}$), $CH_3CN$)}: 201 (115,100), 221 (92,200), 260 (108,400), 292 (sh, 26,100), 396 (25,300), 550 (sh, 5,100), 591 (6,600). **CD** {λ/nm (Δε/M$^{-1}$ cm$^{-1}$), $CH_3CN$}: ΔΔ: 225 (73), 248 (92), 257 (74), 283 (-117), 293 (-120), 325 (sh, -16), 394 (13), 433 (-10); ΛΛ: 225 (-62), 248 (-86), 257 (-71), 283 (107), 293 (110), 325 (sh, 15), 394 (-10), 433 (14).

**[{Ru(Me$_2$phen)$_2$}$_2$(μ-bpm)](PF$_6$)$_4$** [118] was isolated as a dark green solid in a relatively low yield of approximately 60%. The low yield may be attributed to the fact that a significant amount of the crude reaction material stuck to the Sephadex column during the initial purification step. This phenomenon was found to occur with all complexes featuring Me$_2$phen terminal ligands. Chromatographic separation of the *meso* (first band) and *rac* (second band) diastereoisomers was achieved with an ECL of *ca.* 1 m. Resolution of the ΔΔ (first band) and ΛΛ (second band) enantiomers required an ECL of *ca.* 1 m. **UV/Vis** {λ/nm (ε/M$^{-1}$ cm$^{-1}$), $CH_3CN$)}: 205 (110,900), 226 (66,700), 261 (120,500), 408 (27,000), 607 (5,700). **CD** {λ/nm (Δε/M$^{-1}$ cm$^{-1}$), $CH_3CN$}: ΔΔ: 234 (sh, 34), 244 (51), 287 (-85), 375 (4), 431 (-9); ΛΛ: 234 (sh, -31), 244 (-51), 287 (89), 375 (-4), 431 (10).

**[{Ru(bpy)$_2$}$_2$(μ-HAT)](PF$_6$)$_4$** [10, 117, 119] was isolated as a dark purple/brown solid. Like all of the HAT-bridged species, the dinuclear complex was only obtained in yields of approximately 40% due to the formation of a dark blue trinuclear species which was isolated in similar yields. Chromatographic separation of the *meso* (first band) and *rac* (second band) diastereoisomers was achieved with an ECL of *ca.* 5 m. Resolution of the ΔΔ (first band) and ΛΛ (second band) enantiomers required an ECL of *ca.* 3 m. **UV/Vis** {λ/nm (ε/10$^3$ M$^{-1}$ cm$^{-1}$), $CH_3CN$)}: 254 (sh, 38,400), 279 (100,400), 412 (15,700), 455 (sh, 13,800), 564 (14,300). **CD** {λ/nm (Δε/M$^{-1}$ cm$^{-1}$), $CH_3CN$}: ΔΔ: 203 (-49), 222 (19), 228 (19), 268 (33), 288 (-108), 320 (-59), 401 (14), 452 (4); ΛΛ: 203 (54), 222 (-20), 228 (-19), 268 (-32), 288 (110), 320 (63), 401 (-15), 452 (-3).

**[{Ru(Me$_2$bpy)$_2$}$_2$(μ-HAT)](PF$_6$)$_4$** [117] was isolated as a dark purple/brown solid. Chromatographic separation of the *meso* (first band) and *rac* (second band) diastereoisomers was achieved with an ECL of *ca.* 3 m. Resolution of the ΔΔ (first band) and ΛΛ (second band) enantiomers required an ECL of *ca.* 3 m. **UV/Vis** {λ/nm (ε/M$^{-1}$ cm$^{-1}$), $CH_3CN$)}: 205 (114,900), 249 (sh, 40,200), 280 (97,700), 413 (14,900), 464 (14,100), 575 (12,800). **CD** {λ/nm (Δε/M$^{-1}$ cm$^{-1}$), $CH_3CN$}: ΔΔ: 211 (-79), 227 (29), 268 (32), 288 (-125), 319 (-51), 387 (11); ΛΛ: 211 (89), 227 (-30), 268 (-35), 288 (136), 319 (54), 387 (-13).

**[{Ru(phen)$_2$}$_2$(μ-HAT)](PF$_6$)$_4$** [10, 119] was isolated as a dark purple/brown solid. Chromatographic separation of the *meso* (first band) and *rac* (second band) diastereoisomers

was achieved with an ECL of *ca.* 40 cm. Resolution of the ΔΔ (first band) and ΛΛ (second band) enantiomers required an ECL of *ca.* 3 m. **UV/Vis** {λ/nm (ε/$M^{-1}$ $cm^{-1}$), $CH_3CN$)}: 222 (109,300), 262 (138,000), 370 (sh, 16,000), 410 (19,600), 559 (15,900). **CD** {λ/nm (Δε/$M^{-1}$ $cm^{-1}$), $CH_3CN$}: ΔΔ: 217 (64), 255 (231), 270 (-191), 296 (-206), 398 (17); ΛΛ: 217 (-59), 255 (-231), 270 (182), 296 (204), 398 (-16).

**[{Ru(Me$_2$phen)$_2$}$_2$(μ-HAT)](PF$_6$)$_4$** was isolated as a dark purple/brown solid. Chromatographic separation of the *meso* (first band) and *rac* (second band) diastereoisomers was achieved with an ECL of *ca.* 1.5 m. Resolution of the ΔΔ (first band) and ΛΛ (second band) enantiomers required an ECL of *ca.* 70 cm. **UV/Vis** {λ/nm (ε/$M^{-1}$ $cm^{-1}$), $CH_3CN$)}: 205 (203,500), 262 (185,500), 408 (25,100), 558 (17,400). **CD** {λ/nm (Δε/$M^{-1}$ $cm^{-1}$), $CH_3CN$}: ΔΔ: 221 (48), 258 (280), 271 (-256), 295 (-147), 395 (6); ΛΛ: 221 (-48), 258 (-301), 271 (267), 295 (161), 395 (-5).

**[{Ru(bpy)$_2$}$_2$(μ-ppz)](PF$_6$)$_4$** [94] was isolated as a dark purple solid. Chromatographic separation of the *meso* (first band) and *rac* (second band) diastereoisomers was achieved with an ECL of *ca.* 2 m. Resolution of the ΔΔ (first band) and ΛΛ (second band) enantiomers required an ECL of *ca.* 3 m. **UV/Vis** {λ/nm (ε/$M^{-1}$ $cm^{-1}$), $CH_3CN$)}: 252 (65,100), 283 (110,200), 333 (sh, 15,100), 424 (18,700), 569 (22,400). **CD** {λ/nm (Δε/$M^{-1}$ $cm^{-1}$), $CH_3CN$}: ΔΔ: 234 (28), 267 (30), 295 (-149), 400 (-21); ΛΛ: 234 (-24), 268 (-36), 296 (155), 400 (22).

**[{Ru(Me$_2$bpy)$_2$}$_2$(μ-ppz)](PF$_6$)$_4$** was isolated as a dark green solid. Chromatographic separation of the *meso* (first band) and *rac* (second band) diastereoisomers was achieved with an ECL of *ca.* 60 cm. Resolution of the ΔΔ (first band) and ΛΛ (second band) enantiomers required an ECL of *ca.* 3 m. **UV/Vis** {λ/nm (ε/$M^{-1}$ $cm^{-1}$), $CH_3CN$)}: 205 (144,700), 258 (77,800), 282 (128,700), 333 (sh, 18,400), 424 (21,700), 585 (26,000). **CD** {λ/nm (Δε/$M^{-1}$ $cm^{-1}$), $CH_3CN$}: ΔΔ: 214 (-77), 229 (29), 250 (34), 271 (18), 291 (-166), 332 (-29), 400 (21); ΛΛ: 214 (81), 229 (-31), 250 (-34), 271 (-26), 291 (174), 332 (27), 401 (-21).

**[{Ru(phen)$_2$}$_2$(μ-ppz)](PF$_6$)$_4$** was isolated as a dark purple solid. Chromatographic separation of the *meso* (first band) and *rac* (second band) diastereoisomers was achieved with an ECL of *ca.* 60 cm. Resolution of the ΔΔ (first band) and ΛΛ (second band) enantiomers required an

ECL of *ca.* 2.5 m. **UV/Vis** {λ/nm (ε/$M^{-1}$ $cm^{-1}$), $CH_3CN$)}: 223 (108,700), 262 (156,600), 335 (13,500), 382 (sh, 17,300), 421 (20,300), 572 (21,800). **CD** {λ/nm (Δε/$M^{-1}$ $cm^{-1}$), $CH_3CN$}: ΔΔ: 217 (51), 267 (-335), 298 (-191), 409 (17); ΛΛ: 217 (-51), 267 (-335), 298 (190), 409 (-14).

**[{Ru(Me$_2$phen)$_2$}$_2$(μ-ppz)](PF$_6$)$_4$** was isolated as a dark green solid. Chromatographic separation of the *meso* (first band) and *rac* (second band) diastereoisomers was achieved with an ECL of *ca.* 1.5 m. Resolution of the ΔΔ (first band) and ΛΛ (second band) enantiomers required an ECL of *ca.* 2 m. **UV/Vis** {λ/nm (ε/$M^{-1}$ $cm^{-1}$), $CH_3CN$)}: 205 (220,500), 226 (sh, 123,500), 261 (173,500), 415 (22,300), 585 (20,600). **CD** {λ/nm (Δε/$M^{-1}$ $cm^{-1}$), $CH_3CN$}: ΔΔ: 222 (42), 256 (246), 268 (-396), 299 (-128), 409 (9); ΛΛ: 222 (-40), 256 (-250), 268 (405), 299 (132), 409 (-5).

**[{Ru(bpy)$_2$}$_2$(μ-2,3-dpp)](PF$_6$)$_4$** [24] was isolated as a dark purple/red solid. Chromatographic separation of the *meso* (first band) and *rac* (second band) diastereoisomers was achieved with an ECL of *ca.* 5 m. Attempts at effecting a complete resolution of the enantiomers of [{Ru(bpy)$_2$}$_2$(μ-2,3-dpp)]$^{4+}$, like all of the 2,3-dpp-bridged complexes, proved futile. Clipping the leading and trailing ends of the single complex band after an ECL greater than 30 m revealed some small degree of enantioenrichment, however complete separation of the enantiomers was found to be impracticable. **UV/Vis** {λ/nm (ε/$M^{-1}$ $cm^{-1}$), $CH_3CN$)}: 244 (42,600), 253 (sh, 38,000), 284 (91,100), 347 (sh, 21,500), 425 (15,500), 526 (23,200).

**[{Ru(Me$_2$bpy)$_2$}$_2$(μ-2,3-dpp)](PF$_6$)$_4$** was isolated as a dark purple/red solid. Chromatographic separation of the *meso* (first band) and *rac* (second band) diastereoisomers was achieved with an ECL of *ca.* 4 m. Again, complete resolution of enantiomers could not be attained, however after extensive recycling the front and back of the single band were enriched in the ΔΔ and ΛΛ enantiomers, respectively. **UV/Vis** {λ/nm (ε/$M^{-1}$ $cm^{-1}$), $CH_3CN$)}: 205 (126,100), 247 (42,400), 258 (41,200), 281 (94,300), 427 (15,500), 536 (23,200).

**[{Ru(phen)$_2$}$_2$(μ-2,3-dpp)](PF$_6$)$_4$** was isolated as a dark purple/red solid. Chromatographic separation of the *meso* (first band) and *rac* (second band) diastereoisomers was achieved with an ECL of *ca.* 70 cm. Again, complete resolution of enantiomers could not be attained, however after extensive recycling the front and back of the single band were enriched in the ΔΔ and ΛΛ

enantiomers, respectively. **UV/Vis** {λ/nm (ε/$M^{-1}$ $cm^{-1}$), $CH_3CN$)}: 201 (72,800), 223 (102,100), 261 (125,200), 344 (21,500), 368 (19,900), 424 (18,300), 526 (22,300).

**[{Ru($Me_2$phen)$_2$}$_2$(μ-2,3-dpp)]($PF_6$)$_4$** was isolated as a dark purple/red solid. Chromatographic separation of the *meso* (first band) and *rac* (second band) diastereoisomers was achieved with an ECL of *ca.* 30 cm. Attempts at chromatographic resolution were unsuccessful. **UV/Vis** {λ/nm (ε/$M^{-1}$ $cm^{-1}$), $CH_3CN$)}: 205 (137,600), 226 (90,000), 262 (156,200), 377 (22,900), 419 (21,900), 537 (23,400).

**[{Ru(bpy)$_2$}$_2$(μ-2,5-dpp)]($PF_6$)$_4$** [39] was isolated as a dark green solid. Chromatographic separation of the *rac* (first band) and *meso* (second band) diastereoisomers was achieved with an ECL of *ca.* 3 m. Note the diastereoisomer elution order of 2,5-dpp bridged complexes is opposite that which is observed for all of the other bridging ligands described here. Resolution of the ΔΔ (first band) and ΛΛ (second band) enantiomers required an ECL of *ca.* 4 m. **UV/Vis** {λ/nm (ε/$M^{-1}$ $cm^{-1}$), $CH_3CN$)}: 243 (39,100), 285 (116,600), 326 (38,400), 355 (38,500), 433 (21,200), 584 (20,000). **CD** {λ/nm (Δε/$M^{-1}$ $cm^{-1}$), $CH_3CN$}: ΔΔ: 202 (-56), 222 (38), 283 (11), 297 (-39), 328 (-61), 401 (22); ΛΛ: 202 (55), 222 (-36), 283 (-11), 297 (41), 328 (59), 401 (-21).

**[{Ru($Me_2$bpy)$_2$}$_2$(μ-2,5-dpp)]($PF_6$)$_4$** [117] was isolated as a dark green solid. Chromatographic separation of the *rac* (first band) and *meso* (second band) diastereoisomers was achieved with an ECL of *ca.* 250 cm. Resolution of the ΔΔ (first band) and ΛΛ (second band) enantiomers required an ECL of *ca.* 4 m. **UV/Vis** {λ/nm (ε/$M^{-1}$ $cm^{-1}$), $CH_3CN$)}: 204 (132,700), 283 (114,700), 330 (41,200), 355 (36,000), 434 (21,100), 600 (20,300). **CD** {λ/nm (Δε/$M^{-1}$ $cm^{-1}$), $CH_3CN$}: ΔΔ: 210 (-120), 228 (91), 292 (-76), 327 (-107), 393 (36); ΛΛ: 210 (127), 228 (-91), 292 (74), 327 (108), 393 (-40) .

**[{Ru(phen)$_2$}$_2$(μ-2,5-dpp)]($PF_6$)$_4$** [39] was isolated as a dark green solid. Chromatographic separation of the *rac* (first band) and *meso* (second band) diastereoisomers was achieved with an ECL of *ca.* 250 cm. Resolution of the ΔΔ (first band) and ΛΛ (second band) enantiomers required an ECL of *ca.* 3 m. **UV/Vis** {λ/nm (ε/$M^{-1}$ $cm^{-1}$), $CH_3CN$)}: 223 (105,900), 262 (140,300), 346 (44,600), 427 (23,100), 580 (20,800). **CD** {λ/nm (Δε/$M^{-1}$ $cm^{-1}$), $CH_3CN$}: ΔΔ:

216 (-59), 260 (-175), 270 (88), 296 (57), 340 (92), 411 (-24); ΛΛ: 216 (51), 259 (166), 270 (-84), 296 (-56), 340 (-89), 411 (22).

**[{Ru(Me$_2$phen)$_2$}$_2$(μ-2,5-dpp)](PF$_6$)$_4$** was isolated as a dark green solid. Chromatographic separation of the *rac* (first band) and *meso* (second band) diastereoisomers was achieved with an ECL of *ca.* 2 m. Resolution of the ΔΔ (first band) and ΛΛ (second band) enantiomers required an ECL of *ca.* 3 m. **UV/Vis** {λ/nm (ε/M$^{-1}$ cm$^{-1}$), $CH_3CN$}: 206 (135,000), 227 (86,800), 263 (164,100), 347 (39,500), 425 (24,800), 598 (20,600). **CD** {λ/nm (Δε/M$^{-1}$ cm$^{-1}$), $CH_3CN$}: ΔΔ: 261 (322), 269 (-208), 291 (-62), 338 (-86), 414 (21); ΛΛ: 261 (-334), 269 (228), 291 (56), 338 (97), 414 (-20).

## 2.3 RESULTS & DISCUSSION

### 2.3.1 Synthesis

A series of dinuclear polypyridylruthenium(II) complexes of the general form $[\{Ru(pp)_2\}_2(\mu\text{-BL})]^{4+}$ {where pp is a bidentate polypyridyl *terminal* ligand and BL is a di-bidentate polypyridyl *bridging* ligand} were synthesised from appropriate mononuclear precursors of the form $[Ru(pp)_2Cl_2]$. The initial route by which the mononuclear precursor was obtained involved the reaction of $[Ru(DMSO)_4Cl_2]$ with the desired terminal ligand and subsequent isolation of the $[Ru(pp)_2Cl_2]$ complex by means of extraction into dichloromethane.[113] This method has been found to be significantly faster than the alternative techniques of Togano *et al.*[114] and Sullivan *et al.*[120] while still producing generally comparable yields. The "Ruthenium Blue" method of Togano *et al.* involves the reaction of ruthenium trichloride trihydrate with two equivalents of the appropriate terminal ligand in refluxing ethanol for several hours. It is subsequently necessary to reduce the initial Ru(III) product, $[Ru(pp)_2Cl_2]Cl$, to the analogous Ru(II) species using stannous chloride. The method of Sullivan *et al.* also requires the reaction of $RuCl_3.3H_2O$ with two equivalents of the desired terminal ligand, however this technique utilises dimethylformamide as the solvent and the Ru(III) → Ru(II) reduction takes place *in situ*.

Despite being significantly more expedient, the $[Ru(DMSO)_4Cl_2]$-based method was found to be relatively inefficient with regards to isolation of $[Ru(bpy)_2Cl_2]$ and $[Ru(phen)_2Cl_2]$ due to the low solubility of these two species in dichloromethane, whereas the analogous methylated

species demonstrated a greater solubility and were typically isolated in higher yield. As a consequence, the "Ruthenium Blue" technique of Togano *et al.* was adopted as the standard means by which all of the $[Ru(pp)_2Cl_2]$ precursors were synthesised.

Ultimately, the dinuclear species were obtained by combining the appropriate mononuclear precursors and bridging ligands in ethylene glycol at a 2:1 molar ratio and refluxing the mixture in a modified microwave oven for a short period of time.[54] Such microwave techniques produce comparable yields to the thermal techniques classically used to synthesise these dinuclear species[39, 121-125] while offering a considerable improvement in the overall speed of the reaction. The majority of syntheses involved a bridging ligand possessing *two* bidentate ligating moieties, so that the major product of the microwave reaction was the dinuclear species with relatively small traces of monomeric by-products. However, for complexes based upon the HAT bridging ligand which possesses *three* bidentate coordination sites, the formation of *trinuclear* species presents itself as a complicating factor. Isolation of the dinuclear species is accomplished by means of a preliminary chromatographic purification on SP Sephadex C-25 support: cation-exchange techniques with a NaCl solution gradient elution were used to separate the desired dinuclear product from unwanted mono- and trinuclear by-products in the crude microwave reaction mixture. The mono- and trinuclear species were typically eluted at NaCl concentrations of 0.2 M and 1.0 M, respectively, while the dinuclear complex was collected with an intermediate concentration (0.5 M).

The presence of trinuclear HAT by-products adversely affected the yields of the target dinuclear products required for the DNA-binding experiments described in the following chapters of this thesis. A method purporting to increase the proportion of the dinuclear species via gradual addition over several minutes of $[Ru(pp)_2Cl_2]$ to a refluxing solution of HAT[10] was found to have limited success.

## 2.3.2 Chromatography

Chromatographic separations of diastereoisomeric mixtures were performed using a 0.25 M solution of aqueous sodium toluene-4-sulfonate (tosylate) as the eluent. The mechanism responsible for the separation of the *meso* and *rac* forms of a given complex has been identified as differential host-guest interactions (electrostatic, hydrophobic, and π-stacking) between the cationic complex and eluent anions.[55] The extent to which the eluent anion is able to associate

differs between the *meso* and *rac* forms owing to the difference in geometries between the complex diastereoisomers.

The series of complexes described herein are based upon three general classes of bridging ligand which differ in the relative position and orientation of the N—N axis of each chelation site {refer to Figure 2.5(a)}. The simplest case, in which these N—N axes are parallel and the chelation sites are linearly opposite, is exemplified by bpm. The bridging ligands HAT, ppz, and 2,3-dpp are representative of the "angular" class of bridging ligand in which the N—N axes are orientated at an angle of approximately 120° to one another. Finally, 2,5-dpp is described as being "stepped-parallel": the N—N axes remain parallel but the metal chelation sites are no longer directly opposite one another, rather they are offset towards either end of the long axis of the ligand. In the complexes based on linear and stepped-parallel bridging ligands the terminal ligands above and below the plane of the bridge are arranged such that they are approximately orthogonal in the *meso* diastereoisomer and approximately parallel in the *rac* diastereoisomer. Alternatively, in angular-bridged species these relative orientations are essentially reversed {see Figure 2.5(b)}.

In complexes based upon bridging ligands of the linear configuration, the orientation of terminal ligands in the *meso* diastereoisomer gives rise to hydrophobic clefts above and below the plane of the bridge. NMR experiments have suggested that the clefts are capable of accommodating the methylated end of the tosylate anion[55] resulting in a particularly favourable association between the eluent and the complex {see Figure 2.6}. By contrast, the terminal ligands of the *rac* diastereoisomer are orientated in such a manner so as to preclude as favourable an association, and so the *rac* isomer elutes slower than does the *meso*. Despite less pronounced clefts and, as a result, lesser differentiation between stereoisomers, the angular-bridged species also elute in the order *meso* before *rac*, albeit less efficiently (i.e. requiring a larger ECL). Conversely, diastereoisomers based on the stepped linear bridge 2,5-dpp elute in the reverse order (*rac* before *meso*) suggesting that in this instance the *rac* form of the complex participates in a more favourable association with the eluent anion.

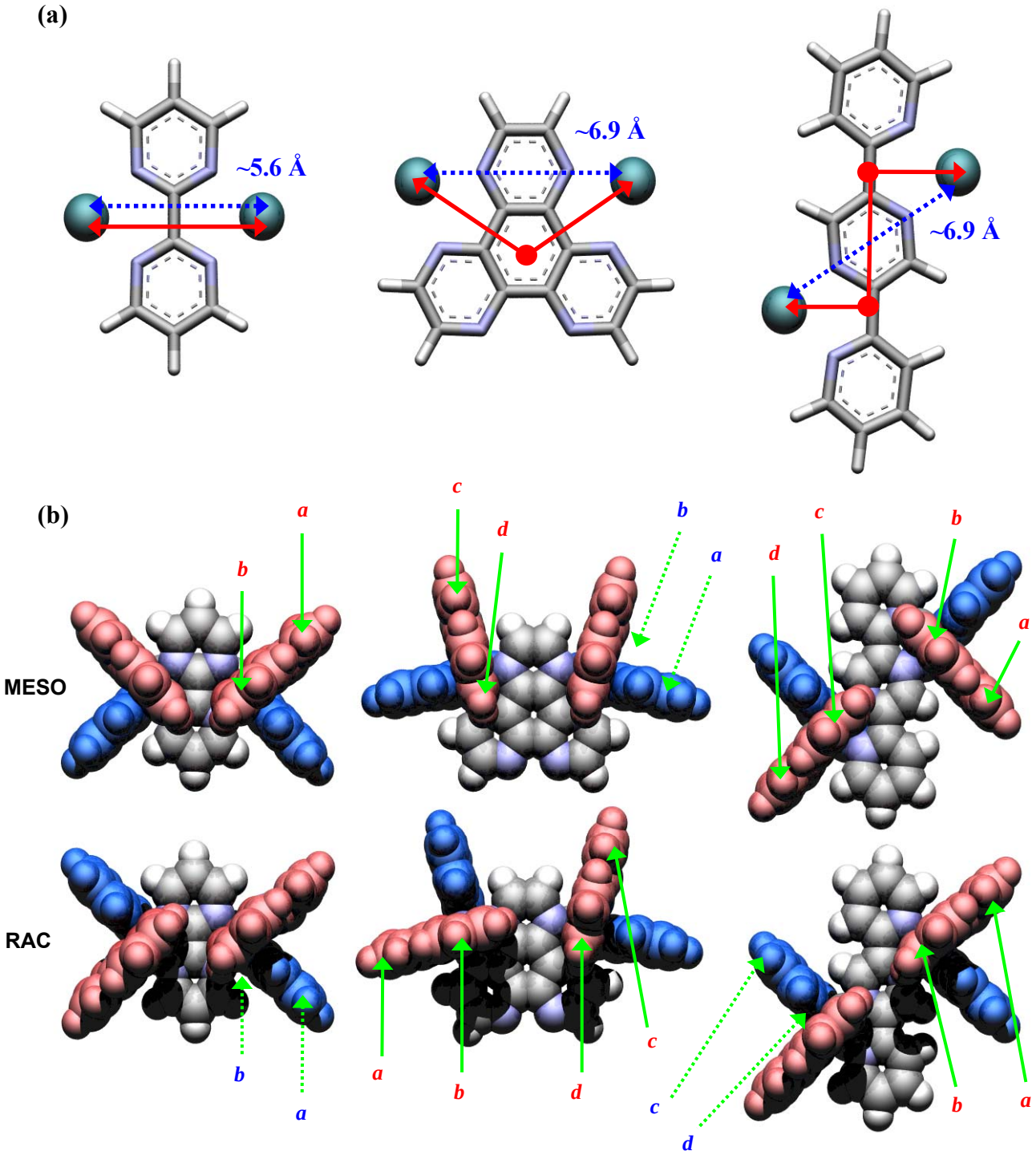


***Figure 2.5***
**Bridging ligand configurations.** (a) The relative orientations (red line) and proximities (blue line) of metal centres in bridging ligands representative of the linear (bpm), angular (HAT) and stepped-parallel (2,5-dpp) classes. (b) Terminal ligand configurations in each class of bridging ligand: red ligands are "above" the plane of the bridge, blue are "below". Ring notation refers to the differing magnetic environments experienced by the halves of each ligand (refer to the NMR section below).

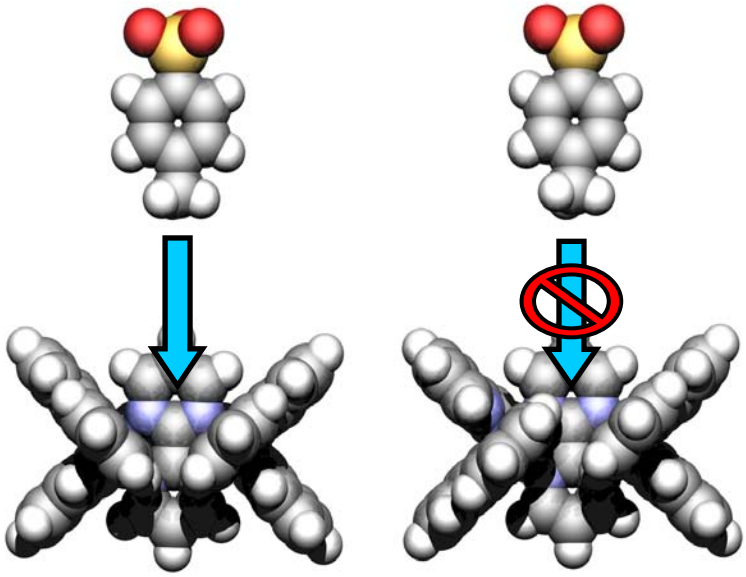

***Figure 2.6***
**Diastereoselective anion association.** Eluent anions can often form stronger associations with one diastereoisomer over the other due to differing cleft dimensions between the two. In the example illustrated here *p*-toluene sulfonate is able to dock neatly within the cleft of *meso*-$[\{Ru(bpy)_2\}_2(\mu\text{-bpm})]^{4+}$ (left), but the arrangement of the terminal ligands in *rac*-$[\{Ru(bpy)_2\}_2(\mu\text{-bpm})]^{4+}$ (right) prohibits this.

The ECLs necessary to achieve separation of the diastereoisomers of each complex were a function of both the bridging *and* terminal ligands. As mentioned above, less favourable associations between the counter-anions of the eluent and complex result in the need for significantly longer ECLs to separate angular- and stepped-parallel-bridged species relative to those possessing a linear bridge. With regards to terminal ligands, methylation has been demonstrated to increase the efficiency of separation for both mononuclear[32] and dinuclear[54] complexes owing to the more favourable hydrophobic associations between eluent counter-anions and complex that arise in such conditions.[32] As an example it has been reported that, using the same cation-exchange chromatographic techniques described herein, $[\{Ru(Me_4bpy)_2\}_2(\mu\text{-bpm})]^{4+}$ {where $Me_4bpy$ = 4,4′,5,5′-tetramethyl-2,2′-bipyridine} was resolved in approximately half the column length required for $[\{Ru(Me_2bpy)_2\}_2(\mu\text{-bpm})]^{4+}$.[54] Similar observations were made in these current studies: for instance, diastereoisomeric separation of $[\{Ru(Me_2bpy)_2\}_2(\mu\text{-2,3-dpp})]^{4+}$ occurred with an ECL approximately 1 m less than the non-methylated analogue, while separation of $[\{Ru(bpy)_2\}_2(\mu\text{-HAT})]^{4+}$ required an ECL approximately 2 m greater than did $[\{Ru(Me_2bpy)_2\}_2(\mu\text{-HAT})]^{4+}$. This effect was also

expected in complexes incorporating phen-based terminal ligands; however, for reasons that are not understood, those complexes possessing $Me_2$phen ligands exhibited significant diffusion on the column. This resulted in "smearing" of the diastereosiomeric bands and a longer apparent ECL to ensure adequate separation. It was generally observed that diastereoisomers of species possessing phen terminal ligands separated with smaller ECLs than the analogous complexes with bpy ligands, again quite possibly due to more favourable hydrophobic interactions between the former species and eluent anions. Additionally, the positioning of methyl substituents was also found to be of importance, as indicated by the shorter ECL required for the separation of the diastereoisomers of $[\{Ru(5,5'\text{-}Me_2bpy)_2\}_2(\mu\text{-bpm})]^{4+}$ relative to the complex possessing the analogous 4,4′-$Me_2$bpy terminal ligands.

Resolutions of racemic mixtures were accomplished using the chromatographic techniques developed by Keene and co-workers: *viz*. cation-exchange chromatography with the chiral eluent disodium (-)-*O*,*O*′-dibenzoyl-L-tartrate.[32, 54, 55] The basis of this resolution is believed to be a synergistic interaction between the complementary chiralities of the eluent anion, the sugar moieties of the Sephadex support, and one of the enantiomers of a racemic mixture of the metal complex.[32] Association between the eluent anion and the cationic complex results in mitigation of the charge on the complex. The chirality of the participants ensures that the association favours one enantiomer (typically ΔΔ) over the other, resulting in a faster elution time for that isomer (although ECLs of several metres are usually required to observe such a resolution). As previously noted, the use of an eluent of the opposite handedness yields the opposite elution order and the chirality of the polysaccharide stationary phase alone has demonstrated some minor resolving power; however the correct choice of chiral eluent undoubtedly enhances the efficiency of enantiomeric resolutions.[54] Additional factors such as the temperature and concentration of the eluent have also been demonstrated to influence the effectiveness of both the separation of diastereoisomers and the resolution of enantiomers.[55]

Despite the general effectiveness of these techniques, the resolution of complexes possessing flexible bridging ligands remains largely problematic.[126] In the studies described herein the ligand 2,3-dpp presented such difficulties: while the other angular-type bridging ligands are relatively rigid and planar due to their fused aromatic ring systems, 2,3-dpp is unfused and has an inherently greater flexibility. This flexibility coupled with steric interactions between the two H*e* protons of the pyridine rings (see Figure 2.8 for ligand structures and proton notation) results in the non-planarity of the two chelating α,α′-diimine moieties.[127, 128]

Two possible conformations arise as the N—N axes of these chelating moieties can be skewed to either side of the mutually planar arrangement; the resultant conformations are actually chiral, thus making the conformational isomers themselves diastereoisomeric (see Figure 2.7).[5] The difficulties in resolving racemic mixture of 2,3-dpp bridged complexes might be attributed to fluctuations between conformers at the ambient temperature; presumably, one conformer interacts more favourably with the chirality of the eluent and/or stationary phase than does the other. The difference in elution speeds between interconverting conformers *within* each enantiomeric band would result in diffusion (smearing and lengthening) of the bands to such an extent that resolving the individual ΔΔ and ΛΛ bands would be very challenging – consistent with what was witnessed in these experiments. Attempts were made to resolve *rac*-$[\{Ru(bpy)_2\}_2(\mu\text{-}2,3\text{-dpp})]^{4+}$, $[\{Ru(Me_2bpy)_2\}_2(\mu\text{-}2,3\text{-dpp})]^{4+}$ and $[\{Ru(phen)_2\}_2(\mu\text{-}2,3\text{-dpp})]^{4+}$, however diffusion necessitated frequent "clipping" of the front and back of the single observed band to prevent the ends from overlapping. After several weeks of such clipping (and over 30 cycles down the metre-long column) some degree of enantioenrichment did become evident in CD measurements of the clippings, yet resolution remained elusive and so further attempts at resolving 2,3-dpp complexes were abandoned. Ultimately, resolution of such complexes might benefit from the use of a different eluent such as sodium (-)-di-*O*,*O*′-*p*-toluoyl-L-tartrate, which has been shown to be more efficient than (-)-*O*,*O*′-dibenzoyl-L-tartrate in the resolution of some complexes.[119] Alternatively, by cooling the chromatographic system it might be possible to slow down the conformational fluctuations and hence decrease the magnitude of the diffusion effects observed at room temperature. Neither variation was pursued in the current work.

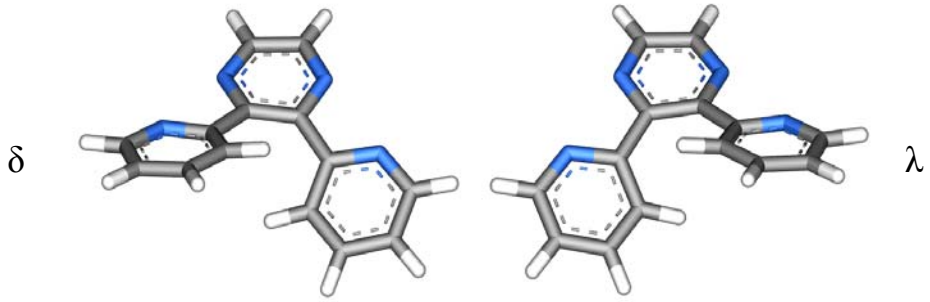


***Figure 2.7***
**Conformational isomers of the 2,3-dpp bridge.** Due to steric clashes between protons on the pyridine rings, the 2,3-dpp ligand is distorted from a planar configuration. This distortion gives rise to a left-handed or right-handed skewing of the chelating moieties, yielding λ and δ conformational isomers, respectively,

## 2.3.3 NMR Spectroscopy

### *2.3.3.1 General Comments*

NMR spectra were recorded in $CD_3CN$ using a 300 MHz spectrometer. Unambiguous structural characterisation of complexes was accomplished through the use of one- and two-dimensional (COSY) proton NMR experiments, and by comparison of the obtained spectra to those previously recorded for the same or similar complexes. The assignment of proton resonances to specific ligands, and by extension the identification of diastereoisomers, was based upon the relative degree of diamagnetic anisotropic interaction expected between terminal and bridging moieties. Enantiomers are indistinguishable by NMR. Proton numbering schemes of all the ligands to be discussed below are presented in Figure 2.8.

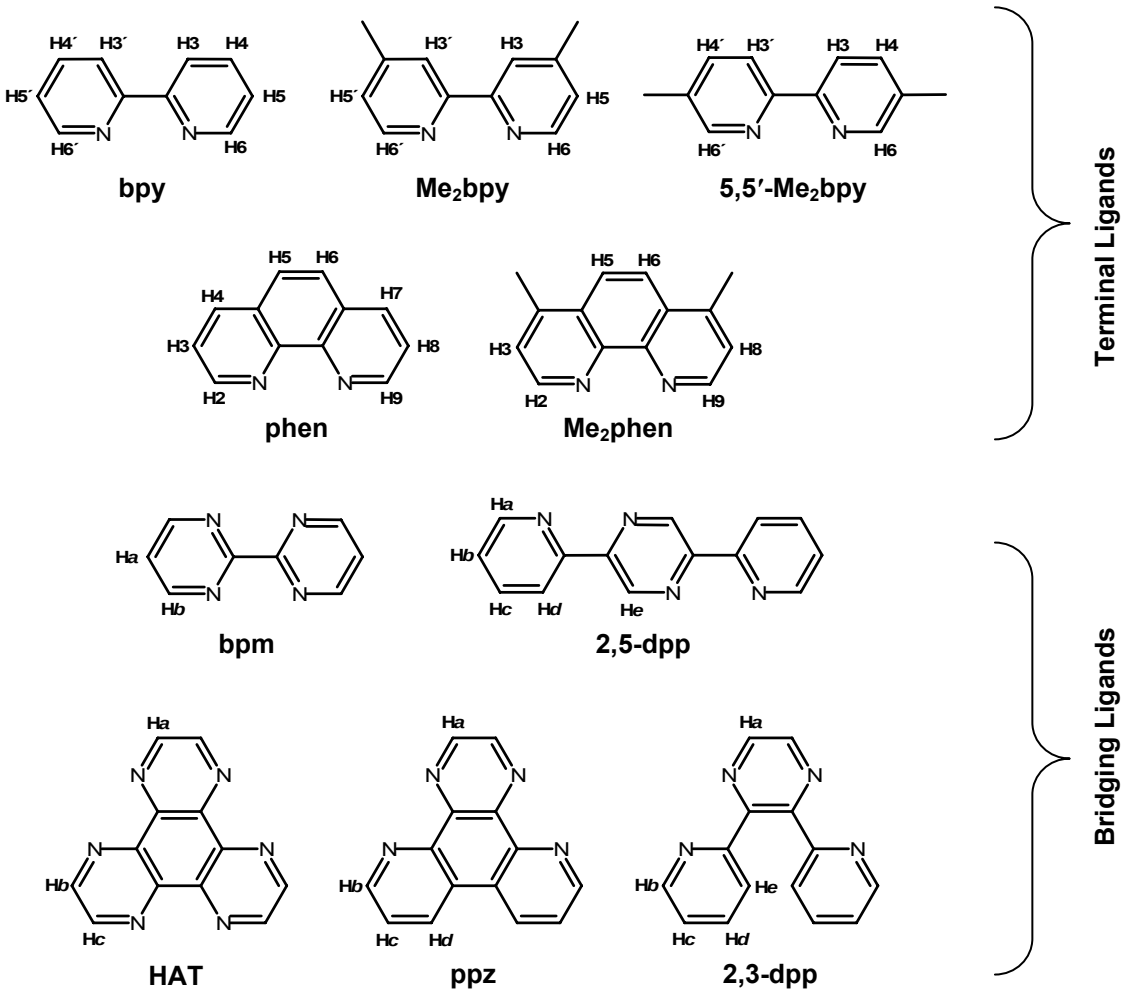


***Figure 2.8***
**Polypyridyl ligands.** Depicted here are the structures and proton numbering schemes of the ligands used in the syntheses discussed in this Chapter.

#### *2.3.3.2 Terminal Ligands*

The bpy- and phen-derived ligands utilised in these syntheses are all of high symmetry ($C_{2v}$ point group); however, when they are incorporated into a dinuclear complex the anisotropic diamagnetic influences of the bridging ligand and those terminal ligands on the opposite metal centre can cause the non-equivalence of individual terminal ligands and/or the *halves* of those ligands. Each half-ligand constitutes a single aromatic ring (one-and-a-half rings in the case of the phenanthroline derivatives) and so each non-equivalent pyridyl moiety may be identified as *ring a*, *ring b* and so on. The specific orientation of these rings is illustrated for the *meso* and *rac* diastereoisomers of each class of complex in Figure 2.5(b).

Spectra arising from bipyridine ligands show AJMX and A′J′M′X′ coupling patterns arising from the non-equivalent H3/H4/H5/H6 and H3′/H4′/H5′/H6′ proton systems in each half of the ligand. The addition of methyl substituents simplifies the aromatic region of the NMR spectrum by lessening the total number of resonances and interrupting the proton coupling system. As a result, each ring of the 4,4′-$Me_2$bpy and 5,5′-$Me_2$bpy substituted systems exhibit resonances in the form of an AM coupling pattern (between H6/H5 for the former ligand, H3/H4 for the latter) and a singlet (from the now-isolated H3 or H6 protons). Methyl substituents typically induced an upfield shift of approximately 0.2-0.3 ppm in the resonances of adjacent protons (in both bipyridine and phenanthroline derivatives). The coupling constants observed for complexes possessing bipyridine-based ligands are in general agreement with those previously reported for such systems:[129] $J_{5/6} = J_{5'/6'} = 5.5$ Hz, $J_{4,5} = J_{4',5'} = 8$ Hz, $J_{3,4} = J_{3',4'} = 8$ Hz, $J_{3,5} = J_{3',5'} = 1$ Hz, $J_{4,6} = J_{4',6'} = 1.5$ Hz.

Phenanthroline exhibits AMX and A′M′X′ coupling pattern arising from the H2/H3/H4 and H7/H8/H9 systems on the non-equivalent halves of the coordinated ligand, as well as an AB coupling between the H5 and H6 protons of the central ring. Again, the addition of methyl groups (to the 4- and 7-positions) simplifies the aromatic region of the spectrum. In a number of cases the H5 and H6 protons are in near-identical magnetic environments resulting in the merging of the inner peaks of their AB-type doublet of doublets signal into what appears to be a singlet (albeit with very small satellite peaks easily lost to the noise of the baseline). Where necessary, the approximate position of the "centre of gravity" of the system (i.e. the singlet) is reported. The coupling constants of the phenanthroline-based ligands were also in general

agreement with reported values for such systems: [29] $J_{2/3} = J_{8/9} = 5$ Hz, $J_{2,4} = J_{7,9} = 1.5$ Hz, $J_{3,4} = J_{7,8} = 8$ Hz, $J_{5,6} = 9$ Hz.

#### *2.3.3.3 Linear-bridged Complexes*

The $D_{2h}$ symmetry of a linear bridge such as bpm results in two magnetically non-equivalent protons (H*a* and H*b* in an $A_2X$ coupling pattern) for the bridging ligand and four equivalent terminal ligands, each comprised of two non-equivalent halves. This non-equivalence arises due to the different shielding environments experienced by the two ends of each terminal ligand {as depicted in Figure 2.5(b)}: *ring a* sits above the plane of the other terminal ligand coordinated to same metal centre, whereas *ring b* is instead situated above the plane of the bpm bridge. The shielding effect of the terminal ligand is greater than that of bpm due to the strong withdrawal of electron density from the bridge by the two chelated ruthenium centres. As a result *ring a* protons (specifically H5′ and H6′ in bpy, H2 and H3 in phen) experience a slightly increased diamagnetic anisotropic effect (i.e. a small upfield shift) relative to *ring b* protons (H5/H6 and H9/H8). COSY analysis facilitated the subsequent assignment of the remaining resonances.

The protons of *ring b* are essential to differentiating between diastereoisomers, again due to differing degrees of shielding. Specifically, while *ring b* protons are orientated over the bpm bridge in both diastereoisomers, the *meso* form ($C_{2h}$ symmetry) is arranged such that the H5/H6 (H9/H8) terminal ligand protons project into the deshielding cone of the comparable terminal ligand on the opposite metal centre. In the *rac* diastereoisomer ($D_2$ symmetry) the planes of the terminal ligands on either side of the bridge are parallel to one another and these characteristic protons experience a greater shielding influence. Accordingly, diastereoisomers of the $[\{Ru(pp)_2\}_2(\mu\text{-bpm})]^{4+}$ series of complexes may be distinguished using NMR based on the knowledge that the H5/H6 (H9/H8) terminal ligand resonances occur at a lower chemical shift in the *rac* form than they do in the *meso*.

Molecular models of the diastereoisomers of each of the bpm-bridged complexes used in these studies are presented alongside their NMR spectra in Figures B.1.1-B.1.5 (Appendix B). Chemical shift data are collated in Table 2.1.

***Table 2.1***
$^{1}$H chemical shifts (ppm; $CD_3CN$ solution)[a,b] of the diastereoisomers of bpm-bridged species.

| | | **[{Ru(bpy)$_2$}$_2$(μ-bpm)]$^{4+}$** | | **[{Ru(Me$_2$bpy)$_2$}$_2$(μ-bpm)]$^{4+}$** | | **[{Ru(5,5′-Me$_2$bpy)$_2$}$_2$(μ-bpm)]$^{4+}$** | |
|---|---|---|---|---|---|---|---|
| | | *meso* | *rac* | *meso* | *rac* | *meso* | *rac* |
| ***bpy ring a (over bpy)*** | H3′ | 8.45 | 8.54 | 8.38 | 8.42 | 8.30 | 8.35 |
| | H4′ | 8.08 | 8.11 | **2.56** | **2.57** | 7.91 | 7.89 |
| | H5′ | 7.44 | 7.41 | 7.30 | 7.25 | **2.20** | **2.15** |
| | H6′ | 7.68 | 7.61 | 7.60 | 7.46 | 7.32 | 7.27 |
| ***bpy ring b (over bpm)*** | H3 | 8.48 | 8.56 | 8.38 | 8.42 | 8.32 | 8.37 |
| | H4 | 8.11 | 8.20 | **2.59** | **2.65** | 7.90 | 7.96 |
| | H5 | 7.61 | 7.43 | 7.49 | 7.28 | **2.35** | **2.18** |
| | H6 | 8.00 | 7.76 | 7.95 | 7.57 | 7.72 | 7.46 |
| ***bpm*** | H*a* | 7.43 | 7.42 | 7.45 | 7.43 | 7.45 | 7.46 |
| | H*b* | 8.03 | 8.08 | 8.02 | 8.06 | 7.97 | 8.07 |

| | | **[{Ru(phen)$_2$}$_2$(μ-bpm)]$^{4+}$** | | **[{Ru(4,7-Me$_2$phen)$_2$}$_2$(μ-bpm)]$^{4+}$** | |
|---|---|---|---|---|---|
| | | *meso* | *rac* | *meso* | *rac* |
| ***phen ring a (over phen)*** | H2 | 7.94 | 7.85 | 7.76 | 7.67 |
| | H3 | 7.66 | 7.61 | 7.47 | 7.44 |
| | H4 | 8.63 | 8.62 | **2.87** | **2.87** |
| | H5 | 8.25 | 8.29 | 8.36 | 8.42 |
| ***phen ring b (over bpm)*** | H6 | 8.29 | 8.37 | 8.40 | 8.50 |
| | H7 | 8.78 | 8.85 | **3.01** | **3.01** |
| | H8 | 8.09 | 7.82 | 7.90 | 7.63 |
| | H9 | 8.68 | 8.29 | 8.44 | 8.08 |
| ***bpm*** | H*a* | 7.23 | 7.22 | 7.19 | 7.19 |
| | H*b* | 7.94 | 8.00 | 7.90 | 7.96 |

[a] Proton chemical shifts depicted in bold are those of the appropriate methyl substituents at those positions.

[b] *Coupling patterns*:

**[{Ru(bpy)$_2$}$_2$(μ-bpm)]$^{4+}$**: H3/3′ (d, *J* = 8.0 Hz, 4H), H4/4′ (dd, *J* = 8.0, 1.5 Hz, 4H), H5/5′ (dd, *J* = 8.0, 1.2 Hz, 4H), H6/6′ (dd, *J* = 6.3, 1.5 Hz, 4H), H*a* (t, *J* = 5.7 Hz, 2H), H*b* (d, *J* = 5.7 Hz, 4H). **[{Ru(4,4′-Me$_2$bpy)$_2$}$_2$(μ-bpm)]$^{4+}$**: H3/3′ (s, 4H), H5/5′ (d, *J* = 5.7 Hz, 4H), H6/6′ (d, *J* = 5.7 Hz, 4H), H*a* (t, *J* = 5.7 Hz, 2H), H*b* (d, *J* = 5.7 Hz, 4H). **[{Ru(5,5′-Me$_2$bpy)$_2$}$_2$(μ-bpm)]$^{4+}$**: H3/3′ (d, *J* = 8.1 Hz, 4H), H4/4′ (dd, 8.1, 1.2 Hz, 4H), H6/6′ (d, 1.2 Hz, 4H), H*a* (t, *J* = 5.7 Hz, 2H), H*b* (d, *J* = 5.7 Hz, 4H), $CH_3CH_3$′ (s, 12H). **[{Ru(phen)$_2$}$_2$(μ-bpm)]$^{4+}$**: H2/9 (d, *J* = 5.2 Hz, 4H), H3/8 (dd, *J* = 8.3, 5.2 Hz, 4H), H4/7 (d, *J* = 8.3 Hz, 4H), H5/6 (d, *J* = 8.8 Hz, 4H), H*a* (t, *J* = 5.7 Hz, 2H), H*b* (d, *J* = 5.7 Hz, 4H). **[{Ru(4,7-Me$_2$phen)$_2$}$_2$(μ-bpm)]$^{4+}$**: H2/9 (d, *J* = 5.4 Hz, 4H), H3/8 (d, *J* = 5.4 Hz, 4H), H5/6 (d, *J* = 9.3 Hz, 4H), H*a* (t, *J* = 5.7 Hz, 2H), H*b* (d, *J* = 5.7 Hz, 4H).

### *2.3.3.4 Angular-bridged Complexes*

The lower symmetry of dinuclear complexes based upon the angular bridging ligands HAT, ppz or 2,3-dpp dictates that there are two magnetically non-equivalent terminal ligands per metal centre, each with two non-equivalent halves. Accordingly there are four different magnetic environments in total: the protons of rings *a* and *c* project away from the bridging ligand into the shielding cone of adjacent terminal ligands, whereas the protons of rings *b* and *d* sit in the shielding cone of the bridging ligand. The *meso* and *rac* diastereoisomers of this class of complex possess $C_s$ and $C_2$ symmetry, respectively. Consequently, the non-equivalent

terminal ligands are positioned on opposite faces of the bridging ligand in the *meso* form, but the same face in the *rac* form. The relative orientations of these ligands in angular-bridged systems may be seen in Figure 2.5(b).

As with the bpm-bridged complexes, these shielding effects are most pronounced in the H5/H5′/H6/H6′ (bpy) or H2/H3/H8/H9 (phen) protons of bpy- or phen-based ligands, respectively, and again allow for differentiation between the *meso* and *rac* forms of this class of complex. In the *rac* diastereoisomer *ring b* of the terminal ligand experiences two shielding effects as it is orientated over the planes of both the bridging ligand and a terminal ligand on the opposite metal centre. As a result *ring b* is subjected to increased diamagnetic anisotropy relative to the other rings and H5 (bpy) or H8 (phen) *ring b* may be assigned to the most shielded (farthest upfield) of the H5/H5′ or H3/H8 resonances, respectively. The H6 (bpy) or H9 (phen) protons of *ring d* are assigned to the farthest downfield resonance since *ring d* lies solely in the shielding cone of the π-electron deficient bridging ligand with no additional shielding influence from other terminal ligands. Further assignments were made via COSY analysis and by comparison to previously reported NMR spectra of HAT,[10, 119] ppz[24, 94] and 2,3-dpp[24] complexes, where available.

In the *meso* diastereoisomer of the angular-bridged complexes, the *ring b* protons actually project into the plane, and hence the *deshielding* cone, of the terminal ligand on the other metal centre. Consequently, the H5/H6 (bpy) or H8/H9 (phen) resonances occur further downfield in the *meso* diastereoisomer. The most upfield of the terminal ligand protons in the *meso* form is the H5 (bpy) or H8 (phen) proton of *ring d* which lies in the shielding cones of both the bridge and a terminal ligand on the opposite metal centre. Subsequent assignments were made as per the *rac* diastereoisomer.

The symmetries of the bridging ligands HAT, ppz and 2,3-dpp ($D_{3h}$, $C_{2v}$ and $C_2$, respectively) are such that there is a $C_2$ axis in the plane of the ligand, making for two equivalent halves. Thus, HAT possesses three non-equivalent protons (H*a* and H*b*/H*c*, yielding a singlet and an AX coupling pattern, respectively), ppz possesses four non-equivalent protons (H*a* and H*b*/H*c*/H*d*, singlet and AMX), and 2,3-dpp should possess five non-equivalent protons (H*a* and H*b*/H*c*/H*d*/H*e*, singlet and AJMX). While HAT and ppz are planar ligands, steric clashes between the H*e* protons (i.e. those at the 3-positions of the pyridine rings) of 2,3-dpp results in a deviation from planarity and further lowers the symmetry of complexes based on this bridge. As detailed in Section 2.2.3, the non-planarity of the two chelating moieties results

in the formation of conformational isomers that subsequently complicate not only the enantiomeric resolution of 2,3-dpp-bridged complexes, but also interpretation of their NMR spectra due to broadening of specific resonaces. Interconversion between the two conformers at room temperature is slow relative to the NMR time-scale, resulting in the broadening of many resonances as they represent a broad average of the two forms. As has previously been demonstrated for the heteroleptic dinuclear species $[\{Ru(bpy)_2\}\{Ru(Me_2bpy)_2\}(\mu\text{-}2,3\text{-dpp})]^{4+}$, temperature-controlled experiments can be used to sharpen up the peaks in the NMR spectrum.[5] At high temperatures the rate of interconversion between conformational states is rapid relative to the NMR time-scale and so a single sharp spectrum corresponding to the average of the two conformational states is observed; alternately, lowering the temperature slows the conformational rate and produces a convoluted NMR signal corresponding to the spectra of the two different conformers. Unfortunately, despite attempts to sharpen the resonances with temperature-controlled experiments, complete assignments of the spectra of the 2,3-dpp-bridged complexes was prohibited by the broadness of many resonances. Nevertheless, the *meso* and *rac* diastereoisomers could be readily distinguished by the chemical shift of their most upfield {H5 (bpy) or H8 (phen)} resonance – as in the other angular-bridged complexes, this resonance occurs at a lower ppm in the *rac* form than it does in the *meso* form.

Molecular models of each of the HAT-, ppz- and 2,3-dpp-bridged complexes used in these studies are presented alongside their NMR spectra in Figures B.1.6-B.1.9, B.1.10-B.1.13 and B.1.14-B.1.17 (Appendix B), respectively. Chemical shift data for the HAT- and ppz-bridged species are tabulated in Tables 2.2 and 2.3, respectively.

***Table 2.2***
$^{1}$H chemical shifts (ppm; $CD_3CN$ solution)[a,b] of the diastereoisomers of HAT-bridged species.

| | | $[\{Ru(bpy)_2\}_2(\mu\text{-HAT})]^{4+}$ | | $[\{Ru(Me_2bpy)_2\}_2(\mu\text{-HAT})]^{4+}$ | |
|---|---|---|---|---|---|
| | | *meso* | *rac* | *meso* | *rac* |
| ***bpy ring a (over bpy)*** | H3′ | 8.63 | 8.61 | 8.45 | 8.44 |
| | H4′ | 8.22 | 8.23 | **2.61** | **2.60** |
| | H5′ | 7.56 | 7.57 | 7.37 | 7.38 |
| | H6′ | 7.76 | 7.77 | 7.54 | 7.54 |
| ***bpy ring b (over HAT)*** | H3 | 8.59 | 8.59 | 8.30 | 8.41 |
| | H4 | 8.16 | 8.09 | **2.54** | **2.48** |
| | H5 | 7.52 | 7.17 | 7.12 | 6.96 |
| | H6 | 7.87 | 7.49 | 7.51 | 7.28 |
| ***bpy ring c (over bpy)*** | H3′ | 8.52 | 8.58 | 8.34 | 8.41 |
| | H4′ | 8.15 | 8.15 | **2.54** | **2.55** |
| | H5′ | 7.47 | 7.48 | 7.32 | 7.28 |
| | H6′ | 7.78 | 7.70 | 7.55 | 7.46 |
| ***bpy ring d (over HAT)*** | H3 | 8.47 | 8.55 | 8.40 | 8.37 |
| | H4 | 8.06 | 8.19 | **2.47** | **2.58** |
| | H5 | 7.31 | 7.42 | 7.27 | 7.20 |
| | H6 | 7.72 | 7.77 | 7.58 | 7.51 |
| ***HAT*** | H*a* | 8.09 | 8.13 | 8.04 | 8.09 |
| | H*b* | 9.26 | 9.26 | 9.21 | 9.20 |
| | H*c* | 8.46 | 8.47 | 8.45 | 8.44 |

| | | $[\{Ru(phen)_2\}_2(\mu\text{-HAT})]^{4+}$ | | $[\{Ru(Me_2phen)_2\}_2(\mu\text{-HAT})]^{4+}$ | |
|---|---|---|---|---|---|
| | | *meso* | *rac* | *meso* | *rac* |
| ***phen ring a (over phen)*** | H2 | 7.97 | 7.95 | 7.85 | 7.82 |
| | H3 | 7.68 | 7.69 | 7.56 | 7.56 |
| | H4 | 8.68 | 8.66 | **2.94** | **3.03** |
| | H5 | 8.28 | *ca.* 8.24 | *ca.* 8.46 | *ca.* 8.43 |
| ***phen ring b (over HAT)*** | H6 | 8.34 | *ca.* 8.24 | *ca.* 8.46 | *ca.* 8.43 |
| | H7 | 8.75 | 8.63 | **2.98** | **2.85** |
| | H8 | 7.86 | 7.49 | 7.73 | 7.33 |
| | H9 | 8.46 | 7.92 | 8.22 | 7.76 |
| ***phen ring c (over phen)*** | H2 | 7.93 | 7.80 | 8.05 | 7.65 |
| | H3 | 7.64 | 7.53 | 7.51 | 7.39 |
| | H4 | 8.55 | 8.57 | **2.82** | **2.90** |
| | H5 | *ca.* 8.14 | 8.25 | *ca.* 8.30 | 8.40 |
| ***phen ring d (over HAT)*** | H6 | *ca.* 8.14 | 8.32 | *ca.* 8.30 | 8.48 |
| | H7 | 8.58 | 8.79 | **2.85** | **2.93** |
| | H8 | 7.61 | 7.80 | 7.47 | 7.65 |
| | H9 | 8.18 | 8.27 | 7.80 | 8.10 |
| ***HAT*** | H*a* | 7.83 | 7.92 | 7.85 | 7.91 |
| | H*b* | 9.10 | 9.10 | 9.10 | 9.11 |
| | H*c* | 8.34 | 8.35 | 8.30 | 8.38 |

[a] Proton chemical shifts depicted in bold are those of the appropriate methyl substituents at those positions.

[b] *Coupling patterns*:

**$[\{Ru(bpy)_2\}_2(\mu\text{-HAT})]^{4+}$**: H3/3′ (d, *J* = 7.8 Hz, 4H), H4/4′ (dd, *J* = 7.8, 7.8 Hz, 4H), H5/5′ (dd, *J* = 7.8, 5.4 Hz, 4H), H6/6′ (d, *J* = 5.4 Hz, 4H), H*a* (s, 2H), H*b* (d, *J* = 3.0 Hz, 4H), H*c* (d, *J* = 3.0 Hz, 4H). **$[\{Ru(4,4'\text{-}Me_2bpy)_2\}_2(\mu\text{-HAT})]^{4+}$**: H3/3′ (s, 4H), H5/5′ (d, *J* = 5.7 Hz, 4H), H6/6′ (d, *J* = 5.7 Hz, 4H), H*a* (s, 2H), H*b* (d, *J* = 3.0 Hz, 2H), H*c* (d, *J* = 3.0 Hz, 2H). **$[\{Ru(phen)_2\}_2(\mu\text{-HAT})]^{4+}$**: H2/9 (dd, *J* = 8.1, 1.2 Hz, 4H), H3/8 (dd, *J* = 8.1, 5.1 Hz, 4H), H4/7 (dd, *J* = 5.1, 1.2 Hz, 4H), H5/6 (d, *J* = 9.0 Hz, 4H), H*a* (s, 2H), H*b* (d, *J* = 2.7 Hz, 2H), H*c* (d, *J* = 2.7 Hz, 2H). **$[\{Ru(4,7\text{-}Me_2phen)_2\}_2(\mu\text{-HAT})]^{4+}$**: H2/9 (d, *J* = 5.4 Hz, 4H), H3/8 (dd, *J* = 5.4, 0.9 Hz, 4H), H5/6 (d, 8.7 Hz, 4H), H*a* (s, 2H), H*b* (d, *J* = 2.9 Hz, 2H), H*c* (d, *J* = 2.9 Hz, 2H).

***Table 2.3***
$^{1}$H chemical shifts (ppm; $CD_3CN$ solution)[a,b] of the diastereoisomers of ppz-bridged species.

| | | $[\{Ru(bpy)_2\}_2(\mu\text{-ppz})]^{4+}$ | | $[\{Ru(Me_2bpy)_2\}_2(\mu\text{-ppz})]^{4+}$ | |
|---|---|---|---|---|---|
| | | *meso* | *rac* | *meso* | *rac* |
| ***bpy ring a (over bpy)*** | H3′ | 8.58 | 8.53 | 8.47 | 8.45 |
| | H4′ | 8.15 | 8.13 | **2.62** | **2.62** |
| | H5′ | 7.50 | 7.51 | 7.38 | 7.22 |
| | H6′ | 7.73 | 7.76 | 7.59 | 7.46 |
| ***bpy ring b (over ppz)*** | H3 | 8.52 | 8.51 | 8.42 | 8.38 |
| | H4 | 8.09 | 8.07 | **2.55** | **2.50** |
| | H5 | 7.39 | 7.02 | 7.27 | 6.93 |
| | H6 | 7.85 | 7.61 | 7.42 | 7.28 |
| ***bpy ring c (over bpy)*** | H3′ | 8.43 | 8.55 | 8.34 | 8.40 |
| | H4′ | 8.06 | 8.15 | **2.55** | **2.55** |
| | H5′ | 7.42 | 7.38 | 7.31 | 7.26 |
| | H6′ | 7.75 | 7.66 | 7.59 | 7.50 |
| ***bpy ring d (over ppz)*** | H3 | 8.39 | 8.48 | 8.31 | 8.42 |
| | H4 | 7.99 | 8.00 | **2.48** | **2.60** |
| | H5 | 7.25 | 7.36 | 7.12 | 7.39 |
| | H6 | 7.54 | 7.42 | 7.66 | 7.60 |
| ***ppz*** | H*a* | 7.93 | 7.96 | 7.97 | 8.00 |
| | H*b* | 9.32 | 9.31 | 9.33 | 9.33 |
| | H*c* | 8.01 | 8.01 | 8.04 | 8.03 |
| | H*d* | 8.23 | 8.23 | 8.28 | 8.27 |

| | | $[\{Ru(phen)_2\}_2(\mu\text{-ppz})]^{4+}$ | | $[\{Ru(Me_2phen)_2\}_2(\mu\text{-ppz})]^{4+}$ | |
|---|---|---|---|---|---|
| | | *meso* | *rac* | *meso* | *rac* |
| ***phen ring a (over phen)*** | H2 | 8.02 | 8.01 | 7.85 | 7.85 |
| | H3 | 7.71 | 7.71 | 7.53 | 7.54 |
| | H4 | 8.69 | 8.68 | **2.94** | **2.98** |
| | H5 | *ca.* 8.32 | 8.28 | 8.45 | *ca.* 8.41 |
| ***phen ring b (over ppz)*** | H6 | *ca.* 8.32 | 8.28 | 8.45 | *ca.* 8.41 |
| | H7 | 8.75 | 8.64 | **2.99** | **2.81** |
| | H8 | 7.89 | 7.48 | 7.70 | 7.29 |
| | H9 | 8.51 | 7.93 | 8.28 | 7.75 |
| ***phen ring c (over phen)*** | H2 | 7.98 | 7.82 | 7.91 | 7.64 |
| | H3 | 7.67 | 7.53 | 7.47 | 7.35 |
| | H4 | 8.55 | 8.57 | **2.82** | **2.86** |
| | H5 | *ca.* 8.16 | 8.26 | 8.28 | 8.38 |
| ***phen ring d (over ppz)*** | H6 | *ca.* 8.16 | 8.34 | 8.28 | 8.47 |
| | H7 | 8.59 | 8.80 | **2.85** | **2.90** |
| | H8 | 7.61 | 7.82 | 7.43 | 7.63 |
| | H9 | 8.08 | 8.17 | 7.79 | 8.00 |
| ***ppz*** | H*a* | 7.78 | 7.82 | 7.76 | 7.79 |
| | H*b* | 9.35 | 9.33 | 9.30 | 9.30 |
| | H*c* | 7.94 | 7.93 | 7.91 | 7.90 |
| | H*d* | 8.21 | 8.19 | 8.20 | 8.19 |

[a] Proton chemical shifts depicted in bold are those of the appropriate methyl substituents at those positions.

[b] *Coupling patterns*:

**$[\{Ru(bpy)_2\}_2(\mu\text{-ppz})]^{4+}$**: H3/3′ (d, *J* = 8.4 Hz, 4H), H4/4′ (dd, *J* = 8.4, 8.4 Hz, 4H), H5/5′ (dd, *J* = 8.4, 5.4 Hz, 4H), H6/6′ (d, *J* = 5.4 Hz, 4H), H*a* (s, 2H), H*b* (d, *J* = 8.4 Hz, 4H), H*c* (dd, *J* = 8.4, 5.4 Hz, 4H), H*d* (d, *J* = 5.4 Hz, 2H). **$[\{Ru(4,4'\text{-}Me_2bpy)_2\}_2(\mu\text{-ppz})]^{4+}$**: H3/3′ (s, 4H), H5/5′ (d, *J* = 5.7 Hz, 4H), H6/6′ (d, *J* = 5.7 Hz, 4H), H*a* (s, 2H), H*b* (d, *J* = 8.4 Hz, 2H), H*c* (dd, *J* = 8.4, 5.4 Hz, 2H), H*d* (d, *J* = 5.4 Hz, 2H). **$[\{Ru(phen)_2\}_2(\mu\text{-ppz})]^{4+}$**: H2/9 (dd, *J* = 5.4, 1.2 Hz, 4H), H3/8 (dd, *J* = 8.4, 5.4 Hz, 4H), H4/7 (dd, *J* = 8.4, 1.2 Hz, 4H), H5/6 (d, *J* = 9.0 Hz, 4H), H*a* (s, 2H), H*b* (d, *J* = 8.7 Hz, 2H), H*c* (dd, *J* = 8.7, 5.1 Hz, 2H), H*d* (d, *J* = 5.1 Hz, 2H). **$[\{Ru(4,7\text{-}Me_2phen)_2\}_2(\mu\text{-ppz})]^{4+}$**: H2/9 (d, *J* = 5.4 Hz, 4H), H3/8 (d, *J* = 5.4 Hz, 4H), H5/6 (d, 8.7 Hz, 4H), H*a* (s, 2H), H*b* (d, *J* = 8.4 Hz, 2H), H*c* (dd, *J* = 8.4, 5.4 Hz, 2H), H*d* (d, *J* = 5.4 Hz, 2H).

#### *2.3.3.5 Stepped Parallel-bridged Complexes*

The $C_2$ symmetry of the 2,5-dpp bridging ligand gives rise to dinuclear complexes of $C_i$ (*meso*) and $C_2$ (*rac*) symmetry. As with the angular-bridged species, the two terminal ligands coordinated to a metal centre are magnetically non-equivalent, and each possesses two non-equivalent halves; however, in this case the non-equivalent terminal ligands are located on the same face in the *meso* form of the complex and on opposite faces in the *rac* diastereoisomer, in contrast to the configuration of the angular-bridged complexes. Once again, the magnetically-distinct pyridyl moieties of *rings a* and *c* are directed away from the bridging ligand while the protons of *rings b* and *d* sit in the shielding cone above (and below) the plane of the bridge. The H5/H5′/H6/H6′ (bpy) and H2/H3/H8/H9 (phen) protons *rings b* and *d* remain the most shielded (farthest upfield). The orientations of the terminal ligands for each diastereoisomer are illustrated in Figure 2.5(b).

*Ring b* of the *meso* diastereoisomer of a 2,5-dpp-bridged complex is oriented so as to sit above the plane of both the bridging ligand and the analogous terminal ligand across the bridge. Consequently, the H5/H6 (bpy) and H8/H9 (phen) protons of *ring b* experience a greater shielding effect than does *ring d*, and so the resonances of the former occur slightly further upfield than do those of the latter. Alternatively, the H6 (bpy) or H9 (phen) protons of *ring b* in the *rac* diastereoisomer lie over the plane of the bridge, but also in the *deshielding* cone of the terminal ligand across the bridge. As a result, these protons experience a slightly decreased shielding influence relative to those of the *meso* diastereoisomer. Likewise, the H6 (bpy) or H9 (phen) protons of *ring d* in the *rac* diastereoisomer are relatively deshielded in comparison to those of the *meso* diastereoisomer. The NMR spectrum of the 2,5-dpp ligand exhibits an AJMX coupling pattern due to the H*b*/H*c*/H*d*/H*e* protons of the terminal pyridyl moieties and a singlet from the sole distinct proton of the central pyrazyl moiety. Further characterisation of the NMR spectra was accomplished through the use of COSY experiments and by comparison to previously reported spectra of similar species.[39, 130] Molecular models and NMR spectra of each of the $[\{Ru(L)_2\}_2(\mu\text{-}2,5\text{-dpp})]^{4+}$ complexes are depicted in Figures B.1.18-B.1.21. Chemical shift data are collected in Table 2.4. Despite considerable effort, the *meso* diastereoisomer of $[\{Ru(Me_2phen)_2\}_2(\mu\text{-}2,5\text{-dpp})]^{4+}$ could not be characterised by NMR spectroscopy. While the *rac* (first) band of the diastereoisomeric mixture was readily isolated using cation-exchange chromatography, the second band (which should have corresponded to the *meso* isomer) had a

particularly broad and convoluted spectrum – much more so than would be expected from the *meso* diastereoisomer alone. The cause of these phenomena remain unknown – attempts to remove any possible impurities by further chromatographic treatment proved fruitless and conformational isomerism seems an unlikely cause of the broadness/complexity in light of the absence of such features in the spectra of other 2,5-dpp-bridged complexes. Consequently, only the *rac* diastereoisomer could be characterised using NMR spectroscopy (the subsequent resolution of this diastereoisomer into ΔΔ and ΛΛ enantiomers proves that it is indeed the *rac* form of the complex).

***Table 2.4***
$^{1}$H chemical shifts (ppm; $CD_3CN$)[a,b] of the diastereoisomers of 2,5-dpp-bridged species.

| | | $[\{Ru(bpy)_2\}_2(\mu\text{-}2,5\text{-}dpp)]^{4+}$ | | $[\{Ru(Me_2bpy)_2\}_2(\mu\text{-}2,5\text{-}dpp)]^{4+}$ | |
|---|---|---|---|---|---|
| | | *meso* | *rac* | *meso* | *rac* |
| ***bpy ring a (over bpy)*** | H3′ | 8.60 | 8.55 | 8.44 | 8.41 |
| | H4′ | 8.23 | 8.17 | **2.63** | **2.61** |
| | H5′ | 7.55 | 7.59 | 7.36 | 7.35 |
| | H6′ | 7.77 | 7.84 | 7.45 | 7.64 |
| ***bpy ring b (over dpp)*** | H3 | 8.57 | 8.55 | 8.35 | 8.40 |
| | H4 | 8.14 | 8.11 | **2.55** | **2.52** |
| | H5 | 7.19 | 7.32 | 7.00 | 7.16 |
| | H6 | 7.55 | 7.51 | 7.39 | 7.34 |
| ***bpy ring c (over bpy)*** | H3′ | 8.58 | 8.55 | 8.43 | 8.40 |
| | H4′ | 8.19 | 8.13 | **2.57** | **2.56** |
| | H5′ | 7.49 | 7.47 | 7.31 | 7.31 |
| | H6′ | 7.66 | 7.51 | 7.42 | 7.38 |
| ***bpy ring d (over dpp)*** | H3 | 8.51 | 8.54 | 8.39 | 8.40 |
| | H4 | 8.08 | 8.20 | **2.60** | **2.63** |
| | H5 | 7.51 | 7.59 | 7.33 | 7.42 |
| | H6 | 7.66 | 8.03 | 7.58 | 7.76 |
| ***2,5-dpp*** | H*a* | 7.77 | 7.78 | 7.75 | 7.78 |
| | H*b* | 7.48 | 7.47 | 7.46 | 7.46 |
| | H*c* | 7.98 | 7.98 | 7.96 | 7.96 |
| | H*d* | 7.90 | 7.88 | 7.90 | 7.86 |
| | H*e* | 8.43 | 8.38 | 8.47 | 8.40 |

| | | $[\{Ru(phen)_2\}_2(\mu\text{-}2,5\text{-}dpp)]^{4+}$ | | $[\{Ru(Me_2phen)_2\}_2(\mu\text{-}2,5\text{-}dpp)]^{4+}$ |
|---|---|---|---|---|
| | | *meso* | *rac* | *rac* |
| ***phen ring a (over phen)*** | H2 | 7.94 | 7.98 | 7.85 |
| | H3 | 7.65 | 7.67 | 7.49 |
| | H4 | 8.84 | 8.66 | **2.93** |
| | H5 | *ca.* 8.32 | *ca.* 8.27 | *ca.* 8.42 |
| ***phen ring b (over dpp)*** | H6 | *ca.* 8.32 | *ca.* 8.27 | *ca.* 8.42 |
| | H7 | 8.64 | 8.59 | **2.86** |
| | H8 | 7.51 | 7.56 | 7.40 |
| | H9 | 8.01 | 7.65 | 7.50 |
| ***phen ring c (over phen)*** | H2 | 7.76 | 7.89 | 7.73 |
| | H3 | 7.61 | 7.66 | 7.47 |
| | H4 | 8.62 | 8.66 | **2.92** |
| | H5 | *ca.* 8.32 | *ca.* 8.27 | *ca.* 8.42 |
| ***phen ring d (over dpp)*** | H6 | *ca.* 8.32 | *ca.* 8.27 | *ca.* 8.42 |
| | H7 | 8.66 | 8.77 | **3.02** |
| | H8 | 7.67 | 8.00 | 7.84 |
| | H9 | 7.96 | 8.56 | 8.34 |
| ***2,5-dpp*** | H*a* | 7.66 | 7.66 | 7.66 |
| | H*b* | 7.28 | 7.26 | 7.26 |
| | H*c* | 7.85 | 7.83 | 7.81 |
| | H*d* | 7.65 | 7.64 | 7.69 |
| | H*e* | 8.47 | 8.39 | 8.44 |

[a] Proton chemical shifts depicted in bold are those of the appropriate methyl substituents at those positions.

[b] *Coupling patterns*:

**$[\{Ru(bpy)_2\}_2(\mu\text{-}2,5\text{-}dpp)]^{4+}$**: H3/3′ (d, *J* = 8.1 Hz, 4H), H4/4′ (dd, *J* = 8.1, 8.1 Hz, 4H), H5/5′ (dd, *J* = 8.1, 5.4 Hz, 4H), H6/6′ (d, *J* = 5.4 Hz, 4H), H*a* (d, *J* = 5.5 Hz, 2H), H*b* (dd, *J* = 8.4, 5.5 Hz, 2H), H*c* (dd, *J* = 8.4, 8.0 Hz, 4H), H*d* (d, *J* = 8.0 Hz, 2H), H*e* (s, 2H). **$[\{Ru(4,4'\text{-}Me_2bpy)_2\}_2(\mu\text{-}2,5\text{-}dpp)]^{4+}$**: H3/3′ (s, 4H), H5/5′ (d, *J* = 5.7 Hz, 4H), H6/6′ (d, *J* = 5.7 Hz, 4H), H*a* (d, *J* = 5.5 Hz, 2H), H*b* (dd, *J* = 8.4, 5.5 Hz, 2H), H*c* (dd, *J* = 8.4, 8.0 Hz, 4H), H*d* (d, *J* = 8.0 Hz, 2H), H*e* (s, 2H). **$[\{Ru(phen)_2\}_2(\mu\text{-}2,5\text{-}dpp)]^{4+}$**: H2/9 (dd, *J* = 5.4, 1.2 Hz, 4H), H3/8 (dd, *J* = 8.4, 5.4 Hz, 4H), H4/7 (dd, *J* = 8.4, 1.2 Hz, 4H), H5/6 (d, *J* = 9.0 Hz, 4H), H*a* (d, *J* = 5.5 Hz, 2H), H*b* (dd, *J* = 8.1, 5.5 Hz, 2H), H*c* (dd, *J* = 8.4, 5.4 Hz, 4H), H*d* (dd, *J* = 5.4, 8.0 Hz, 2H), H*e* (s, 2H). **$[\{Ru(4,7\text{-}Me_2phen)_2\}_2(\mu\text{-}2,5\text{-}dpp)]^{4+}$**: H2/9 (d, *J* = 5.4 Hz, 4H), H3/8 (d, *J* = 5.4 Hz, 4H), H5/6 (d, *J* = 9.0 Hz, 4H), H*a* (d, *J* = 5.5 Hz, 2H), H*b* (dd, *J* = 8.1, 5.5 Hz, 2H), H*c* (dd, *J* = 8.4, 5.4 Hz, 4H), H*d* (dd, *J* = 5.4, 8.0 Hz, 2H), H*e* (s, 2H).

## 2.3.4 Electronic Absorption Spectroscopy

UV/Vis absorption spectra of the hexafluorophosphate salts of each of the complexes were recorded in acetonitrile solution. The spectra of these complexes exhibit the typical characteristics of dinuclear polypyridylruthenium(II) species:[94] strong absorptions in the UV region corresponding to ligand $\pi \rightarrow \pi^*$ electronic transitions, and metal-to-ligand charge transfer (MLCT) absorptions in the visible portion of the spectrum giving such complexes their characteristic intense colouration. These latter absorptions involve the promotion of a ruthenium d-orbital electron to the $\pi^*$ orbital of one of the polypyridyl ligands; transitions involving the bridging ligand occur at lower energies/higher wavelengths (> *ca.* 500 nm) than do those involving the terminal ligands (< *ca.* 500 nm) because of the greater electrostatic energy requirement needed to push an electron onto a terminal ligand away from an electropositive Ru(II) centre.[122] The annotated absorption spectrum of $[\{Ru(bpy)_2\}_2(\mu\text{-bpm})]^{4+}$ is presented in Figure 2.9 to illustrate these characteristics.

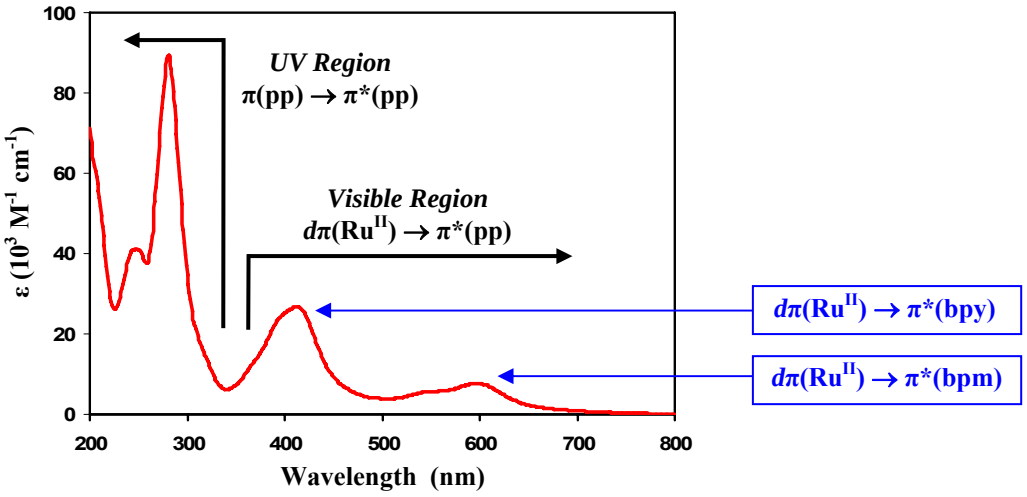


***Figure 2.9***
**Electronic absorption spectrum of $[\{Ru(bpy)_2\}_2(\mu\text{-bpm})]^{4+}$.** Characteristic absorbance regions of dinuclear polypyridylruthenium(II) complexes are shown in black; MLCT transitions specific to this complex are indicated in blue.

More electronegative ligands, or those with more delocalised π-electron systems, possess $\pi^*$ orbitals of greater stability so that transitions involving such ligands are moved to lower energies (longer wavelengths).[131, 132] This effect is particularly obvious in the bridging moiety: transitions involving the ppz ligand occur at lower energies than do those of the HAT bridge

due to the greater aromaticity (and hence delocalisation) of the former.[94, 133, 134] Similarly, absorptions due to the 2,3-dpp bridge occur at comparatively high energies due to the non-planar, non-fused nature of the ligand.[135] Both bpm- and 2,5-dpp-bridged species demonstrated $d\pi(Ru^{II}) \rightarrow \pi^*(BL)$ transitions at lower energies than the analogous angular-bridged complexes, in agreement with the long-wavelength absorptions previously reported for such species.[135, 136] Spectra for each of the complexes synthesised in this Chapter can be found in Appendix C. In the current experiments, little difference was observed between the absorption spectra of diastereoisomers; any discrepancies fell within the bounds of experimental error and so the spectra presented are those of the diastereoisomeric mixture. However, it should be noted that partial or full oxidation of the complex and solvent/anion-association effects are known to exaggerate spectral differences arising from diastereoisomerism.[24, 25, 137]

Circular dichroism spectra were used to establish the absolute configuration – ΔΔ or ΛΛ – of resolved enantiomers. The phenomenon of circular dichroism essentially arises from the difference in the absorbance of left- and right-handed circularly-polarised light due to the chirality of a molecule. Such optical activity is commonly explained using exciton theory[138] – polarisation of the directions of specific electronic transitions within a chiral molecule – and the method has been successfully applied to inorganic species.[139] Notably, X-ray diffraction studies confirmed the Λ configuration of (-)-$[Fe(phen)_3]^{2+}$, in accordance with the configuration implied by the exciton theory.[140] Bosnich further validated the theory with studies into numerous polypyridylruthenium(II) species and devised a general rule for the assignment of absolute configuration of such complexes: in regions of the ligand long-axis-polarised $\pi \rightarrow \pi^*$ transitions (*ca.* 260-290 nm), the CD signal will appear strongly positive at lower energies and strongly negative at higher energies[†] if the absolute configuration is related to (-)-$[Fe(phen)_3]^{2+}$ (i.e. the Λ configuration), and vice versa.[141, 142] While CD spectra of dinuclear species are potentially complicated by transitions involving the bridging ligand, the general rule still applies. Accordingly, assignments of the enantiomers resolved in these studies were made by comparison of their CD spectra with those reported for similar species[143] and, by extension, using Bosnich's rule. A representative spectrum (that of $[\{Ru(bpy)_2\}_2(\mu\text{-bpm})]^{4+}$) is depicted in Figure 2.10, while individual CD spectra for each of the resolved enantiomers employed in these studies may be seen in Appendix C.

[†] It is not uncommon for the higher-energy transition to be diminished somewhat through overlap and mixing with other transitions of the system.

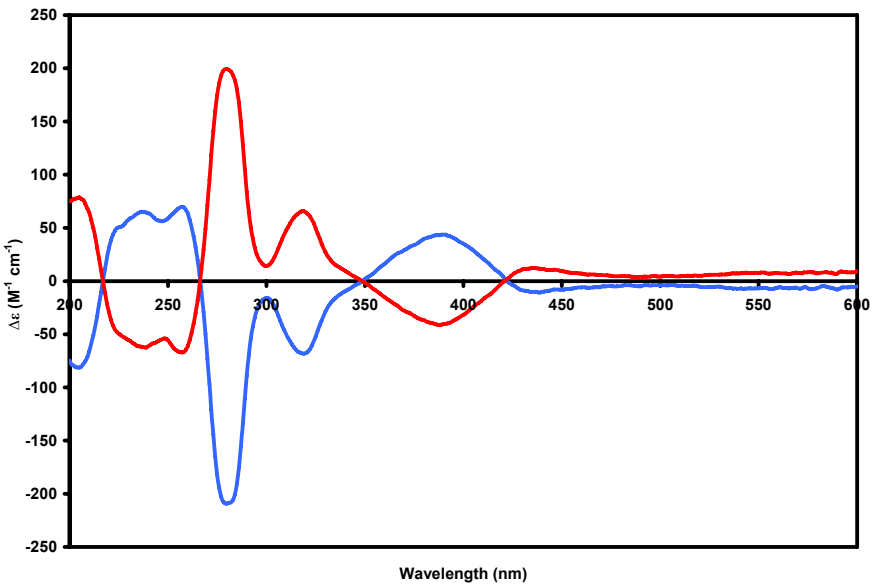


***Figure 2.10***
**Circular dichroism spectra of the ΔΔ (blue) and ΛΛ (red) enantiomers of $[\{Ru(bpy)_2\}_2(\mu\text{-bpm})]^{4+}$.** Spectra collected as the $PF_6^-$ salts of the complexes in acetonitrile solution.

## 2.4 SUMMARY

A series of dinuclear polypyridylruthenium(II) complexes were synthesised for the purpose of studies into structure-specific nucleic acid-binding (as described in subsequent Chapters). These complexes encompassed a variety of different geometries and shapes so as to best enable the elucidation of the structural features that govern the efficiency of their association with oligonucleotides. Systematic variations in the ligand environment of the complexes was accomplished through the use of different terminal ligands, methylation of those ligands, and by utilising bridging ligands of three general classes – linear, angular and stepped-parallel – that altered the proximity and relative configuration of the metal centres (and attached terminal ligands) in these species. Furthermore, cation-exchange chromatography was used to isolate individual diastereoisomeric and enantiomeric species, permitting the study of the role of stereochemistry in mediating metal complex—nucleic acid interactions. Complexes were characterised through the use of NMR and electronic absorption spectroscopy, the latter consisting of both UV/Vis and CD experiments.

The complexes prepared here represent just a small fraction of the many geometries that can be attained through the well-established synthetic chemistry of polypyridyl transition metal complexes. A myriad of potential terminal and bridging ligands exist which may be utilised and

modified in the synthesis of potential probes of nucleic acid structure and function. Future studies involving this class of complex will likely incorporate enhanced functionality into the terminal ligands in the form of hydrogen-bonding groups, and expansion of the complexes into oligo- and polynuclear species with the potential to span ever-larger potential target sites and sequences.

## 2.5 REFERENCES


1. The Royal Swedish Academy of Sciences, *The Nobel Prize in Chemistry 1987*, 12 October **1987**, http://nobelprize.org/nobel_prizes/chemistry/laureates/1987/
2. J.-M. Lehn, *Science*, **1993**, *260*, 1762-1763.
3. F. Blau, *Ber. Dtsch. Chem. Ges.*, **1888**, *21*, 1077-1078.
4. F. R. Keene, *Coord. Chem. Rev.*, **1997**, *166*, 122-159.
5. F. R. Keene, *Chem. Soc. Rev.*, **1998**, *27*, 185-193.
6. A. L. Barra, J. B. Robert and L. Wiesenfeld, *BioSystems*, **1987**, *20*, 57-61.
7. T. J. Rutherford, M. G. Quagliotto and F. R. Keene, *Inorg. Chem.*, **1995**, *34*, 3857-3858.
8. D. A. Reitsma and F. R. Keene, *J. Chem. Soc., Dalton Trans.*, **1993**, 2859-2860.
9. B. T. Patterson, F. M. Foley, D. Richards and F. R. Keene, *Dalton Trans.*, **2003**, 709-714.
10. T. J. Rutherford, O. Van Gijte, A. Kirsch-De Mesmaeker and F. R. Keene, *Inorg. Chem.*, **1997**, *36*, 4465-4474.
11. T. J. Rutherford and F. R. Keene, *J. Chem. Soc., Dalton Trans.*, **1998**, 1155-1162.
12. G. Denti, S. Campagna, S. Serroni, M. Ciano and V. Balzani, *J. Am. Chem. Soc.*, **1992**, *114*, 2944-2950.
13. M. Sommovigo, G. Denti, S. Serroni, S. Campagna, C. Mingazzini, C. Mariotti and A. Juris, *Inorg. Chem.*, **2001**, *40*, 3318-3323.
14. S. D. Ernst and W. Kaim, *Inorg. Chem.*, **1989**, *28*, 1520-1528.
15. Y. Nakabayashi, N. Iwamoto, H. Inada and O. Yamauchi, *Inorg. Chem. Commun.*, **2006**, *9*, 1033-1036.
16. H. Su and J. R. Kincaid, *J. Raman Spectrosc.*, **2003**, *34*, 907-916.
17. E. Brauns, S. W. Jones, J. A. Clark, S. M. Molnar, Y. Kawanishi and K. J. Brewer, *Inorg. Chem.*, **1997**, *36*, 2861-2867.
18. E. Ishow, A. Gourdon, J.-P. Launay, P. Lecante, M. Verelst, C. Chiorboli, F. Scandola and C.-A. Bignozzi, *Inorg. Chem.*, **1998**, *37*, 3603-3609.
19. T. J. Rutherford, D. A. Reitsma and F. R. Keene, *J. Chem. Soc., Dalton Trans.*, **1994**, 3659-3666.
20. J. A. Treadway, P. Chen, T. J. Rutherford, F. R. Keene and T. J. Meyer, *J. Phys. Chem. A*, **1997**, *101*, 6824-6826.
21. A. Velders, H. Kooijman, A. L. Spek, J. G. Haasnoot, D. de Vos and J. Reedijk, *Inorg. Chem.*, **2000**, *39*, 2966-2967.
22. L. S. Kelso, D. A. Reitsma and F. R. Keene, *Inorg. Chem.*, **1996**, *35*, 5144-5153.
23. B. D. Yeomans, L. S. Kelso, P. A. Tregloan and F. R. Keene, *Eur. J. Inorg. Chem.*, **2001**, 239-246.
24. D. M. D'Alessandro, *Stereochemical Effects on Intervalence Charge Transfer*, PhD Thesis, James Cook University, Townsville, **2006**.
25. D. M. D'Alessandro and F. R. Keene, *Chem. Phys.* , **2006**, *324*, 8-25.
26. F. H. Burstall, *J. Chem. Soc.*, **1936**, 173-175.
27. F. P. Dwyer and E. C. Gyarfas, *J. Proc. Roy. Chem. Soc. N.S.W.*, **1949**, *83*, 170-173.
28. B. Bosnich and F. P. Dwyer, *Aust. J. Chem.*, **1966**, *19*, 2229-2233.
29. X. Hua and A. von Zelewsky, *Inorg. Chem.*, **1995**, *34*, 5791-5797.
30. R. T. Watson, J. L. Jackson, J. D. Harper, K. A. Kane-Maguire, L. A. P. Kane-Maguire and N. A. P. Kane-Maguire, *Inorg. Chim. Acta*, **1996**, *249*, 5-7.
31. H. Yoneda, *J. Chromatogr.*, **1984**, *313*, 59-91.

32. T. J. Rutherford, P. A. Pellegrini, J. Aldrich-Wright, P. C. Junk and F. R. Keene, *Eur. J. Inorg. Chem.*, **1998**, 1677-1688.
33. J. W. Vaughn, *Inorg. Chem.*, **1983**, *22*, 844-845.
34. L. J. Boucher, *Inorg. Chem.*, **1970**, *9*, 1202-1207.
35. Y. Kushi, M. Kuramoto and H. Yoneda, *Chem. Lett.*, **1976**, 663-664.
36. K. Garbett and R. D. Gillard, *J. Chem. Soc. A*, **1966**, 802-805.
37. O. Maury, J. Lacour and H. Le Bozec, *Eur. J. Inorg. Chem.*, **2001**, 201-204.
38. J. Lacour, C. Goujon-Ginglinger, S. Torche-Haldiman and J. J. Jodry, *Angew. Chem. Int. Ed.*, **2003**, *39*, 3695-3697.
39. X. Hua, *Chiral Building Blocks Ru(L^L)$_2$ for Coordination Compounds*, PhD Thesis, University of Fribourg (Switzerland), Fribourg, **1993**.
40. A. von Zelewsky and O. Mamula, *J. Chem. Soc., Dalton Trans.*, **2000**, 219-231.
41. F. M. MacDonnell, M.-J. Kim and S. Bodige, *Coord. Chem. Rev.*, **1999**, *185-186*, 535-549.
42. J. R. Keubler, Jr. and J. C. Bailar, Jr., *J. Am. Chem. Soc.*, **1952**, *74*, 3535-3538.
43. B. E. Douglas and S. Yamada, *Inorg. Chem.*, **1965**, *4*, 1561-1565.
44. J. H. Dunlop and R. D. Gillard, *J. Chem. Soc.*, **1965**, 6531-6541.
45. J. I. Legg, D. W. Cooke and B. E. Douglas, *Inorg. Chem.*, **1967**, *6*, 700-706.
46. M. J. Hannon, I. Meistermann, C. J. Isaac, C. Blomme, J. R. Aldrich-Wright and A. Rodger, *Chem. Commun.*, **2001**, 1078-1079.
47. L. T. Taylor and D. H. Busch, *J. Am. Chem. Soc.*, **1967**, *89*, 5372-5376.
48. F. P. Dwyer, T. E. MacDermott and A. M. Sargeson, *J. Am. Chem. Soc.*, **1963**, *85*, 2913-2916.
49. T. S. Piper, *J. Am. Chem. Soc.*, **1961**, *83*, 3908-3909.
50. Y. Yoshikawa and K. Yamasaki, *Coord. Chem. Rev.*, **1979**, *28*, 205-229.
51. Y. Yoshikawa and K. Yamasaki, *Bull. Chem. Soc. Jpn.*, **1972**, *45*, 179-184.
52. F. R. Keene and G. H. Searle, *Chem. Commun.*, **1970**, 784-786.
53. G. H. Searle, *Aust. J. Chem.*, **1977**, *30*, 2625-2637.
54. N. C. Fletcher, P. C. Junk, D. A. Reitsma and F. R. Keene, *J. Chem. Soc., Dalton Trans.*, **1998**, 133-138.
55. N. C. Fletcher and F. R. Keene, *J. Chem. Soc., Dalton Trans.*, **1999**, 683-689.
56. A. Inagaki, S. Yatsuda, S. Edure, A. Suzuki, T. Takahashi and M. Akita, *Inorg. Chem.*, **2007**, *46*, 2432-2445.
57. S. Rau, D. Walther and J. G. Vos, *Dalton Trans.*, **2007**, 915-919.
58. E. Amouyal, *Sol. Energy Mater. Sol. Cells*, **1995**, *38*, 249-276.
59. F. Szemes, D. Hesek, Z. Chen, S. W. Dent, M. G. B. Drew, A. J. Goulden, A. R. Graydon, A. Grieve, R. J. Mortimer, T. Wear, J. S. Weightman and P. D. Beer, *Inorg. Chem.*, **1996**, *35*, 5868-5879.
60. P. D. Beer and F. Szemes, *J. Chem. Soc., Chem. Commun.*, **1995**, 2245-2247.
61. J. N. Demas and B. A. DeGraff, *J. Chem. Ed.*, **1997**, *74*, 690-695.
62. P. D. Beer, R. J. Mortimer, N. R. Stradiotto, F. Szemes and J. S. Weightman, *Anal. Proc. Incl. Anal. Commun.*, **1995**, *32*, 419-421.
63. P. D. Beer and J. Cadman, *Coord. Chem. Rev.*, **2000**, *205*, 131-155.
64. G. Orellana, M. C. Moreno-Bondi, E. Segovia and M. D. Marazuela, *Anal. Chem.*, **1992**, *64*, 2210-2215.
65. J. M. Price, W. Xu, J. N. Demas and B. A. DeGraff, *Anal. Chem.*, **1998**, *70*, 265-270.
66. V. W.-W. Yam and A. S.-F. Kai, *Inorg. Chim. Acta*, **2000**, *300-302*, 82-90.

67. S. Rau, T. Büttner, C. Temme, M. Ruben, H. Görls and D. Walther, *Inorg. Chem.*, **2000**, *39*, 1621-1624.
68. B. J. Coe, J. P. Essex-Lopresti, J. A. Harris, S. Houbrechts and A. Persoons, *Chem. Commun.*, **1997**, 1645-1646.
69. W. Suna, T. H. Patton, L. K. Stultz and J. P. Claudec, *Opt. Commun.*, **2003**, *218*, 189–194.
70. A. Juris, S. Barigelletti, S. Campagna, V. Balzani, P. Belser and A. von Zelewsky, *Coord. Chem. Rev.*, **1988**, *84*, 85-277.
71. T. H. Uyeda, Y. Zhao, K. Wostyn, I. Asselberghs, K. Clays, A. Persoons and M. J. Therien, *J. Am. Chem. Soc.*, **2002**, *124*, 13806-13813.
72. H. Le Bozec and T. Renouard, *Eur. J. Inorg. Chem.*, **2000**, 229-239.
73. S. Di Bella, *Chem. Soc. Rev.*, **2001**, *90*, 355-366.
74. D. Pomeranc, D. Jouvenot, J.-C. Chambron, J.-P. Collin, V. Heitz and J.-P. Sauvage, *Chem. Eur. J.*, **2003**, *9*, 4247-4254.
75. J.-P. Sauvage, *Chem. Commun.*, **2005**, 1507-1510.
76. B. Champin, P. Mobian and J.-P. Sauvage, *Chem. Soc. Rev.*, **2007**, *36*, 358-366.
77. J.-P. Collin, D. Jouvenot, M. Koizumi and J.-P. Sauvage, *Eur. J. Inorg. Chem.*, **2005**, 1850-1855.
78. Y. Liu, S.-H. Song, Y. Chen, Y.-L. Zhao and Y.-W. Yang, *Chem. Commun.*, **2005**, 1702-1704.
79. V. Balzani and F. Scandola, *Supramolecular Photochemistry*, Ellis Horwood, Chichester (U.K.), **1991**.
80. P. Belser, S. Bernhard, C. Blum, A. Beyeler, L. De Cola and V. Balzani, *Coord. Chem. Rev.*, **1999**, *190-192*, 155-169.
81. A. P. de Silva, H. Q. N. Gunaratne, T. Gunnlaugsson, A. J. M. Huxley and C. P. McCoy, *Chem. Rev.*, **1997**, *97*, 1515-1566.
82. V. Balzani, R. Ballardini, F. Bolletta, M. T. Gandolfi, A. Juris, M. Maestri, M. F. Manfrin, L. Moggi and N. Sabbatini, *Coord. Chem. Rev.*, **1993**, *125*, 75-88.
83. A. von Zelewsky, P. Belser, P. Hayoz, R. Dux, X. Hua, A. Suckling and H. Stoecklievans, *Coord. Chem. Rev.*, **1994**, *132*, 75-85.
84. J. G. Vos and J. M. Kelly, *Dalton Trans.*, **2006**, 4869-4883.
85. V. Balzani, *Photochem. Photobiol. Sci.*, **2003**, *2*, 459-476.
86. M. Querol Sans and P. Belser, *Coord. Chem. Rev.*, **2002**, *229*, 59-66.
87. R. Ballardini, V. Balzani, M. Clemente-León, A. Credi, M. T. Gandolfi, E. Ishow, J. Perkins, J. F. Stoddart, H.-R. Tseng and S. Wenger, *J. Am. Chem. Soc.*, **2002**, *124*, 12786-12795.
88. B. Schlicke, P. Belser, L. De Cola, E. Sabbioni and V. Balzani, *J. Am. Chem. Soc.*, **1999**, *121*, 4207 - 4214.
89. M. Plevoets, F. Vögtle, L. De Cola and V. Balzani, *New J. Chem.*, **1999**, 63-69.
90. V. Balzani, S. Campagna, G. Denti, A. Juris, S. Serroni and M. Venturi, *Acc. Chem. Res.*, **1998**, *31*, 26-34.
91. V. Balzani and A. Juris, *Coord. Chem. Rev.*, **2001**, *211*, 97-115.
92. D. M. D'Alessandro and F. R. Keene, *Chem. Soc. Rev.* , **2006**, *35*, 424-440.
93. D. M. D'Alessandro and F. R. Keene, *Chem. Rev.*, **2006**, *106*, 2270-2298.
94. D. M. D'Alessandro and F. R. Keene, *Dalton Trans.*, **2006**, 1060-1072.
95. Y. Xiong and L.-N. Ji, *Coord. Chem. Rev.*, **1999**, *185-186*, 711-733.

96. S. Fukuzumi, M. Tanaka, M. Nishimine and K. Ohkubo, *J. Photochem. Photobio*, **2005**, *175*, 79-88.
97. M. E. Núñez and J. K. Barton, *Curr. Opin. Chem. Biol.*, **2000**, *4*, 199-206.
98. J. K. Barton, *Pure Appl. Chem.*, **1998**, *70*, 873-879.
99. S. E. Evans, S. Mon, R. Singh, L. R. Ryzhkov and V. A. Szalai, *Inorg. Chem.*, **2006**, *45*, 3124-3132.
100. C. W. Crean, Y. T. Kavanagh, C. M. O'Keefe, M. P. Lawler, M. P. Stevenson, R. J. Davies, P. H. Boyle and J. M. Kelly, *Photochem. Photobiol. Sci.*, **2002**, *1*, 1024-1033.
101. M. Liang, S. Liu, M. Wei and L.-H. Guo, *Anal. Chem.*, **2006**, *78*, 621-623.
102. Y. Liu, H. Chao, J. Yao, L. Tan, Y. Yuan and L. N. Ji, *Inorg. Chim. Acta.*, **2005**, *358*, 1904-1910.
103. Y. Liu, H. Chao, Y. Yuan, H. Yu and L. N. Ji, *Inorg. Chim. Acta.*, **2006**, *359*, 3807-3814.
104. X.-W. Liu, J. Li, H. Li, K. Zheng, H. Chao and L. Ji, *J. Inorg. Biochem.*, **2005**, *99*, 2372-2380.
105. E. V. Bichenkova, X. Yu, P. Bhadra, H. Heissigerova, S. J. A. Pope, B. J. Coe, S. Faulkner and K. T. Douglas, *Inorg. Chem.*, **2005**, *44*, 4112-4114.
106. J. L. Morgan, D. P. Buck, A. G. Turley, J. G. Collins and F. R. Keene, *J. Biol. Inorg. Chem.*, **2006**, *11*, 824-834.
107. C. B. Spillane, J. L. Morgan, N. C. Fletcher, J. G. Collins and F. R. Keene, *Dalton Trans.*, **2006**, 3122-3133.
108. A. C. G. Hotze, B. M. Kariuki and M. J. Hannon, *Angew. Chem. Int. Ed.*, **2006**, *45*, 4839-4842.
109. H.-Y. Mei and J. K. Barton, *J. Am. Chem. Soc.*, **1986**, *108*, 7414-7416.
110. P. U. Maheswari, V. Rajendiran, M. Palaniandavar, R. Parthasarathi and V. Subramanian, *Bull. Chem. Soc. Jpn.*, **2005**, *78*, 835-844.
111. D. M. P. Mingos and D. R. D. Baghurst, *Chem. Soc. Rev.*, **1991**, *20*, 1-47.
112. I. P. Evans, A. Spencer and G. Wilkinson, *J. Chem. Soc., Dalton Trans.*, **1973**, 204-209.
113. P. A. Anderson, R. F. Anderson, M. Furue, P. C. Junk, F. R. Keene, B. T. Patterson and B. D. Yeomans, *Inorg. Chem.*, **2000**, *39*, 2721-2728.
114. T. Togano, N. Nagao, M. Tsuchida, H. Kumakura, K. Hisamatsu, F. S. Howell and M. Mukaida, *Inorg. Chim. Acta*, **1992**, *195*, 221-225.
115. F. M. Foley, *DNA Interactions of Mono- and Dinuclear Polypyridylruthenium(II) Complexes*, Honours Thesis, James Cook University, Townsville, **2000**.
116. F. M. Foley, F. R. Keene and J. G. Collins, *J. Chem. Soc., Dalton Trans.*, **2001**, 2968-2974.
117. J. A. Smith, *Dinuclear Ruthenium Complexes as Sequence- and Structure-Selective Binding Agents for DNA*, Honours Thesis, James Cook University, Townsville, **2003**.
118. J. L. Morgan, D. P. Buck, A. G. Turley, J. G. Collins and F. R. Keene, *Inorg. Chim. Acta*, **2006**, *359*, 888-898.
119. T. J. Rutherford, *Stereochemistry in Mono- and Oligo-nuclear Assemblies Based in the* $[Ru(\alpha,\alpha'\text{-diimine})_3]^{2+}$ *Chromophore*, PhD Thesis, James Cook University, Townsville, **1997**.
120. B. P. Sullivan, D. J. Salmon and T. J. Meyer, *Inorg. Chem.*, **1978**, *17*, 3334-3341.
121. K. A. Goldsby and T. J. Meyer, *Inorg. Chem.*, **1984**, *23*, 3002-3010.
122. E. V. Dose and L. J. Wilson, *Inorg. Chem.*, **1978**, *17*, 2660-2666.
123. P. Rillema and K. B. Mack, *Inorg. Chem.*, **1982**, *21*, 3849-3854.

124. M. Krejcik and A. A. Vlcek, *Inorg. Chem.*, **1992**, *31*, 2390-2395.
125. M. Hunziker and A. Ludi, *J. Am. Chem. Soc.*, **1977**, *99*, 7370-7371.
126. J. L. Morgan, C. B. Spillane, J. A. Smith, D. P. Buck, J. G. Collins and F. R. Keene, *Dalton Trans.*, **2007**, 4333-4342.
127. C. H. Braunstein, A. D. Baker, T. C. Strekas and H. D. Gafney, *Inorg. Chem.*, **1984**, *23*, 857-864.
128. D. P. Rillema, D. G. Taghdiri, D. S. Jones, C. D. Keller, L. A. Worl, T. J. Meyer and H. A. Levy, *Inorg. Chem.*, **1987**, *26*, 578-585.
129. E. C. Constable and J. Lewis, *Inorg. Chim. Acta*, **1983**, *70*, 251-253.
130. D. M. D'Alessandro and F. R. Keene, *New J. Chem.*, **2006**, *30*, 228-237.
131. A. Chouai, S. E. Wicke, C. Turro, J. Bacsa, K. R. Dunbar, D. Wang and R. P. Thummel, *Inorg. Chem.*, **2005**, *44*, 5996-6003.
132. Y. Fuchs, S. Lofters, T. Dieter, W. Shi, T. C. Morgan, T. C. Strekas, H. D. Gafney and A. D. Baker, *J. Am. Chem. Soc.*, **1987**, *109*, 2691-2697.
133. D. M. D'Alessandro and F. R. Keene, *Chem. Eur. J.*, **2005**, *11*, 3679-3688.
134. L. Jacquet and A. Kirsch-De Mesmaeker, *J. Chem. Soc., Faraday Trans.*, **1992**, *88*, 2471-2480.
135. G. Denti, S. Campagna, L. Sabatino, S. Serroni, M. Ciano and V. Balzani, *Inorg. Chem.*, **1990**, *29*, 4750-4758.
136. K. Kalyanasundaram and M. K. Nazeeruddin, *Inorg. Chem.*, **1990**, *29*, 1888-1897.
137. E. A. Fellows and F. R. Keene, *J. Phys. Chem. B*, **2007**, *111*, 6667-6675.
138. W. Moffitt, *J. Chem. Phys.*, **1956**, *25*, 467.
139. A. J. McCaffery and S. F. Mason, *Proc. Chem. Soc.*, **1963**, 211-212.
140. D. H. Templeton, A. Zalkin and T. Ueki, *Acta Cryst. Suppl.*, **1966**, *21*, A154.
141. B. Bosnich, *Inorg. Chem.*, **1968**, *7*, 2379-2386.
142. B. Bosnich, *Inorg. Chem.*, **1968**, *7*, 178-180.
143. S. G. Telfer, N. Tajima and R. Kuroda, *J. Am. Chem. Soc.* , **2004**, *126*, 1408-1418.

# Chapter 3

## *Fluorescence and Electronic Absorption Spectroscopy Investigations into the DNA-Binding Properties of Dinuclear Ruthenium Complexes*

## 3.1 INTRODUCTION

### 3.1.1 Methods of Investigating Metal Complex-Nucleic Acid Interactions

A variety of different techniques – ranging from the biophysical to the photophysical, the electrochemical to the theoretical – have been applied to the study of metal complex-nucleic acid interactions. Comprehensive investigations typically employ several complementary techniques in order to provide a detailed picture of the association in question, encompassing such aspects as binding affinity, geometry, site and mode.

Amongst the most useful techniques employed in nucleic acid binding studies is nuclear magnetic resonance (NMR) spectroscopy which is discussed in greater depth in the following Chapter. Despite lacking the sensitivity of some other techniques, a thorough application of one- and two-dimensional NMR experiments can yield detailed information regarding the nature of the solution phase interactions of metal complexes and nucleic acids. Conversely, complementary solid-state structural data can notionally be obtained using X-ray crystallography; however, while this technique has been extensively applied to organic nucleic acid-binders,[1-7] useful crystals of metal complex-nucleic acid adducts are notoriously difficult to obtain. The few examples of crystal structures of non-covalently bound polypyridyl species are those of rhodium metallointercalators prepared by Barton and co-workers.[8, 9]

Mass spectrometry (MS), widely employed in the elucidation of the primary structure of biopolymers, has also been applied to the study of nucleic acid-binding metal complexes.[10] While these investigations have been largely confined to covalently-binding species,[10-14] the relatively gentle nature of electrospray isonisation mass spectrometry (ESI-MS) has facilitated studies of noncovalently-bound metal complexes.[15-17] ESI-MS experiments, like many of the techniques used to assess nucleic acid-metal complex interactions, can provide information regarding the stoichiometry, relative binding affinity and sequence selectivity of these interactions. However, other than the determination of binding constants, there are only a few instances in which the thermodynamics of nucleic acid-binding has been examined in any great detail. Such studies are typically based upon isothermal calorimetry (ITC) experiments,[18-21] in which the various thermodynamic parameters ($\Delta H$, $\Delta G$, $\Delta S$) of the system are assessed in order to quantitate the relative electrostatic versus nonelectrostatic contributions to the interaction.

Equilibrium dialysis experiments are commonly used to ascertain the degree of enantioselectivity exhibited by chiral noncovalently-binding metal complexes,[22-24] but can also

be used to derive quantitative data including binding constants.[25, 26] Circular dichroism (CD) measurements are used to determine the chirality of the favoured enantiomer in such experiments, but CD techniques can also be used to observe topological changes in nucleic acids upon binding.[27-30] A related technique, linear dichroism (LD), can unambiguously determine the orientation of a metal complex relative to the nucleic acid to which it is bound;[30-34] based upon this binding geometry, one can infer the mode by which the complex is binding. Thermal denaturation profiles are commonly used to assess the relative overall DNA-binding strength of a metal complex:[28, 33, 35-37] "melting" of double-stranded DNA (i.e. thermal dissociation of the two strands) is monitored through the accompanying hyperchromism at the $\lambda_{max}$ of the DNA – bound metal complexes alter the denaturation temperature of a given nucleic acid relative to the strength of their association. As previously mentioned in the Introduction, classical intercalative binding has another notable physical effect on nucleic acids: it causes a lengthening of the helix that can be detected using a number of different techniques. Most commonly this lengthening is measured using viscosity experiments in which the relative electrophoretic mobility of a duplex to which an intercalator is bound is reduced due to the increased length of the rod-like DNA molecule.[18, 27, 28, 37-40] Similarly, intercalators are known to unwind supercoiled plasmid DNA, causing it to migrate more slowly through an electrophoretic gel. The extent to which the DNA is unwound (and thus, the degree to which its electrophoretic migration is retarded) again directly correlates to the intercalative ability of the complex.[25, 41, 42] Non-intercalative complexes typically have little effect on the viscosity of the DNA to which they are bound. A relatively recent innovation in the detection of duplex lengthening/plasmid unwinding upon the intercalation of a metal complex is the application of atomic force microscopy (AFM). This technique can provide an image of the DNA being studied and directly measure any lengthening/unwinding of the molecule, inferring an intercalative or non-intercalative binding mode and, in some instances, deriving a binding constant based upon the degree of lengthening/unwinding.[43-45]

Biochemical assays – specifically, inhibiting the association of nucleic acid-binding enzymes and impairing their function – are another routine means of assessing the relative affinity and selectivity of metal complex-nucleic acid interactions.[35, 46-50] Additionally, the rich photophysical properties of many polypyridylruthenium(II) complexes also make them amenable to the photocleavage of nucleic acids: many such complexes are able to induce cleavage of plasmid DNA upon irradiation at specific wavelengths, thus showing promise as

potential photoactive drugs.[51-56] While such assays are undertaken *in vitro*, they provide an invaluable insight into not only the DNA-binding capabilities of these metal complexes, but also the mechanisms by which such species exert cytotoxic effects *in vivo*.[57-61]

In many cases experimental investigations have been supplemented by theoretical studies into the nature of specific metal complex-nucleic acid interactions. While density functional theory (DFT) analyses of intercalating complexes have been used to explain their relative intercalative abilities,[40, 62, 63] the sheer complexity of the interactions between small molecules and biomacromolecules hinders accurate predictive modeling of binding scenarios. The majority of theoretical binding studies to date have been molecular mechanics-based geometry/energy-optimisation procedures based upon available experimental data,[30, 64-67] with the end result being a model of the metal complex-nucleic acid adduct which reflects the experimental observations. Inferences regarding the binding mode of the complex can be made on the basis of specific orientations, configurations and close contacts observed in the model.

As previously stated, polypyridylruthenium(II) complexes possess electrochemical and photophysical properties that make them particularly amenable to the study of nucleic acid binding interactions. By monitoring perturbations to these phenomena it is possible to discern the nature of various aspects of the metal complex-nucleic acid interaction. For example, the exceptional redox properties of this class of metal complex facilitate the assessment of their binding interactions using voltammetric experiments. Decreases in peak current upon binding to DNA have been used to infer the degree of enantioselectivity, binding constants and binding site sizes of several ruthenium complexes.[24, 67, 68] Similarly, spectral variations induced by hydrophobic- and π-interactions between aromatic ligands and the bases of a nucleic acid can be used to estimate binding modes and affinities. Typically, strong metal complex-nucleic acid interactions manifest themselves as hypochromism and bathochromic shifts in absorption spectra,[23, 69-71] and enhanced emission intensity and luminescence lifetimes in luminescence spectra.[29, 37, 40, 72, 73] More recently, resonance Raman spectroscopy has shown considerable promise as a means by which to probe the vibrational structure of metal complexes in nucleic acid interactions, thus providing information from which the binding mode of the complex may be deduced.[74-78]

### 3.1.2 The Fluorescent Dye Displacement Assay

Through the use of the techniques described above it is possible to accumulate a large amount of data from which the nature of specific metal complex-nucleic acid interactions may be ascertained. Unfortunately, most of these techniques are relatively labour- and time-intensive and are therefore not amenable to a high-throughput screening process.

Our laboratory has recently adopted and adapted the high-throughput fluorescent intercalator displacement (FID) assay of Boger *et al.*[79-81] to facilitate the screening of large numbers of metal complex-oligonucleotide interactions within a relatively short period of time. The technique involves the treatment of the oligonucleotide of interest with an intercalative fluorescent dye {such as ethidium bromide (EthBr) or thiazole orange (TO)} that exhibits a significant fluorescence increase upon binding to DNA.[†] Upon addition of a DNA-binding analyte compound, the dye is displaced to an extent proportional to the binding affinity of the compund, thus inducing a concordant decrease in fluorescence. Conducting the assay in multi-well plates incorporating a variety of DNA-binding compounds and potential target oligonucleotides allows for a rapid survey of numerous systems with minimal technical demands. The data obtained from the assay facilitates a comprehensive qualitative comparison of the relative binding affinities of many compounds as well as their respective sequence- and structure-selectivities.

Boger and colleagues have successfully applied the technique to a study of the binding affinity and sequence selectivity of a series of organic minor-groove binders interacting with a library of hairpin oligonucleotides,[79] protein-DNA interactions[82] and the association of hairpin polyamides.[81] The technique has also been employed in the study of DNA-binding antibiotics,[83] potential quadruplex-binders,[84] and helix 3 homeodomain analogue peptides.[85] In a recent paper, Goodwin *et al.* reported on the coupling of the FID procedure to a high-resolution crystallographic technique, allowing them to study both the general selectivity and intricate structural details of the DNA-interactions of a "highly twisted" benzimidazole-diamidine within a relatively short period of time.[86]

[†] Accommodation of the fluorophore within the hydrophobic core of a DNA molecule shields it from quenching solvent molecules, enhancing its fluorescence manifold.

### 3.1.3 Present Studies

Our goal was to adapt the FID technique to qualitatively assess the general DNA-binding capabilities of a range of inert dinuclear ruthenium(II) complexes against numerous different oligonucleotides. It was our intent to identify those systems which would be of most interest for more in-depth studies, specifically NMR experiments. The series of complexes studied by the author were those of the general formula $[\{Ru(pp)_2\}_2(\mu\text{-BL})]^{4+}$, where pp represents the polypyridyl terminal ligands bpy, $Me_2$bpy, phen and $Me_2$phen, and BL represents the polypyridyl bridging ligands bpm, HAT, ppz, 2,3-dpp and 2,5-dpp. FID assays were used to study the binding of these complexes to a variety of different oligonucleotides incorporating various sequences and secondary structures for the purpose of identifying specific structural selectivies of the assorted metal complexes. Over the course of these studies it became clear that more accurate results could be obtained using an adaptation of the FID assay which employs a dye possessing a binding mode more akin to that of the complexes being investigated; the experimental justifications for this are detailed below.

Additionally, several of the complexes utilised in the FID assay were employed in electronic absorption titration experiments with calf thymus DNA and/or yeast tRNA in order to quantitate their affinities for these nucleic acids. By monitoring perturbations to the spectra of the metal complexes upon interaction with the nucleic acids it was possible to calculate binding constants for those particular species. The general trends reflected in these quantitative assessments were found to be in accord with those implied by the FID assays, thus asserting an overall pattern of selectivity for complexes of this type.

## 3.2 EXPERIMENTAL

### 3.2.1 Materials

All oligonucleotides (listed in Table 3.1) were obtained from GeneWorks with the exception of the quadruplex sequences which were supplied by Dr. Max Keniry at the Research School of Chemistry, Australian National University. Calf thymus DNA (CT DNA) and baker's yeast tRNA (type X-SA) were obtained from Sigma. Ethidium bromide (EthBr; 95%, Aldrich), 4′,6-diamidino-2-phenylindole (DAPI; ≥ 98%, Fluka), sodium chloride (Ajax; AR),

tris(hydroxymethyl)aminomethane (Tris; 99.9+%, Aldrich), and 1X8-200 Dowex anion-exchange resin ($Cl^-$ form; Sigma-Aldrich) were used as supplied.

***Table 3.1***
Oligonucleotides used in these studies.

| | Oligonucleotide Sequence[a] | Description |
|---|---|---|
| **1** | d(ATATATATATAT)$_2$ | Canonical duplex, repeating AT sequence |
| **2** | d(AATTAATTAATT)$_2$ | Canonical duplex, repeating AATT sequence |
| **3** | d(CGCGCGCGCGCG)$_2$ | Canonical duplex, repeating CG sequence |
| **4** | d(CCGGCCGGCCGG)$_2$ | Canonical duplex, repeating CCGG sequence |
| **5** | d(CGCGAATTCGCG)$_2$ | Canonical duplex, Dickerson-Drew sequence |
| **6** | d(CCGGAATTCCGG)$_2$ | Canonical duplex, control version of bulge oligomers 7-11 |
| **7** | d(CCG**A**GAATTCCGG)$_2$ | Duplex containing adenine bulge site(s) |
| **8** | d(CCG**C**GAATTCCGG)$_2$ | Duplex containing cytosine bulge site(s) |
| **9** | d(CCG**T**GAATTCCGG)$_2$ | Duplex containing thymine bulge site(s) |
| **10** | d(CCG**G**GAATTCCGG)$_2$ | Duplex containing guanine bulge site(s) |
| **11** | d(CCG**AA**GAATTCCGG)$_2$ | Duplex containing two-adenine bulge site(s) |
| **12** | d(GCATCG**AAA**GCTACG)•d(CGTAGCCGATGC) | Duplex containing a centralised three-adenine bulge site |
| **13** | d(GCATCG**AAAAA**GCTACG)•d(CGTAGCCGATGC) | Duplex containing a centralised five-adenine bulge site |
| **14** | d(GCATCG**AATAA**GCTACG)•d(CGTAGCCGATGC) | Duplex containing a centralised AATAA bulge site |
| **15** | d(CACTGGT**CTCT**ACCAGTG) | Hairpin loop containing a CTCT 4-base loop sequence |
| **16** | d(CACTGGT**AAAA**ACCAGTG) | Hairpin loop containing an AAAA 4-base loop sequence |
| **17** | d(CACTGGT**CTCTCT**ACCAGTG) | Hairpin loop containing a CTCTCT 6-base loop sequence |
| **18** | d(CACTGGT**AGAGAG**ACCAGTG) | Hairpin loop containing an AGAGAG 6-base loop sequence |
| **19** | d(CACTGGT**AAAAAA**ACCAGTG) | Hairpin loop containing an AAAAAA 6-base loop sequence |
| **20** | d(CACTGGT**CCCCCC**ACCAGTG) | Hairpin loop containing a CCCCCC 6-base loop sequence |
| **21** | d(CACTGGT**GGGGGG**ACCAGTG) | Hairpin loop containing a GGGGGG 6-base loop sequence |
| **22** | d(CACTGGT**TTTTTT**ACCAGTG) | Hairpin loop containing a TTTTTT 6-base loop sequence |
| **23** | d(GGTTGGTGTGGTTGG) | Quadruplex-forming sequence; thrombin aptamer |
| **24** | d(TGGGGT)$_4$ | Quadruplex-forming sequence |
| **25** | d(GGGGTTTTGGGG)$_2$ | Quadruplex-forming sequence |

[a] Unpaired (bulge or loop) bases depicted in red.

Metal complexes were synthesised as described in Chapter 2 and converted to the water-soluble chloride salts: the hexafluorophosphate salt of the complex of interest was dissolved in a minimum volume of acetone to which approximately one gram of anion-exchange resin was added and the volume increased by 50% by the addition of distilled water. The mixture was stirred for 20 minutes before being filtered; the acetone was removed using a rotary evaporator and the aqueous solution lyophilised to yield the solid, dry chloride salt. The complexes

$[\{Ru(phen)_2\}_2(\mu\text{-dppm})]^{4+}$ {dppm = 4,6-bis(2-pyridyl)pyrimidine} and $[\{Ru(phen)_2\}_2(\mu\text{-bb7})]^{4+}$ {bb7 = 1,7-bis[4(4′-methyl-2,2′-bipyridyl)]heptane} were supplied by Dr. Joy Morgan (JCU).

### 3.2.2 Physical Measurements

UV/Visible absorbance measurements/titrations were performed on a Cary 5E spectrophotometer. Oligonucleotide concentrations were determined from UV absorbance at 260 nm using extinction coefficients provided by the supplier; polynucleotide concentrations (reported as base pair concentrations {bp} unless otherwise noted) were determined using the established extinction coefficients for CT DNA (6,600 $M^{-1}$ $cm^{-1}$ $nucleotide^{-1}$)[87] and tRNA (7,700 $M^{-1}$ $cm^{-1}$ $nucleotide^{-1}$).[88] Fluorescence assays were carried out using a Perkin-Elmer Wallac Victor$^3$ V multilabel plate counter, and circular dichroism (CD) spectra were measured on a Jasco J-715 spectropolarimeter.

### 3.2.3 Fluorescent Intercalator Displacement (FID) Assay

The methods of Boger *et al.*[79, 80] were adapted as follows. Oligonucleotides to be used in the FID assay were rehydrated with Tris buffer solution (100 mM Tris, 100 mM NaCl, pH 7.8)[†] and their concentrations determined spectrophotometrically. Each well of a Costar black flat-bottomed 96-well plate was loaded with EthBr (88 μL of 6 μM solution in Tris buffer) and the appropriate oligonucleotide {20 μL of 12 μM (bp) in Tris buffer}. Using a plate reader ten fluorescence readings were taken on each cell ($\lambda_{ex}$ = 545 nm, $\lambda_{em}$ = 595 nm) at 25 °C, providing a baseline emission value arising from fully-bound intercalating dye. The wells were subsequently loaded with the appropriate ruthenium complex solutions (10 μL of 1 mM complex chloride salt in $H_2O$), with four wells dedicated to each metal complex/oligonucleotide combination. Hence, before the addition of the metal complex well occupancy was 108 μL [4.9 μM EthBr, 2.2 μM DNA (bp)], and after the addition of the metal complex the total volume was 118 μL [4.5 μM EthBr, 2.2 μM DNA (bp), 85 μM Ru]. A further ten emission readings were performed on each well after an incubation period of ten minutes, giving a total of forty data points for each interaction being studied. The difference in fluorescence between the metal

[†] In preparing solutions of the quadruplex oligonucleotides (**23-25**) the Tris buffer solution contained KCl instead of NaCl.

complex-free emission and the emission in the presence of the metal complex were calculated for each well and averaged for each sample. Results are presented as a percentage decrease in the initial, metal-free emission. A variance of approximately 10% was observed between wells, consistent with the observations of Boger *et al.* who attributed it to surface effects such as bubbles or dust.[79]

### 3.2.4 Fluorescent Minor Groove-Binder Displacement Assay

This method was further adapted for use with the fluorescent DNA minor groove-binder DAPI. The effective dye:oligonucleotide ratio was found to be significantly lower than that required for the FID assay. A DAPI to double-stranded oligonucleotide ratio of 1:1 was found to provide the best resolution between complex stereoisomers for a given oligonucleotide, whereas higher ratios (approximately 3:1) were found to better facilitate comparisons between oligonucleotides. Likewise, the metal complex:oligonucleotide ratio necessary to induce a significant decrease in fluorescence was considerably lower than in the FID technique. Accordingly, a higher DNA concentration was used in these experiments, with the molarity of the solutions reported as oligonucleotide concentration, rather than base-pair concentration.

In a typical experiment each well of the 96-well plate was loaded with DAPI (88 μL of 32 μM solution in Tris buffer) and the oligonucleotide of interest {17 μL of 165 μM (oligonucleotide concentration), rehydrated in Tris buffer as per the FID assay}. Ten fluorescence measurements were recorded for each well at 25 °C using a plate reader ($\lambda_{ex}$ = 358 nm, $\lambda_{em}$ = 461 nm), providing the full emission reading. The wells were subsequently loaded with the appropriate ruthenium complex solution (11 μL of 1 mM complex in $H_2O$), with four wells dedicated to each metal complex/oligonucleotide combination. Well occupancy before the addition of the metal complex was therefore 105 μL [27 μM DAPI, 27 μM DNA (oligonucleotide)]; after addition of t he metal complex it was 116 μL [24 μM DAPI, 24 μM DNA (oligonucleotide), 96 μM Ru]. A further ten emission readings were made on each well in the presence of the metal complex, thus providing forty data points for each metal complex-oligonucleotide combination which were subsequently averaged to yield the reported fluorescence percentage decrease values. Once again, a variance of approximately 10% was observed between wells.

### 3.2.5 Electronic Absorption Titrations

The absorption spectra (200-800 nm) of several complexes at a fixed conccentration were recorded in the presence of varying concentrations of CT DNA or yeast tRNA {0-50 μM (nucleotide concentration, nt)}. Two solutions were prepared for each complex: Solution A, containing the metal complex (*ca.* 5 μM) and CT DNA/tRNA {*ca.* 150 μM (nt)} in Tris buffer (100 mM Tris, 100 mM NaCl, pH 7.8), and Solution B containing just the metal complex (*ca.* 5 μM) in Tris buffer. Aliquots of Solution A (100 μL each) were titrated into Solution B (2500 μL) for a total of 10-15 titrations per complex. The UV/Vis absorption spectrum of Solution B was measured after each addition, with the resultant data fitted to the equations of Wolfe *et al.*[89] in order to obtain an intrinsic binding constant, $K_b$:

$$[\text{DNA}]/(\varepsilon_a - \varepsilon_f) = [\text{DNA}]/(\varepsilon_b - \varepsilon_f) + 1/K_b(\varepsilon_b - \varepsilon_f) \qquad \textbf{(Equation 3.1)}$$

where [DNA] is the concentration of DNA in *base-pairs* (i.e. half the nt concentration)[†] and $\varepsilon_a$, $\varepsilon_b$ and $\varepsilon_f$ are the apparent, bound and free metal complex extinction coefficients, respectively. A plot of $[\text{DNA}]/(\varepsilon_a - \varepsilon_f)$ versus [DNA] gave a slope of $1/(\varepsilon_b - \varepsilon_f)$ with a *y*-intercept equal to $1/K_b(\varepsilon_b - \varepsilon_f)$; $K_b$ was calculated from the ratio of the slope to the *y*-intercept.

## 3.3 Results & Discussion

### 3.3.1 Overview of the FID Assay

FID assays were used to assess the relative binding affinities of a series of dinuclear ruthenium complexes of the general form $[\{Ru(pp)_2\}_2(\mu\text{-BL})]^{4+}$ {pp = polypyridyl terminal ligand: bpy, $Me_2$bpy, phen, or $Me_2$phen; BL = polypyridyl bridging ligand: bpm, HAT, ppz, 2,3-dpp, or 2,5-dpp} for a variety of different oligonucleotides (see Table 3.1). This technique – a modification of that used by Boger *et al.* to assess the hairpin-binding capabilities of several organic minor groove-binding compounds[79] – is a simple high-throughput means of surveying many potential metal complex-oligonucleotide interactions within a relatively small period of time. The oligonucleotides of interest were loaded into a 96-well plate and treated with an intercalating dye that underwent a significant increase in fluorescence upon binding to DNA.

[†] Base-pair concentrations were used for both CT DNA and tRNA, despite large regions of unpaired bases in the latter polynucleotide.

For the series of complexes discussed here the dye used in the FID assay was EthBr – its emission maximum is at 595 nm, well clear of the longer wavelength visible/NIR emissions expected of the rigid dinuclear ruthenium complexes. However, in applying the technique to the study of mononuclear species[29, 60] or dinuclear complexes joined through a flexible bridge,[90] a judicious use of dye is necessary to avoid competing emissions. Thiazole orange has been found useful in such cases as the wavelength of its emission maximum (535 nm) is sufficiently removed from the typical emission maximum of these complexes (*ca.* 600 nm). Upon the addition of a metal complex, the fluorescence of the system decreased to an extent that correlates to the relative affinity of the metal complex for the target oligonucleotide. Comparing the relative fluorescence decreases induced by different metal complexes and/or stereoisomers facilitates a rapid, qualitative appraisal of the strength of many complex-oligonucleotide interactions simultaneously. The data derived from such an assay not only identifies those systems of most interest for more detailed (but time-consuming) studies such as NMR experiments, but also makes apparent any specific trends with regards to the selectivity of the interactions being investigated.

## 3.3.2 General Trends Observed in the FID Assay

### *3.3.2.1 Terminal Ligands*

As previously discussed in Chapter 1, the nature of the terminal ligands of a metal complex significantly influences the extent to which that complex can associate with nucleic acids. Generally speaking, an increase in the aromatic bulk of a terminal ligand and/or the inclusion of methyl substituents will increase the potential binding affinity of a complex containing that ligand through enhanced hydrophobic and van der Waals interactions.[18, 24, 39, 91] Furthermore, terminal ligands of increased bulk can serve to exaggerate any stereoselective effects in binding to chiral nucleic acid polymers through unfavourable steric clashes on the part of specific stereoisomers.[64, 92-94] Conversely, a poor match between the shape and size of the metal complex (arising, at least in part, from the size and orientation of the terminal ligands) and the geometry of the groove to which the complex is binding will ultimately result in weak binding.

The series of complexes used in the present studies incorporated either 2,2′-bipyridine or 1,10-phenanthroline terminal ligands or their dimethylated derivatives, 4,4′-dimethyl-2,2′-bipyridine or 4,7-dimethyl-1,10-phenanthroline. Bpm-bridged complexes with 5,5′-dimethyl-

2,2′-bipyridine terminal ligands were also synthesised, but both the current FID assay and prior NMR studies[95] suggested that the 5,5′-derivative had a very similar binding profile to the analogous 4,4′-derivative; consequently the 5,5′-dimethyl-2,2′-bipyridine ligand was not used in the synthesis of complexes based on other bridging ligands. The phen ligands differ from the bpy ligands by the inclusion of a third fused aromatic ring; the larger size of the phen ligands coupled with their greater aromaticity results in an increased hydrophobicity. Derivitisation of each ligand with methyl substituents does not exaggerate the size variation between the bpy and phen ligands because the substitution positions (designated 4,4′ in the former, 4,7 in the latter) are in actuality equivalent sites on the two non-derived ligands (refer to Figure 1.22 for the structures of these ligands). The influence of methyl groups on the DNA-binding behaviour of dinuclear polypyridylruthenium(II) complexes has been previously demonstrated in NMR collaborations between the laboratories of F. R. Keene (James Cook University) and J. G. Collins (University of New South Wales, Australian Defence Force Academy): a bpm-bridged complex with $Me_2$bpy ligands on one metal centre but bpy ligands on the other binds to the bulge-containing duplex d(CCGAGAATTCCGG)$_2$ such that the methylated ligands project into the minor groove,[96] while the analogous complex featuring only $Me_2$bpy terminal ligands binds to the same bulge sequence with a greater affinity than the complex with only bpy terminal ligands.[96, 97]

The results of the current FID assay suggest that, overall, complexes possessing phen terminal ligands induce a larger fluorescence decrease than do the analogous complexes with bpy ligands, while methylated ligands induce a larger decrease than do their non-methylated analogue. Thus, the general trend in relative binding affinity amongst a series of complexes possessing the same bridging ligand is found to be $Me_2$phen > phen > $Me_2$bpy > bpy (with respect to induced fluorescence decrease and, by implication, binding affinity). This trend is most apparent in *meso* diastereoisomers; enantiomers (or the *rac* form) tended to exhibit greater variability, most likely due to exaggeration in chiral and steric incompatibility between specific metal complexes and oligonucleotides. Nevertheless, the trend in *meso* diastereoisomers is generally very consistent across all of the oligonucleotides tested – canonical and non-canonical sequences alike. For example, upon binding to the 6-base hairpin loop sequence d(CACTGGT**CTCTCT**ACCAGTG) the *meso* diastereoisomers of a series of ppz-bridged complexes induced fluorescence decreases that vary from 52% for complex with bpy termini to 90% for the complex with $Me_2$phen termini, while the bpm-bridged complexes varied from

15% (bpy) to 62% ($Me_2$phen) {see Figure 3.1(a)}. When these same complexes are added to a canonical Dickerson-Drew sequence {d(CGCGAATTCGCG)$_2$} the overall trend remained the same, albeit with a much smaller difference between the effect of the terminal ligands: the induced fluorescence decreases of the ppz-bridged complexes varied from 47% for bpy to 67% for $Me_2$phen, while the bpm-bridged versions only varied from 27% (bpy) to 39% ($Me_2$phen) {see Figure 3.1(b)}. The anomalously large effect of *meso*-[{Ru(phen)$_2$}$_2$($\mu$-bpm)]$^{4+}$ seen in Figure 3.1(b) is most likely an aberration in that particular assay given the clear trend evident amongst the other terminal ligands.

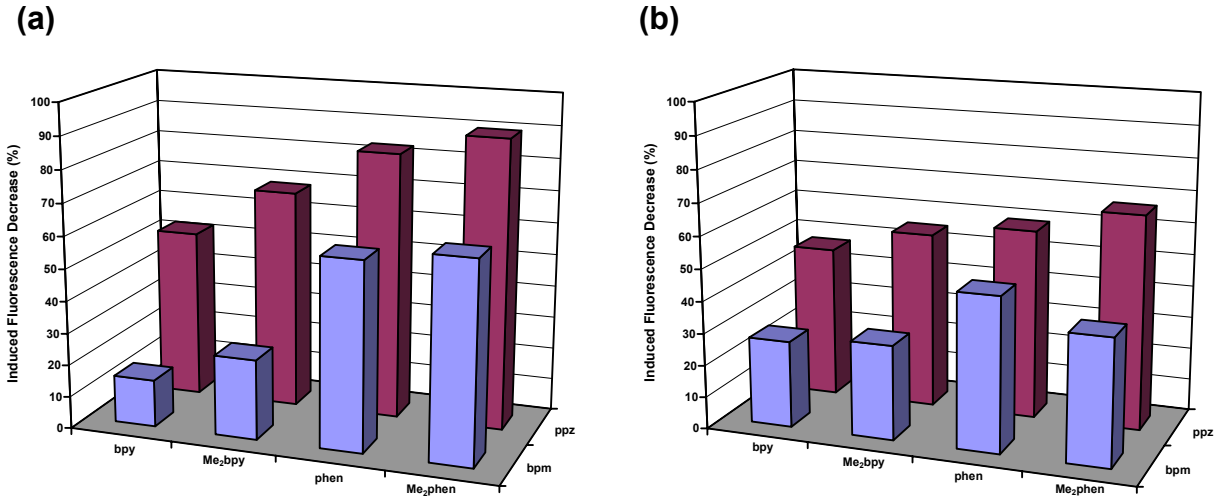


***Figure 3.1***
**The effect of terminal ligand identity on binding affinity.** The relative binding affinities of a series of ppz- and bpm-bridged complexes (*meso* diastereoisomers only) with systematically varied terminal ligands as assessed using the FID assay. Each chart shows the metal complex-induced decrease in the fluorescence of EthBr bound to **(a)** a 6-base hairpin loop sequence {d(CACTGGT**CTCTCT**ACCAGTG)} and **(b)** the canonical duplex Dickerson-Drew sequence {d(CGCGAATTCGCG)$_2$}. Larger decreases imply higher affinities.

### *3.3.2.2 Bridging Ligands*

The FID data also clearly illustrates the effect of bridging ligand-induced geometry changes on the nucleic acid-binding properties of dinuclear metal complexes. In general, those complexes based upon the "angular" class of bridging ligand (defined in Chapter 2) induced greater decreases in fluorescence than did the "stepped parallel" class of bridging ligand, which itself had a larger effect than did complexes of the "linear" bridging ligand. Figure 3.2 shows the average extent to which complexes containing each class of bridging ligand induced a decrease in the fluorescence of EthBr bound to a specific type of oligonucleotide: canonical

duplexes (oligonucleotides **1-6** of Table 3.1), single-base bulge sequences (**7-10**), multi-base bulge sequences (**11-14**), 4-base hairpin loop sequences (**15** and **16**), and 6-base hairpin loop sequences (**17-22**); the quadruplex sequences **23-25** were not included in these averages as they were not assayed against a large variety of metal complexes. The reported values are the average fluorescence decrease (%) induced by all complexes of the nominated bridging ligand class, including all three stereoisomers and all varieties of terminal ligand. It should be noted that several enantiomers of the 2,3-dpp-bridged complexes were excluded from the assay due to the chromatographic difficulties described in Chapter 2. Furthermore, the results describing the effect of the "stepped-parallel" bridging ligand class only incorporates FID data pertaining to the bpy and $Me_2$bpy variants of the 2,5-dpp-bridged complex as the other complexes were unavailable at the time of the assay. If the trend of terminal ligand affects holds true, the phen and $Me_2$phen variants of the 2,5-dpp-bridged complexes should exhibit a higher nucleic acid-affinity than their bpy and $Me_2$bpy analogues; as such, the "stepped-parallel"-induced average fluorescence decrease reported in Figure 3.2 may be understating the actual nucleic acid affinity of this class of complexes.

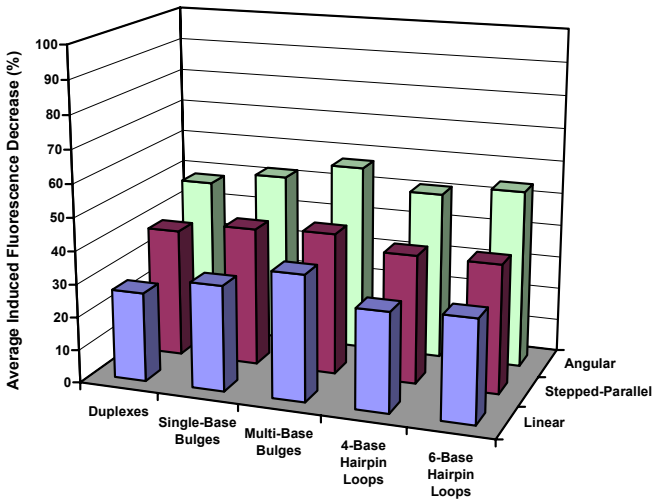


***Figure 3.2***
**The effect of bridging ligand identity on binding affinity.** Reported here are the average decreases in EthBr fluorescence induced by each class of bridging ligand (linear, stepped-parallel and angular) for each general type of oligonucleotide. The averages incorporate the FID data for all complexes (ΔΛ, ΔΔ and ΛΛ stereoisomers, and bpy, $Me_2$bpy, phen, $Me_2$phen terminal ligands), where available.

Against all oligonucleotides (excluding the quadruplexes) the "angular", "stepped-parallel" and "linear" classes of metal complex induced average fluorescence decreases of 52%, 40% and 32%, respectively. This implies that the "angular"-bridged complexes have a higher overall

affinity for nucleic acids than do the other classes of bridging ligand, and the oligonucleotide-specific breakdown illustrated in Figure 3.2 suggests that this greater affinity is uniform across all types of oligonucleotides.

While the "stepped-parallel" and "linear" classes were represented by a single bridging ligand each in this assay, the "angular" class is comprised of three ligands (HAT, ppz and 2,3-dpp) that vary to some extent in their apparent individual affinities. Of these angular ligands it was the ppz-bridged complexes that induced the greatest decrease in fluorescence, followed by 2,3-dpp-bridged and HAT-bridged species (see Figure 3.3). The observed disparity between the effects of the ppz- and HAT-bridged complexes is noteworthy because these two ligands (and complexes based upon them) are structurally identical with the exception of a third, vacant chelation site in the HAT ligand. NMR experiments also suggest differential binding modes and/or affinities between ppz- and HAT-bridged complexes (see Chapter 4), however the reason for this remains uncertain. It should be cautioned that the average relative affinity of the 2,3-dpp-bridged species may be exaggerated due to the absence of FID data relating to the enantiomers of 2,3-dpp complexes – significant enantioselectivity in the binding of 2,3-dpp-bridged species could very well negatively impact the average induced fluorescence decrease of those complexes.

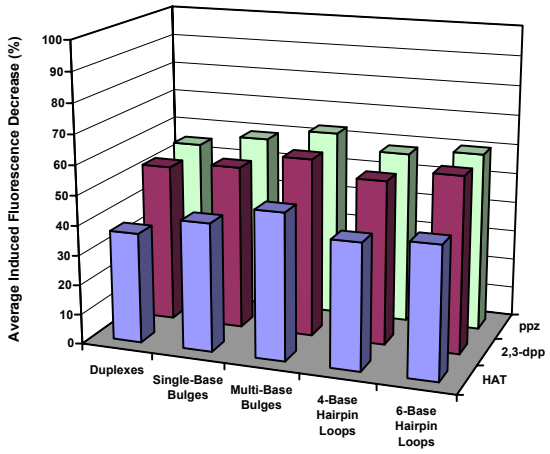


***Figure 3.3***
**Differences in the relative binding affinities of the "angular" class of bridging ligand.** Reported here are the average decreases in EthBr fluorescence induced by each specific type of "angular" bridging ligand (HAT, 2,3-dpp and ppz) for each general type of oligonucleotide. The averages incorporate the FID data for all complexes (ΔΛ, ΔΔ and ΛΛ stereoisomers, and bpy, $Me_2$bpy, phen, $Me_2$phen terminal ligands), where available.

It is unlikely that the enhanced affinity exhibited by the "angular" class of bridging ligand is due solely to direct, favourable interactions between the bridging moiety and the nucleic acid

target. In both HAT- and ppz-bridged dinuclear complexes one end of the planar polyaromatic bridging ligand is relatively exposed, providing what appears to be an ideal moiety to insert into a nucleic acid groove; however, complexes based on the 2,3-dpp bridge bind with a similar affinity to those based on HAT and ppz, yet it lacks the extended aromaticity and planarity of the multi-azatriphenylene ligands. Instead, the similar FID results complexes based on these ligands is most likely attributable to their commonality of shape – they share an "angular" orientation between chelation sites that results in a terminal ligand configuration which, presumably, complements the minor groove of nucleic acids more efficiently than do the "linear" and "stepped-parallel"-type ligands. This complementarity, most evident in the *meso* diastereoisomers of each complex (see the following Section), is made apparent in molecular modelling experiments (based on NMR data) described in Chapter 4.

#### *3.3.2.3 Stereoisomers*

From the FID data it is clear that, of the three stereoisomers (ΔΛ, ΔΔ and ΛΛ) of the metal complexes used in these studies, it was most often the *meso* diastereoisomers that induced the greatest decrease in EthBr fluorescence upon addition to an oligonucleotide. This observation is applicable across all terminal ligands, bridging ligands and oligonucleotides, however the disparity in binding affinity between the *meso* form and either enantiomer is most pronounced amongst the angular-bridged complexes. The relative affinity of the two enantiomers for a given oligonucleotide is considerably less consistent, varying dramatically with the nature of the bridging and terminal ligands as well as the identity of the oligonucleotide to which the complexes are binding. Surprisingly, the ΛΛ enantiomer often induced a greater decrease in fluorescence than did the ΔΔ enantiomer, an observation that is relatively rare in dinuclear species[98, 99] and at odds with the usual preference for the Δ enantiomer of mononuclear complexes.[22, 25, 92, 100] The degree of enantioselectivity is relatively low in complexes possessing bpy or $Me_2$bpy terminal ligands, but is significantly magnified in the analogous complexes with phen or $Me_2$phen ligands, and upon associating with oligonucleotides having less open and/or flexible binding sites (i.e. canonical duplexes). This observation might be attributed to an exaggeration of the detrimental steric interactions between the less-favoured enantiomer and groove walls of the oligonucleotide at the preferred binding site. The increased bulk of the phen-based ligands and the less-accommodating grooves of duplex sequences are both likely to

promote such an effect. Figure 3.4 illustrates this phenomenon for bpm- and HAT-bridged complexes binding to the least- and most-accommodating oligonucleotides {the bulge control duplex (**6**) and AATAA bulge sequence (**14**), respectively}. Figure 3.4(a) shows very little stereoselectivity amongst bpm-bridged complexes with bpy-based terminal ligands (left-hand cluster of columns), but the inclusion of phen-based ligands (right-hand cluster) results in a pronounced disparity (a difference of 19%) between the relative binding affinities of the ΔΔ and ΛΛ isomers. Figure 3.4(b) illustrates the same effect for HAT-bridged ligands; note the increased enantioselectivity when binding to the bulge control sequence relative to that seen when binding to the AATAA bulge (particularly with phen-based terminal ligands – a 15% difference between enantiomers upon binding to the bulge control sequence, no difference between enantiomers upon binding to the AATAA bulge).

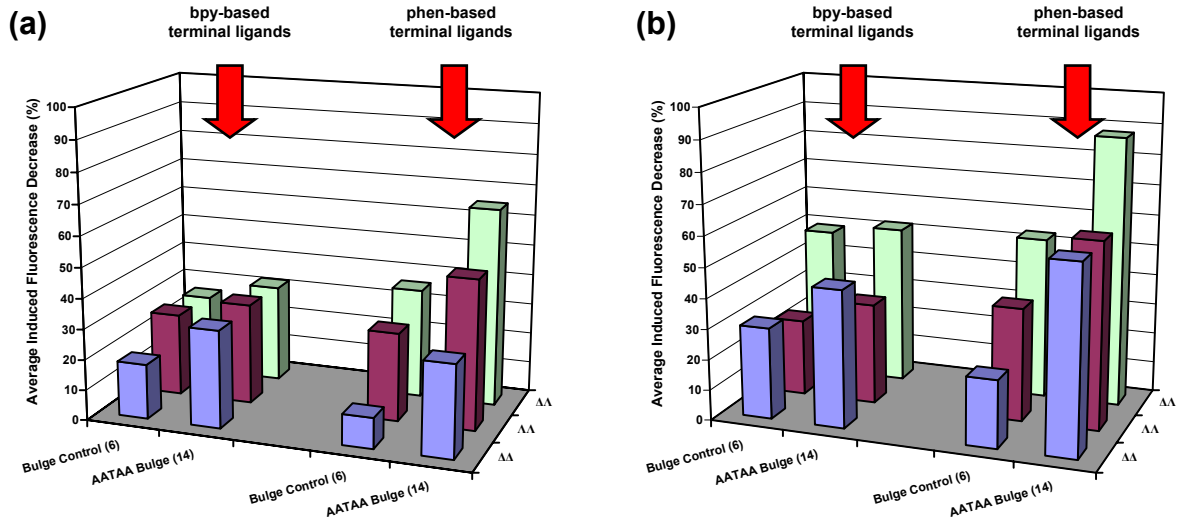


***Figure 3.4***
**Differences in the relative binding affinities of stereoisomers.** Reported here are the average decreases in EthBr fluorescence induced by the addition of the ΔΛ, ΔΔ and ΛΛ stereoisomers of dinuclear metal complexes to oligonucleotides **6** and **14**. FID data is divided into those results obtained from complexes with bpy-based ligands (left-hand side grouping; bpy or $Me_2$bpy) and those with phen-based ligands (right-hand side grouping; phen or $Me_2$phen). Chart **(a)** refers to bpm-bridged dinuclear complexes; chart **(b)** refers to HAT-bridged dinuclear complexes.

Generally, the FID data imply that enantioselectivity is much less evident in the nucleic acid binding of bpm-bridged complexes than it is in HAT-bridged ligands. Intriguingly, ppz-

bridged species demonstrate negligible enantioselectivity overall,[†] which is very surprising given the essentially identical structures of analogous ppz- and HAT-bridged complexes. Similarly, 2,5-dpp-bridged complexes were found to possess very little enantioselectivity on average (although only those complexes with bpy-based ligands were investigated), while little inference can be made about 2,3-dpp-bridged species given the difficulty in obtaining enantiomerically pure samples.

#### *3.3.2.4 Oligonucleotides*

Figure 3.5 illustrates the average decrease in fluorescence in a given oligonucleotide as induced by *all* of the dinuclear metal complexes used in the FID assay. While averaging out the data in this manner results in a relatively uniform affinity across all oligonucleotides, the maxima and minima in this chart (which differ by only 16%) *are* representative of those oligonucleotides that partake in the strongest and weakest associations, respectively, with individual metal complexes. Indeed, based on prior NMR experiments it was proposed that rigid dinuclear ruthenium complexes of the type being considered here would preferentially bind oligonucleotides with more open and/or flexible binding sites. This is exactly what is suggested by the results of the FID survey: the largest decreases in fluorescence were induced in oligonucleotides **13** and **14** (large, 5-base bulges), with other notably large decreases in oligonucleotides **20**-**22** (6-base hairpin loop sequences) and **7**-**12** (single- and multi-base bulge sites). Each of these oligonucleotides possesses non-canonical features (bulges or loops) that potentially increase groove flexibility and/or stand out as more accommodating binding sites. The lowest fluorescence decreases were generally observed amongst the canonical duplex sequences (oligonucleotides **2**-**6**), which conceivably possess less flexible (and therefore, less accommodating) minor grooves in which metal complexes would conceivably bind. Oligonucleotides **1**, **17** and **19** stand out as notable exceptions to this trend – **1**, a duplex consisting of alternating AT-pairs, demonstrates a relatively high affinity for a canonical double-stranded oligonucleotide, while **17** and **19** are both 6-base hairpin loop sequences that demonstrate a comparatively low overall affinity for the metal complexes being investigated in these studies. The remarkable general affinity for the AT sequence may most likely be

[†] This is not to say that enantioselectivity was not observed in specific complex-oligonucleotide interactions, just that the average effect across *all* terminal ligands/oligonucleotides was not very distinct.

attributed to the enhanced electronegativity and flexibility inherent in the minor groove of AT-rich sequences,[101-104] thus making the minor groove of oligonucleotide **1** both more attractive and more accommodating. An explanation for the uncharacteristically low affinity for oligonucleotides **17** and **19** remains elusive. On the basis of NMR evidence (see Chapter 4) it is assumed that rigid dinuclear polypyridylruthenium(II) complexes bind to hairpin loop sequence at the stem-loop interface on the minor groove-side of the oligonucleotide. Given that the nucleobases C and T have a near-identical profile in the minor groove of DNA, oligonucleotide **17**, featuring a CTCTCT loop, should conceivably present a binding target that is not dissimilar to oligonucleotides **20** and **22**, which feature identical stems and CCCCCC and TTTTTT loops, respectively. Similarly, oligonucleotide **19**, which possesses an AAAAAA loop, demonstrated a weaker average association with the metal complexes than did the analogous sequence with a GGGGGG loop (oligonucleotide **21**). This is somewhat counter-intuitive: one would expect the adenine loop to be more accommodating than the guanine loop because the latter structure has amino groups projecting into the minor groove where they would potentially serve as steric impediments to strong metal complex associations. The reason for the unusually low affinities towards these particular stem-loop oligonucleotides is unknown; however the overall average affinity for these sequences is biased towards lower values due to the especially poor affinities exhibited by the "linear" and "stepped-parallel"-bridged complexes towards oligonucleotides **17** and **19**. This observation alone is however insufficient to explain the phenomenon because the affinity of the "angular"-bridged complexes for these same sequences is also relatively low (see Figure 3.6).

Figure 3.6 demonstrates that the average overall oligonucleotide affinities seen in Figure 3.5 are reflected in the trends of individual bridging ligand classes. It is evident from these data that inert dinuclear polypyridylruthenium(II) complexes exhibit a preference for non-duplex features over canonical double-stranded sequences. Furthermore, the affinity is generally greatest for larger single-stranded regions of oligonucleotide (specifically, the 5-base bulges and 6-base loops). This observation can possibly be attributed to the relatively large size of these complexes; the comparatively small binding site of the minor groove of canonical duplex DNA yielded relatively low fluorescence decreases, implying a low binding affinity. The prominent exception to these results was a significant affinity for the AT sequence (oligonucleotide **1**) by the "angular"- and "stepped-parallel"-bridged complexes. These trends also extend to individual complexes – several interactions that are representative of the

extremes of the trend (i.e. specific complexes exhibiting particularly high or low affinities) are discussed in the following Section.

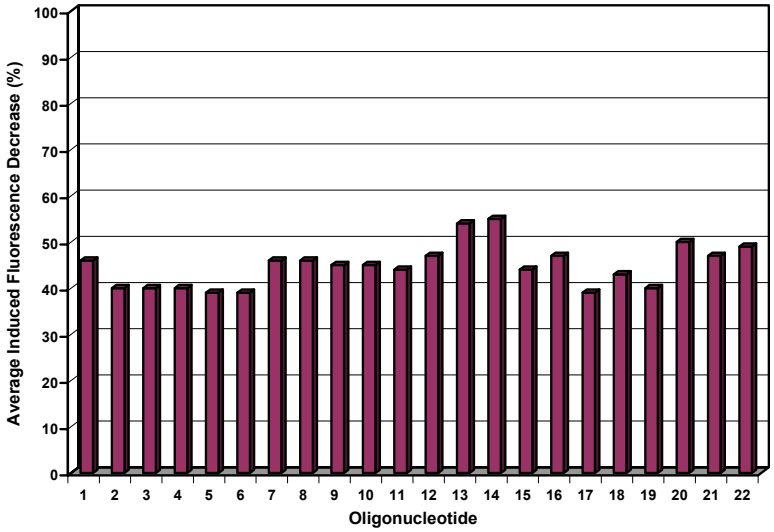


***Figure 3.5***
**The relative binding affinities of *all* dinuclear polypyridylruthenium(II) complexes by oligonucletoide.** This chart shows the average fluorescence decreases for oligonucleotides **1-22** as induced by all complexes (stereoisomers/terminal ligands/bridging ligands) used in the FID assay. The results relating to oligonucleotides **23-25** are not depicted here as they were tested only with as small subset of complexes.

Due to limitations on the quantities of metal complex and oligonucleotide available at the time of FID assay, the quadruplex-forming oligonucleotides **23-25** were only examined against a selection of HAT- and ppz-bridged complexes with phen-based ligands. The results indicate a moderate affinity by these complexes for the quadruplexes (average fluorescence decreases on the order of *ca.* 60-65%), however such results were relatively underwhelming in comparison to the affect of the same complexes on more favourable oligonucleotides such as the larger bulges and hairpin loops (average fluorescence decreases of *ca.* 80-90%). Consequently, quadruplexes are assumed to be poor targets for the genre of bulky metal complex used in these studies; indeed, the most promising quadruplex-binding molecules have been found to be large planar macrocyclic structures that bind externally to the quadruplex.[105-109]

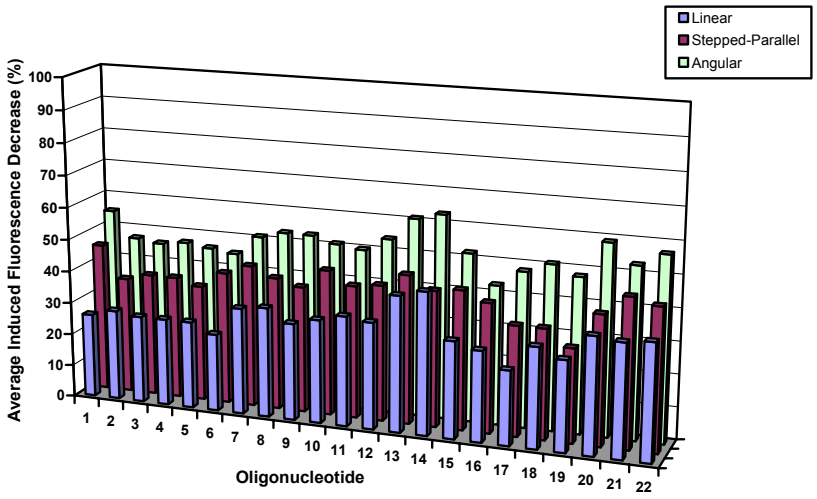


***Figure 3.6***
**The relative binding affinities of each bridging ligand class by oligonucleotide.** This chart shows the average fluorescence decreases for oligonucleotides **1-22** as induced by all complexes of each bridging ligand class used in the FID assay. The results relating to oligonucleotides **23-25** are not depicted here as they were tested only with as small subset of complexes.

### *3.3.2.5 Notable Specific Interactions*

As previously alluded to, the *meso* diastereoisomers of complexes featuring an "angular" bridging ligand and $Me_2$phen terminal ligands exhibited the greatest overall affinity for the oligonucleotides used in these studies. *Meso*-$[\{Ru(Me_2phen)_2\}_2(\mu\text{-HAT})]^{4+}$ appeared to be the strongest-binding complex overall as it induced fluorescence decrease of approximately 85-90% in most DNA sequences. The analogous ppz-bridged complex demonstrated a similarly uniform high affinity across those sequences possessing non-duplex features, as well as the AT-rich duplex oligonucleotides **1** and **2**.

Both *meso*-$[\{Ru(phen)_2\}_2(\mu\text{-HAT})]^{4+}$ and *meso*-$[\{Ru(phen)_2\}_2(\mu\text{-ppz})]^{4+}$ demonstrated a greater selectivity between oligonucleotides than did the corresponding complexes with $Me_2$phen terminal ligands, albeit at the cost of binding affinity. For example, *meso*-$[\{Ru(Me_2phen)_2\}_2(\mu\text{-HAT})]^{4+}$ induced fluorescence decreases of 88, 87 and 91% for oligonucleotides **1**, **15** and **17**, respectively, while *meso*-$[\{Ru(phen)_2\}_2(\mu\text{-HAT})]^{4+}$ affected a decrease of 69% in oligonucleotide **17**, but only 50 and 54% for oligonucleotides **1** and **15**. *meso*-$[\{Ru(phen)_2\}_2(\mu\text{-ppz})]^{4+}$ induced large fluorescence decreases in the 5-base bulge sequences (88 and 89% for oligonucleotides **13** and **14**, respectively) and several hairpin sequences (83, 83 and 82% for oligonucleotides **16**, **20** and **22**, respectively), but it also demonstrated a particularly high affinity

for the standard AT duplex (oligonucleotide **1**, 83% fluorescence decrease). It is interesting to note that amongst the bpm-bridged complexes those with phen terminal ligands exhibit a higher overall affinity than do those with $Me_2$phen ligands – the interaction between the stereoisomers of $[\{Ru(phen)_2\}_2(\mu\text{-bpm})]^{4+}$ and oligonucleotide **7**, an interaction that appeared to be significantly stronger than those involving any of the other single-base bulge sequences, have been examined in detail using NMR experiments, the results of which have been previously published.[110] FID data pertaining to each individual metal complex-oligonucleotide interaction may be found in Appendix D.

### 3.3.3 Discrepancies in the FID Assay

It has been found that the results of these FID assays were generally consistent with the binding affinities and stereoselectivities observed using other techniques such as NMR, affinity chromatography and equilibrium dialysis. However, there were a small number of instances in which the affinities implied by FID data were not in agreement with other experimental results. Three notable cases are summarised in Table 3.2.

***Table 3.2***
Comparison of the DNA-binding stereoselectivities of interactions between dinuclear ruthenium complexes and the bulge-containing oligonucleotide d(CCG**A**GAATTCCGG)$_2$ as observed using different techniques.

| Complex | NMR | Dialysis | Chromatography[a] | FID Assay[b] | DAPI Assay[c] |
|---|---|---|---|---|---|
| $[\{Ru(Me_2bpy)_2\}_2(\mu\text{-bpm})]^{4+}$ | $\Delta\Delta > \Lambda\Lambda$[111] | – | $\Delta\Delta > \Lambda\Lambda$ | $\Delta\Delta \approx \Lambda\Lambda$ | $\Delta\Delta > \Lambda\Lambda$ |
| $[\{Ru(phen)_2\}_2(\mu\text{-dppm})]^{4+}$ | – | – | $\Delta\Delta >$ *meso* | $\Delta\Delta \approx$ *meso*[112] | $\Delta\Delta >$ *meso* |
| $[\{Ru(phen)_2\}_2(\mu\text{-bb7})]^{4+}$ | – | $\Delta\Delta > \Lambda\Lambda$[113] | $\Delta\Delta > \Lambda\Lambda$ | $\Lambda\Lambda > \Delta\Delta$ | $\Delta\Delta > \Lambda\Lambda$ |

[a] Affinity chromatography experiments as described in Chapter 5.
[b] FID assays, employing either EthBr or TO as the fluorescent dye.
[c] Modified FID assay incorporating DAPI as the fluorescent dye.

The first and most notable inconsistency encountered in the FID assay was in the results pertaining to the binding of the enantiomers of the complex $[\{Ru(Me_2bpy)_2\}_2(\mu\text{-bpm})]^{4+}$ to the tridecanucleotide featuring an adenine bulge site {number **7**, d(CCG**A**GAATTCCGG)$_2$}. In the FID assay both the $\Delta\Delta$ and $\Lambda\Lambda$ enantiomers induced a fluorescence decrease of 29% in the bound EthBr, implying that the two enantiomers possess identical binding affinities {see Figure 3.7(a)}. This contradicts the findings of NMR studies in which the stereoisomers of this

complex were found to exhibit total enantioselectivity (ΔΔ > ΔΛ > ΛΛ, with regards to affinity and selectivity) for this same oligonucleotide.[96, 111] These NMR results were supported by DNA-affinity chromatography experiments in which ΔΔ-[{Ru($Me_2$bpy)$_2$}$_2$($\mu$-bpm)]$^{4+}$ was found to have a significantly higher affinity for a column coated in oligonucleotide **7** than did the analogous ΛΛ enantiomer (see Chapter 5), thus confirming the discrepancy in the FID results.

A second significant anomaly in the FID results was in the binding of *meso*- and ΔΔ-[{Ru(phen)$_2$}$_2$($\mu$-dppm)]$^{4+}$ to the same bulge oligonucleotide (**7**). The FID assay implied no discernable difference in binding affinity between the diastereoisomers, both causing a 52% reduction in fluorescence {see Figure 3.7(b)}.[112] This was in sharp contrast to DNA-affinity chromatography experiments in which the *meso* isomer eluted from the column before the ΔΔ enantiomer (refer to Chapter 5 for further details), reflecting the relative binding affinities of these diastereoisomers with oligonucleotide **7** (ΔΔ > ΔΛ).

The third discrepancy evident in the FID results related to the binding of the enantiomers of [{Ru(phen)$_2$}$_2$($\mu$-bb7)]$^{4+}$ to oligonucleotide **7**. FID data indicated that the ΛΛ enantiomer was possessed of the higher binding affinity, causing a 66% reduction in fluorescence compared to the 46% decrease induced by the ΔΔ form {see Figure 3(c)}. Once again, these results were at odds with DNA-affinity chromatography elution orders (see Chapter 5), and equilibrium dialysis experiments, both of which implied stronger/preferential binding by the ΔΔ enantiomer.

As cautioned by Boger *et al.*,[79] the FID assay is at best a semiquantitative technique. The mechanism by which the minor groove-binding metal complexes used in these studies are able to induce a decrease in the fluorescence of intercalated dyes (EthBr or TO) is uncertain. A direct competition between dye and complex might be envisioned in which both potential binding agents exhibit an affinity for the same binding site – while a direct expulsion of the dye by the complex is unlikely, the resultant dynamic equilibria and concentration differences may effectively exclude the dye from the binding site. Alternatively, an indirect displacement of the DNA-bound dye could be contributing to the decrease in fluorescence of the system. It is likely that binding of the metal complex induces structural changes in the oligonucleotide which may alter the binding affinity of the dye. Such a mechanism could effectively exclude the fluorescent dye from regions of the oligonucleotide other than the immediate binding site of the complex.

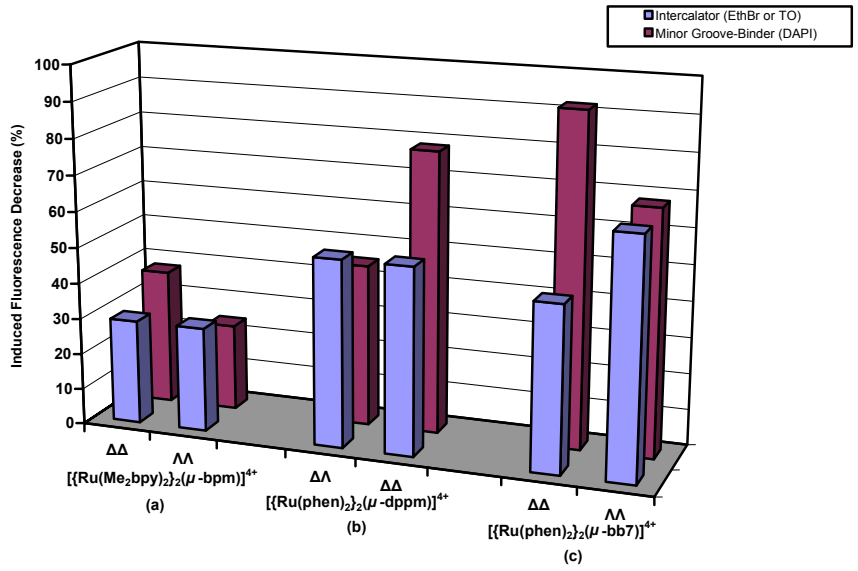


***Figure 3.7***
**Comparison of fluorescent DNA-binding dye displacement assays.** Fluorescence decreases induced in dye-bound oligonucleotide **7** by stereoisomers of **(a)** $[\{Ru(Me_2bpy)_2\}_2(\mu\text{-bpm})]^{4+}$, **(b)** $[\{Ru(phen)_2\}_2(\mu\text{-dppm})]^{4+}$ and **(c)** $[\{Ru(phen)_2\}_2(\mu\text{-bb7})]^{4+}$. The affect of each complex on the intercalating dye {EthBr for **(a)** and **(b)**, TO for **(c)**} is depicted in blue, the affect on the minor groove-binding dye (DAPI) in maroon.

If the complexes being assayed were targeting the same binding site, and the dye being used bound to each binding site with the same affinity, then comparisons between the fluorescence decreases induced by each complex could be used to make quantitative inferences regarding the binding affinities of each complex. Unfortunately, the reality of the situation is considerably more complicated as metal complexes (and their stereoisomers) and dyes do indeed vary in their affinity for different binding sites on a given oligonucleotide. For example, in the NMR experiments demonstrating the enantioselectivity of $[\{Ru(Me_2bpy)_2\}_2(\mu\text{-bpm})]^{4+}$ in its binding to oligonucleotide **7**, the ΔΔ enantiomer bound specifically to the bulge site while the ΛΛ form exhibited a significantly lower affinity and selectivity, binding weakly to the AT-rich centre of the oligonucleotide as well as the frayed ends.[96, 111] It has been reported that EthBr binds to bulge sites with a greater affinity than regular duplex DNA,[114] a fact which may have contributed to anomalous identical FID results for ΔΔ- and ΛΛ-$[\{Ru(Me_2bpy)_2\}_2(\mu\text{-bpm})]^{4+}$: the more readily "displaced" dye at the favoured binding sites of the ΛΛ form may compensate for its relatively poor binding affinity, thus inducing a fluorescence increase that appears identical to that of the stronger-binding ΔΔ enantiomer (which has to contend with a more strongly-bound dye at the bulge site).

The relationship between the binding affinities of such metal complexes and the extent to which they induce a fluorescence decrease in the DNA-bound dye is further complicated by the different binding *modes* adopted by the complex and the dye: the genre of rigid dinuclear polypyridylruthenium(II) complexes studied here are known to be minor groove-binders, whereas the dyes used in the FID assay – EthBr or TO – are both intercalators. This dichotomy concerns not only the physical manner by which the complexes/dyes interact with DNA, but also the preferred binding sites of each (minor groove-binders favour AT-rich sequences whereas intercalators tend to preferentially bind GC-rich sequences). Thus, the use of an intercalating agent as the fluorescent dye in the assay introduces another level of obfuscation to the possible "displacement" mechanism, possibly contributing to the anomalous results obtained detailed above. For this reason it was decided to modify the FID assay; we hypothesised that a more efficient and accurate assay could be attained through the use of a fluorescent minor groove-binding dye, rather than the intercalators of the conventional FID.

### 3.3.4 Modification of the FID Assay to Use DAPI

The minor groove-binding dye selected for the modified FID assay was 4′,6-diamidino-2-phenylindole (DAPI). DAPI undergoes a relatively modest (i.e. 20-fold) increase in fluorescence upon binding to DNA, but like other such minor groove-binding dyes it has a considerable selectivity for double-stranded rather than single-stranded DNA and does not cause elongation of the duplex upon binding (in contrast to intercalators such as EthBr).[115] The ability of DAPI to pass through an intact cell membrane has enabled its widespread application as a marker fluorescent DNA stain, particularly in microscopy experiments.[116] In the present context, the excitation and emission maxima of the dye are distinct from those of EthBr, a feature which is advantageous when dealing with ruthenium complexes that have competing emissions with EthBr (specifically, mononuclear species or dinuclear complexes with a sufficiently flexible bridging ligand such as bb7).[90] These spectroscopic properties, in addition to the minor groove-binding nature of the dye, have been exploited in several studies intended to identify the site of interaction – major or minor groove – of DNA-binding polypyridylruthenium(II) complexes.[117-120]

As a means of assessing the utility of the modified technique we used it to assay those systems that yielded anomalous results using the conventional FID method (as detailed in Table

3.2 and the previous section). It was found that the DAPI-based assay did indeed reflect the stereoselectivities observed using alternative techniques, thereby improving on the original FID assay. Using DAPI the ΔΔ and ΛΛ enantiomers of $[\{Ru(Me_2bpy)_2\}_2(\mu\text{-bpm})]^{4+}$ were found to induce fluorescence decreases that differed by 15% {see Figure 3.7(a)}, with the greater decrease being caused by the ΔΔ form, suggesting stronger binding by this isomer. Likewise, ΔΔ-/ΔΛ-$[\{Ru(phen)_2\}_2(\mu\text{-dppm})]^{4+}$ differed by 33% {ΔΔ inducing the greater decrease; see Figure 3.7(b)} and ΔΔ-/ΛΛ-$[\{Ru(phen)_2\}_2(\mu\text{-bb7})]^{4+}$ differed by 24%, also favouring the ΔΔ enantiomer {the opposite of the selectivity implied by the FID assay; see Figure 3.7(c)}. Wider application of the technique was also successful, with the general trends in oligonucleotide selectivity and affinity mirroring those seen in the FID assay.

Despite the successes of the DAPI-modified fluorescent dye displacement technique, the mechanism of the fluorescence decrease remains ambiguous. It has been noted that DNA-mediated resonance energy transfer from DAPI to a DNA-bound polypyridylruthenium(II) complex can result in an efficient quenching of fluorescence that is related to binding geometry rather than any real "displacement" of the dye.[118, 119] However, such a mechanism is dependent upon the metal complex being an intercalator, while the complexes examined here are incapable of classical intercalation.[18] Furthermore, the degree of resonance energy transfer quenching, although dependent upon binding *geometry*, still largely correlates to the binding *affinity* of the complex. In any case, physical displacement of DAPI from DNA by the metal complexes used in these studies can be seen in CD titration experiments. For example, Figure 3.8 shows a decrease in the DAPI-induced CD peak of CT DNA upon the addition of increasing amounts of $[\{Ru(phen)_2\}_2(\mu\text{-ppz})]^{4+}$ implying displacement of the DAPI by the ruthenium complex.

The ambiguity of the mechanism of the decrease in fluorescence has hindered attempts to apply the phenomenon to a quantitative assessment of binding affinity. While titrations of DAPI-bound DNA with solutions of dinuclear polypyridylruthenium(II) complexes do induce fluorescence decreases that are proportional to the amount of ruthenium added, the fluorescence of the system eventually drops below the level of *free* DAPI. From this observation one might infer that extraneous ruthenium complex-DAPI interactions are occurring without the participation of the DNA, complicating interpretation of the results in terms of assigning binding constants. Titrations in the absence of DNA yield similarly anomalous results, as do experiments in which EthBr is substituted for DAPI. While ongoing collaborations between the

laboratories of Keene and J. Aldrich-Wright (University of Western Sydney) are intended to elucidate upon the specific equilibria involved, at present the multiple factors contributing to the fluorescence decrease of a DNA-bound dye upon the addition of a metal complex sufficiently complicate the situation to such an extent as to make any real quantitation of the results of these assays (FID or the DAPI-modified variant) problematic. Nevertheless, the assay does provide a high-throughput means by which to qualitatively assess and compare the relative binding affinities of numerous metal complexes for a variety of different oligonucleotides at a single concentration. The general trends in binding affinity observed via this technique are in general concordance with those suggested by other experimental methods and from the accumulated data a number of particularly compelling metal complex-oligonucleotide interactions have been selected and studied in greater detail.

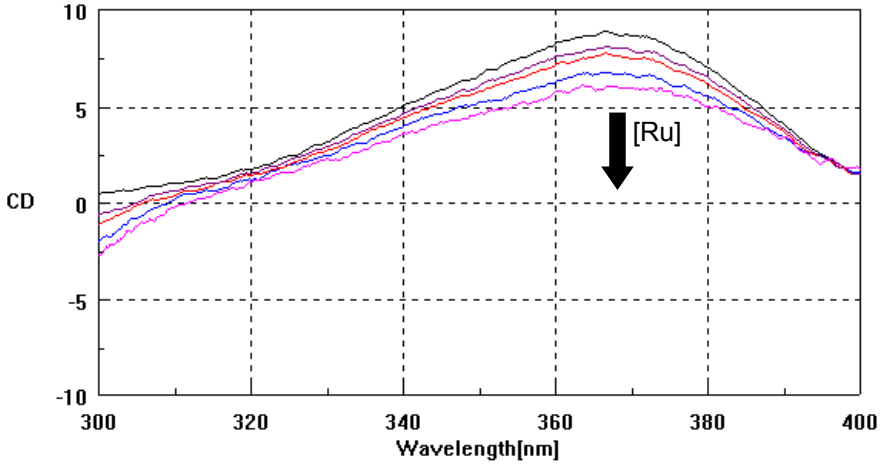


***Figure 3.8***
**Displacement of DAPI from calf thymus DNA by $[\{Ru(phen)_2\}_2(\mu\text{-ppz})]^{4+}$.** These spectra show the reduction in the magnitude of the DAPI-induced CD peak (*ca.* 365 nm) of calf thymus DNA upon increasing concentrations of ruthenium complex. DNA concentration is 50 μM (bp), DAPI concentration is 10 μM (i.e. 1 DAPI per 5 bp), and ruthenium complex concentration varies from 0-100 μM {i.e. varying from 0 (black line) to 2 (magenta line) Ru per bp}.

## 3.3.5 Quantitation of Binding Affinity by Absorption Spectroscopy

Interactions between metal complexes and nucleic acids are typically accompanied by perturbations to the spectral properties of the metal complex. The spectra of all of the metal complexes employed in the present studies exhibited hypochromism upon interaction with calf thymus DNA, with most MLCT bands decreasing in absorbance by 5-10% (see Appendix E for

these spectra). Complexes that interact predominantly on an electrostatic basis ($[Ru(bpy)_3]^{2+}$, for example) have been found to undergo negligible spectral perturbation upon association with DNA.[121, 122] Conversely, complexes possessing strong intercalating ligands often demonstrate a large degree of hypochromism (20-50% at similar [DNA]:[Ru] ratios).[23, 26, 69, 71, 99, 123, 124] This decrease in absorbance is believed to arise due to strong stacking interactions between aromatic ligands and DNA bases. Accordingly, the extent of the hypochromism induced in a particular complex is often related to the degree to which that complex intercalates with DNA: those complexes with large planar aromatic ligands more conducive to intercalation have typically demonstrated larger absorbance changes than those with smaller ligands.[42] For example, Barnard and Vagg report on the series of complexes *cis*-*α*-$[Ru(picenMe_2)L]^{2+}$ {$picenMe_2$ = 1,6-di(2′-pyridyl)-2,5-dimethyl-2,5-diazahexane; L = bpy, phen or dpq} binding to CT DNA in which they found that the degree of hypochromism exhibited was proportional to the aromatic surface area (and, therefore, intercalative ability) of the ligand L (bpy < phen < dpq).[69] Being intermediate in magnitude between electrostatic binders and intercalators, the hypochromism exhibited by the complexes studied herein is more consistent with a groove-binding association. Indeed, the 14% MLCT hypochromism observed in the complex $[Ru(NH_3)_2dppz]^{2+}$ upon binding to CT DNA[125] has been described as being at the threshold of intercalative/non-intercalative binding[121] – although those measurements were performed at a significantly smaller [DNA]:[Ru] ratio than the present experiments. Nevertheless, several of the present complexes did demonstrate particularly large levels of hypochromism upon titration with ctDNA, most notably the ppz-bridged complexes with phen-based ligands that demonstrated a particularly high affinity for DNA in the fluorescence assays. In the most impressive example, ΔΛ-$[\{Ru(Me_2phen)_2\}(\mu\text{-ppz})]^{4+}$ exhibited absorbance decreases of 25%, 14% and 15% at 261, 412 and 593 nm, respectively (see Figure E.1.13, Appendix E). While classical intercalative binding is ruled out for these complexes (a conclusion of the NMR/modelling experiments discussed in Chapter 4), relatively large levels of hypochromism such as this could be indicative of a semi-intercalative binding mode. It has been demonstrated that the ligand via which a metal complex interacts with DNA can be identified by a disproportionately large hypochromism associated with the intraligand transition band of that ligand,[70, 71] however such peaks were typically difficult to resolve in the present spectra and so no inferences of this nature are made.

As with the induced hypochromism described above, bathochromic shifts in the absorption bands of metal complex spectra are also taken to be indicative of the degree to which the complex interacts with DNA – specifically, the extent to which it intercalates. Commonly, strong intercalators such as $[Ru(bpy)_2(phi)]^{2+}$,[42] *cis*-$\alpha$-$[Ru(picenMe_2)(dpq)]^{2+}$ [69] and $[\{Ru(bpy)_2\}_2(\mu\text{-bdptb})]^{4+}$ [99] {bdptb = 2,2′-bis(5,6-diphenyl-1,2,4-triazin-3-yl)-4,4′-bipyridine} have previously been shown to undergo large MLCT band red shifts (*ca.* 10-20 nm) upon binding to CT DNA, while once again the spectra of electrostatic binders remain relatively unperturbed.[121, 122] However, other complexes also known to bind strongly via intercalation undergo only moderate bathochromic shifts – $[Ru(phen)_2(dppz)]^{2+}$, for instance, undergoes a red shift of only 3 nm in its 437 nm MLCT band upon binding to CT DNA.[122] The dinuclear polypyridylrutheium(II) complexes used in the present studies generally underwent small-to-negligible changes in MLCT band wavelengths that encompassed both bathochromic and *hypsochromic* shifts. While not without precedent, the blue shift of MLCT spectral features upon binding to CT DNA (coupled with the relatively small magnitude of these shifts) implies a non-intercalative binding mode consistent with the minor groove-binding nature of these complexes. Even so, there were several complexes for which significant bathochromic shifts were noted, and these instances were typically in concordance with those complexes that also exhibited larger levels of hypochromism. Once again, the most notable case was found to be the spectrum of ΔΛ-$[\{Ru(Me_2phen)_2\}(\mu\text{-ppz})]^{4+}$ in which a red shift of 10 nm was observed in the MLCT band at 593 nm. Since this peak relates to metal-to-*bridging* ligand charge transfer, and given that the metal-to-*terminal* ligand charge transfer band does not undergo a wavelength shift, one might infer the bridging ligand of this complex plays a particularly significant role in its interaction with DNA.

By monitoring the hypochromism of the more intense MLCT band (specifically, the metal-to-*terminal* ligand band) of each complex as a function of CT DNA added, it was possible to calculate the intrinsic binding affinity of several complexes through the application of Equation 3.1 (results collected in Table 3.3). The plots from which the binding constants were derived may be found with the associated metal complex spectra in Appendix E. Overall, the trends observed in the binding constants obtained using this technique are in reasonable agreement with the relative binding affinities implied by the fluorescent dye-displacement techniques. While these absorption titration experiments were undertaken using CT DNA (a generic canonical duplex polymer consisting of approximately 42% GC base pairs, 48% AT base pairs),

the results correlate particularly well to the affinities obtained from fluorescence assays containing analogous mixed-sequence duplexes (i.e. oligonucleotides **5** and **6**). As with the fluorescence assays, the binding affinities of series of complexes possessing the same bridging ligand largely correlates to the hydrophobicity of their terminal ligands, such that bpy < $Me_2$bpy < phen < $Me_2$phen with regards to intrinsic binding constants. This is illustrated in Figure 3.9 by a comparison of the relative binding affinities of a series of ppz-bridged complexes as inferred from absorption titration and FID experiments; the chart confirms that the relative orders of affinity obtained from the two different techniques are in agreement with one another. Furthermore, the enhanced affinity of those complexes possessed of an "angular"-type bridging ligand relative to those with a "linear"-type ligand (i.e. bpm) is also evident, as is the greater affinity of the *meso* diastereoisomers of each complex in most instances. Those complexes with "stepped-parallel" (2,5-dpp) bridging ligands exhibited somewhat anomalous results in that they demonstrated binding affinities well in excess of those implied by the results of the FID assays. It is noteworthy that *meso*-$[\{Ru(phen)_2\}_2(\mu\text{-}2,5\text{-dpp})]^{4+}$ – a complex not used in prior FID assays – exhibited some of the largest binding constants. While the DNA-interactions of this class of complex were not examined in any further detail in the present studies, these results suggest that "stepped-parallel"-type species may be of particular interest in future studies.

The binding constants exhibited by the complexes used in these studies varied in magnitude from mid-$10^4$ to low-$10^5$ $M^{-1}$ (see Table 3.3), placing them at a level of affinity an order of magnitude higher than $[Ru(phen)_3]^{2+}$ for CT DNA.[25, 45, 126, 127] This range is consistent with a groove-binding mode intermediate in affinity between an electrostatic interaction (e.g. $[Ru(bpy)_3]^{2+}$, $K_b < 10^3$ $M^{-1}$)[42, 128] and classical intercalation (e.g. $[Ru(phen)_2(dppz)]^{2+}$, $K_b \approx 10^6$ $M^{-1}$),[18, 45] and is of a similar magnitude to the affinities demonstrated by a number of other dinuclear species.[71, 98, 99] While binding constants of this magnitude imply a relatively unimpressive affinity for CT DNA, they are in accord with the thesis that rigid dinuclear polypyridylruthenium(II) complexes of this type preferentially bind to non-canonical DNA features that are more open and/or flexible; the generic CT DNA used here represents a particularly poor target for these complexes.

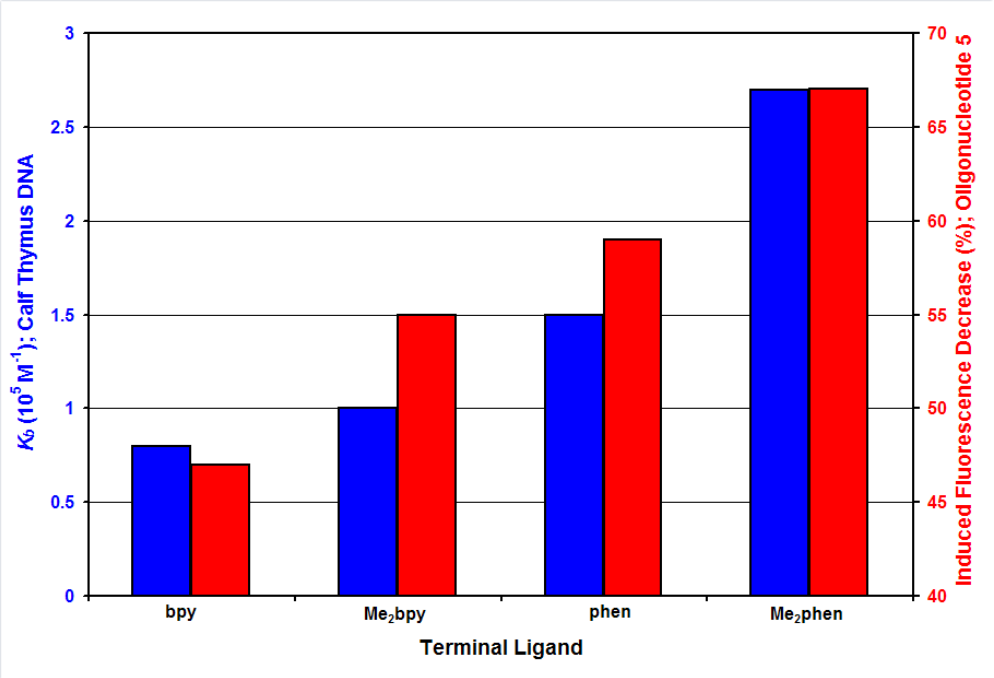


***Figure 3.9***
**The relative binding affinities of ppz-bridged complexes as established using different electronic spectroscopy techniques.** Electronic absorption titration experiments (blue bars) and fluorescent dye-displacement assays (red bars) yield comparable orders of affinity for a series of ppz-bridged complexes (*meso* diastereoisomers) with varying terminal ligands. Absorption data are reported as the intrinsic binding constant of each complex as it associates with calf thymus DNA; fluorescence data is reported as the extent to which the complex of interest induced a decrease in the fluorescence of ethidium bromide bound to oligonucleotide **5** (a canonical, mixed base sequence).

Titrations were also performed with several of the metal complexes and yeast tRNA (see Table 3.4 for results; spectra are collected in Appendix E) in order to compare and contrast binding between the two polynucleotides. As with the CT DNA titrations, all metal complexes demonstrated MLCT band hypochromism (typically 5-15%, slightly higher than seen with CT DNA) upon the addition of tRNA. Once again the largest spectral perturbations were experienced by those complexes with $Me_2$phen terminal ligands, with the MLCT band of ΔΛ-$[\{Ru(Me_2phen)_2\}_2(\mu\text{-ppz})]^{4+}$ having undergone a red-shift of some 10 nm (see Figure E.2.9, Appendix E). In contrast to the CT DNA titrations, the intrinsic binding constants determined from these perturbations (using Equation 3.1) did not demonstrate any notable trends. While tRNA binding constants were found to be of the same general magnitude as those of CT DNA, there were no clear correlation between those binding constants and the identity of terminal- or bridging-ligands. Additionally, stereoselectivity was generally negligible or the relative order of binding affinities of the stereoisomers varied dramatically between complexes. The only notable exception to these observations was in the selectivity of the 2,3-dpp-bridged complexes

in which the *meso* diastereoisomer invariably had a significantly higher affinity for tRNA than did the *rac* diastereoisomer.

***Table 3.3***
Spectral perturbations of dinuclear polypyridylruthenium(II) complexes (*ca.* 5 μM) upon titration with calf thymus DNA {*ca.* 50 μM (nt)}, and the associated intrinsic binding constants of each.

| | | Perturbations Upon Titration with ctDNA | | |
|---|---|---|---|---|
| **Complex** | **MLCT λ (nm)** | **Δλ (nm)** | **ΔA (%)** | **$K_b$ ($10^5$ $M^{-1}$)** |
| ΛΛ-[{Ru(bpy)$_2$}$_2$($\mu$-bpm)]$^{4+}$ | 410 | +1 | -4 | 0.8 |
| ΔΛ-[{Ru(Me$_2$bpy)$_2$}$_2$($\mu$-bpm)]$^{4+}$ | 413 | +1 | -6 | 0.8 |
| ΔΛ-[{Ru(phen)$_2$}$_2$($\mu$-bpm)]$^{4+}$ | 407 | -2 | -7 | 1.0 |
| ΔΛ-[{Ru(bpy)$_2$}$_2$($\mu$-HAT)]$^{4+}$ | 407 | +1 | -7 | 1.0 |
| ΔΔ-[{Ru(bpy)$_2$}$_2$($\mu$-HAT)]$^{4+}$ | 407 | 0 | -4 | 0.6 |
| ΔΛ-[{Ru(Me$_2$bpy)$_2$}$_2$($\mu$-HAT)]$^{4+}$ | 407 | 0 | -8 | 2.0 |
| ΔΔ-[{Ru(Me$_2$bpy)$_2$}$_2$($\mu$-HAT)]$^{4+}$ | 407 | 0 | -9 | 0.7 |
| ΔΛ-[{Ru(phen)$_2$}$_2$($\mu$-HAT)]$^{4+}$ | 404 | 0 | -4 | 1.9 |
| ΔΔ-[{Ru(phen)$_2$}$_2$($\mu$-HAT)]$^{4+}$ | 404 | 0 | -11 | 1.2 |
| ΔΛ-[{Ru(bpy)$_2$}$_2$($\mu$-ppz)]$^{4+}$ | 421 | +1 | -7 | 0.8 |
| ΔΛ-[{Ru(Me$_2$bpy)$_2$}$_2$($\mu$-ppz)]$^{4+}$ | 420 | 0 | -8 | 1.0 |
| ΔΛ-[{Ru(phen)$_2$}$_2$($\mu$-ppz)]$^{4+}$ | 419 | +4 | -10 | 1.5 |
| ΔΛ-[{Ru(Me$_2$phen)$_2$}$_2$($\mu$-ppz)]$^{4+}$ | 412 | 0 | -14 | 2.7 |
| ΔΔ-[{Ru(Me$_2$phen)$_2$}$_2$($\mu$-ppz)]$^{4+}$ | 412 | 0 | -11 | 1.2 |
| ΛΛ-[{Ru(Me$_2$phen)$_2$}$_2$($\mu$-ppz)]$^{4+}$ | 412 | 0 | -11 | 0.5 |
| *meso*-[{Ru(bpy)$_2$}$_2$($\mu$-2,3-dpp)]$^{4+}$ | 422 | +1 | -7 | 1.7 |
| *rac*-[{Ru(bpy)$_2$}$_2$($\mu$-2,3-dpp)]$^{4+}$ | 422 | 0 | -6 | 0.5 |
| *meso*-[{Ru(Me$_2$bpy)$_2$}$_2$($\mu$-2,3-dpp)]$^{4+}$ | 424 | -1 | -4 | 2.4 |
| *rac*-[{Ru(Me$_2$bpy)$_2$}$_2$($\mu$-2,3-dpp)]$^{4+}$ | 424 | 0 | -3 | 1.4 |
| *rac*-[{Ru(phen)$_2$}$_2$($\mu$-2,3-dpp)]$^{4+}$ | 422 | +1 | -8 | 0.8 |
| ΔΛ-[{Ru(bpy)$_2$}$_2$($\mu$-2,5-dpp)]$^{4+}$ | 431 | -1 | -4 | 0.5 |
| ΔΔ-[{Ru(Me$_2$bpy)$_2$}$_2$($\mu$-2,5-dpp)]$^{4+}$ | 432 | 0 | -7 | 1.3 |
| ΛΛ-[{Ru(Me$_2$bpy)$_2$}$_2$($\mu$-2,5-dpp)]$^{4+}$ | 432 | 0 | -5 | 0.4 |
| ΔΛ-[{Ru(phen)$_2$}$_2$($\mu$-2,5-dpp)]$^{4+}$ | 427 | +1 | -5 | 3.2 |

The structure of tRNA is considerably more complicated than that of CT DNA: tRNA consists of several large loops of unpaired bases interspersed between regions of double-helical base-paired RNA in an A-type conformation, all of which is folded into an intricate three-dimensional structure (refer to Figure 1.15 for an example). Based on the experimental evidence presented in this thesis it is evident that rigid dinuclear metal complexes possess a particular affinity for more open and/or flexible nucleic acid structures much like the loops of tRNA. Furthermore, the hydrophobic pockets and folds of the tertiary structure of tRNA represent additional potential binding sites for a polypyridyl metal complex. Conversely, the

narrower minor groove present in A-type structures may prove to adversely affect the binding affinity of these bulky complexes. Unfortunately, the lack of notable trends within the tRNA-binding affinities prohibits speculation into the extent to which these factors are influencing binding. While investigations into the RNA-binding behaviour of polypyridylruthenium(II) complexes have been relatively limited, a study by Xu *et al*. suggests that the very different structures of CT DNA and tRNA have significant effects on binding behaviour.[19] They report that the binding of a mononuclear intercalating complex to CT DNA is driven primarily by a large enthalpy decrease, while binding to tRNA is governed by a moderately favourable enthalpy decrease combined with a moderately favourable entropy increase. A recent NMR investigation involving the author has demonstrated that dinuclear groove-binding complexes do still interact with the minor groove of RNA, while retaining their enhanced affinity for more accommodating structures within duplex stretches of nucleic acid.[129] However, these experiments were conducted with short, synthetic duplexes devoid of tertiary structure; clearly further research is needed to elucidate the nature of the interactions between metal complexes and biologically-relevant RNAs.

***Table 3.4***
Spectral perturbations of dinuclear polypyridylruthenium(II) complexes (*ca*. 5 μM) upon titration with yeast tRNA {*ca.* 50 μM (nt)}, and the associated intrinsic binding constants of each.

| | | Perturbations Upon Titration with tRNA | | |
|---|---|---|---|---|
| **Complex** | **MLCT λ (nm)** | **Δλ (nm)** | **ΔA (%)** | **$K_b$ ($10^5$ $M^{-1}$)** |
| ΔΛ-[{Ru(phen)$_2$}$_2$($\mu$-HAT)]$^{4+}$ | 404 | 0 | -6 | 4.6 |
| ΔΔ-[{Ru(phen)$_2$}$_2$($\mu$-HAT)]$^{4+}$ | 404 | 0 | -6 | 0.5 |
| ΔΔ-[{Ru(Me$_2$phen)$_2$}$_2$($\mu$-HAT)]$^{4+}$ | 407 | +1 | -17 | 1.2 |
| ΛΛ-[{Ru(Me$_2$phen)$_2$}$_2$($\mu$-HAT)]$^{4+}$ | 407 | -4 | -15 | 0.8 |
| ΔΛ-[{Ru(Me$_2$bpy)$_2$}$_2$($\mu$-ppz)]$^{4+}$ | 420 | +1 | -12 | 1.4 |
| ΔΛ-[{Ru(phen)$_2$}$_2$($\mu$-ppz)]$^{4+}$ | 419 | +2 | -5 | 1.1 |
| ΔΔ-[{Ru(phen)$_2$}$_2$($\mu$-ppz)]$^{4+}$ | 419 | 0 | -1 | 2.3 |
| ΛΛ-[{Ru(phen)$_2$}$_2$($\mu$-ppz)]$^{4+}$ | 419 | 0 | -2 | 1.3 |
| ΔΛ-[{Ru(Me$_2$phen)$_2$}$_2$($\mu$-ppz)]$^{4+}$ | 412 | +10 | -14 | 1.4 |
| ΔΔ-[{Ru(Me$_2$phen)$_2$}$_2$($\mu$-ppz)]$^{4+}$ | 412 | +1 | -15 | 1.0 |
| ΛΛ-[{Ru(Me$_2$phen)$_2$}$_2$($\mu$-ppz)]$^{4+}$ | 412 | +2 | -10 | 1.3 |
| *meso*-[{Ru(bpy)$_2$}$_2$($\mu$-2,3-dpp)]$^{4+}$ | 422 | 0 | -7 | 2.5 |
| *rac*-[{Ru(bpy)$_2$}$_2$($\mu$-2,3-dpp)]$^{4+}$ | 422 | 0 | -8 | 0.1 |
| *meso*-[{Ru(Me$_2$bpy)$_2$}$_2$($\mu$-2,3-dpp)]$^{4+}$ | 424 | 0 | -7 | 1.1 |
| *rac*-[{Ru(Me$_2$bpy)$_2$}$_2$($\mu$-2,3-dpp)]$^{4+}$ | 424 | +1 | -6 | 0.5 |
| *meso*-[{Ru(phen)$_2$}$_2$($\mu$-2,3-dpp)]$^{4+}$ | 422 | +3 | -7 | 1.5 |
| ΔΛ-[{Ru(bpy)$_2$}$_2$($\mu$-2,5-dpp)]$^{4+}$ | 431 | -1 | -9 | 0.4 |
| ΔΔ-[{Ru(Me$_2$bpy)$_2$}$_2$($\mu$-2,5-dpp)]$^{4+}$ | 431 | 0 | -4 | 0.4 |

## 3.4 CONCLUSIONS

Overall, the FID assay has proven itself as an efficient and practical means by which to qualitatively assess the binding affinities and selectivities of a large library of metal complexes in the minimum amount of time. The technique is ideally suited to the identification of those specific interactions that would be most relevant to more comprehensive binding studies. While the relative orders of binding affinities implied by the fluorescent intercalator-based assay were generally quite consistent, there were several instances in which the assay conflicted with the results of alternative experiments. However, it was found that by utilising the minor groove-binder DAPI in place of the intercalative dye all inconsistencies were rectified; this has been attributed to the fact that DAPI and the metal complexes being assayed interact with DNA via the same binding mode. Attempts to obtain quantitative binding information via DAPI displacement/fluorescence decrease titrations proved to be fruitless due to extraneous complex-DAPI interactions.

The trends apparent in the results of the fluorescent dye displacement assays reaffirmed several of the traits observed in prior studies of mononuclear species. Of particular note was the relationship between the hydrophobicity of the terminal ligands and the binding affinity of the complex. Also evident in these studies was the previously-established predilection of bulky dinuclear ruthenium(II) complexes to preferentially bind to more open and/or flexible nucleic acid structures. The complexes uniformly bound to oligonucleotides featuring non-duplex structures (bulges, hairpins, etc.) with a greater affinity than they did to standard duplex sequences (the exception being several complexes that exhibiting an exceptionally high affinity for the AT sequence of oligonucleotide **1**). Complexes based upon the "angular" bridging ligand class demonstrated a greater overall affinity for the nucleotides, most likely attributable to the orientation of the terminal ligands in such species.

On the basis of prior studies into the stereoselective DNA-binding of mononuclear species and previous examples of enantioselectivity in dinuclear species (both of which imply preferential binding by the right-handed enantiomer, Δ or ΔΔ) it was somewhat surprising to see that the *meso* (ΔΛ) diastereoisomer was typically the strongest-binding. Intriguingly, the ΛΛ enantiomer often exhibited a greater affinity for the oligonucleotides than did the ΔΔ form.

The relative affinities observed in the fluorescent dye displacement assay were largely reflected in the binding constants ascertained using electronic absorption titrations. While these titrations were performed against generic, duplex calf thymus DNA, the relative trends in binding affinity are analogous to those of the fluorescence assay with respect to their relationship to the identity of bridging and terminal ligands as well as the stereochemistry of the complex. The parallels between the two techniques are particularly evident when comparing the absorption data with fluorescence assay results pertaining to that duplex sequence that most closely matches the mixed sequence of calf thymus DNA (oligonucleotide **5**).

Ultimately, it was the HAT- and ppz-bridged species (especially those with phen-based ligands) that demonstrated the greatest potential as DNA-binding agents, particularly against sequences with large non-duplex features. The interactions of these complexes with select oligonucleotides were examined in greater detail using NMR experiments, the results of which are reported in the following Chapter.

## 3.5 REFERENCES


1. M.-H. Hou, H. Robinson, Y.-G. Gao and A. H.-J. Wang, *Nucleic Acids Res.*, **2002**, *30*, 4910-4917.
2. N. Narayana, N. Shamala, K. N. Ganesh and M. A. Viswamitra, *Biochemistry*, **2006**, *45*, 1200-1211.
3. G. A. Leonard, T. W. Hambley, K. McAuley-Hecht, T. Brown and W. N. Hunter, *Acta Crystallogr. D: Biol. Crystallogr.*, **1993**, *49*, 458-467.
4. J. R. Quintana, A. A. Lipanov and R. E. Dickerson, *Biochemistry*, **1991**, *30*, 10294-10306.
5. M. L. Kopka, C. Yoon, D. Goodsell, P. Pjura and R. E. Dickerson, *Proc. Natl. Acad. Sci. USA*, **1985**, *82*, 1376-1380.
6. M. Coll, C. A. Frederick, A. H.-J. Wang and A. Rich, *Proc. Natl. Acad. Sci. USA*, **1987**, *84*, 8385-8389.
7. A. H.-J. Wang, G. J. Quigley and A. Rich, *Nucleic Acids Res.*, **1979**, *6*, 3879-3890.
8. C. L. Kielkopf, K. E. Erkkila, B. P. Hudson, K. Barton and D. C. Rees, *Nature Struct. Biol.*, **2000**, *7*, 117-121.
9. V. C. Pierre, J. T. Kaiser and J. K. Barton, *Proc. Natl. Acad. Sci. USA*, **2007**, *104*, 429-434.
10. J. L. Beck, M. L. Colgrave, S. F. Ralph and M. M. Sheil, *Mass Spectrom. Rev.*, **2001**, *20*, 61-87.
11. H. T. Chifotides, J. M. Koomen, M. Kang, S. E. Tichy, K. R. Dunbar and D. H. Russell, *Inorg. Chem.*, **2004**, *43*, 6177-6187.
12. M. B. L. Janik, A. Hegmans, E. Freisinger and B. Lipert, *J. Biol. Inorg. Chem.*, **1999**, *4*, 130-139.
13. N. Xu, L. Paša-Tolić, R. D. Smith, S. Ni and B. D. Thrall, *Anal. Biochem.*, **1999**, *272*, 26-33.
14. P. Iannitti-Tito, A. Weimann, G. Wickham and M. M. Sheil, *Analyst*, **2000**, *125*, 627-634.
15. J. L. Beck, R. Gupta, T. Urathamakul, N. L. Williamson, M. M. Sheil, J. R. Aldrich-Wright and S. F. Ralph, *Chem. Commun.*, **2003**, 626-627.
16. T. Urathamakul, J. L. Beck, M. M. Sheil, J. R. Aldrich-Wright and S. F. Ralph, *Dalton Trans.*, **2004**, 2683-2690.
17. K. X. Wan, T. Shibue and M. L. Gross, *J. Am. Chem. Soc.*, **2000**, *122*, 300-307.
18. I. Haq, P. Lincoln, D. C. Suh, B. Nordén, B. Z. Chowdhry and J. B. Chaires, *J. Am. Chem. Soc.*, **1995**, *117*, 4788-4796.
19. H. Xu, Y. Liang, P. Zhang, F. Du, B.-R. Zhou, J. Wu, J.-H. Liu, Z. Liu and L.-N. Ji, *J. Biol. Inorg. Chem.* , **2005**, *10*, 529-538.
20. H. Xu, J.-H. Liu, Z.-G. Liu, Y. Liang, P. Zhang, F. Du, B.-R. Zhou and L.-N. Ji, *Chinese J. Chem.*, **2005**, *23*, 659-661.
21. C. Rajput, R. Rutkaite, L. Swanson, I. Haq and J. A. Thomas, *Chem. Eur. J.*, **2006**, *12*, 4611-4619.
22. L.-N. Ji, X.-H. Zou and J.-G. Liu, *Coord. Chem. Rev.*, **2001**, *216-217*, 513-536.
23. H. Chao, Y. Yuan, F. Zhou and L. Ji, *Transit. Metal Chem.*, **2006**, *31*, 465-469.
24. P. U. Maheswari, V. Rajendiran, M. Palaniandavar, R. Parthasarathi and V. Subramanian, *J. Inorg. Biochem.*, **2006**, *100*, 3-17.

25. J. K. Barton, A. T. Danishefsky and J. M. Goldberg, *J. Am. Chem. Soc.*, **1984**, *106*, 2172-2176.
26. R. J. Morgan, S. Chatterjee, A. D. Baker and T. C. Strekas, *Inorg. Chem.*, **1991**, *30*, 2687-2692.
27. S. Shi, J. Liu, K. C. Zheng, C. P. Tan, L. M. Chen and L. N. Ji, *Dalton Trans.*, **2005**, 2038-2046.
28. P. U. Maheswari, V. Rajendiran, M. Palaniandavar, R. Parthasarathi and V. Subramanian, *Bull. Chem. Soc. Jpn.*, **2005**, *78*, 835-844.
29. C. B. Spillane, J. L. Morgan, N. C. Fletcher, J. G. Collins and F. R. Keene, *Dalton Trans.*, **2006**, 3122-3133.
30. D. Z. M. Coggan, I. S. Haworth, P. J. Bates, A. Robinson and A. Rodger, *Inorg. Chem.*, **1999**, *38*, 4486-4497.
31. P. Lincoln and B. Norden, *J. Phys. Chem.*, **1998**, *102*, 9583-9594.
32. F. Westerlund, F. Pierard, M. P. Eng, B. Norden and P. Lincol, *J. Phys. Chem.*, **2005**, *109*, 17327-17332.
33. S.-D. Choi, M.-S. Kim, S. K. Kim, P. Lincoln, E. Tuite and B. Nordén, *Biochemistry*, **1997**, *36*, 214-223.
34. B. Önfelt, P. Lincoln, B. Nordén, J. S. Baskin and A. H. Zewail, *Proc. Natl. Acad. Sci. USA*, **2000**, *97*, 5708-5713.
35. P. K.-L. Fu, P. M. Bradley and C. Turro, *Inorg. Chem.*, **2003**, *42*, 878-884.
36. M. Han, L. Gao and K. Wang, *New J. Chem.* , **2005**, *30*, 209-214.
37. M. Mariappan and M. B. G., *Eur. J. Inorg. Chem.*, **2005**, 2164-2173.
38. C. Metcalfe, C. Rajput and J. A. Thomas, *Inorg. Biochem.*, **2006**, *100*, 1314-1319.
39. D. Lawrence, V. G. Vaidyanathab and B. U. Nair, *J. Inorg. Biochem.* , **2006**, *100*, 1244-1251.
40. H. Deng, J. Li, K. C. Zheng, Y. Yang, H. Chao and L. N. Ji, *Inorg. Chim. Acta.*, **2005**, *358*, 3430-3440.
41. J. M. Kelly, A. B. Tossi, D. J. McConnell and C. OhUigin, *Nucleic Acids Res.*, **1985**, *13*, 6017-6029.
42. A. M. Pyle, J. P. Rehmann, R. Meshoyrer, C. V. Kumar, N. J. Turro and J. K. Barton, *J. Am. Chem. Soc.*, **1989**, *111*, 3051-3058.
43. J. E. Coury, J. R. Anderson, L. McFailIsom, L. D. Williams and L. A. Bottomley, *J. Am. Chem. Soc.*, **1997**, *119*, 3792-3796.
44. A. Garcia-Raso, J. J. Fiol, M. J. Prieto, V. Moreno, I. Mata, E. Molins, T. Bunic, A. Golobic and I. Turel, *Inorg. Chem. Comm.*, **2005**, *5*, 800-804.
45. A. Mihailovic, I. Vladescu, M. McCauley, E. Ly, M. C. Williams, E. M. Spain and M. E. Nunez, *Langmuir*, **2006**, *22*, 4699-4709.
46. P. K.-L. Fu and C. Turro, *Chem. Commun.*, **2001**, 279-280.
47. F. Gao, H. Chao, J.-Q. Wang, Y.-X. Yuan, B. Sun, Y.-F. Wei, B. Peng and L.-N. Ji, *J. Biol. Inorg. Chem.*, **2007**, *12*, 1015-1027.
48. M. Pauly, I. Kayser, M. Schmitz, M. Dicato, A. Del Guerzo, I. Kolber, C. Moucheron and A. Kirsch-De Mesmaeker, *Chem. Commun.*, **2002**, 1086-1087.
49. M. Chandra, A. N. Sahay, D. S. Pandey, R. P. Tripathi, J. K. Saxena, V. J. M. Reddy, M. C. Puerta and P. Valerga, *J. Organometal. Chem.*, **2004**, *689*, 2256-2267.
50. D. T. Odom, C. S. Parker and J. K. Barton, *Biochemistry*, **1999**, *38*, 5155-5163.
51. J.-P. Lecomte, A. K.-D. Mesmaeker, M. M. Feeney and J. M. Kelly, *Inorg. Chem.*, **1995**, *34*, 6481-6491.

52. A. A. Holder, *Inorg. Chem.*, **2004**, *43*, 303-308.
53. Y. Liu, H. Chao, J. Yao, L. Tan, Y. Yuan and L. N. Ji, *Inorg. Chim. Acta.*, **2005**, *358*, 1904-1910.
54. Y. Liu, H. Chao, Y. Yuan, H. Yu and L. N. Ji, *Inorg. Chim. Acta.*, **2006**, *359*, 3807-3814.
55. S. Swavey and K. J. Brewer, *Inorg. Chem.*, **2002**, *41*, 6196-6198.
56. M. B. Fleisher, K. C. Waterman, N. J. Turro and J. K. Barton, *Inorg. Chem.*, **1986**, *25*, 3549-3551.
57. O. Nováková, J. Kaspárková, O. Vrána, P. M. van Vliet, J. Reedijk and V. Brabec, *Biochemistry*, **1995**, *34*, 12369-12378.
58. L. Mishra, R. Sinha, H. Itokawa, K. F. Bastow, Y. Tachibana, Y. Nakanishi, N. Kilgorec and K.-H. Leeb, *Bioorg. Med. Chem.*, **2001**, *9*, 1667-1671.
59. D.-L. Ma, C.-M. Che, F.-M. Siu, M. Yang and K.-Y. Wong, *Inorg. Chem.*, **2007**, *46*, 740-749.
60. C. B. Spillane, N. C. Fletcher, S. M. Rountree, H. van den Berg, S. Chanduloy, J. L. Morgan and F. R. Keene, *J. Biol. Inorg. Chem.*, **2007**, *12*, 797-807.
61. M. J. Clarke, *Coord. Chem. Rev.*, **2002**, *232*, 69-93.
62. X. W. Liu, J. Li, H. Deng, K. C. Zheng, Z. W. Mao and L. N. Ji, *Inorg. Chim. Acta*, **2005**, *358*, 3311-3319.
63. X.-W. Liu, J. Li, H. Li, K. Zheng, H. Chao and L. Ji, *J. Inorg. Biochem.*, **2005**, *99*, 2372-2380.
64. P. U. Maheswari, V. Rajendiran, H. Stoeckli-Evans and M. Palaniandavar, *Inorg. Chem.*, **2006**, *45*, 37-50.
65. A. Broo and P. Lincoln, *Inorg. Chem.* , **1997**, *36*, 2544-2553.
66. D. Han, H. Wang and N. Ren, *J. Molec. Struc.* , **2004**, *711*, 185-192.
67. V. G. Vaidyanathan and B. U. Nair, *Dalton Trans.* , **2005**, 2842-2848.
68. S. Mahadevan and M. Palaniandavar, *Inorg. Chem.*, **1998**, *37*, 693-700.
69. P. J. Barnard and R. S. Vagg, *J. Inorg. Biochem.*, **2005**, *99*, 1009-1017.
70. C. Hiort, P. Lincoln and B. Nordén, *J. Am. Chem. Soc.*, **1993**, *115*, 3448-3454.
71. J.-Z. Wu and L. Yuan, *J. Inorg. Biochem.*, **2004**, *98*, 41-45.
72. C. V. Kumar, J. K. Barton and N. J. Turro, *J. Am. Chem. Soc.*, **1985**, *107*, 5518-5523.
73. J. K. Barton, J. M. Goldberg, C. V. Kumar and N. J. Turro, *J. Am. Chem. Soc.*, **1986**, *108*, 2081-2088.
74. B. Abraham, C. V. Sastri, B. G. Maiya and S. Umapathy, *J. Raman Spectrosc.*, **2004**, *35*, 13-18.
75. C. G. Coates, L. Jacquet, J. J. McGarvey, S. E. J. Bell, A. H. R. Al-Obaidi and J. M. Kelly, *J. Am. Chem. Soc.*, **1997**, *119*, 7130-7136.
76. C. G. Coates, J. J. McGarvey, P. L. Callaghan, M. Coletti and J. G. Hamilton, *J. Phys. Chem. B*, **2001**, *105*, 730-735.
77. E. Gaudry, J. Aubard, H. Amouri, G. Levi and C. Cordier, *Biopolymers*, **2005**, *82*, 399-404.
78. C. G. Coates, P. Callaghan, J. J. McGarvey, J. M. Kelly, L. Jacquet and A. Kirsch-De Mesmaeker, *J. Mol. Struct.*, **2001**, *598*, 15-25.
79. D. L. Boger, B. E. Fink, S. R. Brunette, W. C. Tse and M. P. Hedrick, *J. Am. Chem. Soc.*, **2001**, *123*, 5878-5891.
80. D. L. Boger and W. C. Tse, *Bioorg. Med. Chem.*, **2001**, *9*, 2511-2518.
81. W. C. Tse and D. L. Boger, *Acc. Chem. Res.*, **2004**, *37*, 61-69.

82. Y.-W. Ham, W. C. Tse and D. L. Boger, *Bioorg. Med. Chem. Lett.*, **2003**, *13*, 3805-3807.
83. M. A. Lewis and E. C. Long, *Bioorg. Med. Chem.* , **2006**, *14*, 3481-3490.
84. D. Monchaud, C. Allain and M.-P. Teulade-Fichou, *Bioorg. Med. Chem. Lett.*, **2006**, *16*, 4842-4845.
85. Y.-H. Shim, P. B. Arimondo, A. Laigle, A. Garbesi and L. S., *Org. Biomol. Chem.*, **2004**, *2*, 915-921.
86. K. D. Goodwin, M. A. Lewis, F. A. Tanious, R. R. Tidwell, W. D. Wilson, M. M. Georgiadis and E. C. Long, *J. Am. Chem. Soc.*, **2006**, *128*, 7846-7854.
87. M. E. Reichmann, S. A. Rice, C. A. Thomas and P. Doty, *J. Am. Chem. Soc.*, **1954**, *76*, 3047-3053.
88. K. A. Meadows, F. Liu, J. Sou, B. P. Hudson and D. R. Mcmillin, *Inorg. Chem.*, **1993**, *32*, 2919-2923.
89. A. Wolfe, G. H. J. Shimer and T. Meehan, *Biochemistry*, **1987**, *26*, 6392-6396.
90. J. L. Morgan, C. B. Spillane, J. A. Smith, D. P. Buck, J. G. Collins and F. R. Keene, *Dalton Trans.*, **2007**, 4333-4342.
91. A. Greguric, I. D. Greguric, T. W. Hambley, J. R. Aldrich-Wright and J. G. Collins, *J. Chem. Soc., Dalton Trans.*, **2002**, 849-855.
92. J. G. Collins, J. R. Aldrich-Wright, I. D. Greguric and P. A. Pellegrini, *Inorg. Chem.*, **1999**, *38*, 5502-5509.
93. R. Caspar, L. Musatkina, A. Tatosyan, H. Amouri, M. Gruselle, C. Guyard-Duhayon, R. Duval and C. Cordier, *Inorg. Chem.*, **2004**, *43*, 7986-7993.
94. H.-Y. Mei and J. K. Barton, *Proc. Natl. Acad. Sci. USA*, **1988**, *85*, 1339-1343.
95. J. A. Smith, *Dinuclear Ruthenium Complexes as Sequence- and Structure-Selective Binding Agents for DNA*, Honours Thesis, James Cook University, Townsville, **2003**.
96. B. T. Patterson, J. G. Collins, F. M. Foley and F. R. Keene, *J. Chem. Soc., Dalton Trans.*, **2002**, 4343-4350.
97. B. T. Patterson, *Stereochemistry and Applications of Mono- and Oligo-nuclear Complexes of Iron, Ruthenium and Osmium*, PhD Thesis, James Cook University, Townsville, **2002**.
98. C.-W. Jiang, H. Chao, X.-L. Hong, H. Li, W.-J. Mei and L.-N. Ji, *Inorg. Chem. Commun.*, **2003**, *6*, 773-775.
99. C.-W. Jiang, *Eur. J. Inorg. Chem.*, **2004**, 2277-2282.
100. P. P. Pellegrini and J. R. Aldrich-Wright, *Dalton Trans.*, **2003**, 176-183.
101. S. Neidle, *Nat. Prod. Rep.*, **2001**, *18*, 291-309.
102. P. E. Pjura, K. Grzeskowiak and R. E. Dickerson, *J. Mol. Biol.*, **1987**, *197*, 257-271.
103. R. Lavery and B. Pullman, *Nucleic Acids Res.*, **1982**, *10*, 4383-4395.
104. A. V. Fratini, M. L. Kopka, H. R. Drew and R. E. Dickerson, *J. Biol. Chem.*, **1982**, *257*, 14686-14707.
105. G. N. Parkinson, R. Gosh and S. Neidle, *Biochemistry*, **2007**, *46*, 2390-2397.
106. M. A. Read, A. A. Wood, J. R. Harrison, S. M. Gowan, L. R. Kelland, H. S. Dosanjh and S. Neidle, *J. Med. Chem.*, **1999**, *42*, 4538-4546.
107. C. M. Barbieri, A. R. Srinivasan, S. G. Rzuczek, J. E. Rice, E. J. LaVoie and D. S. Pilch, *Nucleic Acids Res.*, **2007**, *35*, 3272-3286.
108. M.-Y. Kim, H. Mankayalapati, K. Shin-ya, K. Wierzba and L. H. Hurley, *J. Am. Chem. Soc.*, **2002**, *124*, 2098-2099.

109. A. D. Moorhouse, A. M. Santos, M. Gunaratnam, M. Moore, S. Neidle and J. E. Moses, *J. Am. Chem. Soc.*, **2006**, *128*, 15972-15973.
110. J. L. Morgan, D. P. Buck, A. G. Turley, J. G. Collins and F. R. Keene, *Inorg. Chim. Acta*, **2006**, *359*, 888-898.
111. J. A. Smith, J. G. Collins, B. T. Patterson and F. R. Keene, *Dalton Trans.*, **2004**, 1277-1283.
112. J. L. Morgan, D. P. Buck, A. G. Turley, J. G. Collins and F. R. Keene, *J. Biol. Inorg. Chem.*, **2006**, *11*, 824-834.
113. C. B. Spillane, J. A. Smith, J. L. Morgan and F. R. Keene, *J. Biol. Inorg. Chem.*, **2007**, *12*, 819-824.
114. J. W. Nelson and J. Tinoco, I., *Biochemistry*, **1985**, *24*, 6416-6421.
115. W. D. Wilson, F. A. Tanious, J. Barton, R. L. Jones, K. Fox, R. L. Wydra and L. Strekowski, *Biochemistry*, **1990**, *29*, 8452-8461.
116. C. Bustamante, *Annu. Rev. Biophys. Biophys. Chem.*, **1991**, *20*, 415-446.
117. B. H. Yun, J.-O. Kim, B. W. Lee, P. Lincoln, B. Nordén, J.-M. Kim and S. K. Kim, *J. Phys. Chem. B*, **2003**, *107*, 9858-9864.
118. M. R. Youn, S. J. Moon, B. W. Lee, D. Lee, J. Kim, S. K. Kim and C. Lee, *Bull. Korean Chem. Soc.* , **2005**, *26*, 537-542.
119. B. W. Lee, S. J. Moon, M. R. Youn, J. H. Kim, H. G. Jang and S. K. Kim, *Biophys. J.*, **2003**, *85*, 3865-3871.
120. F. Westerlund, L. M. Wilhelmsson, B. Norden and P. Lincol, *J. Phys. Chem. B*, **2005**, *109*, 21140-21144.
121. X.-H. Zou, *J. Chem. Soc., Dalton Trans.*, **1999**, 1423-1428.
122. G. Yang, J. Z. Wu, L. Wang, L. N. Ji and X. Tian, *J. Inorg. Biochem.*, **1997**, *66*, 141-144.
123. F. Liu, K. Wang, G. Bai, Y. Zhang and L. Gao, *Inorg. Chem.*, **2004**, *43*, 1799-1806.
124. J.-Z. Wu, B.-H. Ye, L. Wang, L.-N. Ji, J.-Y. Zhou, R.-H. Li and Z.-Y. Zhou, *J. Chem. Soc., Dalton Trans.*, **1997**, 1395-1401.
125. R. B. Nair, E. S. Teng, S. L. Kirkland and C. J. Murphy, *Inorg. Chem.*, **1998**, *37*, 139-141.
126. S. Satyanarayana, J. C. Dabrowiak and J. B. Chaires, *Biochemistry*, **1993**, *32*, 2573-2584.
127. S. Mahadevan and M. Palaniandavar, *Bioconjugate Chem.*, **1996**, *7*, 138-143.
128. W. A. Kalsbeck and H. H. Thorp, *J. Am. Chem. Soc.*, **1993**, *115*, 7146-7151.
129. C. B. Spillane, J. A. Smith, D. P. Buck, J. G. Collins and F. R. Keene, *Dalton Trans.*, **2007**, 5290-5296.